

CERTIFICATE OF ORIGINALITY

This is to certify that I am responsible for the work submitted in this thesis, that the original work is my own except as specified in acknowledgments or in footnotes, and that neither the thesis nor the original work contained therein has been submitted to this or any other institution for a degree.

Synthesis of Fluorinated Heterocyclic Compounds and Study of their Interaction with DNA

By

Fatemeh Zeinali

A thesis submitted in the partial fulfilment of the requirements for
the award of

Doctor of Philosophy

Loughborough University

Department of Chemistry

Research Supervisors

Dr. George Weaver

Dr. Paul Lucas

Dr. Mark Elsegood

2016

Dedication

This research work is dedicated to my Father, Mother, and my children Matin, Mahta, and to all my family and friends.

Acknowledgement

I would like to express deepest gratitude to my supervisors Dr. George Weaver, Dr. Paul Lucas and Dr. Mark Elsgood for their full support, expert guidance, encouragement, enthusiastic supervision, and invaluable advice throughout the duration of the research project and allowing me to grow as a research scientist. Without their incredible patience and timely wisdom and counsel, my thesis work would have been a frustrating and overwhelming pursuit.

I would like to record a special thanks to the technical and support staff for all their assistance. They include Dr. Mark Elsgood for X-ray crystallography, Dr. Mark Edgar for NMR spectroscopy and Mr. Alastair Daley for elemental analysis and for GC mass spectrometry. I would like to thank Dr Sweta Ladwa for help with the antibacterial activity. I would like to thank Dr Vladimir Kryštof of Palacky University, Czech Republic, for the anti-cancer screening. I acknowledge the EPSRC National mass spectrometry facility, Swansea University, for mass spectrometry.

Thanks also go to the Weaver research group and all research students in laboratories F009 and F001 for their help and assistance and friendship.

I am thankful to Loughborough University for support.

Finally, I would like to express thankfulness to my parents (specially my father) and children for their unconditional support and patience throughout these studies. I would not have been able to complete this thesis without my father's continuous encouragement and love.

Abstract

Over fifty, structurally diverse, novel fluorinated heteroarenes, have been successfully synthesised by S_NAr reaction of a range of fluorinated arenes including pentafluoropyridine, hexafluorobenzene, and methyl pentafluorobenzoate by introduction of a range of groups such as imidazole, triazole, benzimidazole, benzotriazole, and carbazole. Different water solubilising side chains were introduced to some of the successfully synthesised fluorinated heteroarenes to improve water solubility and potential biological activity. X-ray crystal structures of over 10 compounds were obtained including those of two macrocyclic compounds containing 21- and 24-membered rings. The synthesised compounds have been characterized by elemental analysis, IR, 1H and ^{19}F spectroscopy and high resolution mass spectrometry. These compounds have been screened for their biological activities and possible interaction with DNA by methods including UV-visible spectroscopy, fluorescence spectroscopy, co-crystallization for X-ray diffraction analysis, and antimicrobial activity. A number of the fluoroaryl benzimidazole derivatives have been tested against K-562 and MCF-7 cell lines and G361 and HOS cell lines. From the all tested compounds three tethered fluoroaryl benzimidazole derivatives demonstrated micromolar inhibition against K-562 and MCF-7 cell lines. These compounds, in addition to 1-tetrafluoropyrid-4-yl-2-tetrafluoropyrid-4-ylsulfanyl-1H-benzimidazole, also demonstrated micromolar inhibition against G361 and HOS cell lines. Two of the compounds were found to activate caspases leading to apoptosis.

Abbreviations

• ACTD	Actinomycin D
• A	Adenine
• AFM	Atomic-force microscopy
• ChI	Chlorambucil
• C	Cytosine
• COX-2	Cyclooxygenase-2
• CDKs	Cyclin-dependent kinases
• Cu(OTf)₂	Copper(II) triflate
• CT-DNA	Calf thymus-DNA
• DNA	Deoxyribonucleic acid
• DMF	Dimethylformamide
• DCM	Dichloromethane
• DMSO	Dimethylsulfoxide
• Et₃N	Triethylamine
• EB	Ethidium boromide
• Eq.	Equation
• EGFR	Epidermal growth factor receptor
• EN	Electronegativity
• ESI-MS	Electrospray ionisation mass spectrometry
• ERK	Extracellular Regulated Kinase
• GC-MS	Gas chromatography mass spectrometry
• FT-IR	Fourier transform infrared
• G	Guanine
• ΔG	Gibbs free energy
• g	Grams
• h	Hours
• 5HT1D	5-hydroxytryptamine receptor 1D
• HOS	Human Osteosarcoma cell
• IR	Infra-red
• IC₅₀	Half maximal inhibitory concentration
• K	Binding constant

- **K_{sv}** Stern-Volmer quenching constant
- **mL** Millilitres
- **m.p.** Melting point
- **MCF-7** Michigan cancer foundation-7
- **MAPK** Mitogen-activated protein kinase
- **NMR** Nuclear magnetic mesonance
- **NaH** Sodium hydride
- **NaHCO₃** Sodium bicarbonate
- **ppm** Parts per million
- **PPA** Polyphosphoric acid
- **PTKs** Protein tyrosine kinases
- **RNA** Ribonucleic acid
- **RT** Room temperature
- **S_NAr** Aromatic nucleophilic substitution
- **SS-DNA** Salmon sperm-DNA
- **T** Thymine
- **TS** Thymidylate synthase
- **tRNA** Transfer ribonucleic acid
- **TKI** Tyrosine-kinase inhibitor
- **THF** Tetrahydrofuran
- **TLC** Thin layer chromatography
- **UV** Ultraviolet

Contents

CERTIFICATE OF ORIGINALITY	i
Dedication	iii
Acknowledgement.....	iv
Abstract.....	v
Abbreviations.....	vii
List of schemes.....	xix
List of figures.....	xxi
List of tables.....	xxiv

Chapter 1: Introduction

1. Introduction	1
1.1. Fluorine in medicinal chemistry	1
1.1.1. Physical characteristics of fluorine	2
1.1.2. Improving metabolic stability with fluorine	3
1.1.3. The effect of fluorine on the pKa and bioavailability	5
1.1.4. The effect of fluorine on molecular lipophilicity.....	6
1.1.5. Fluorinated heterocyclic compounds based on natural products	7
1.1.5.1. Nucleosides.....	7
1.1.5.2. Alkaloids.....	8
1.1.5.3. Steroids	9
1.2. Heterocyclic chemistry.....	10
1.2.1. Imidazole in medicinal chemistry	11
1.2.2. Benzimidazole in medicinal chemistry	12
1.2.3. Triazole in medicinal chemistry.....	14
1.2.4. Benzotriazole in medicinal chemistry.....	16
1.2.5. Reactions of perfluorinated arenes and heteroarenes.....	18
1.2.5.1. Perfluorinated pyridine	25
1.3. Fluorinated heterocyclic compounds as potential DNA binding ligands	30
1.3.1. DNA double helix structure	30

1.3.2.	Type of DNA-drug interactions	31
1.3.3.	Modes of drug-DNA binding.....	32
1.3.3.1.	Covalent mode of binding	32
1.3.3.2.	Non-covalent mode of binding	33
1.3.3.3.	Groove binding drug-DNA interaction.....	33
1.3.3.4.	Intercalating binding agents.....	36
1.3.4.	Techniques used to study drug–DNA interactions	38
1.3.4.1.	UV–visible absorption spectroscopy	38
1.3.4.2.	Fluorescence spectroscopy	38
1.3.4.3.	Macromolecular X-ray crystallography.....	40
1.3.4.4.	Vapour diffusion crystallization	40
1.4.	Fluorinated heterocyclic compounds as protein kinases inhibitors	41

Chapter 2: Results and discussion

2.	Results and discussion.....	46
2.1.	Outcome of organic synthesis.....	46
2.1.1.	Synthesis of perfluoro heterocyclic compounds	46
2.1.1.1.	Reaction of pentafluoropyridine with imidazole	46
2.1.1.2.	Reaction of pentafluoropyridine with benzimidazole	47
2.1.1.3.	Reaction of benzimidazolyltetrafluoropyridine derivative (109) with Benzimidazole.....	48
2.1.1.4.	Reaction of pentafluoropyridine with triazole.....	50
2.1.1.5.	Reaction of pentafluoropyridine with benzotriazole	51
2.1.1.6.	Reaction of pentafluoropyridine with carbazole	52
2.1.1.7.	Reaction of 2-bromophenol with compound (109)	53
2.1.1.8.	Reaction of 2-aminothiophenol with compound (109)	54
2.1.1.9.	Reaction of 2-aminobenzenethiol with 4-nitrobenzoyl chloride	55
2.1.1.10.	Reaction of 2-bromothiophenol with compound (109)	57
2.1.2.	Synthesis of bis N-heterocyclic compounds as starting materials for reaction with fluoroarenes	59
2.1.2.1.	Reaction of the glyoxalin with ammonium acetate	59
2.1.3.	Synthesis of 2,2-(1,4-butanediyl)-bis-1H-imidazole (132) and 2,2-(1,4-butanediyl)-bis-1H-benzimidazole (134)	59

2.1.3.1.	Reaction of adipoyl chloride with aminoacetaldehyde dimethyl acetal	59
2.1.3.2.	Reaction of adipoyl chloride with <i>o</i> -phenylenediamine.....	60
2.1.3.3.	Reaction of adiponitrile with aminoacetaldehyde dimethyl acetal.....	61
2.1.3.4.	Synthesis of imidate and formation of the target compound (132) and (134)	62
2.1.4.	Synthesis of bis-imidazole and bis-benzimidazole containing perfluoro heterocyclic derivatives.....	67
2.1.4.1.	Reaction of the pentafluoropyridine with 1H,1H-2,2'-biimidazole	67
2.1.4.2.	Reaction of the hexafluorobenzene with 1H,1H-2,2'-biimidazole.....	68
2.1.4.3.	Reaction of pentafluorobenzaldehyde with 1H,1H-2,2'-biimidazole	69
2.1.4.4.	Reaction of pentafluoropyridine with bis-benzimidazole (134)	70
2.1.4.5.	Reaction of the hexafluorobenzene with bis-benzimidazole (134)	71
2.1.4.6.	Reaction of pentafluorobenzaldehyde with bis-benzimidazole (134)	72
2.1.4.7.	Reaction of compound (134) with methyl pentafluorobenzoate	73
2.1.5.	Synthesis of bis-linked binding agents via formation of an amide bond.....	74
2.1.5.1.	Reaction of pentafluorobenzoyl chloride and 2,2'-(ethylenedioxy)bis(ethylamine)	74
2.1.5.2.	Substitution reaction of benzimidazole with fluorinated bis-linked scaffold (151)	75
2.1.5.3.	Substitution reaction of carbazole with fluorinated bis-linked scaffold (151)	77
2.1.5.4.	Substitution reaction of 2-mercaptobenzimidazole with fluorinated bis-linked scaffold (151)	78
2.1.5.5.	Substitution reaction of imidazole with fluorinated bis-linked scaffold (151)	79
2.1.5.6.	Substitution reaction of indole with fluorinated bis-linked binding scaffold (151)	81
2.1.5.7.	Substitution reaction of benzotriazole with fluorinated bis-intercalator scaffold (151)	82
2.1.5.8.	Substitution reaction of 1,2,4 triazole with fluorinated bis-intercalator scaffold (151)	83
2.1.6.	Synthesis of bis-linked binding agents by introducing of aliphatic hydrophilic link to synthesised fluorinated heterocyclic compounds.	84
2.1.6.1.	Reaction of compound (109) with 2,2'-(ethylenedioxy)bis(ethylamine)	84
2.1.6.2.	Reaction of further perfluoropyridine derivatives with 2,2'-(ethylenedioxy)bis(ethylamine)	86

2.1.6.3.	Reaction of different perfluoropyridine derivatives with 2-(2-aminoethoxy) ethylamine.....	88
2.1.7.	Further functionalization to make bis-linked binding agents	91
2.1.7.1.	Reaction of compound (148) with hydrazine	91
2.1.7.2.	Reaction of compound (148) with 2-aminopyridine	92
2.1.7.3.	Reaction of ester compound (148) with acetamide hydrochloride.....	93
2.1.8.	Addition of hydrophilic side chains to the successfully synthesised fluorinated heterocyclic compounds.	94
2.1.8.1.	Reaction of the compound (138) with cysteine	94
2.1.8.2.	Reaction of the compound (143) with cysteine	95
2.1.8.3.	Study the Reaction of compound (143) with 2,2-(ethylenedioxy)bis(ethylamine)	96
2.1.8.4.	Investigation of the reaction of compound (143) with 2-(2-aminoethoxy)ethylamine	98
2.1.8.5.	Study of the reaction of perfluoro bis-benzimidazole derivative (143) with hexamethylenediamine	100
2.1.8.6.	Study of the reaction of compound (143) with ethylenediamine	101
2.1.8.7.	Investigation of the reaction of compound (143) with 2-(2-aminoethoxy) ethanol	102
2.1.8.8.	Investigation of the reaction of compound (143) with (\pm)-3-amino-1,2-propanediol	103
2.1.8.9.	Reaction of compound (143) with ethanolamine	104
2.1.8.10.	Reaction of pentafluoropyridine with 2-mercaptobenzimidazole	105
2.1.8.11.	Investigation of further substitution of fluorine in scaffold (194) by ethanolamine	106
2.1.8.12.	Substitution reaction of scaffold (194) with ethylenediamine	107
2.1.8.13.	Substitution reaction of scaffold (194) with morpholine.....	107
2.1.8.14.	Investigation of reaction of morpholine with the tethered bis-benzimidazolyl pyridine (163)	108
2.1.9.	Investigation of reaction perfluoroarenes with aliphatic side chain which contain thiol	109
2.1.9.1.	Reaction of compound (109) with 3,6-dioxa-1,8-octanedithiol	110

2.2. DNA binding studies	112
2.2.1. UV absorption spectroscopy experiment	112
2.2.1.1. UV-visible spectroscopy of ACTD as known intercalate agent and naproxen as known groove binder	113
2.2.1.2. Studies of UV absorption results and cooperation of binding constant data.....	115
2.2.2. Ethidium bromide (EB) fluorescence displacement experiment	117
2.2.2.1. EB fluorescence displacement assay of ACTD as intercalating agent.....	118
2.2.2.2. EB fluorescence displacement assay of naproxen as groove binding agent reference.	119
2.2.2.3. Binding constant comparison of synthesis compound using EB quenching assay.....	120
2.3. Anticancer activity <i>in vitro</i>	121
2.4. Antibacterial activity of synthesised compounds	123
2.5. Hanging drop DNA crystallization	124
3. Conclusions and future work.....	125

Chapter 3: Experimental

4. Experimental.....	127
4.1. General.....	127
4.2. Organic synthesis.....	128
4.2.1. 2,3,5,6-Tetrafluoro-4-(1H-imidazol-1-yl)pyridine (108).....	128
4.2.2. 1-(Perfluoropyridin-4-yl)-1H-benzo[d]imidazole (109).....	128
4.2.3. 1,1'-(3,5,6-Trifluoropyridine-2,4-diyl)bis(1H-benzo[d]imidazole) (110)	129
4.2.4. 2,3,5,6-Tetrafluoro-4-(1H-1,2,3-triazol-1-yl)pyridine (111) and 2,3,5,6-tetrafluoro-4-(2H-1,2,3-triazol-2-yl)pyridine (112)	130
4.2.5. 1-(Perfluoropyridin-4-yl)-1H-benzo[d][1,2,3]triazole (113)	131
4.2.6. 9,9'-(3,4,6-Trifluoropyridine-2,5-diyl)bis(9H-carbazole) (114)	131
4.2.7. 1-(2,6-is(2-Bromophenoxy)-3,5-difluoropyridin-4-yl)-1H-benzo[d]imidazole (115).132	
4.2.8. 2-(((4-(1H-benzo[d]imidazol-1-yl)-3,5,6-trifluoropyridin-2-yl)thio)aniline) (118).....	133
4.2.9. N-(2-Mercaptophenyl)-4-nitrobenzamide (121)	134
4.2.10. 2-(4-Nitrophenyl)benzo[d]thiazole (122)	134

4.2.11.	1-(2,5-bis((2-Bromophenyl)thio)-3,6-difluoropyridin-4-yl)-1H-benzo[d]imidazole (126)	135
4.2.12.	1H,1'H-2,2'-Biimidazole (130)	136
4.2.13.	N1,N6-bis(2,2-Dimethoxyethyl)adipamide (131)	136
4.2.14.	1,4-di(1H-imidazol-2-yl)butane (132)	137
4.2.15.	N1,N6-bis(2-Aminophenyl)adipamide (133)	137
4.2.16.	1,4-bis(1H-benzo[d]imidazol-2-yl)butane (134)	138
4.2.17.	N1,N6-bis(2,2-Dimethoxyethyl)adipimidamide (135)	138
4.2.18.	Diethyl adipimidate dihydrochloride (136)	139
4.2.19.	5,7,8-Trifluorodiimidazo[1,2-a:2',1'-c]pyrido[3,4-e]pyrazine (137) and 1- (perfluorophenyl)-1'-(perfluoropyridin-4-yl)-1H,1'H-2,2'-biimidazole (138)	13939
4.2.20.	5,6,7,8-Tetrafluorodiimidazo[1,2-a:2',1'-c]quinoxaline (140)	140
4.2.21.	5,7,8-Trifluorodiimidazo[1,2-a:2',1'-c]quinoxaline-6-carbaldehyde (141)	141
4.2.22.	1,4-bis-1-Tetrafluoropyrid-4-yl-1H-benzimidazol-2-ylbutane (143)	141
4.2.23.	1,4-bis-1-(4-Methoxycarbonyltetrafluorophenyl)-1H-benzimidazol-2-ylbutane	148 . 142
4.2.24.	2,2-(Ethylenedioxy)-bis-ethyl pentafluorobenzamide (151)	143
4.2.25.	2,2'-(Ethylenedioxy)-bis-ethyl 4-benzimidazol-1-yltetrafluorobenzamide (152) and N- (2-(2-(2-(4-(1H-benzo[d]imidazol-1-yl)-2,3,5,6-tetrafluorobenzamido)ethoxy)ethoxy)ethyl)- 2,3,4,5,6-pentafluorobenzamide (151)	144
4.2.26.	N,N'-((Ethane-1,2-diylbis(oxy))bis(ethane-2,1-diyl))bis(2,3,5,6-tetrafluoro-4-(1H- imidazol-1-yl)benzamide) (158) and 2,3,4,5,6-pentafluoro-N-(2-(2-(2-(2,3,5,6-tetrafluoro-4- (1H-imidazol-1-yl)benzamido)ethoxy)ethoxy)ethyl)benzamide (159)	145
4.2.27.	N,N'-((Ethane-1,2-diylbis(oxy))bis(ethane-2,1-diyl))bis(4-(1H-benzo[d][1,2,3]triazol- 1-yl)-2,3,5,6-tetrafluorobenzamide) (161)	146
4.2.28.	2,3,4,5,6-Pentafluoro-N-(2-(2-(2-(2,3,5,6-tetrafluoro-4-(4H-1,2,4-triazol-4- yl)benzamido)ethoxy)ethoxy)ethyl)benzamide (162)	147
4.2.29.	N,N'-((Ethane-1,2-diylbis(oxy))bis(ethane-2,1-diyl))bis(4-(1H-benzo[d]imidazol-1-yl)- 3,5,6-trifluoropyridin-2-amine) (163)	148

4.2.30. N,N'-((Ethane-1,2-diylbis(oxy))bis(ethane-2,1-diyl))bis(4-(1H-benzo[d][1,2,3]triazol-1-yl)-3,5,6-trifluoropyridin-2-amine) (164)	149
4.2.31. N,N'-((Ethane-1,2-diylbis(oxy))bis(ethane-2,1-diyl))bis(3,5,6-trifluoro-4-(1H-1,2,3-triazol-1-yl)pyridin-2-amine) (165).....	150
4.2.32. N,N'-((Ethane-1,2-diylbis(oxy))bis(ethane-2,1-diyl))bis(3,5,6-trifluoro-4-(1H-imidazol-1-yl)pyridin-2-amine) (166)	151
4.2.33. N,N'-(Oxybis(ethane-2,1-diyl))bis(4-(1H-benzo[d]imidazol-1-yl)-3,5,6-trifluoropyridin-2-amine) (168).....	152
4.2.34. N,N'-(Oxybis(ethane-2,1-diyl))bis(4-(1H-benzo[d][1,2,3]triazol-1-yl)-3,5,6-trifluoropyridin-2-amine) (169).....	153
4.2.35. N,N'-(Oxybis(ethane-2,1-diyl))bis(3,5,6-trifluoro-4-(1H-1,2,3-triazol-1-yl)pyridin-2-amine) (170)	154
4.2.36. N,N'-(Oxybis(ethane-2,1-diyl))bis(3,5,6-trifluoro-4-(1H-imidazol-1-yl)pyridin-2-amine) (171)	154
4.2.37. Methyl 2,3,5,6-tetrafluoro-4-(2-(4-(1-(5,6,8-trifluoro-2-methyl-4-oxo-1,4-dihydroquinazolin-7-yl)-1H-benzo[d]imidazol-2-yl)butyl)-1H-benzo[d]imidazol-1-yl)benzoate (176).....	155
4.2.38. Reaction of 1,4-bis-1-tetrafluoropyrid-4-yl-1H-benzimidazol-2-ylbutane 143 with 2,2-(ethylenedioxy)bis(ethylamine): macrocycle (181).....	156
4.2.39. Reaction of 1,4-bis-1-tetrafluoropyrid-4-yl-1H-benzimidazol-2-ylbutane 143 with 2-(2-aminoethoxy)ethylamine: macrocycle (183)	157
4.2.40. Reaction of 1,4-bis-1-tetrafluoropyrid-4-yl-1H-benzimidazol-2-ylbutane 143 with 2-(2-aminoethoxy)ethylamine : macrocycle (185)	158
4.2.41. 1,4-bis-1-[2-(2-Aminoethylamino)-trifluoropyrid-4-yl-1H-benzimidazol-2-yl]butane (187).....	159
4.2.42. 1,4-bis-1-{2-[2-(2-Hydroxyethoxy)ethylamino)-trifluoropyrid-4-yl]}-1H-benzimidazol-2-ylbutane (189).....	159
4.2.43. 1,4-bis-1-[2-(2,3-Dihydroxypropylamino)-trifluoropyrid-4-yl]-1H-benzimidazol-2-ylbutane (191).....	160

4.2.44.	1,4-bis-1-[2-(2-Hydroxyethylamino)-trifluoropyrid-4-yl]-1H-benzimidazol-2-ylbutane (193)	161
4.2.45.	1-Tetrafluoropyrid-4-yl-2-tetrafluoropyrid-4-ylsulfanyl-1H-benzimidazole (194).....	161
4.2.46.	2-((3,5,6-Trifluoro-4-((1-(2,3,5-trifluoro-6-((2-hydroxyethyl)amino)pyridin-4-yl)-1H- benzo[d]imidazol-2-yl)thio)pyridin-2-yl)amino)ethan-1-ol (196)	162
4.2.47.	N1-(4-((1-(2-((2-Aminoethyl)amino)-3,5,6-trifluoropyridin-4-yl)-1H- benzo[d]imidazol-2-yl)thio)-3,5,6-trifluoropyridin-2-yl)ethane-1,2-diamine (197)	163
4.2.48.	4-(3,5,6-Trifluoro-4-((1-(2,3,5-trifluoro-6-morpholinopyridin-4-yl)-1H- benzo[d]imidazol-2-yl)thio)pyridin-2-yl)morpholine (199).....	164
4.2.49.	N-(2-(2-(2-((4-(1H-benzo[d]imidazol-1-yl)-3,5,6-trifluoropyridin-2- yl)amino)ethoxy)ethoxy)ethyl)-4-(1H-benzo[d]imidazol-1-yl)-3,5-difluoro-6- morpholinopyridin-2-amine (201)	165
4.2.50.	2-(2-(2-((4-(1H-benzo[d]imidazol-1-yl)-3,5,6-trifluoropyridin-2- yl)thio)ethoxy)ethoxy)ethane-1-thiol (203).....	166
4.3.	Biological activity studies.....	167
4.3.1.	Preparation of Tris base buffer.....	167
4.3.2.	Preparation of DNA stock solution.....	167
4.3.3.	Preparation of synthesis and reference compounds solution	167
4.3.4.	Method of UV absorption assay	167
4.3.5.	Method of fluorescence displacement assay	167
4.3.6.	Hanging drop DNA crystallization method	168
4.3.6.1.	Preparation of DNA solution	168
4.3.6.2.	Preparation of the DNA-compound complex sample.....	168
4.3.7.	Antimicrobial activity studies	168
5.	References.....	169
6.	Appendix.....	179
6.1.	X-ray crystallography data	179
6.1.1.	Compound (109) X-ray crystal structure data	179
6.1.2.	Compound (110) X-ray crystal structure data	1806.1.3.
	Compound (111 X isomer) X-ray crystal structure data	182

6.1.4.	Compound (114) X-ray crystal structure data	183
6.1.5.	Compound (126) X-ray crystal structure data.....	185
6.1.6.	Compound (134) X-ray crystal structure data	187
6.1.7.	Compound (137) X-ray crystal structure data	188
6.1.8.	Compound (151) X-ray crystal structure data	190
6.1.9.	Compound (152) X-ray crystal structure data	192
6.1.10.	Compound (181) X-ray crystal structure data	193
6.1.11.	Compound (183) X-ray crystal structure data	195
6.2.	UV-Visible spectroscopy data	198
6.2.1.	UV-visible spectroscopy of compound (108)	198
6.2.2.	UV-visible spectroscopy of compound (111)	199
6.2.3.	UV-visible spectroscopy of compound (113)	200
6.2.4.	UV-visible spectroscopy of compound (114)	201
6.2.5.	UV-visible spectroscopy of compound (137)	202
6.2.6.	UV-visible spectroscopy of compound (138)	203
6.2.7.	UV-visible spectroscopy of compound (143)	204
6.2.8.	UV-visible spectroscopy of compound (148)	205
6.2.9.	UV-visible spectroscopy of compound (151)	206
6.2.10.	UV-visible spectroscopy of compound (152)	207
6.2.11.	UV-visible spectroscopy of compound (161)	208
6.2.12.	UV-visible spectroscopy of compound (162)	209
6.2.13.	UV-visible spectroscopy of compound (163)	210
6.2.14.	UV-visible spectroscopy of compound (164)	211
6.2.15.	UV-visible spectroscopy of compound (165)	212
6.2.16.	UV-visible spectroscopy of compound (166)	213
6.2.17.	UV-visible spectroscopy of compound (169)	214
6.2.18.	UV-visible spectroscopy of compound (170)	215

6.2.19.	UV-visible spectroscopy of compound (171)	216
6.2.20.	UV-visible spectroscopy of compound (181)	217
6.2.21.	UV-visible spectroscopy of compound (183)	218
6.2.22.	UV-visible spectroscopy of compound (187)	219
6.2.23.	UV-visible spectroscopy of compound (189)	220
6.2.24.	UV-visible spectroscopy of compound (191)	221
6.2.25.	UV-visible spectroscopy of compound (195)	222
6.2.26.	UV-visible spectroscopy of compound (196)	223
6.2.27.	UV-visible spectroscopy of compound (198)	224
6.3.	Fluorescence spectroscopy data for the ethidium boromide displacement assay	225
6.3.1.	Fluorescence spectra of compound (108)	225
6.3.2.	Fluorescence spectra of compound (111)	226
6.3.3.	Fluorescence spectra of compound (113)	226
6.3.4.	Fluorescence spectra of compound (114)	227
6.3.5.	Fluorescence spectra of compound (137)	227
6.3.6.	Fluorescence spectra of compound (138)	228
6.3.7.	Fluorescence spectra of compound (143)	228
6.3.8.	Fluorescence spectra of compound (148)	229
6.3.9.	Fluorescence spectra of compound (151)	229
6.3.10.	Fluorescence spectra of compound (152)	230
6.3.11.	Fluorescence spectra of compound (161)	230
6.3.12.	Fluorescence spectra of compound (162)	231
6.3.13.	Fluorescence spectra of compound (163)	231
6.3.14.	Fluorescence spectra of compound (164)	232
6.3.15.	Fluorescence spectra of compound (165)	232
6.3.16.	Fluorescence spectra of compound (166)	233
6.3.17.	Fluorescence spectra of compound (169)	233

6.3.18.	Fluorescence spectra of compound (170)	234
6.3.19.	Fluorescence spectra of compound (181)	234
6.3.20.	Fluorescence spectra of compound (183)	235
6.3.21.	Fluorescence spectra of compound (187)	235
6.3.22.	Fluorescence spectra of compound (189)	236
6.3.23.	Fluorescence spectra of compound (191)	236
6.3.24.	Fluorescence spectra of compound (195)	237
6.3.25.	Fluorescence spectra of compound (196)	237
6.3.26.	Fluorescence spectra of compound (198)	238

List of Schemes

Scheme 1: Commercial synthesis of 5-fluorouracil.....	2
Scheme 2. Development of Ezetimibe 4 by optimization of the lead.....	4
Scheme 3. Discovery of the COX 2 inhibitor Celecoxib 6 by replacing the a fluorine group with methyl group which is reduces the very long half-life to an acceptable level.	4
Scheme 4. Syntheses of trifluridine.	8
Scheme 5. synthesis of vinflunine.	9
Scheme 6. Synthesis of fulvestrant	9
Scheme 7. Synthesis of dustasteride	10
Scheme 8. Synthesis of benzimidazole from ortho-phenylene diamine	13
Scheme 9. Synthesis of benzotriazole.....	17
Scheme 10. Mechanism of nucleophilic substitution reaction.....	19
Scheme 11. Examples of S _N Ar reactions of hexafluorobenzene	20
Scheme 12. Reaction of hexafluorobenzene with methanethiolate	21
Scheme 13. Reaction of hexafluorobenzene with 2-bromophenol	21
Scheme 14. Addition of second nucleophilic substituent to pentafluorobenzene derivative	21
Scheme 15. Examples where a second nucleophilic substituent attaches to 1,2,3,4,5-pentafluoro-6-(trifluoromethyl)benzene	22
Scheme 16. S _N Ar reaction of pentafluorobenzaldehyde with dimethyl amine.....	24
Scheme 17. Reaction of <i>ortho</i> -dipyrrol-3-ylbenzene and hexafluorobenzene	24
Scheme 18. General reaction of pentafluoropyridine with difunctional nucleophiles	25
Scheme 19. S _N Ar reactions of pentafluoropyridine	26
Scheme 20. Di- and tri-substitution reactions of pentafluoropyridine	27
Scheme 21. Reaction of pentafluoropyridine with 2-iminopiperidine	27
Scheme 22. Reaction of pentafluoropyridine with acetamidine	28
Scheme 23. Smiles reaction in lithiation of 4-(2-bromophenoxy)tetrafluoropyridine	29
Scheme 24. Cyclization of thioether(93) with n-BuLi.....	29
Scheme 25. Reaction of pentafluoropyridine with imidazole.....	47
Scheme 26. Reaction of pentafluoropyridine with benzimidazole	48
Scheme 27. Reaction of compound (109) with benzimidazole	49
Scheme 28. Reaction of pentafluoropyridine with 1,2,3-triazole	51
Scheme 29. Reaction of pentafluoropyridine with benzotriazole.....	52
Scheme 30. Reaction of pentafluoropyridine with carbazole	52

Scheme 31. Reaction of the 2-bromophenol with compound (109)	54
Scheme 32. Reaction of the 2-aminothiophenol with compound (109)	55
Scheme 33. Reaction of 2-aminobenzenethiol with 4-nitrobenzoyl chloride	56
Scheme 34. Reaction of 2-boromothiophenol with compound (109).....	58
Scheme 35. Reaction of the glyoxalin with ammonium acetate	59
Scheme 36. Reaction of adipoyl chloride with aminoacetaldehyde dimethyl acetal.....	60
Scheme 37. Reaction of adipoyl chloride with aminoacetaldehyde methyl ester.....	61
Scheme 38. Reaction of adiponitrile with aminoacetaldehyde dimethyl acetal	62
Scheme 39. Synthesis of bis-imidate to form linked imidazole and benzimidazoles (132) and (134)	64
Scheme 40. Reaction of the pentafluoropyridine with 1H,1H-2,2'-biimidazole.....	67
Scheme 41. Reaction of the pentafluoropyridine with 1H,1H-2,2'-biimidazole.....	69
Scheme 42. Reaction of pentafluorobenzaldehyde with 1H,1H-2,2'-biimidazole.....	70
Scheme 43. Reaction of the pentafluoropyridine with bis-benzimidazole (134).....	71
Scheme 44. Reaction of the pentafluoropyridine with bis-benzimidazole (134).....	72
Scheme 45. Reaction of pentafluorobenzaldehyde with bis-benzimidazole (134).....	73
Scheme 46. Reaction of compound (134) with methyl pentafluorobenzoate.....	73
Scheme 47. Reaction of pentafluorobenzoylchloride and 2,2-(ethylenedioxy)bis(ethylamine).....	74
Scheme 48. Reaction of benzimidazole with fluorinated bis-linked scaffold (151).....	76
Scheme 49. Attempted reaction of carbazole with fluorinated bis-linked scaffold (151)	77
Scheme 50. Reaction of 2-mercaptobenzimidazole with fluorinated bis-linked scaffold (151).....	79
Scheme 51. Reaction of imidazole with fluorinated bis-linked scaffold (151)	80
Scheme 52. Reaction of indole with fluorinated bis-linked binding scaffold (151).....	81
Scheme 53. reaction of benzotriazole with fluorinated bis-intercalator scaffold (159).....	83
Scheme 54. reaction of 1,2,4 triazole with fluorinated bis-intercalator scaffold (151)	84
Scheme 55. Reaction of compound (109) with 2,2'-(ethylenedioxy)bis(ethylamine).....	85
Scheme 56. Reaction of compound (148) with hydrazine	91
Scheme 57. Reaction of compound (148) with 2-aminopyridine	92
Scheme 58. Reaction of ester compound (148) with acetamidine hydrochloride	93
Scheme 59. Reaction of the compound (138) with cysteine.....	95
Scheme 60. Reaction of the compound (143) with cysteine	96
Scheme 61. Reaction of compound (143) with 2,2-(ethylenedioxy)bis(ethylamine).....	97
Scheme 62. Reaction of compound (143) with 2-(2-aminoethoxy)ethylamine.....	99

Scheme 63. reaction of perfluoro bis-benzimidazole derivative (143) with hexamethylenediamine	100
Scheme 64. Reaction of compound (143) with ethylenediamine	101
Scheme 65. Reaction of compound (188) with 2-(2-aminoethoxy)ethanol	102
Scheme 66. Reaction of compound (143) with (\pm)-3-amino-1,2-propanediol	104
Scheme 67. Reaction of compound (143) with ethanolamine	105
Scheme 68. Reaction of pentafluoropyridine with 2-mercaptobenzimidazole	106
Scheme 69. Reaction of scaffold (194) with ethanolamine	106
Scheme 70. Reaction of scaffold (194) with ethylenediamine	107
Scheme 71. Reaction of scaffold (194) with morpholine	108
Scheme 72. Reaction of morpholine with tethered compound (163)	109
Scheme 73. Reaction of compound (109) with 3,6-dioxa-1,8-octanedithiol	111

List of figures

Figure 1. Effect of pKa value on the receptor binding and bioavailability for a set of 5HT1D agonists.	6
Figure 2. Fundamental heterocyclic rings.....	11
Figure 3. Some clinical imidazole-based anticancer drugs.....	12
Figure 4. Benzimidazole-based structures drugs	14
Figure 5. Pair of triazole isomers.....	15
Figure 6. Examples of antitumor triazole-base compounds in vitro.....	16
Figure 7. Examples of clinical antitumor BTA-based compounds.....	18
Figure 8. DNA double helix structure.....	31
Figure 8a. DNA base paire structure which bind together by hydrogen binding.....	31
Figure 9. (A) Cisplatin covalently bonded to DNA. B. (a) Modes of binding of cisplatin to guanine (G) and adenine (A); (b) 1,2-Intrastrand GpG (structure a), 1,2-intrastrand	32
Figure 10. B-DNA conformation, with the main structural dimensions.....	33
Figure 11. A) Minor groove filled with two drug molecules of diimidazole lexitropsin. 18 B) major groove binding of DMAADD molecule.	34
Figure 12. Netropsin is an example of a polypyrrole which bind to A/T-rich sites, and acts as potent inhibitor of Werner and Bloom helicases.	35
Figure 13. Hoechst 33258 (pibenzimol) is an example of a bis-(benzimidazole) which binds to AT-sites, and acts as potent cytotoxic drug by inhibition of topoisomerase and DNA helicase.....	35
Figure 14. SN 6999 is an example of bis-quaternary ammonium heterocycles which bind to AT tracts with at least 4 base pairs, related to polyamidines, and causes significant distortion of the DNA structure as well as inhibition of DNA and RNA polymerases.	35
Figure 15. Structure of 1R-Chl which binds to a specific sequence of DNA and acts as inhibitor of cell proliferation in different cancer cell lines with no apparent cytotoxicity.	36
Figure 16. Intercalation of a planar aromatic molecule in the DNA base pairs by hydrophobic interaction and van der Waals forces.	37
Figure 17. Example of DNA-intercalating agents	37
Figure 18. Emission spectra of EB bound to CT-DNA in the presence of free Ni complex [Ni ₂ (L) ₂ (NO ₃) ₂] (a) Fluorescence quenching curves of EB bound to CT-DNA Ni complex (b). (Plots of I ₀ /I vs. [Compound])	39

Figure 19. Vapour diffusion crystallization methods. a) Sitting drop, b) hanging drop, c) sandwich drop.	41
Figure 20. Oncogene activation of the ERK MAPK cascade.	42
Figure 21. Protein Kinase Inhibitors in the clinic and in development	44
Figure 22. X-ray crystal structure of compound (109) which crystallises with one molecule of water with hydrogen bonds to the N-9 atoms of two benzimidazole rings.	48
Figure 23. Crystal structure of compound (110).....	50
Figure 24. Crystal structure of compound (110).....	51
Figure 25. Crystal structure of compound (114).....	53
Figure 26. Crystal structure of compound (126).....	58
Figure 27. ¹ H NMR (400 MHz, DMSO-d ₆) spectrum of compound (132)	65
Figure 28. ¹ H NMR (400 MHz, methanol-d ₄) spectrum of compound (132).....	66
Figure 29. Crystal structure of compound (134).....	66
Figure 30. Crystal structure of compound (134).....	68
Figure 31. Crystal structure of compound (151).....	75
Figure 32. Crystal structure of compound (152).....	76
Figure 33. X-ray crystal structure of (181 ·2½·H ₂ O) showing the 24-membered macrocycle with 2½ hydrogen bonded water molecules. The molecule lies on a 2-fold axis. O(3) and O(3A) are each ¼ occupied.	97
Figure 34. X-ray crystal structure of (183) showing the 21-membered macrocycle with a hydrogen-bonded ethanol solvate molecule.	99
Figure 35. Absorption spectra of 1 x 10 ⁻⁵ M ACTD in absence (a) and presence of 9.6 µM (b), 18 µM (c), 27 µM (d), 35 µM (e), 43 µM (f) and 50 µM (g) of DNA.	113
Figure 36. Absorption spectra of 1 x 10 ⁻⁵ M of naproxen in absence (a) and presence of 9.6 µM (b), 18 µM (c), 27 µM (d), 35 µM (e), 43 µM (f) and 50 µM (g) DNA.....	114
Figure 37. UV absorption of synthesised compounds with different concentrations of DNA. Each bar in this graph represents the binding constant of different synthesised compounds.	116
Figure 38. Emission spectra of EB 1 x 10 ⁻⁶ M in the absence of DNA and b) Emission spectra in presence of DNA 3.17 x 10 ⁻⁵ M.....	118
Figure 39. Emission spectra of SS-DNA-EB in tris-HCl buffer on titration of ACTD.....	118
Figure 40. Emission spectra of SS-DNA-EB in tris-HCl buffer on titration of naproxen.....	119
Figure 41. EB displacement assay of synthesis compound. Each bar in this graph represents binding constant of different synthesised compounds. ACTD and naproxen were used as references.....	120

Figure 42. Effect of studied compounds on the cell cycle of MCF7 and K562 cells treated for 24 h
..... 122

Figure 43. Fluorimetric caspase activity assay. K562 cells treated with studied compounds for 24 h
were lysed and the activities of caspases were measured using the fluorogenic substrate Ac-DEVD-
AMC and normalised to untreated control..... 123

List of tables

Table 1. Typical S _N Ar reactions of pentafluoroaniline, pentafluoro-N-methylaniline and pentafluoro-N,N-dimethyl aniline.	23
Table 2. Different reaction conditions of compound (109) with benzimidazole.....	49
Table 3. different reaction condition of cyclization of compound (132).....	60
Table 4. different reaction conditions attempted for the formation of compound (135).	62
Table 5. Different reaction conditions attempted for the of carbazole with fluorinated bis-linked scaffold (151).....	77
Table 6. different reaction condition of 2-mercaptobenzimidazole with fluorinated bis-linked scaffold (151).....	78
Table 7. Different reaction conditions for the attempted reaction of indole with fluorinated bis-linked scaffold (151).....	81
Table 8. Different reaction conditions for the attempted reaction of benzotriazole with fluorinated bis-linked scaffold (151).....	82
Table 9. Different methods for synthesising target compound (163).....	85
Table 10. Reaction of different perfluoropyridine derivatives with 2,2'-(ethylenedioxy)bis(ethylamine).....	86
Table 11. Reaction of different perfluoropyridine derivatives with 2-(2-aminoethoxy) ethylamine ..	88
Table 12. Different condition attempted for synthesising target compound (172).....	91
Table 13. Different condition attempted for synthesising target compound (174).....	92
Table 14. Different condition for synthesising target compound (176).....	94
Table 15. Different reaction conditions for compound (138) with cysteine.....	95
Table 16. Different reaction conditions for compound (143) with (±)-3-amino-1,2-propanediol.....	103
Table 17. Different reaction conditions for compound (109) with 3,6-dioxa-1,8-octanedithiol	110
Table 18. Changing absorption by synthesised compound and DNA interaction	115
Table 19. Cytotoxicity of fluoroarylbenzimidazole derivatives	121
Table 20. Cytotoxicity of lead derivatives.....	122
Table 21. Antimicrobial activity of some fluorinated, synthesized compounds.....	124

1. Introduction

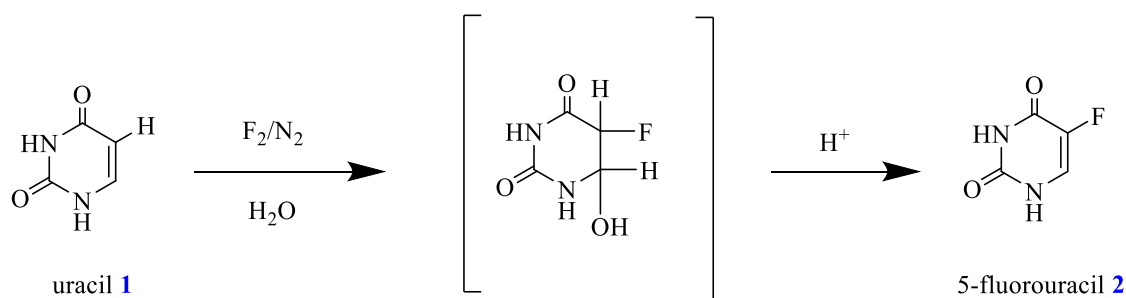
Heterocyclic compounds are the largest of the traditional divisions of organic chemistry and are of huge importance biologically and industrially. For more than one century heterocyclic chemistry has been the largest area for research in organic chemistry. Heterocycles have been used in the development of biologically active compounds, and also in the understanding of living processes, and in improving the quality of life. Large numbers of drugs such as morphine, atropine, procaine, codeine, and reserpine are heterocycles.^{1,2} Also many synthetic drugs such as diazepam, chlorpromazine, isoniazid, metronidazole, azidothymidine are heterocycles due to their useful solubility profile and their rigid structures which can bind to a broad range of receptors for valuable biological activity.^{3,4} Therefore heterocyclic chemistry is very important in the pharmaceutical industry for the synthesis of new drugs including antibacterial, antifungal, antimycobacterial, anti-inflammatory and especially anti-cancer agents because cancer is a leading cause of premature deaths in the world. In cancer, abnormal cells divide rapidly without control and are able to invade and destroy healthy tissues.^{1,5} These uncontrolled, unregulated cells which divide rapidly and grow abnormally produce malignant tumours which affect and invade nearby parts of the body leading to human death. It has been estimated that in the United States over 1 million cases of cancer are reported per year and it is expected that by the year 2017 cancer-related deaths will reach 12 million world-wide.¹ Therefore in recent years, a wide range of research has been carried out in the field of anti-cancer drug development.¹ On the other, hand fluorine use in medicinal chemistry has exploded over recent decades and significant improvement in pharmaceutical and biological activity of drugs containing fluorine has been shown. Therefore fluorination of a heterocyclic compound or combination of heterocycles with fluorinated arenes is a major concern in drug design and discovery, and is the main focus of this thesis.

1.1. Fluorine in medicinal chemistry

Fluorinated compounds have shown important improvement of biological activity of pharmaceutical compounds and drugs in medicinal chemistry. The fundamental properties of fluorine impart significant improvement on the biological activity of the fluorinated molecules. Therefore many fluorinated analogues of natural compounds have been synthesised and investigated due to the increase in understanding of the impact of fluorination on the biological properties of a molecule. This has supported the design and synthesis of more active and selective pharmaceutical agents

during the last 15 years, and development of synthetic methodologies in organic fluorine chemistry. There are more than 150 fluorinated compounds among those marketed pharmaceutical drugs in the world which is a huge number compared with other halogen-containing pharmaceuticals. Organochlorine and -bromine compounds are far more abundant as natural compounds.⁶

As a good example of the effect of a fluorine atom modifying the activity of the parent compound is introduction of fluorine into quinolone derivatives which led to the first fluoroquinolone, (norfloxacin) that is a broad-spectrum antibiotic. Replacing a CH bond by a CF bond improves metabolic stability. Also replacement of hydrogen with fluorine in uracil **1** gives 5-fluorouracil **2** which shows potent antitumor activity (Scheme 1).^{6,7} The fluorinated version of the molecule binds irreversibly to the active site of thymidylate synthetase preventing thymine biosynthesis in tumour cells.



Scheme 1: Commercial synthesis of 5-fluorouracil.

1.1.1. Physical characteristics of fluorine

Among all elements fluorine has the highest electronegativity value (EN) of 4 (on the Pauling scale) with very low polarizability and very low bond dissociation energy (155 kJ/mol).⁸

The low polarizability effect of fluorine and the three non-bonding electron pairs are important physical characteristics of biological activity of fluorinated compounds.^{6, 9, 10}

The high electronegativity of fluorine causes it to attract electrons more powerfully than any other element and it is never found as the free element in the natural environment. Moreover, the bonding between the ligand and the target in the active centre of a protein molecule possessing fluorophobic and fluorophilic areas can be improved due to the electronegativity of the fluorine atom which causes particular dipole-type interactions. It is necessary to mention that in organic compounds, the fluorine

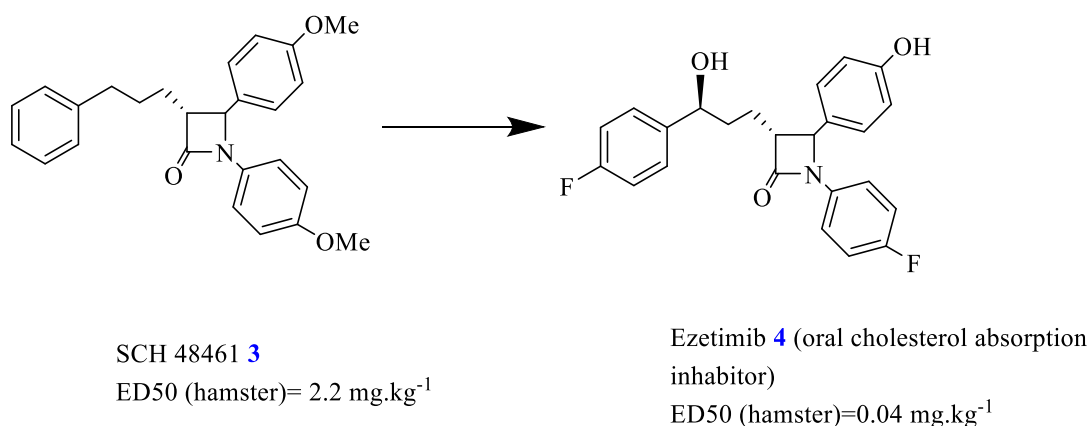
atoms can accept hydrogen bonds only in the absence of better acceptors, such as oxygen or nitrogen, as fluorine is more electronegative and not able to compete with stronger hydrogen-bond acceptors.¹¹ The fluorine atom has the second smallest van der Waals radius, (1.47 Å) which is sited between hydrogen (1.20 Å)¹² and oxygen (1.52 Å)¹¹² and allows fluorine to behave like a hydroxyl group and contribute in hydrogen bonding interactions.¹⁰ Also the C-F bond has greater strength than C-H bond which results in high chemical stability of fluorinated compounds.^{10,13}

Furthermore, fluorine containing substituents (especially perfluorinated groups, like CF₃, C₆F₅, OCF₃) can provide significant steric volume distressing the arrangement of the parent molecule and its isomers, conformations or transition states. Therefore it affects chemical properties such as solubility, acidity, basicity and metabolic stability of molecules. In addition the incorporation of fluorine into organic molecules often leads to increasing lipophilicity thereby enhancing their affinity for natural receptors.¹¹

In nuclear magnetic resonance spectroscopy, ¹⁹F deserves special attention due to its desirable characteristics (nuclear spin ½, relatively narrow lines, high sensitivity, short longitudinal relaxation time, and 100% abundance). Therefore, ¹⁹F NMR spectroscopy is ideally suited to following the fate of fluorinated drug molecules. The selective detection of molecules containing fluorine reduces the background and interfering signals. In addition, this method is very sensitive to changes in the environment due to larger chemical shifts than ¹H NMR. ¹⁹F NMR can be used in laboratory research; for example in studying the mechanism of interaction with receptors in tumour and normal tissue localization of anti-cancer drugs. Moreover, ¹⁹F NMR spectroscopy can be useful as a tool for therapeutic monitoring of fluoropyrimidine analogues and their prodrugs. ¹⁹F NMR spectroscopy studies of the metabolism of the successful fluoropyrimidine anti-cancer drugs, such as fluorouracil, and prodrug capecitabine, as well as antifungal agents have been carried out.^{9,11}

1.1.2. Improving Metabolic Stability with Fluorine

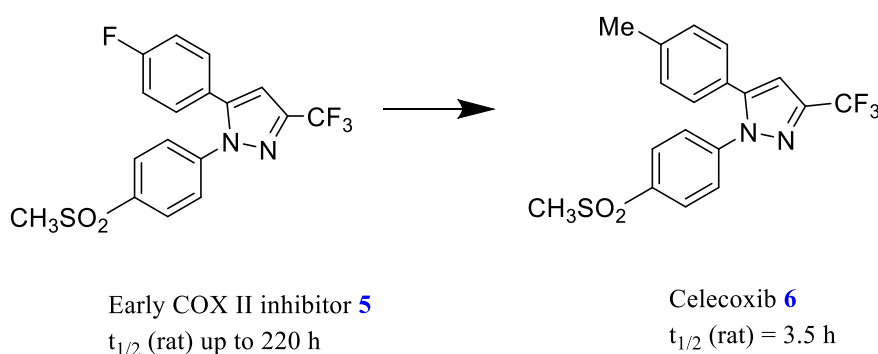
One of the problems in many drug discovery projects is low metabolic stability because lipophilic compounds are likely to be oxidized by liver enzymes, especially cytochrome P450. There are different approaches to minimise this problem such as increasing the polarity of the molecule. Another strategy is to introduce a fluorine substituent to block the metabolically labile site and optimally the fluorine atom will not harm the bonding to the target protein. Certainly, this method is commonly employed and results in many successful compounds. The discovery of the cholesterol-absorption inhibitor Ezetimibe **4** (Scheme 2) is counted as one of the nicest examples of this strategy.^{14,15,16}



Scheme 2. Development of Ezetimibe 4 by optimization of the lead.

As seen in (Scheme 2), the target compound SCH58235 (Ezetimibe) was afforded by introducing two fluorine substituents to starting compound SCH48461, which is a very effective compound that was recently approved by the FDA. By substitution of hydrogen by fluorine the phenyl ring does not oxidize to a phenol, and dealkylation of the methoxy group is prevented by replacement of OMe by F on the N-phenyl substituent.

Another significant example indicating the strong effect of fluorine on metabolic stability is the development of cyclo-oxygenase 2 (COX-2), inhibitor **4** (Scheme 3). In this case, fluorine was replaced by a metabolically labile methyl group to reduce the very long biological half-life to a more acceptable level by really decreasing the metabolic stability of the lead compound. Interestingly, there are also a few cases known for which the introduction of a fluorine substituent does not prevent oxidation at that site. This phenomenon is observed in particular for phenyl rings with a nitrogen substituent in the para position to the fluorine substituent.^{17,18}



Scheme 3. Discovery of the COX 2 inhibitor Celecoxib 6 by replacing the a fluorine group with methyl group which is reduces the very long half-life to an acceptable level.^{14,17,18}

1.1.3. The effect of fluorine on the pKa and bioavailability

Fluorine has a very strong effect on the basicity or acidity (pKa) of neighbouring functional groups. pKa shift changing will be depend to the position of the fluorine substituent relative to the acidic or basic group in the molecule. For example, the pKa's of ethylamine and its β -fluorinated analogues decrease in almost linear fashion by introduction of fluorine, $\text{CH}_3\text{CH}_2\text{NH}_2 = 10.7$, $\text{CH}_2\text{FCH}_2\text{NH}_2 = 8.97$, $\text{CHF}_2\text{CH}_2\text{NH}_2 = 7.52$, and $\text{CF}_3\text{CH}_2\text{NH}_2 = 5.7$. Similarly, the acidities or pKa's of acetic acid and its α -fluorinated analogues increase with $\text{CH}_3\text{COOH} = 4.76$, $\text{CH}_2\text{FCOOH} = 2.59$, $\text{CHF}_2\text{COOH} = 1.24$ and $\text{CF}_3\text{COOH} = 0.23$ ^{14,19}

Also, the pKa value of the piperidine ring decreases about 2 log units by substitution of fluorine at the position 3 and 4. A change in the pKa has a result on both the pharmacokinetic properties of the molecule and its binding affinity. For example, for binding within a certain leads series a strongly basic group is essential, however simultaneously this basic group may cause low bioavailability of compounds as a result of the partial ability of a strong basic group to pass through membranes. Therefore a drug discovery project team should be trying to finding an optimum between these conflicting effects. This challenge is well emphasised by the work of van Niel et al.²⁰ on the development of novel fluorinated indole derivatives as selective 5HT1D receptor ligands.

As seen in figure 1, the pKa values of the compounds significantly decrease by amalgamation of fluorine. This reduction of basicity was shown potent effect on oral absorption or bioavailability but associated weakening of the affinity to the receptor.^{20,21,22}

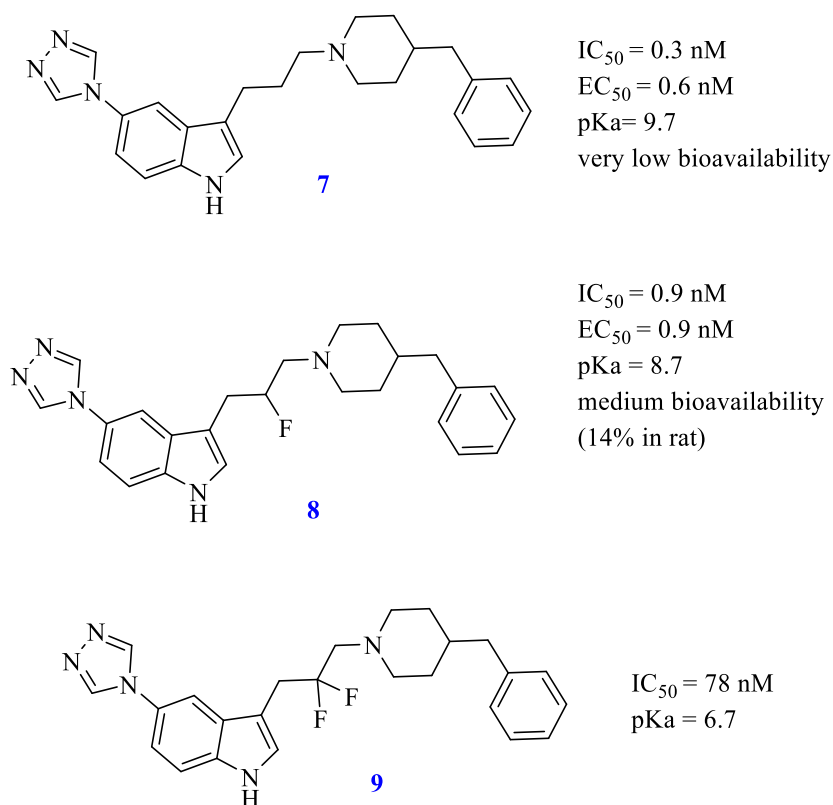


Figure 1. Effect of pKa value on the receptor binding and bioavailability for a set of 5HT1D agonists.²⁰

The nonfluorinated parent compound **7** has very low bioavailability but it is a very strong receptor binding ligand. The monofluorinated compound **8** has a lower pKa which is still well-matched with the requirements for receptor binding, but significantly increased bioavailability of compound. The difluoro compound **9** is basic enough to achieve high binding affinity for the 5HT1D receptor due to low pKa value of 6.7.

1.1.4. The effect of fluorine on molecular lipophilicity

One of the important molecular parameters in medicinal chemistry is lipophilicity. Naturally the ligand needs appropriate lipophilicity for good binding affinity to the target protein but too high lipophilicity will reduce solubility and causes other undesirable properties for a compound.¹⁴ Thus, the equilibrium between required lipophilicity and a certain minimal overall polarity of the molecule is another regular challenge for medicinal chemists. To improve the effect of fluorine on the lipophilicity of compound the hydrogen atom was replaced by fluorine atom in 293 pairs of molecules and log D values (logarithmic coefficient of the distribution of the compound between octanol and water at a given pH) was measured. The result indicated lipophilicity slightly increased

by substitution of hydrogen with fluorine.²³ Interestingly, in the compounds which are characterized by the presence of an oxygen atom close to the fluorine substitution show decreased lipophilicity. Possibility the fluorine polarizes the neighbouring oxygen atom causing stronger hydrogen bonds between the oxygen and neighbouring water molecules. Therefore the idea of H/F exchange should be used with care because it does not always increase lipophilicity, however in general an additional fluorine substituent will improve the binding affinity due to an increase in the lipophilicity of the molecule.^{14,23}

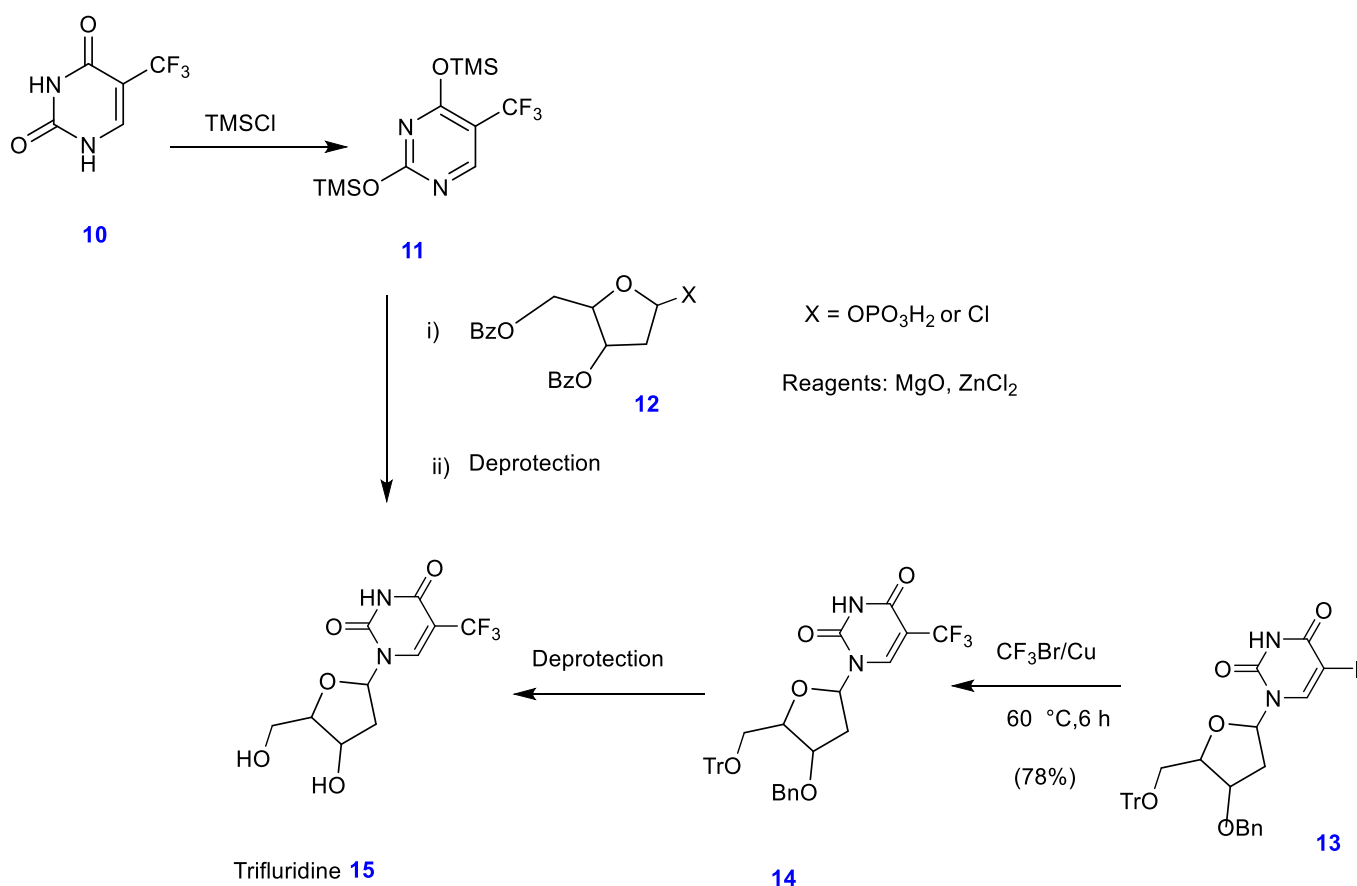
1.1.5. Fluorinated heterocyclic compounds based on natural products

In many therapeutic classes the presence of fluorinated drugs and drug candidates based on natural compounds, such as fluorocorticoid and fluorouracil derivatives are still used as major drugs for many clinical therapeutic classes, and recent research focuses on fluorinated nucleosides, alkaloids, macrolides, steroids, amino acids and prostaglandins. Most of the applications are found in anti-cancer, anti-viral and anti-infectious fields.^{6,24}

1.1.5.1. Nucleosides

Fluorinated analogues of nucleosides, such as trifluridine **15**, have been developed as anti-cancer and anti-infection drugs, due to their interaction either with DNA and RNA, or their effect on an enzymatic reaction. The main targeted enzymes by fluoronucleosides and fluoronucleobases are thymidylate synthesis, ribonucleotide diphosphate reductase (RDPR), DNA polymerases and viral reverse transcriptases.

For example thymidylate synthesis (TS) is one of the main enzymes for DNA synthesis effecting transformation of 2-deoxyuridine monophosphate into thymidine monophosphate, which trifluridine as anti-viral drug can inactivate by blocking release of the substrate and co-factor from the active site.^{6,24} Trifluridine **15** can be formed in two ways; it can be formed by trifluoromethylation of the protected idonucleosides **13** or by radical trifluoromethylation of uracil followed by enzymatic or chemical coupling with the protected deoxyribose **12** as seen in Scheme 4.⁶

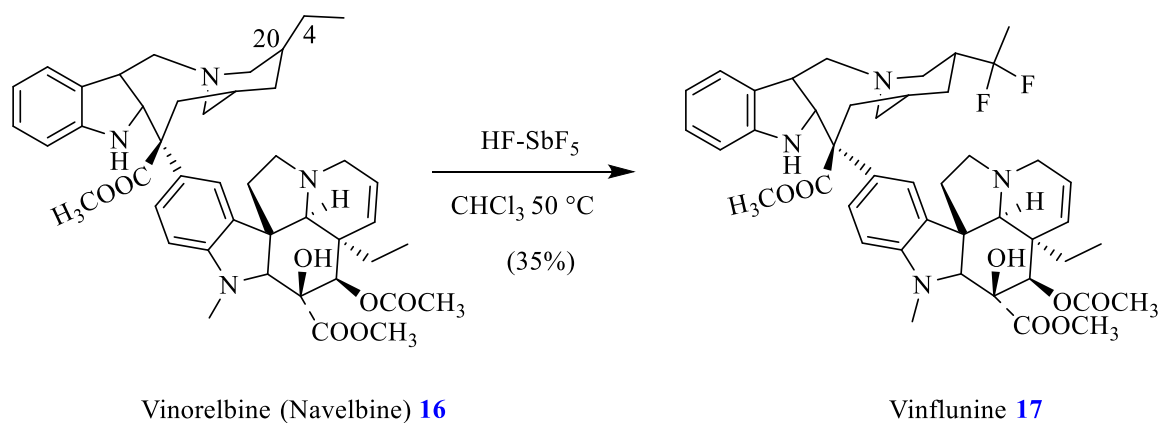


Scheme 4. Syntheses of trifluridine.

1.1.5.2. Alkaloids

Vinblastine and its analogue vinorelbine are anticancer drugs based Vinca indole dimer alkaloids which work by binding to tubulin and inhibiting polymerisation into microtubules. It is important to mention that second-generation vinca dimer alkaloids, (e.g. vinflumine) show a better therapeutic effect in cancer therapy and are more active than vinorelbine.^{25,6}

Vinflunine **17** is formed by fluorination of vinorelbine **16** in presence of super-acid media (HF-SbF_5) and trichloromethane (CHCl_3) which generated a super-electrophilic agent such as difluoromethylation to abstract hydrogen from protonated alkaloid. Difluorination extraordinarily takes place selectively at C-4 of the clavamine part (Scheme 5).⁶



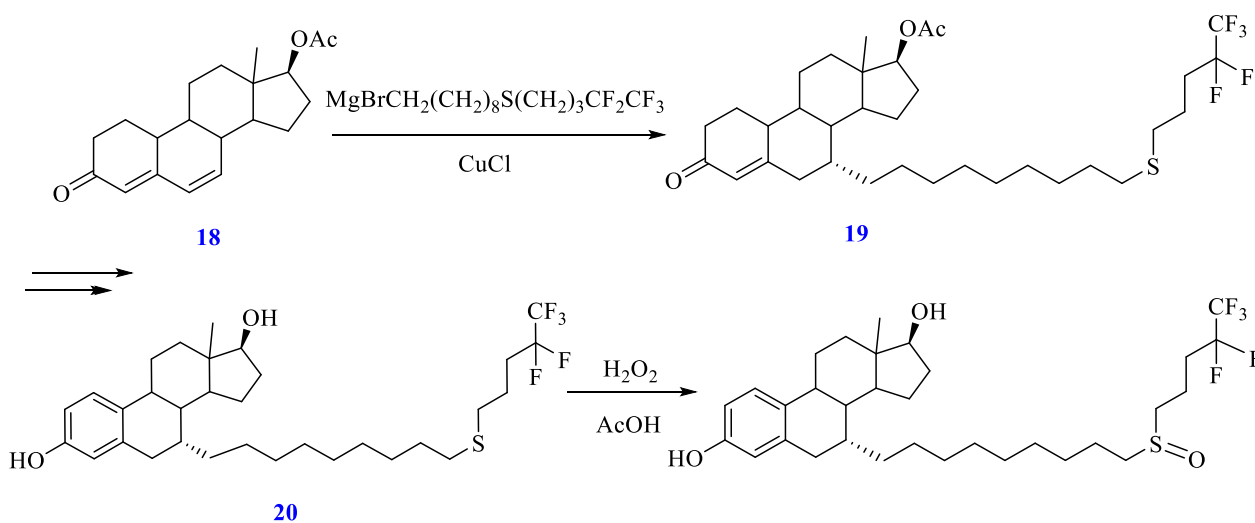
Scheme 5. Synthesis of vinflunine.⁶

1.1.5.3. Steroids

Pharmaceutical research in the fluorocorticoid field is now essentially devoted to the search for new formulation of registered drugs. Nevertheless, there has been recently a renewal of interest for steroids in medicinal chemistry. It mainly concerns selective ligands for steroid hormone receptors for the treatment of several hormonal disorders.

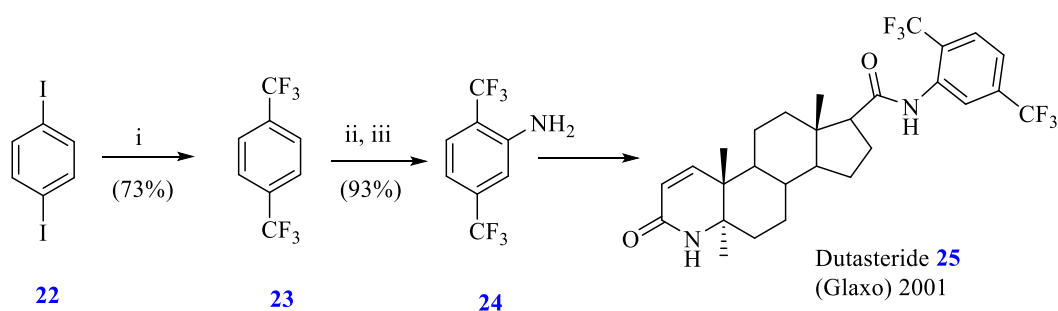
One of the most important drugs acting on steroid hormone receptors is Fulvestrant **21**, which works by binding to the oestrogen receptor in a competitive way with estradiol with similar affinity. Therefore fulvestrant can be used as a treatment for hormone-dependent breast cancer.^{6,26}

Fulvestrant **21** has been synthesised as shown in (Scheme 6), and contains a long-chain substituent with the terminal two carbons fluorinated.



Scheme 6. Synthesis of fulvestrant.⁶

Dutasteride is another fluorinated steroid drug which is a 4-azasteroid. It works by inhibition of type 1 and 2, 5α -reductases, enzymes which convert testosterone to dihydrotestosterone in the prostate. Therefore Dutasteride **25** can be used to treat the Benign Prostatic Hyperplasia (BPH). In the synthesis of Dutasteride **25** the fluorine containing starting compound 2,4-bis(trifluoromethyl)aniline **24** can be formed by trifluoromethylation of the corresponding di-iodobenzene **22**, followed by nitration and reduction (Scheme 7).⁶



i) CF_3COONa , CuI , NMP ; ii) HNO_3 , H_2SO_4 ; iii) H_2 , Ni , $i\text{PrOH}$

Scheme 7. Synthesis of dustasteride.⁶

1.2. Heterocyclic chemistry

The cyclic compounds in which the ring contains carbon plus one or more atoms of other elements are called heterocyclic compounds, and the non-carbon atoms are named as hetero atoms. The most common hetero atoms are nitrogen, oxygen and sulphur. Among heterocyclic compounds, those containing five to six atoms in the ring are generally the most important. Heterocyclic compounds are widely distributed in nature and they are mostly important due to extensive variety of physiological activity attributed to them.

Some of the significant compounds containing heterocyclic rings are antibiotics, amino acids, dyes, drugs, enzymes, the genetic material DNA, and so on. A few of the fundamental ring systems of the heterocyclic compounds which were used in this study are listed below (Figure 2).²⁷

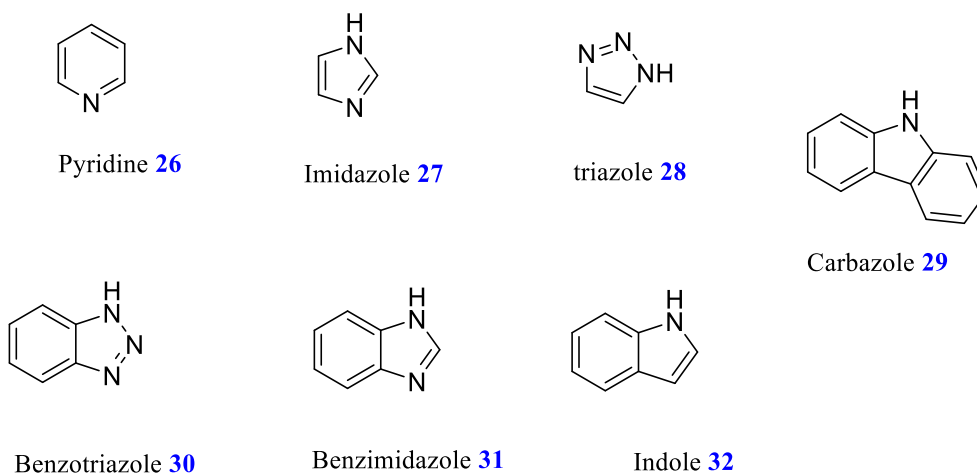


Figure 2. Fundamental heterocyclic rings.

1.2.1. Imidazole in medicinal chemistry

Imidazole is one of the heterocyclic compounds which is common and is very important in medicinal chemistry. Imidazole is a 5-membered planar ring containing two nitrogen atoms which is highly polar and therefore soluble in water and other polar solvents, due to its two nitrogen atoms easily leading to the formation of hydrogen bonds. It exists as two tautomers since the hydrogen can move and locate on either nitrogen atom. The imidazole contains a sextet of π -electrons, two electrons from the protonated nitrogen, and four from the remaining atoms in the ring therefore it is classified as an aromatic compound. Imidazole is amphoteric so it can act as an acid or a base.^{5,28,29}

Also, because of these special structural features of imidazole ring, its derivatives can freely bind with a range of enzymes and receptors in biological systems through hydrogen bonds, ion-dipole, π - π stacking, and van der Waals forces, thus showing broad bioactivity.^{5,30}

In fact, the imidazole ring is part of many natural compounds such as purine, histamine, histidine and nucleic acid.^{31,32} Mainly, imidazole-based compounds are very important in medicinal chemistry and encouraged medicinal chemists to synthesize novel imidazole containing chemotherapeutic agents such as anticancer (dacarbazine), antifungal (clotrimazole), antiparasitic (metronidazole), antihistaminic (cimetidine) and antihypertensive (losartan) drugs which have been widely used to treat various types of diseases with high therapeutic potency.^{33,34}

In terms of anti-cancer activity imidazole derivatives could delay DNA synthesis through weak interactions such as hydrogen bond or π - π stacking which stop cell growth or division.

Temporarily, imidazole could bind to protein molecules much easily compared with other heterocyclic rings. More importantly, incessant work has been done leading to synthesis newimidazole-based anticancer agents targeting various enzymes or receptors such as topoisomerases, microtubule, cytochrome P450 enzymes, rapidly accelerated fibrosarcoma (RAF) kinases and so on.⁵

So far, many imidazole derivatives as anticancer and antitumour drugs such as dacarbazine **33**, zoledronic acid **34** and azathioprine **35** have been widely used in the clinic (Figure 3).^{5,35,36,37}

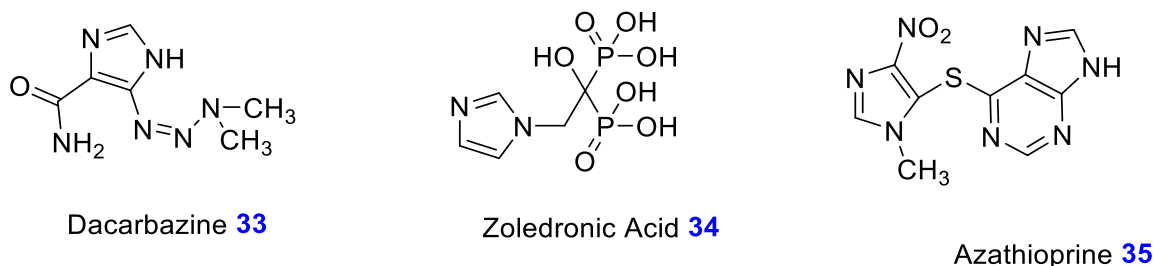


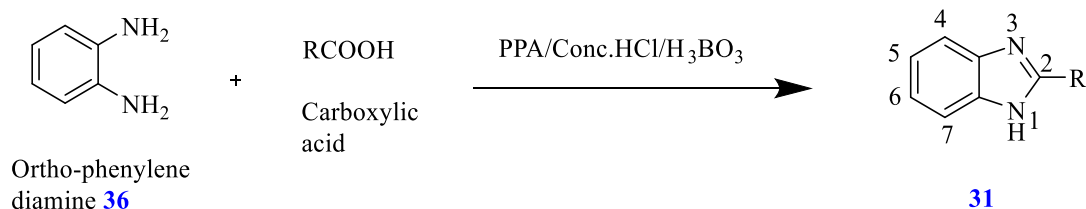
Figure 3. Some clinical imidazole-based anticancer drugs.⁵

1.2.2. Benzimidazole in medicinal chemistry

Benzimidazole is a heterocyclic aromatic organic compound which results from the formal fusion of benzene and imidazole. It is an essential pharmacophore and an advantaged or privileged structure in medicinal chemistry.^{38,39}

Benzimidazole is typically soluble in polar solvents and less soluble in non-polar ones due to the imide nitrogen. The solubility in non-polar solvents increases by introducing other non-polar substituents in various positions of the benzimidazole ring. On the other hand, by introducing a polar group into the molecule the solubility in polar solvents will be improved. Benzimidazoles are sufficiently acidic to be usually soluble in aqueous alkali. Also they are weakly basic. Benzimidazole is slightly less basic than imidazole and is usually soluble in dilute acids. Benzimidazole with unsubstituted NH groups, show fast prototropic tautomerism which leads to equilibrium mixtures of asymmetrically substituted compounds. benzimidazole ring is very stable and unaffected by strong acid such as concentrated sulfuric acid or hot hydrochloric acid in addition to alkalis. Is it fairly resistant to oxidation and reduction. A further characteristic of benzimidazoles is that they have the ability to form salts.³⁹⁻⁴¹

Benzimidazoles **31** are generally synthesised from the reaction of 1, 2-diaminobenzenes **36** with carbonyl-containing compounds (carboxylic acids) under tough dehydrating reaction conditions, using strong acids such as polyphosphoric acid (PPA), hydrochloric acid, or boric acid (Scheme 8).²⁷



Scheme 8. Synthesis of benzimidazole from ortho-phenylene diamine.²⁷

The benzimidazole nucleus is a vital core in many compounds acting at different targets to cause a range of pharmacological effects. However all seven positions in the benzimidazole nucleus can be substituted with different chemical units, but in the most of the biologically benzimidazole based compounds functional groups are located at the 1, 2, 5 or 6 positions. Therefore, the compounds might be mono-, di- or tri-substituted derivatives of the nucleus. Suitably substituted benzimidazole derivatives have established different therapeutic applications such as in antimicrobial³⁹ antiviral, antifungal, anticancer, antiulcer, antihypertensive and antihistaminics^{1, 29,42,43}.

The optimization of benzimidazole-based structures led to several drugs which are presently on the market.(Figure 4).²⁸

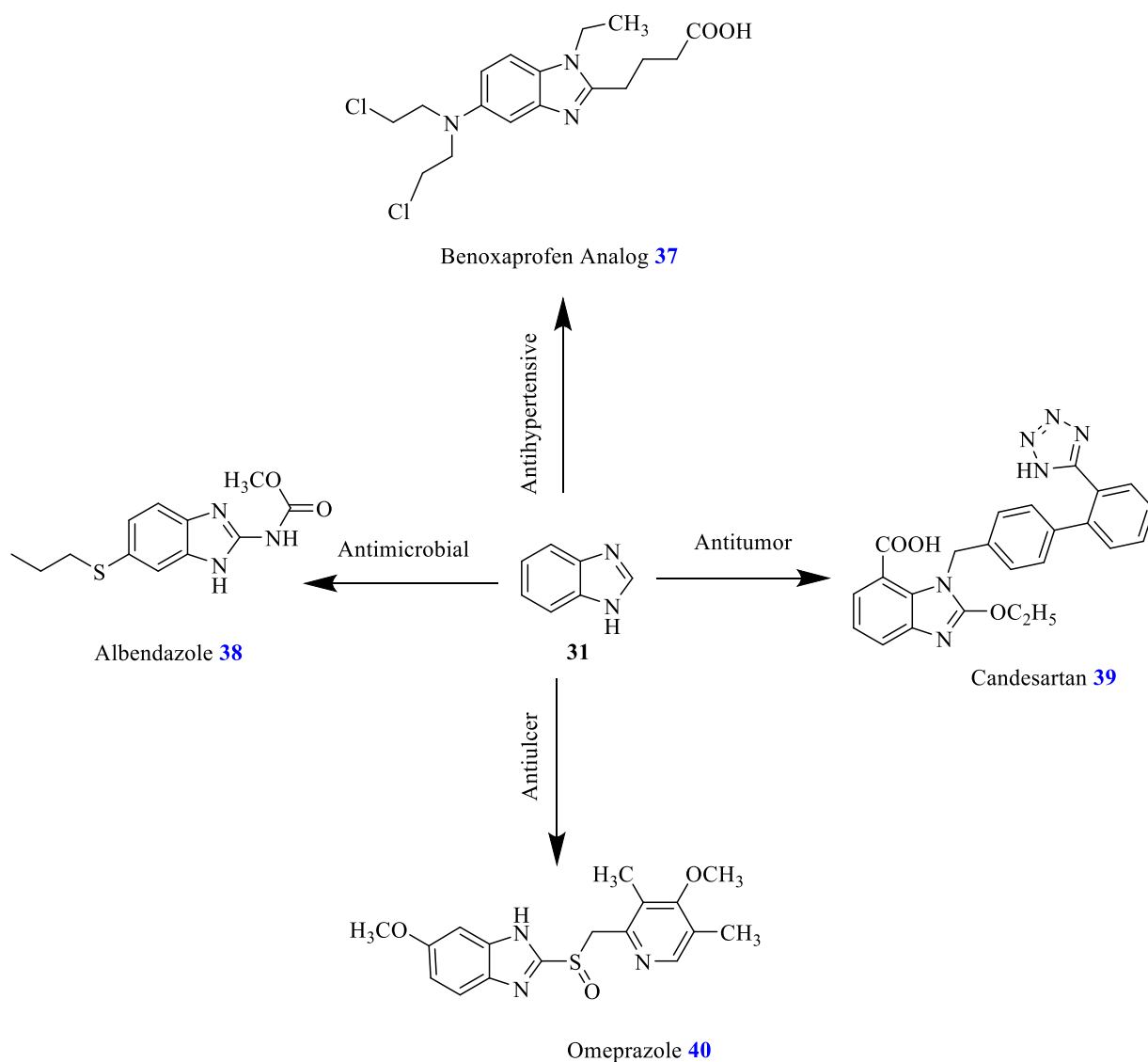


Figure 4. Benzimidazole-based structures drugs.²⁸

1.2.3. Triazole in medicinal chemistry

Triazole is one of the organic heterocyclic compounds consisting of a five-membered ring structure. It contains three nitrogen atoms and two carbon atoms. Triazole is pale yellow crystalline solid which is soluble in water and alcohol. It exists as a pair of isomeric compounds, 1,2,3-triazole **28** and 1,2,4-triazole **41** (Figure 5) depending on whether the carbon atoms are adjacent or not.^{43,44,45}

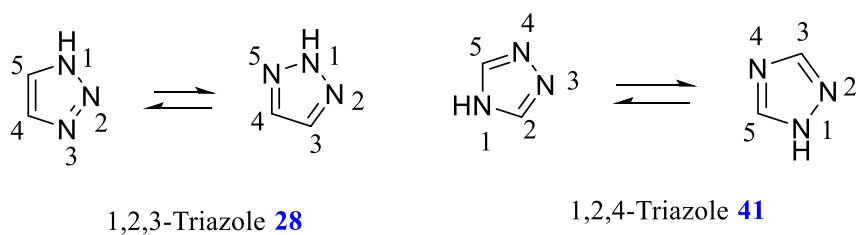
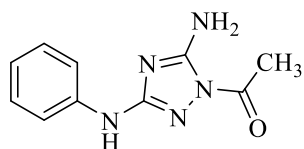


Figure 5. Pair of triazole isomers.

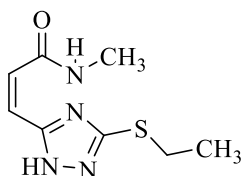
This unique structure of triazole allows its derivatives to freely bind with a range of receptors and enzymes in biological systems and to show an extensive spectrum of biological activity.⁴⁶⁻⁴⁸ Moreover, the triazole ring can be combined with different pharmacophore groups to create novel drug molecules as an attractive linker. Therefore it provides a useful and effective pathway to develop different bioactive molecules.⁴⁹⁻⁵¹

Triazole based compounds with pharmacological activity indicated some advantages such as low toxicity, high bioavailability, less multi-drug resistance, broad spectrum activity, better therapeutic effect, and fewer adverse effects. Therefore they have been regularly applied in the treatment of different types of disease including cancer.⁵²⁻⁵⁴ In general, triazole derivatives have various pharmacological activities such as antifungal, antihistaminic, antimicrobial, anti-inflammatory, and antineoplastic. in addition to anticancer activities which is a major target for medicinal chemists (Figure 6).^{43,55}



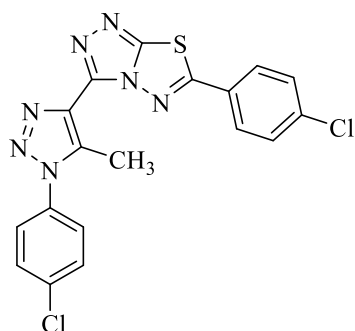
This compound indicated powerful and selective cyclin-dependent kinase CDK inhibitory activities and inhibited in vitro cellular propagation in different tumour cells.⁷⁸

1-(5-amino-3-(phenylamino)-1H-1,2,4-triazol-1-yl)ethan-1-one **42**



This compound showed clearly anti-proliferative effect in breast carcinoma cells in vitro with the less cytotoxicity against of normal cell ⁷⁹

(Z)-3-(3-(ethylthio)-1H-1,2,4-triazol-5-yl)-N-methylacrylamide **43**



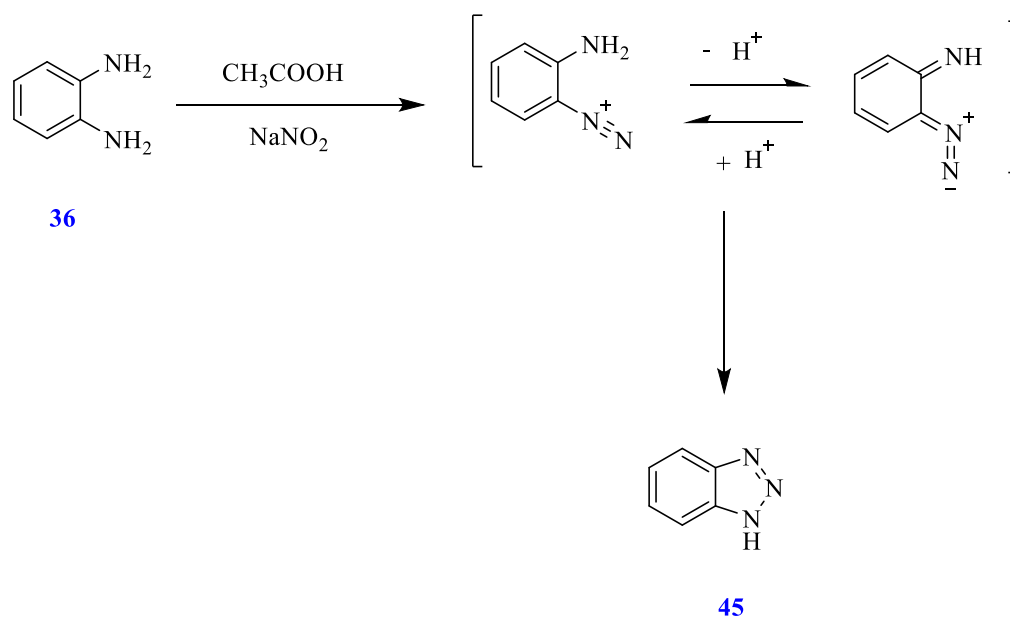
TDZ showed antitumor activity against of two different human cell line in vitro and in vivo it indicated inhibition of DNA replication ⁶⁵

6-(4-chlorophenyl)-3-(1-(4-chlorophenyl)-5-methyl-1H-1,2,3-triazol-4-yl)-[1,2,4]thiazolo[3,4-b][1,3,4]thiadiazole (TDZ) **44**

Figure 6. Examples of antitumor triazole-base compounds in vitro.⁴³

1.2.4. Benzotriazole in medicinal chemistry

Benzotriazole **45** is another of the important scaffolds found in many biologically active compounds and drugs. It is an inexpensive, non-toxic, highly stable, aromatic nitrogen heterocycle consisting of a benzene ring fused to a triazole. Benzotriazole can be produced by diazotization of one the amine groups in benzene-1,2-diamine **36** with sodium nitrite and an acid (often a carboxylic acid) (Scheme 9). The reaction is usually best conducted at lower temperature (5-10 °C) to avoid loss of nitrous acid or decomposition of the unstable diazonium intermediate.⁵⁶⁻⁵⁹



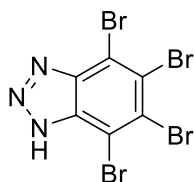
Scheme 9. Synthesis of benzotriazole.⁵⁹

Benzotriazole, because of its fused, more highly conjugated structure, can form stronger π - π stacking interactions compared to triazole. In addition, the three nitrogen atoms allow it to form coordination and hydrogen bonds easily. Therefore the benzotriazole-based compounds can bind to enzymes and receptors in biological systems more easily through different non-covalent binding modes which results in an extensive spectrum of biological activity. Moreover, benzotriazole can form BTA-containing metal complexes by binding the benzotriazole nucleus to different metal ions which could exert a double action mechanism to overcome drug resistance, due to both benzotriazole derivatives themselves and their supramolecular agent activity.⁶⁰ For the above reasons, the benzotriazole moiety has been regularly employed to design novel drug molecules.⁶¹⁻⁶³

Recently, medicinal chemists working on benzotriazole derivatives have reached great improvement. They have discovered a number of BTA-base compounds with effective pharmacological properties, low toxicity, few side effects, little multi-drug resistance, good water solubility, promising bioavailability, diversity of drug administration, as well as a broad bioactivity spectrum.⁶²⁻⁶⁴

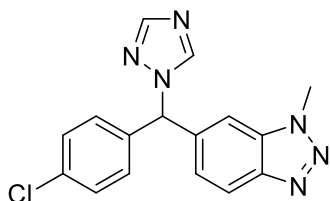
Generally, bioactive BTA-based compounds are being extremely investigated all over the world to treat different types of disease including cancers.

Some anticancer benzotriazole derivatives such as Vorozole and TBB have been in clinical use (Figure 7). The successful examination of these drug encourages continuation of work to make the new BTA-based anticancer compounds targeting different kinases or receptors.⁶⁵⁻⁶⁸



TBB has pro-apoptotic effect on a number of different tumor cell by inhibition of protein kinase CK2^{91,92}

4,5,6,7-Tetrabromobenzotriazole (TBB) **46**



Vorozole is potent and selective antineoplastic agent which causes reversible inhibition of cytochrome P450 aromatase^{93,91}

6-[(4-Chlorophenyl)(1,2,4-triazol-1-yl)methyl]-1-methylbenzotriazole (Vorozole) **47**

Figure 7. Examples of clinical antitumor BTA-based compounds.

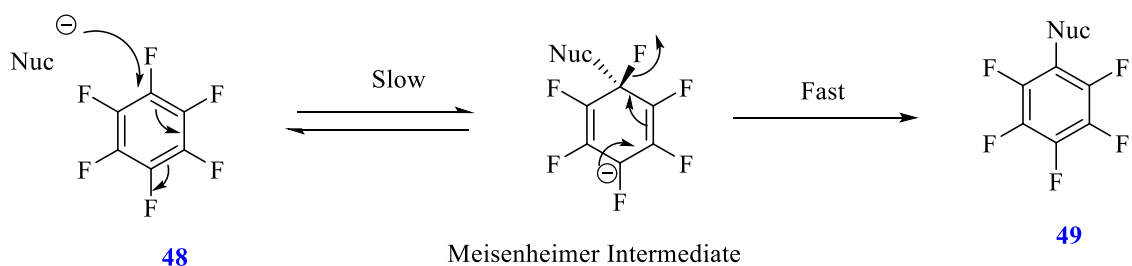
1.2.5. Reactions of Perfluorinated Arenes and Heteroarenes

Examining fluorinated arene and heteroarene systems for the chemical synthesis of a wide range of polyfunctional carbo- and hetero-cyclic derivatives, has been one of the early research programs that has been pursued in organofluorine chemistry since the 1960s. For synthesis of a wide range of highly functionalised heteroaromatic and ring fused polycyclic systems, perfluoroarenes such as pentafluoropyridine, and hexafluorobenzene can be used as core scaffolds.⁶⁹

Reaction of a perfluoroaromatic as an acceptor moiety with various nucleophiles as the donor moiety involves nucleophilic aromatic substitution (S_NAr) and occurs readily under usually mild conditions. The reaction can involve displacement of fluorine from highly fluorinated aromatic systems by carbon, nitrogen, oxygen and sulphur centred nucleophiles, due to the strong electron withdrawing effect of the fluorine substituents, rendering the compounds extremely sensitive towards nucleophilic attack.

The majority of reactions of perfluoroaromatic systems proceed by the two-step addition-elimination nucleophilic aromatic substitution (S_NAr) mechanism. The first step of the reaction involves the flouting of the aromaticity of the fluoroaromatic ring and creation of a tetrahedral intermediate (the

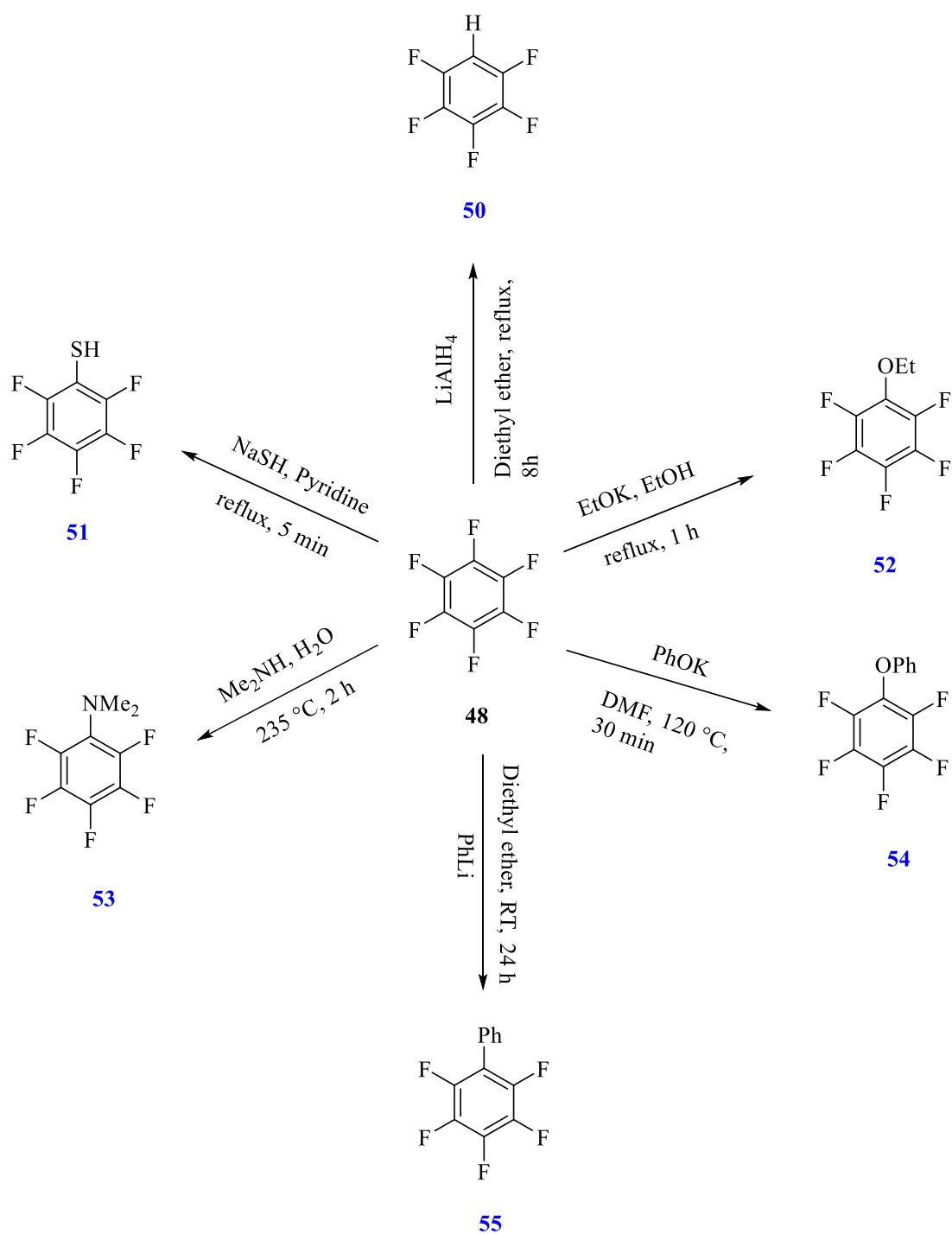
so-called Meisenheimer intermediate). The Meisenheimer intermediate usually breaks down quickly through the ejection of a fluoride ipso to the site of initial nucleophilic attack therefore aromaticity is recouped (Scheme 10).⁷⁰



Scheme 10. Mechanism of nucleophilic substitution reaction.⁷¹

Highly fluorinated systems are more receptive towards S_NAr reaction compared to chlorinated or brominated complements, because the rate of reaction depends on the electrophilicity of the aromatic ring and the electronic stabilisation of the Meisenheimer intermediate.

S_NAr reactions of hexafluorobenzene **48** are well documented and interesting. Relevant examples have been selected for more detailed discussion.⁷⁰

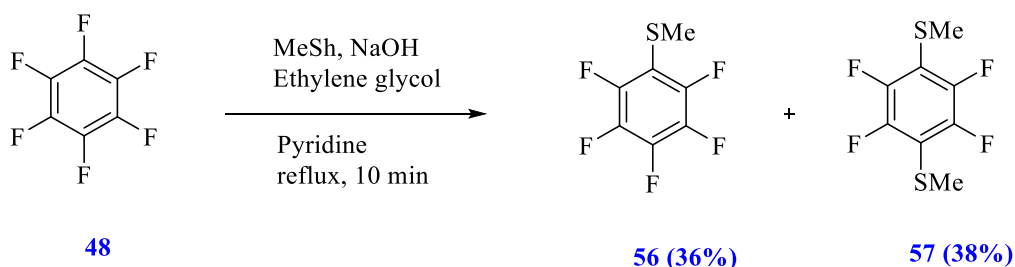


Scheme 11. Examples of $\text{S}_{\text{N}}\text{Ar}$ reactions of hexafluorobenzene.

As the examples shown in Scheme 11 these $\text{S}_{\text{N}}\text{Ar}$ reactions show how an extensive variety of substituted pentafluorobenzene derivatives may be formed in a single synthetic step.⁷⁰

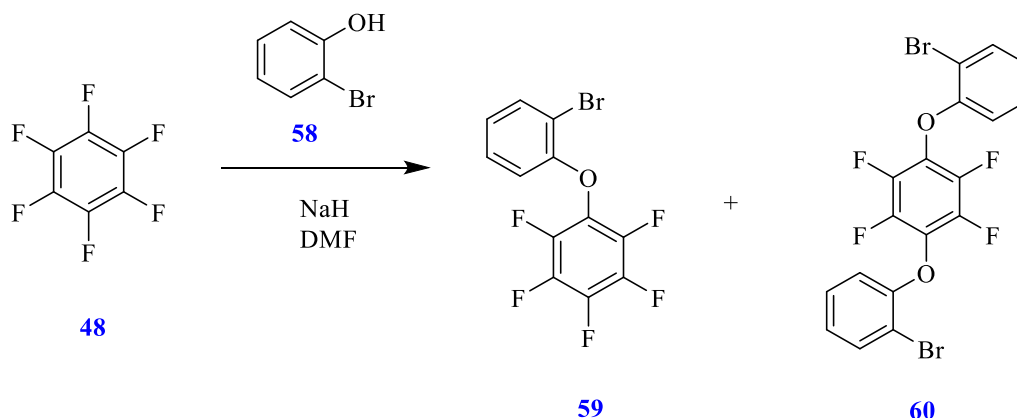
There is no selectivity matter regarding the first nucleophilic substitution due to the symmetrical structure of hexafluorobenzene **48**. Occasionally, some di-substituted product is isolated as well as the mono-substituted compound in $\text{S}_{\text{N}}\text{Ar}$ reactions of hexafluorobenzene **48** especially when the

added functional group is more activating than fluorine itself. For example, the reaction of sodium methanethiolate with an excess of hexafluorobenzene **48** which resulted in formation of mono- and di-substituted compounds **56** and **57** in approximately equal amounts from a single pot reaction (Scheme 12).⁷²



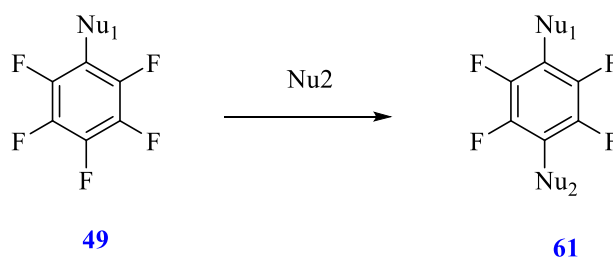
Scheme 12. Reaction of hexafluorobenzene **48 with methanethiolate.⁷²**

Also, the reaction of hexafluorobenzene **48** with 2-bromophenol **58** is another example of mono and di-substituted formation in single step of S_NAr reactions (Scheme 13).⁷³



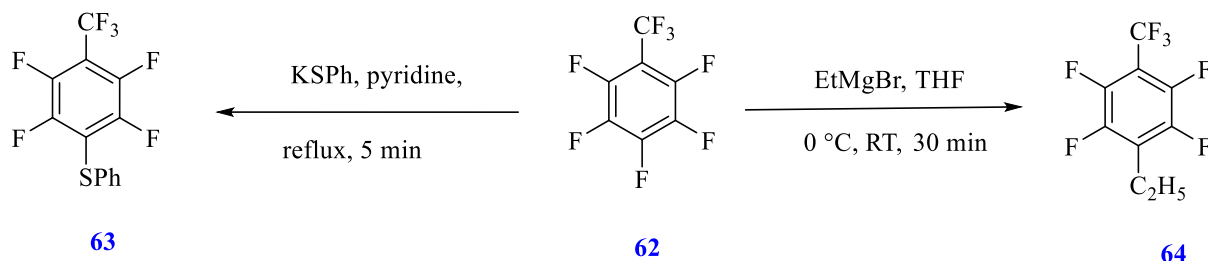
Scheme 13. Reaction of hexafluorobenzene **48 with 2-bromophenol **58**.⁷³**

As seen in scheme 14, addition of a further nucleophile to mono-substituted perfluorobenzene is possible. The same, or a different, nucleophile substituent can add to pentafluorobenzene **49** derivatives.⁷⁴



Scheme 14. Addition of second nucleophilic substituent to pentafluorobenzene derivative.⁷⁴

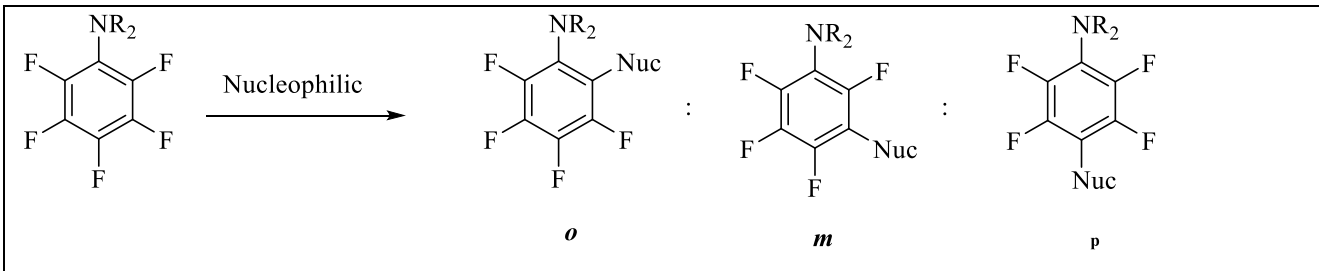
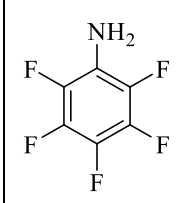
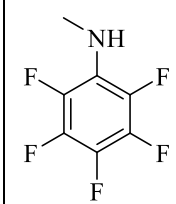
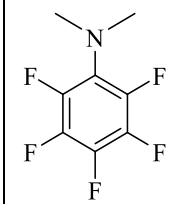
In the vast majority of cases, the 1,4-disubstituted product is obtained and nucleophilic substitution occurs preferentially at para position due to the destabilizing effect of a para-fluorine (Scheme 15). The lone pair on the fluorine atom is believed to repel the build up of charge at the centre of the pentadienyl anion system of the incipient Meisenheimer complex.



Scheme 15. Examples where a second nucleophilic substituent attaches to 1,2,3,4,5-pentafluoro-6-(trifluoromethyl)benzene.⁷⁰

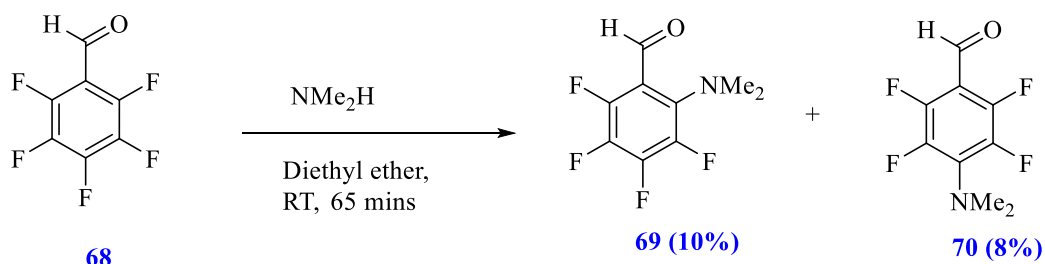
However, significant variation from total selectivity of *para* substituent is observed in several cases. (Table 1). Initially, S_NAr reactions of pentafluoroaniline **65** with ammonia, primary and secondary amines and alkoxide nucleophiles indicated nucleophilic substitution to occur mainly at the *meta* position. Corresponding reactions of pentafluoro-N-methylaniline **66** give about equal amounts of *meta* and *para*-substituted products, however practically exclusive *para* substitution is observed for reactions of pentafluoro-N,N-dimethylaniline **67**. The observed results indicate the amino group powerfully deactivated the *ortho* and *para* positions due to the resonance donation of electron density into the aromatic ring by the amino group lone pair. However as the dimethylamino group is much larger, and twists out of the plane, the lone pair can no longer conjugate with the π -system, and therefore cannot successfully deactivate the *ortho* and *para* sites.⁷¹

Table 1. Typical S_NAr reactions of pentafluoroaniline, pentafluoro-N-methylaniline and pentafluoro-N,N-dimethyl aniline.⁷¹

				
Substrate	Nucleophile	Isomer substitution %		
		<i>Ortho</i>	<i>Meta</i>	<i>Para</i>
 65	NH ₃ MeNH ₂ Me ₂ NH NaOMe	0 0 0 5	87 88 90 79	13 12 10 16
 66	NH ₃ MeNH ₂ Me ₂ NH NaOMe	0 0 0 5	40 60 52 43	60 40 48 52
 67	NH ₃ MeNH ₂ Me ₂ NH NaOMe	0 0 3 1	7 6 5 2	93 94 92 97

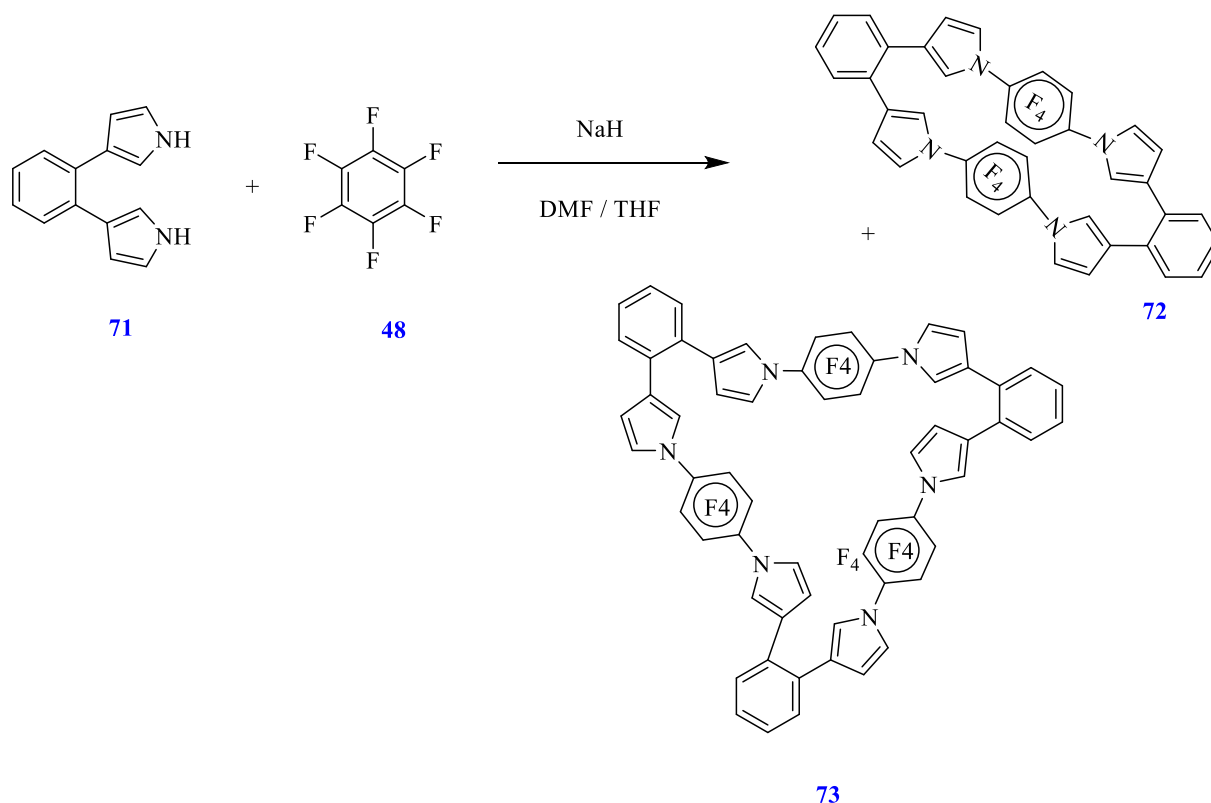
Similarly, reaction of pentafluorobenzaldehyde **68** with dimethylamine (Me₂NH) results in the formation of *ortho* and *para* substituted products in one step S_NAr reaction in diethyl ether as solvent (Scheme 16).⁷⁵ Hydrogen bonding of the amine to the carbonyl oxygen may be involved in directing

attack at the ortho position which would involve addition para to a fluorine with the associated repulsion effect of the fluorine lone pair.



Scheme 16. S_NAr reaction of pentafluorobenzaldehyde **68 with dimethyl amine.⁷⁵**

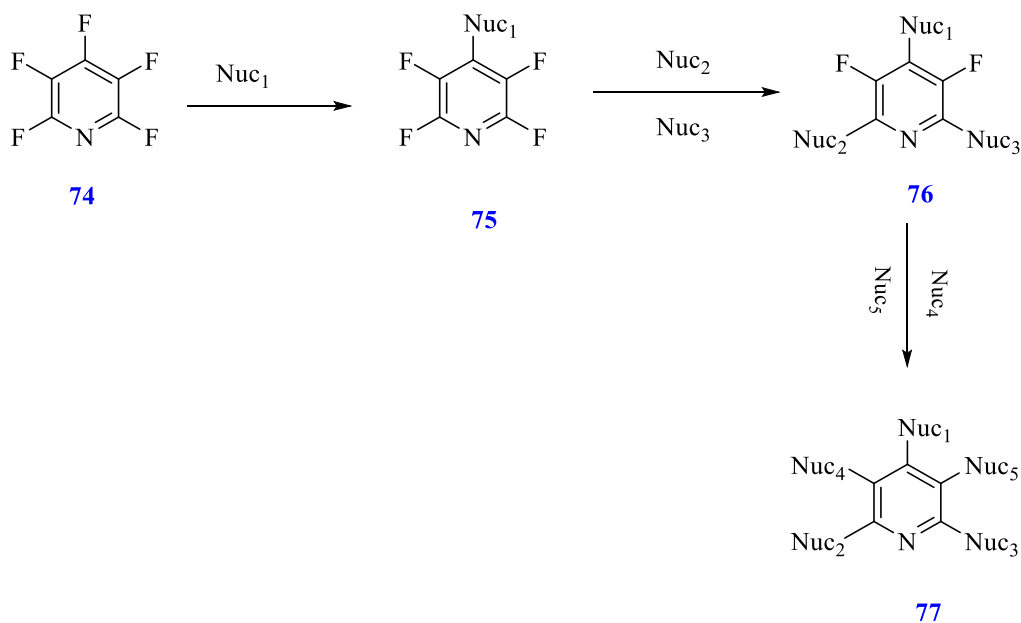
Another recent reaction of a perfluoroaromatic as acceptor moiety with various difunctional nucleophiles with nitrogen as the donor atom involved nucleophilic aromatic substitution (S_NAr) of ortho-dipyrrol-3-ylbenzene **71** with hexafluorobenzene **48** in the presence of NaH as base in DMF and THF to form the macrocyclic stacked fluoroarenes **72** and **73**, which can be used in the field of molecular electronics as conductors and field effect transistors (FET) due to the π -stacked structure (Scheme 17).



Scheme 17. Reaction of ortho-dipyrrol-3-ylbenzene and hexafluorobenzene

1.2.5.1. Perfluorinated pyridine

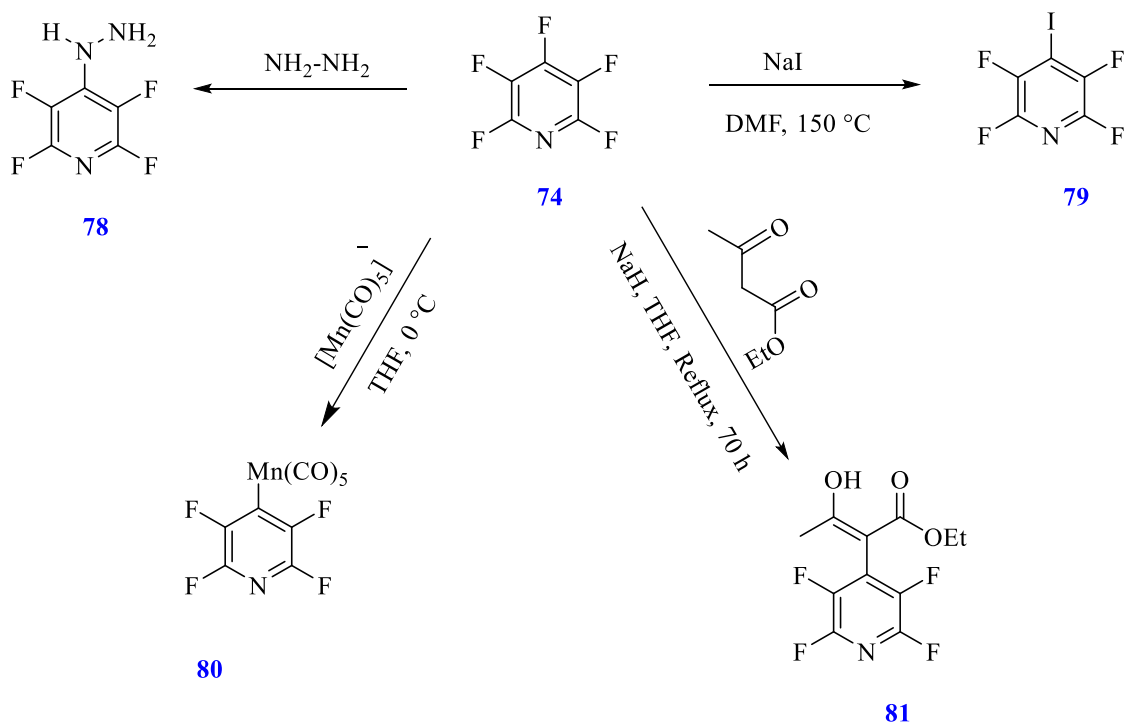
The perfluoroheteroaromatic systems such as pentafluoropyridine **74** are exceptional core scaffolds for the synthesis of different functionalized heteroaromatic and ring fused polycyclic compounds. Pentafluoropyridine, because of presence of five highly electronegative fluorine atoms and the ring nitrogen atom, is very reactive toward nucleophilic attack and all the five fluorine atoms can be replaced by nucleophiles in S_NAr reactions.⁷⁶



Scheme 18. General reaction of pentafluoropyridine **74 with difunctional nucleophiles.**⁷⁷⁻⁷⁹

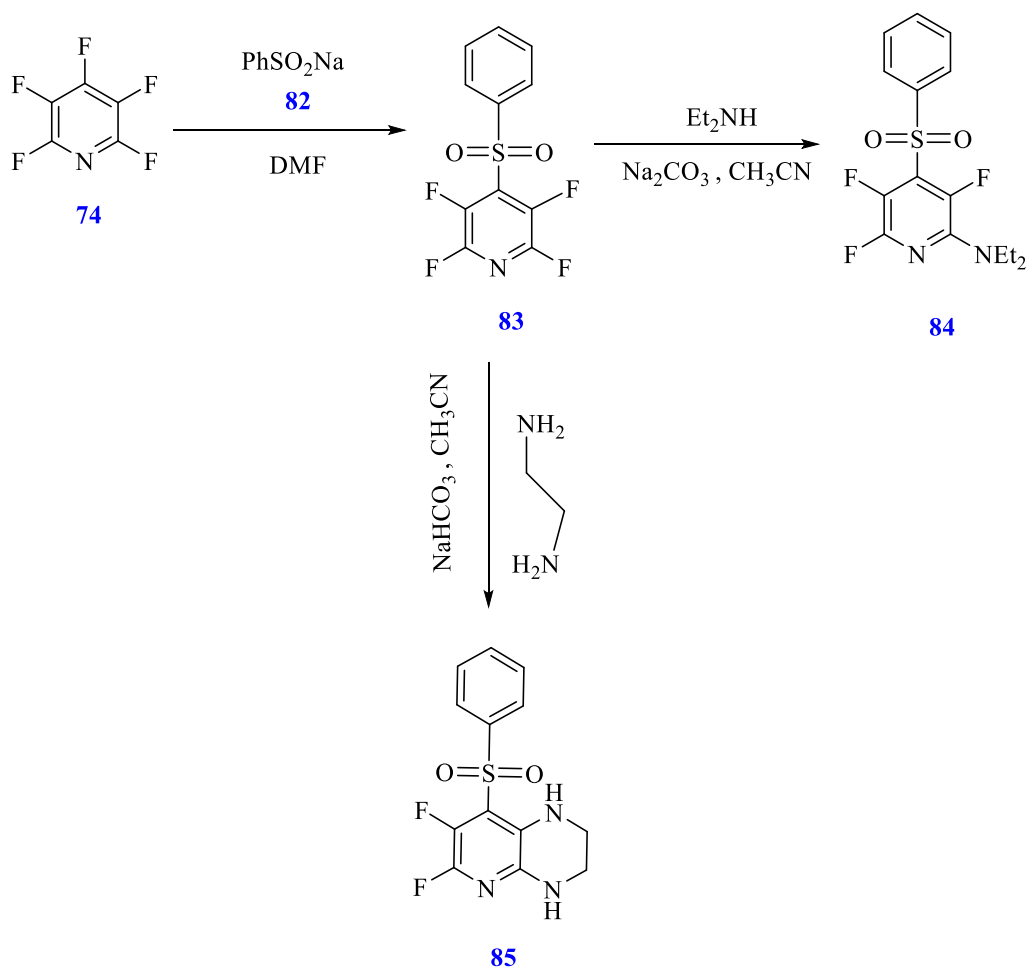
As seen in the above (Scheme 18), the first nucleophile adds at *para* position (4-position) of pentafluoropyridine **74** which is most active site, to the stabilizing nitrogen, and avoiding the repulsion of a *para*-fluorine atom. Following nucleophiles then attack at C-2 and C-6 of compound **75** which are adjacent to the ring nitrogen. The final nucleophiles tend to add to C-3 and C-5 of compound **76** to give final compound **77**.

Scheme 19 shows some examples of the one-step nucleophilic substitution of pentafluoropyridine in which all the nucleophilic substituents added at the *para* position as most active site.⁸⁰⁻⁸²



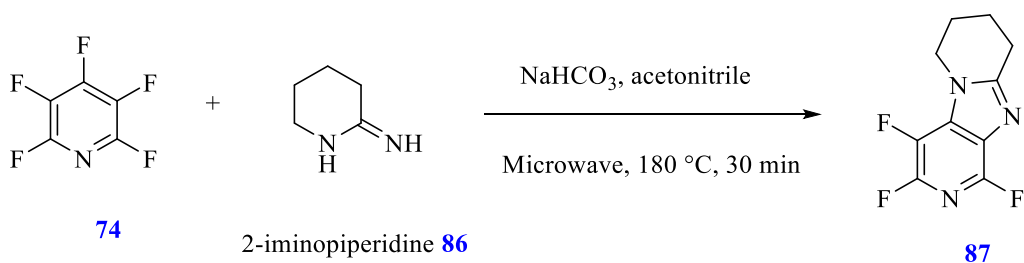
Scheme 19. S_NAr reactions of pentafluoropyridine.

Di- and tri-substitution is possible as shown by the examples in Scheme 20.^{78, 83} The sodium salt of benzenesulfonic acid **82** reacted with pentafluoropyridine **74** to form compound **83** which was in turn treated with a second nucleophile (diethylamine) which added to the ortho position to form di-substituted compound **84** in moderate yield. On the other hand reaction of compound **83** with ethylenediamine led to the tri-substitution product. In this case addition is most likely to have occurred firstly at ortho (C-2) position and the other amino group then attacking the less reactive, but geometrically accessible, meta position (C-3) to form the piperazine ring. This reaction shows the possibility of forming an additional fused ring.^{78,84}



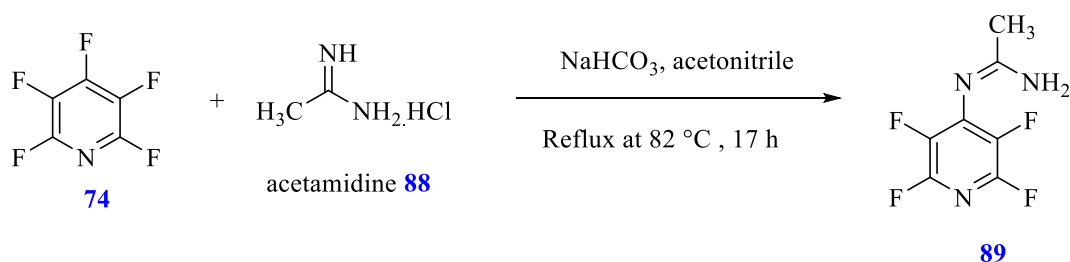
Scheme 20. Di- and tri-substitution reactions of pentafluoropyridine.⁷⁸

An additional example of ring formation involved the reaction of pentafluoropyridine **74** with 2-iminopiperidine **86** to form the tricyclic compound **87** after heating with NaHCO_3 at 180 °C for 30 minutes under microwave irradiation. Initial attack at the para position is most likely to have occurred, followed by a second $\text{S}_{\text{N}}\text{Ar}$ reaction at the meta position to close the imidazole ring (Scheme 21).⁷⁸



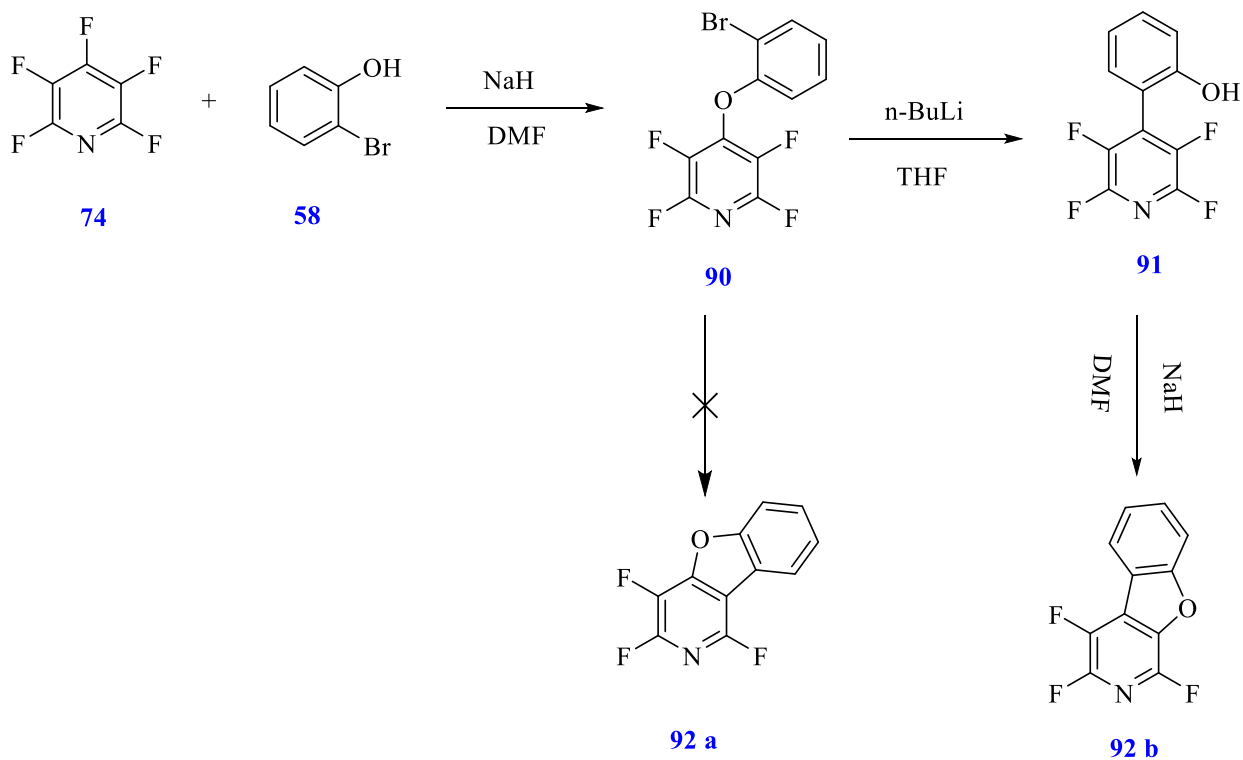
Scheme 21. Reaction of pentafluoropyridine with 2-iminopiperidine.⁷⁸

However, in some case the cyclization failed and a ring did not form (Scheme 22). As seen in the reaction of pentafluoropyridine **74** with acetamidine **88** in the presence of NaHCO₃ under reflux in acetonitrile for 17 h which gave the uncyclised amidine derivative **89**.⁷⁸



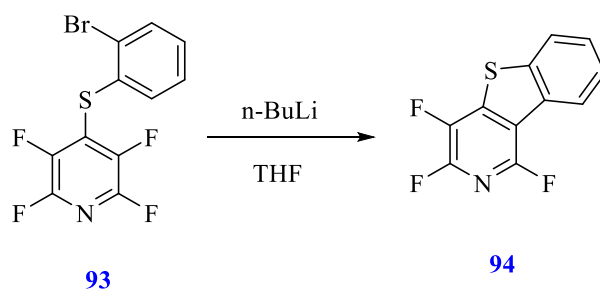
Scheme 22. Reaction of pentafluoropyridine with acetamidine.

Ring formation of fluorinated aryl ethers is another aim of the Weaver research group. As seen in Scheme 23, lithium-bromine exchange in ether was predicted to generate an aryllithium which would lead to intramolecular substitution of the fluorine at C-3 of the pyridine ring to close the furan ring forming **92a**. But treatment of the compound **34** with n-BuLi in THF at -78 °C followed by warming to room temperature gave a compound **91** which was not the expected tricyclic furan **92a**. The compound (2-(tetrafluoropyrid-4-yl)phenol) **91** was isolated indicating that the reaction had proceeded by a Smiles-type rearrangement. It seems that the aryllithium formed prefers to attack at C-4 rather than at C-3 to avoid the destabilizing effect of a para-fluorine. Treatment of the unexpected compound **91** with sodium hydride in DMF did then give the fused benzofuran **92b** quantitatively with the phenoxide oxygen effecting nucleophilic substitution of the fluorine atom at 3-position of the pyridine ring.⁷³



Scheme 23. Smiles-type reaction in lithiation of 4-(2-bromophenoxy)tetrafluoropyridine.⁷³

On the other hand, when the corresponding thioether **93** was treated with *n*-BuLi, direct cyclization occurred by S_NAr reaction at C-3 and no rearrangement was observed. The anion stabilizing effect of the sulfur is thought to lower the activation energy for attack at C-3 overcoming the repulsive effect of the para-fluorine (Scheme 24).⁷³



Scheme 24. Cyclization of thioether 93 with *n*-BuLi

1.3. Fluorinated heterocyclic compounds as potential DNA binding ligands

1.3.1. DNA double helix structure

Deoxyribonucleic acid (DNA) is a double-stranded molecule where each strand is composed of a mixture of four different types of bases which are named as adenine (A), thymine (T), cytosine (C) and guanine (G). In the strand these bases are connected to deoxyribose sugars to form nucleosides which are joined by phosphodiester links at both the 3'-hydroxyl and 5'-hydroxyl groups (Figure 8). The two strands are held together by Watson Crick hydrogen bonds where A form two hydrogen bonds with T and C forms three hydrogen bonds with G.⁸⁵⁻⁸⁶

DNA plays a significant role in the life process as it carries genetic information which instructs the biological synthesis of enzymes and proteins through the process of transcription and translation of genetic information in living cells. It is a major target for drug interaction as it is the starting point of significant cellular processes of replication, transcription and translation which are vital for cell growth and division. Small ligand molecules bind to DNA and unnaturally change and/or inhibit DNA function. These small ligand molecules are used as drugs when inhibition of DNA function which is essential to treat or control a disease.⁸⁶

The interaction mechanisms of drugs with DNA have an important role in biological studies in drug discovery, and pharmaceutical development procedures, which can be used for the determination of new drugs targeting DNA.⁸⁷

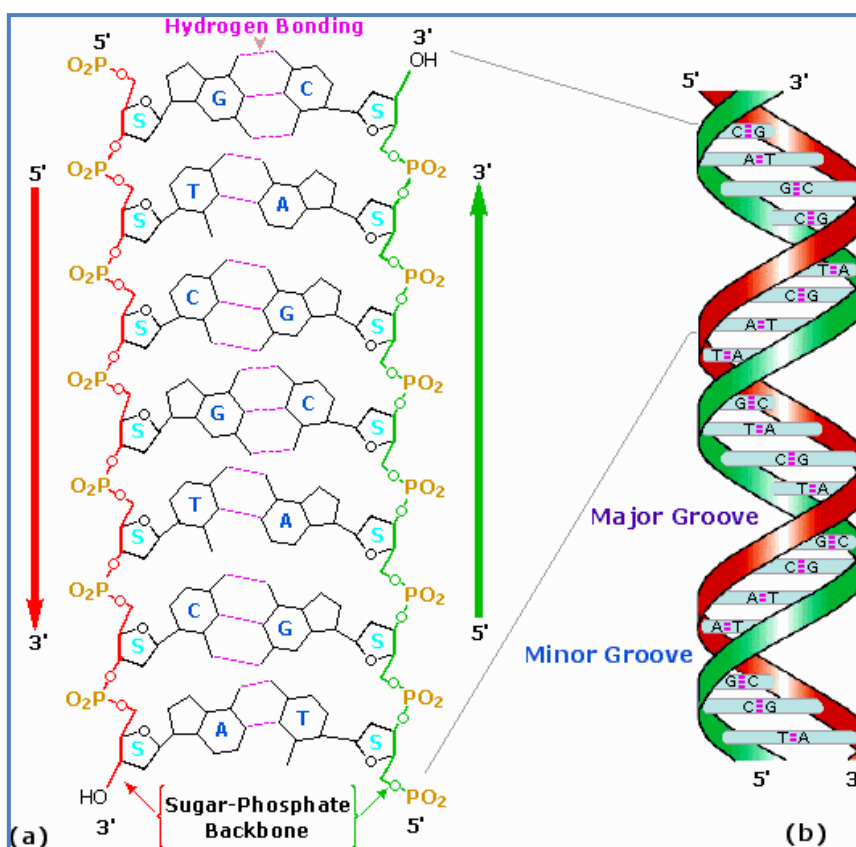


Figure 8. DNA double Helix structure.⁸⁸

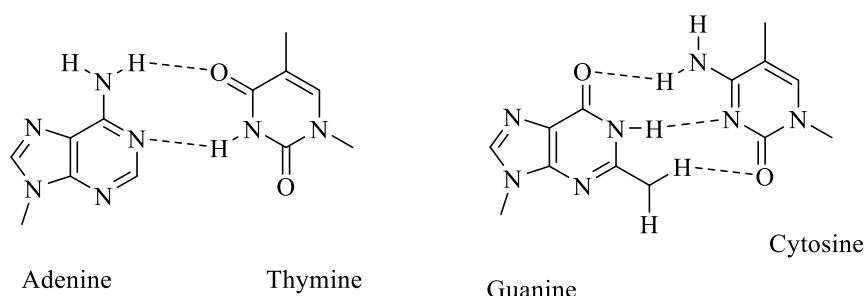


Figure 8a. DNA base pair structure which bind together by hydrogen bonding.

1.3.2. Type of drug-DNA interactions

Drugs can interact with DNA in three different ways. i) by interaction of the drug with proteins that bind to the DNA, which control transcription factors and polymerases. ii) through the RNA binding to double helical DNA to form a triple helix structure, to open DNA single strand regions forming DNA-RNA hybrids that may affect transcriptional action and iii) by interaction of small aromatic drugs with DNA double strand structures. Interaction of drugs with DNA can involve binding of a planar aromatic ring compound between the base pairs of DNA which is called intercalation (for

example actinomycin D and daunomycin), or electrostatic interaction and DNA groove binding interactions of flexible chains which can wrap themselves around either the minor or major grooves.
86,89

1.3.3. Modes of drug-DNA binding

There are two modes of drug–DNA binding, covalent and noncovalent.

1.3.3.1. Covalent mode of binding

Some anticancer drugs bind to DNA through covalent interaction such as via alkylation or inter- and intra-strand cross linking.⁹⁰ In covalent interactions the binding is irreversible and invariably proceeds to complete inhibition of DNA and as a result cell death (apoptosis) will take place. The covalent binders have very high binding strength. In addition, they can cause DNA backbone distortion, which in turn can affect both transcription and replication. The covalent binders are usually alkylating agents, and as a result of adduct formation, they are used in cancer treatment to cross link DNA.⁹ DNA alkylating drugs are the oldest class of anticancer drug, but are still commonly used today. They show significant anti-cancer activity by damaging DNA and can cause cancer cells to undergo apoptosis.⁶ Alkylation usually occurs on the N-7 of guanine in DNA, although alkylation of other positions and other types of cross-links can occur.

Another well-known covalent binder used as an anticancer drug is cis-platin, cis-diamminedichloroplatinum(II) which makes intra- and inter-strand cross-links through replacement of chloride ligands by the nitrogens on the purine bases(Figure 9).⁹¹

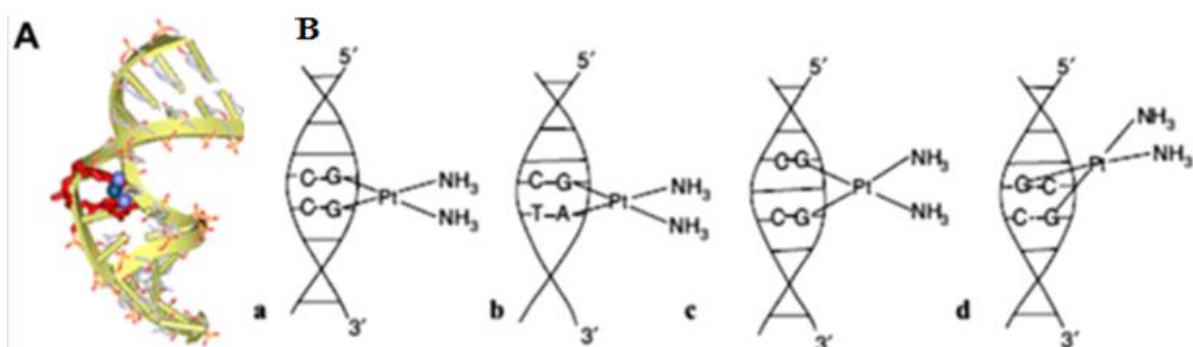


Figure 9. (A) Cisplatin covalently bonded to DNA. B. (a) Modes of binding of cisplatin to guanine (G) and adenine (A); (b) 1,2-intrastrand GpG (structure a), 1,2-intrastrand.

1.3.3.2. *Non-covalent mode of binding*

Non-covalent binding agents are normally considered less cytotoxic than DNA covalent binding agents. The non-covalent binding mode is reversible and is preferred over a covalent interaction which leads to irreversible DNA damage and severe toxic side effects.

Non-covalent binders cause DNA conformation change, interrupt protein–DNA interactions and potentially initiate DNA strand breaks which substantial effects on gene expression.⁹⁰

The non-covalent mode of drug–DNA binding can be classified into intercalation and groove binding.⁸⁶

1.3.3.3. *Groove binding drug-DNA interaction*

Minor groove binding drugs typically have several aromatic rings, such as pyrrole, furan or benzene connected by bonds possessing torsional freedom. Groove binder drugs can bind with DNA by van der Waals interaction and hydrogen bonding. In addition, these drugs can form hydrogen bonds to bases, typically to N-3 of adenine and O-2 of thymine.

Nucleotide asymmetry generates two grooves with different geometrical characteristics. The major groove is wide and relatively small and shallow, and approximately 22 Å in width. However the minor groove is deeper and narrower, and only about 12 Å in width (Figure 10).^{87,92}

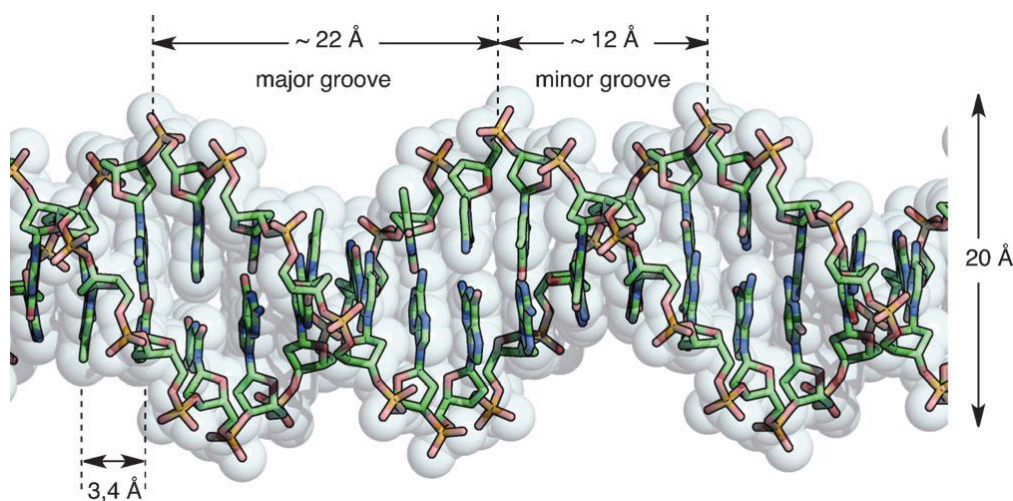


Figure 10. B-DNA conformation, with the main structural dimensions.⁸⁷

Furthermore, studies of the functional groups on the base pairs shows that in the major groove the donor-acceptor pattern is more variable. Actually, in the minor groove A/T and T/A are degenerate while in the major groove all four possible base pairs can be distinguished by particular donor–

acceptor combinations.⁸⁷ In nature, proteins can bind to the major groove, some to the minor groove, and some require binding to both. Most DNA interactive proteins do bind in the major groove which is richer in the number and specificity of the hydrogen bond donor and acceptor sites compared to the minor groove. However, most small molecules of less than 1000 Da bind in the minor groove.⁹²

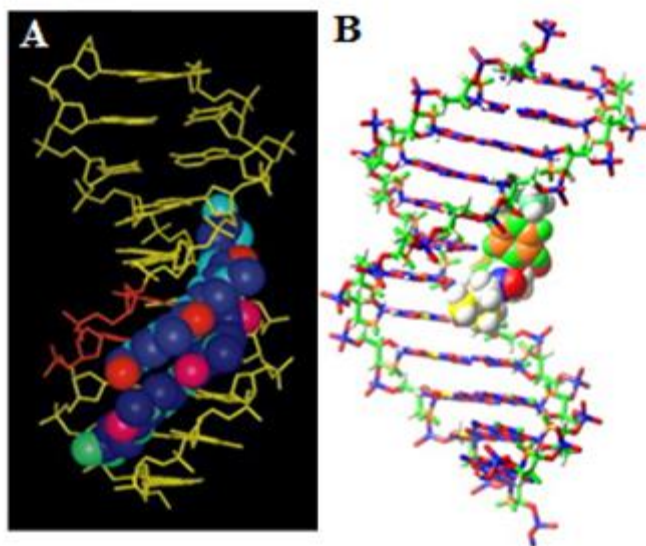
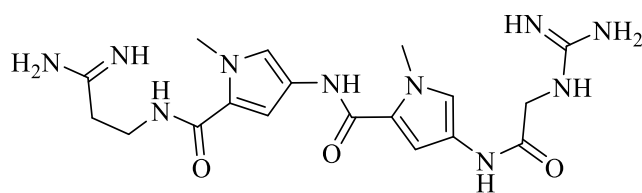


Figure 11. A) Minor groove filled with two drug molecules of diimidazole lexitropsin. B) major groove binding of DMAADD molecule.⁸⁵

The minor groove binders are usually curved in shape, which matches well with the topology of double-stranded DNA, and increasingly are of interest as potential anti-cancer drugs^{87,90} which can bind either non-covalently and covalently to DNA.⁹²

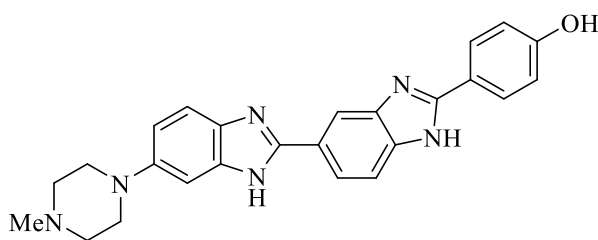
It is important to recognise that due to the sterically obstructive amine groups, G-C base pairs are not good binding sites in most minor groove DNA sections. However the anti-microbial agents that bind to A/T base pairs in the minor groove frequently have anti-tumour activity and are more selective than other typical DNA-reactive anti-tumour drugs which regularly cause wide damage to areas that are also vital for the operating of non-replicative cells. Moreover, such agents can cause damage to normal tissues by producing mutagenic lesions.⁹³

Non-covalent minor groove binding drugs as potential anticancer compounds are interesting to work on. The polypyrrole, Bis (benzimidazole) and the bis-quaternary ammonium heterocycles are some examples of A/T minor groove binding drugs.⁹⁴



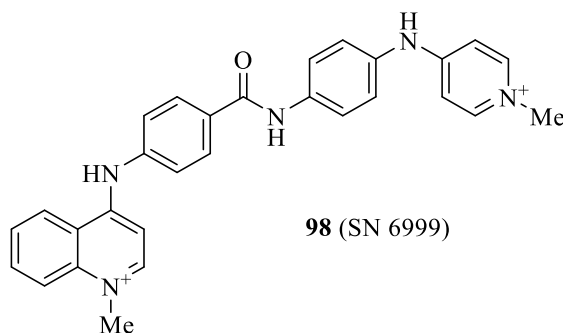
Netropsin **95**

Figure 12. Netropsin is an example of a polypyrrrole which binds to A/T-rich sites, and acts as potent inhibitor of Werner and Bloom helicases.⁹⁴



Hoechst 33258 (pibenzimol) **96**

Figure 13. Hoechst 33258 (pibenzimol) is example of a bis-(benzimidazole) which binds to AT-sites, and acts as potent cytotoxic drug by inhibition of topoisomerase and DNA helicase.⁹⁴



98 (SN 6999)

Figure 14. SN 6999 is example of bis-quaternary ammonium heterocycles which bind to AT tracts with at least 4 base pairs, related to polyamidines, and causes significant distortion of the DNA structure as well as inhibition of DNA and RNA polymerases.^{91, 94}

In addition the pyrrole-imidazole (Py-Im) polyamides show high binding affinity and specificity to the specific DNA sequences. They are effective inhibitors of RNA transcription, and modulate gene expression by modifying chromatin structure. This compound has been linked with the DNA-

alkylating agent chlorambucil (Chl) which then reacts covalently with specific sites of DNA. For example, polyamide 1R-Chl (Figure 16).⁹¹

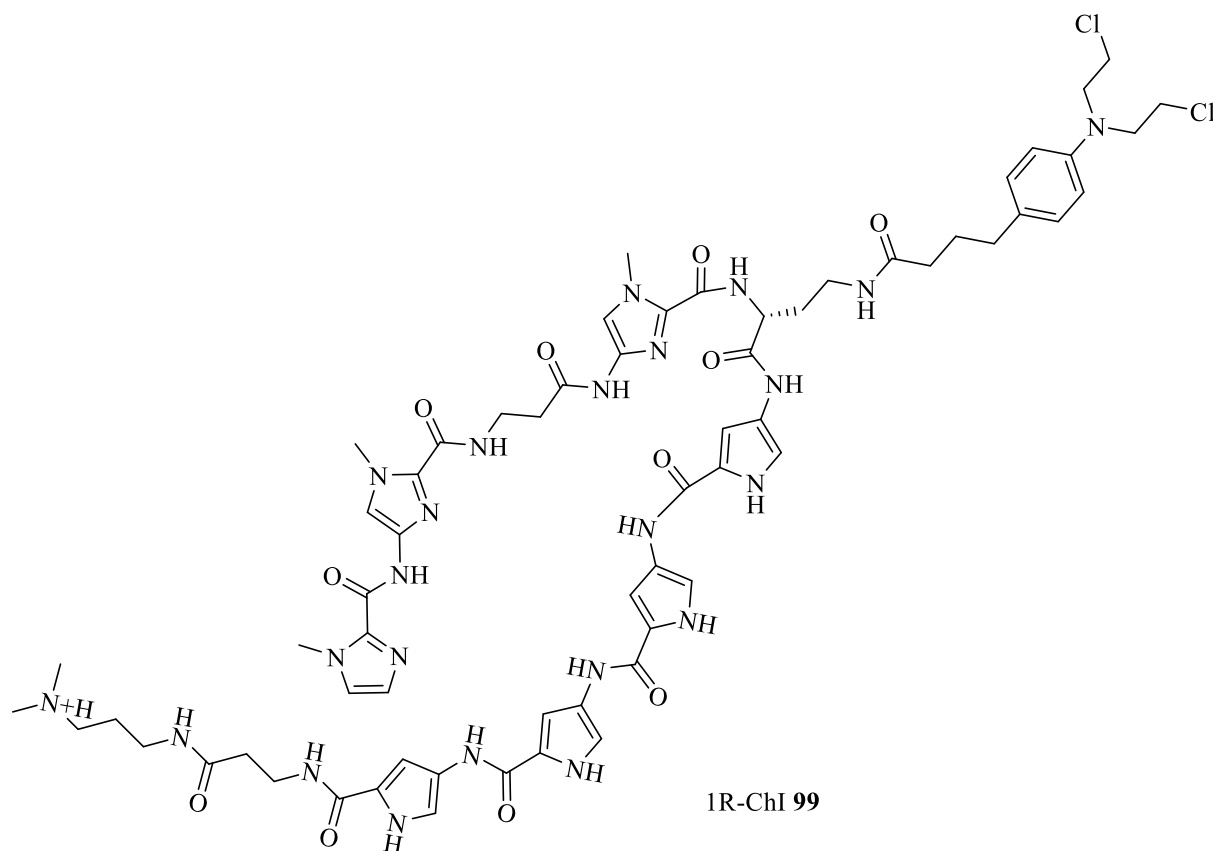


Figure 15. Structure of 1R-Chl which binds to a specific sequence of DNA and acts as inhibitor of cell proliferation in different cancer cell lines with no apparent cytotoxicity.⁹¹

1.3.3.4. Intercalating binding agents

The interaction between DNA base pairs and the acridine proflavone agent was described by Leman as intercalation. Intercalation is the selected binding manner of flat polyaromatic ligands of adequately large surface area and suitable steric properties (Figure 16). Intercalators stack between adjacent DNA base pairs leading to significant π -electron overlap, aligning perpendicular to the DNA backbone without breaking up the hydrogen bonds between the DNA bases. Van der Waals, hydrogen bonding, hydrophobic, and/or charge transfer are the known forces that maintain the stability of the DNA–intercalator complex, even more than DNA alone.^{83,96} In addition the DNA intercalators complex is less sensitive to the ionic strength compared to DNA groove binding complexes due to the stabilization by π - π interaction.

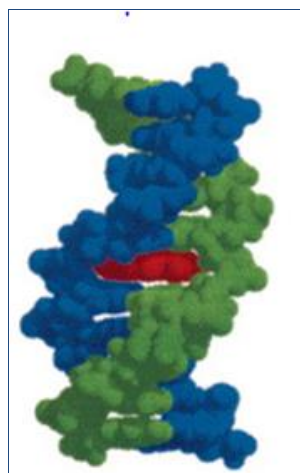
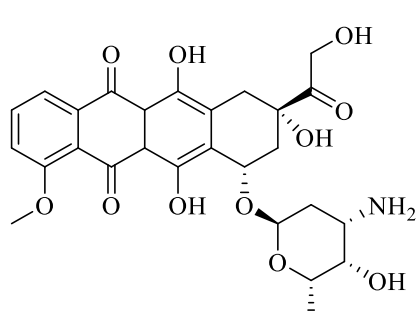


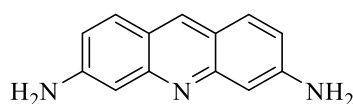
Figure 16. Intercalation of a planar aromatic molecule in the DNA base pairs by hydrophobic interaction and van der Waals forces.⁹⁷

When an intercalating agent is inserted between DNA base pairs, a decrease in the DNA helical twist and lengthening of the DNA occurs that causes delay in cell replication. Therefore such compounds used in chemotherapeutic treatment to inhibit DNA replication in rapidly growing cancer cells.

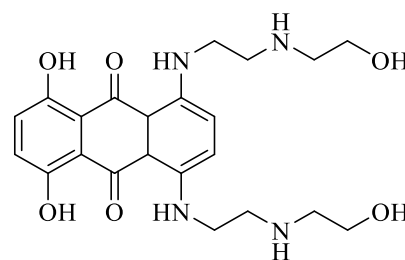
The binding mode can be determined by the size and nature of intercalating chromophore. For effective intercalation, at least a two-ring fused system is necessary, for example naphthalene- type, but these intercalate only if they have pendant cationic side chain, having similar affinities irrespective of the presence of charged or uncharged nitrogen atoms in the aromatic system. In comparison fused three-ring systems such as acridines have adequate stacking interactions to intercalate without the need for appended side chains.⁹³ Figure 17 shows some examples of intercalating clinical drugs.



Doxorubicin **100**



proflavine **101**



Mitoxantrone **102**

Figure 17. Example of DNA-intercalating agents⁹³

1.3.4. Techniques used to study drug–DNA interactions

There are a number of different techniques which can be used to study the interaction of DNA with ligand molecules such as infrared (IR), UV–Visible, and nuclear magnetic resonance (NMR) and fluorescence spectroscopies, as well as macromolecular X-ray crystallography. Atomic force microscopy (AFM), electrophoresis, mass spectrometry, viscosity measurements, thermal denaturation studies, differential pulse voltammetry, Raman and circular dichroism, have also all been employed. All these techniques can be used as methods to characterise drug–DNA complexes, and effect of binding on DNA structure. In this study UV–Visible and fluorescence spectroscopies were used as these are of common use. Macromolecular x-ray crystallography was also attempted to see if co-crystals of DNA-drug adducts could be grown. In addition, some antibacterial activity also studied against one Gram negative strain (*E. coli*) and one gram positive strain (*Staphylococcus aureus*).

1.3.4.1. UV–Visible absorption spectroscopy

UV–Visible absorption spectroscopy is one the simplest and commonly employed instrumental techniques for studying both the stability of DNA and its interactions with small ligand molecules. In this technique, UV–Visible absorption spectra of the free drug are compared with drug–DNA complexes, which are usually different. If a small molecule has intercalated between DNA base pairs hypochromism (reduced absorbance) and bathochromism (red shift) should occur which is due to the stacking interaction between an aromatic chromophore of intercalator and a base pair of DNA. In terms of bathochromism (red shift) the π -orbitals of the DNA base pairs couple with π^* -orbital of the small molecules which causes an energy decrease and a decreasing of $\pi \rightarrow \pi^*$ transition energy. Therefore the absorption of the small molecule shows a red shift. Simultaneously, the empty π^* -orbital is partly filled by electrons, reducing the transition probability, which leads to hypochromism. In case of electrostatic attraction between the DNA and small molecules, a hyperchromic effect should occur, which is due to the corresponding changes of DNA in its conformation and structure after the complex–DNA interaction has occurred. The hyperchromic effect is the exceptional increase in absorbance of DNA upon denaturation.⁸⁶

1.3.4.2. Fluorescence spectroscopy

Fluorescence spectroscopy is another common technique which can indicate interactions between small ligand molecules and DNA. The advantages of this technique compared to other techniques are high sensitivity, selectivity and large linear concentration range. Compounds containing aromatic

functional groups with low-energy π - π transition levels have large number of possible transitions compared to compounds containing aliphatic and alicyclic carbonyl structures or conjugated double-bond structures, and absorb strongly. Such rigid structures can often re-emit the excess energy as light in the form of fluorescence. Therefore aromatic systems usually give the most intense and the most useful fluorescence signals. Also using this technique based on fluorescence emission the mode of drug-DNA binding can often be determined. In the case of intercalation interactions, drugs bound to DNA enhance deactivation through fluorescence emission so a significant increase in the fluorescence emission will usually be observed.

But in other interactions like groove binding, electrostatic, hydrogen bonding or hydrophobic interactions drugs are close to the sugar-phosphate backbone; therefore it is possible to observe a decrease in the fluorescence intensity due to non-radiative energy loss. The quenching fluorescence assay is one method which provides further information about the binding mode of drugs to DNA.

Ethidium bromide (EB) is one of the common fluorophore probes. It can insert to the DNA base pair and bind to DNA strongly as an intercalator, which causes an increase in the fluorescence intensity. The improved fluorescence in presence of EB can be quenched by the addition of a second molecule. Therefore by intercalating a second molecule into DNA, the fluorescence intensity of the EB-DNA will decrease, because it will compete with EB in binding with DNA. In addition the extent of interaction between the drug and DNA can be determined by the extent of fluorescence quenching of EB bound to DNA.⁸⁶ Figure 18, describes the interaction of Ni complex $[\text{Ni}_2(\text{L})_2(\text{NO}_3)_2]$ with EB-DNA. The K_{SV} values of compound is $(7.0 \pm 0.097) \times 10^3 \text{ M}^{-1}$

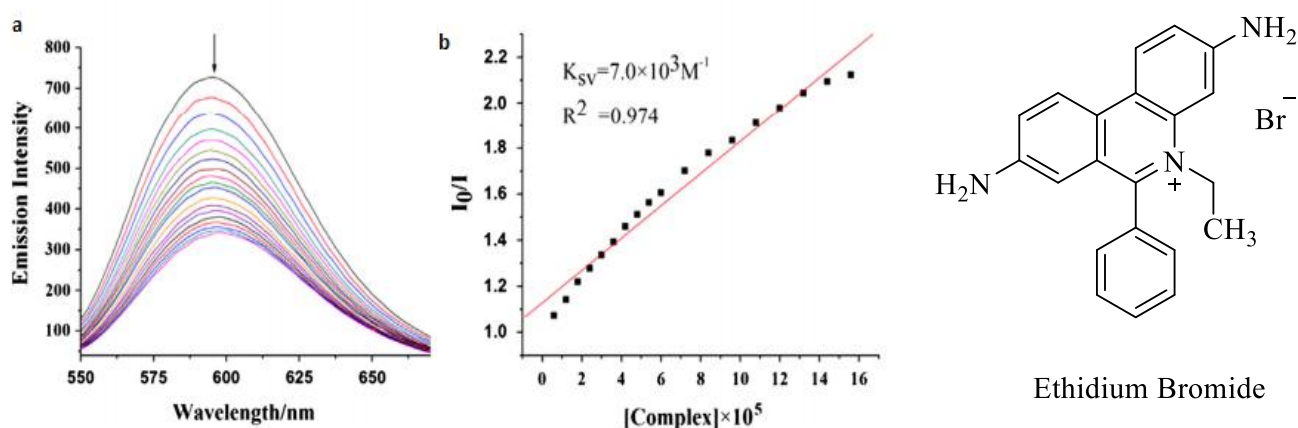


Figure 18. Emission spectra of EB bound to CT-DNA in the presence of free Ni complex $[\text{Ni}_2(\text{L})_2(\text{NO}_3)_2]$ (a) Fluorescence quenching curves of EB bound to CT-DNA Ni complex (b). (Plots of I_0/I vs. $[\text{Compound}]$).⁸⁶

1.3.4.3. Macromolecular X-ray crystallography

One of the useful and important methods which is used to determine the three dimensional structure of DNA-drug complex is macromolecular X-ray crystallography. This method involves growth of a co-crystal of DNA and the drug of interest and X-ray diffraction data collection. There are different methods to grow suitable crystals which all have the aim of bringing the biological macromolecules solution to a supersaturated state. The crystallization process can be affected by different factors which include biophysical and physico-chemical parameters. Biophysical parameters include stabilization, purification, storage and handling of macromolecules, as bacterial contamination are very significant in crystallization of the DNA. Fundamental physico-chemical parameters such as supersaturation (concentration of macromolecules and precipitants), temperature, pH, purity, ionic strength, pressure, magnetic and electric field, viscosity effects and the difference in concentration between DNA/drug solutions crystallizing solution also are significant factor in DNA crystallization. In addition, nucleation and crystal growth can be affected by the method used. Therefore it better to attempt different methods to achieve optimum crystallization. The most common method is the vapour diffusion technique which was investigated in this study.^{98,99}

1.3.4.4. Vapour diffusion crystallization

This technique is suitable for small volumes less than 2 μ l and was used for the first time to crystallize transfer ribonucleic acid (tRNA). In this technique the vapour pressure of a droplet containing biological macromolecule, buffer, crystallizing agent, additives, and any drug expected to bind, and the vapour pressure of a reservoir (containing a solution of crystallizing agent which is more concentrated than the droplet) are allowed to reach to equilibrium by diffusion of the volatile substances such as organic solvent or water molecules from the droplet. Vapour diffusion crystallization can involve different methods which include, hanging drop, sitting drop and sandwich drop as seen in (Figure 19).^{99,37} In the present study the hanging drop method was employed.

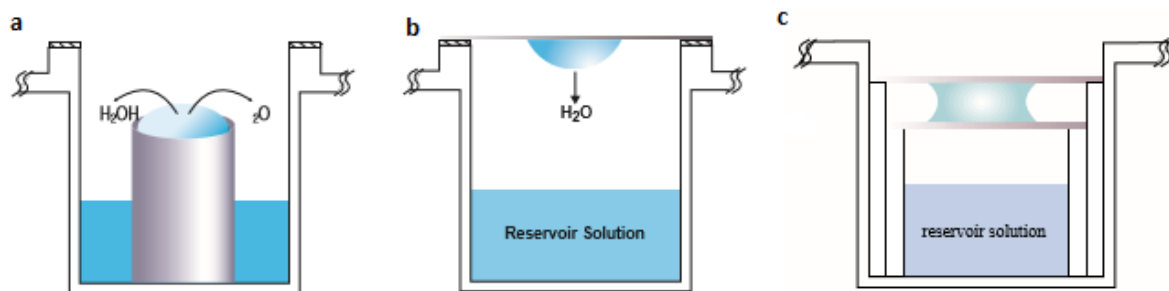


Figure 19. Vapour diffusion crystallization methods. a) Sitting drop, b) hanging drop, c) sandwich drop.³⁷

1.4. Fluorinated heterocyclic compounds as protein kinases inhibitors

Due to toxicity of many anticancer drugs to normal tissues and various side effects of them the medicinal chemist is constantly trying to design and develop new therapeutic agents for the treatment of cancers with high selectivity. An important area where selectivity is hoped for is inhibition against protein kinases and receptors.¹⁰⁰⁻¹⁰² Inhibition of receptors or kinases is one of the greatest pathways to treat cancers due to their significant role of them in cell proliferation.¹⁰³

Cancer cells vary from normal cells in their way of communicating with their neighbours because of abnormality in their signalling network. Therefore the understanding of abnormal signal transduction as the source of the altered phenotype of cancer cells has led to more attention to emerging therapies targeting this abnormality,¹⁰⁴ and identification of these signalling pathway is very important in signal transduction therapy.¹⁰⁵ One of the most important signalling elements are protein tyrosine kinases (PTKs) which were recognized as key drivers of cancer cells in the late 1980s. Protein tyrosine kinases (PTKs) show a crucial role in the regulation of cell proliferation, differentiation, metabolism, migration, and survival. They are classified as receptor PTKs and non-receptor PTKs. Selective receptor and non-receptor PTK inhibitors are known to function as anti-tumor agents. These agents are indicated to prevent various features of cancer cell development, including propagation, survival, incursion, and angiogenesis.¹⁰⁶

Also the groups of serine /threonine kinases, cyclin dependent kinase (CDKs), Erks, Raf, and PKB/Akt, are very important in cell proliferation, cell division, and anti-apoptotic signalling. In addition EGFR (epidermal growth factor receptor), PDGFR (platelet derived growth factor receptor), and VEGFR (vascular endothelial growth factor receptor), were targeted having established their involvement in various malignancies.¹⁰⁷

For example, the Ras-Raf-Mek-Erk pathway is one significant pathway in the hallmark of many cancers which can be activated by receptor-linked tyrosine kinases such as the epidermal growth factor receptor (EGFR). Therefore the inhibition of Raf, Mek, and Erk are very significant and useful for treatment of many cancers as their activities are highly improved because of the extensive oncogenic mutations in ras (Figure 18).¹⁰⁸⁻¹¹⁰ For example sorafenib (a Raf kinase inhibitor) can be useful in preventing activating mutations in B-Raf which occur in 66% of human melanomas.¹¹¹ Selumetinib (AZD6244) (a Mek kinase inhibitor) is used to treat various types of cancer, such as non-small cell lung (Figure 20).¹¹²

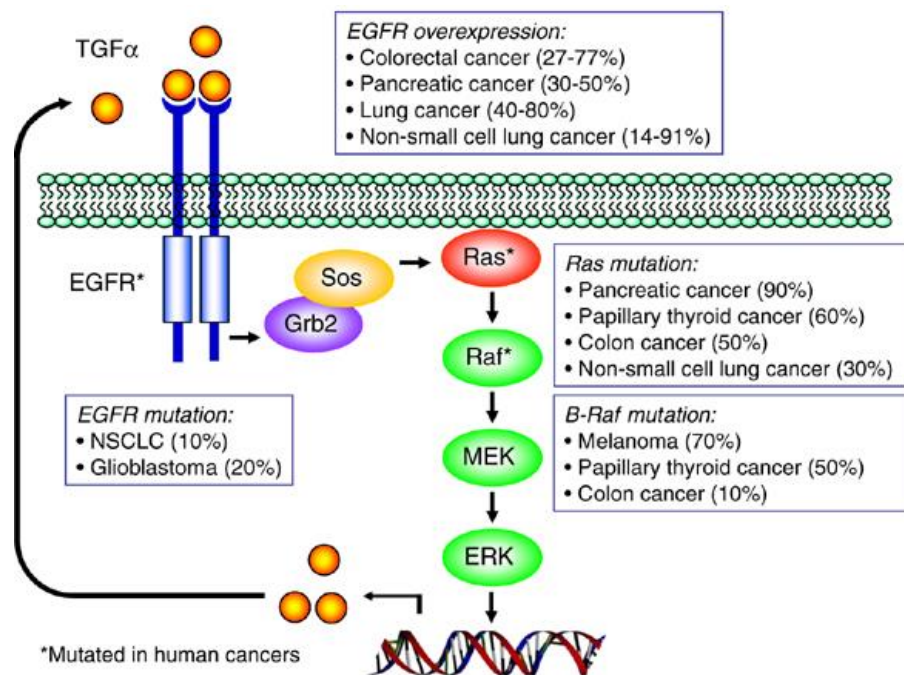
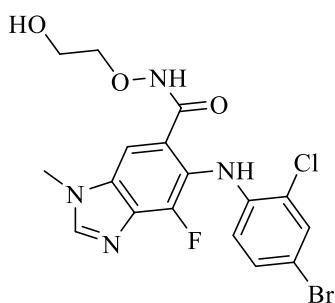


Figure 20. On cogene activation of the ERK MAPK cascade.

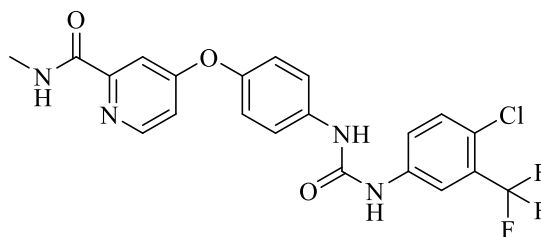
Mutationally activated B-Raf, Ras and mutationally activated and/or overexpressed EGFR causes persistent activation of the ERK MAPK cascade in human cancers. Activated ERKs translocate to the nucleus, where they phosphorylate and control various transcription factors causing changes in gene expression. Especially, ERK-mediated transcription can result in the upregulation of EGFR ligands, such as transforming growth factor alpha (TGF- α), therefore generating an autocrine feedback loop that is critical for Ras-mediated transformation and Raf-mediated gene expression changes.¹⁰⁸

Also epidermal growth factor receptor (EGFR) is a tyrosine kinase cell-surface receptor for members of EGF-Family which contains an extracellular ligand-binding domain, a transmembrane lipophilic

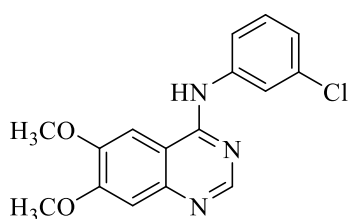
region and an intracellular protein tyrosine kinase domain. EGFR triggered by binding of a specific substrate which leads to cell propagation, invasion and metastasis by activation of signal transduction pathways. By binding EGFR inhibitors to epidermal growth factor receptor the EGFR pathway will be blocked, resulting in inhibition of the proliferation of malignant cells.¹¹³⁻¹¹⁶ Therefore the role of EGFR in treatment of many cancers is found to be very significant. For example, Iressa and Tarceva are active epidermal growth factor receptor tyrosine kinase inhibitors (EGFR-TKI) which prevent the growth and spread of non-small cell lung cancer and pancreatic cancer by blocking the EGFR pathway.¹¹⁷⁻¹¹⁹ Although they show some side effects. Quinazoline AG 147829 is another example of EGFR inhibitor which is in clinical development for the treatment of glioblastoma multiforme (GBM) (Figure 20).¹¹⁵



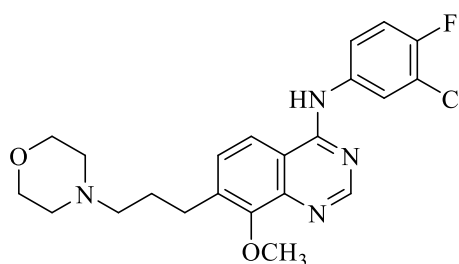
Selumetinib: Mek kinase inhibitor **103**



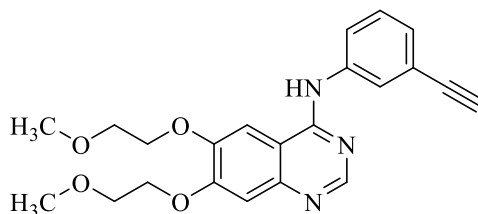
Sorafenib: Raf kinase inhibitor **104**



AG 1498 : EGFR inhibitor **105**



Iressa : EGFR inhibitor **106**



Tarceva: EGFR inhibitor **107**

Figure 21. Protein kinase inhibitors in the clinic and in development

In general this study was aimed at the synthesis of new heteroarene and fluorinated heteroarene compounds with potential bioactivity. In particular for the synthesis of new heterocycles, we planned to exploit the easy S_NAr reaction of fluorinated arenes such as hexafluorobenzene and pentafluoropyridine to introduce a range of groups, specially bisimidazole and bisbenzimidazole derivatives which will allow subsequent ring fusion processes to be carried to generate polycyclic structures, or allow biaryl type links to be set up to generate conformationally flexible polyaryl systems. A further aim was to introduce different water solubilising group into the successfully synthesised polycyclic structures to increase water solubility of the compounds for further

consideration and investigation of the biological activity. The binding properties of the synthesised compounds will be carried out using UV absorption, and ethidium bromide (EB) fluorescence displacement experiments to evaluate interactions between the synthesised compounds as groove or intercalating binding agents with DNA by different binding modes including hydrogen bonding and electrostatic interactions. Biological properties will be assessed by antimicrobial activity assay, and anticancer activity of the synthesised compounds will be investigated against different cancer cell lines. Continuing work should be undertaken to improve biological and anticancer activity of synthesised compounds and to develop the new drugs needed.

2. Results and discussion

As mentioned before fluorinated compounds have shown important improvement in the biological activity of pharmaceutical compounds and drugs in medicinal chemistry. The introduction of a fluorine atom into organic compounds can change the biological properties of the compound and make significant improvement on the biological activity of them by influencing its metabolism. On the other hand N-heterocycles are very important scaffolds found in many biologically active compounds, and drugs containing nitrogen atom play a significant role in interaction of small molecules and drugs target. These compounds have application and their utilization in organic synthesis is important. Therefore this research involves the use of perfluoroarenes, as convenient starting materials to different heterocycles compound especially N-heterocycles for synthesis of novel fluorinated heterocyclic compounds by S_NAr reaction.

2.1. *Outcome of organic synthesis*

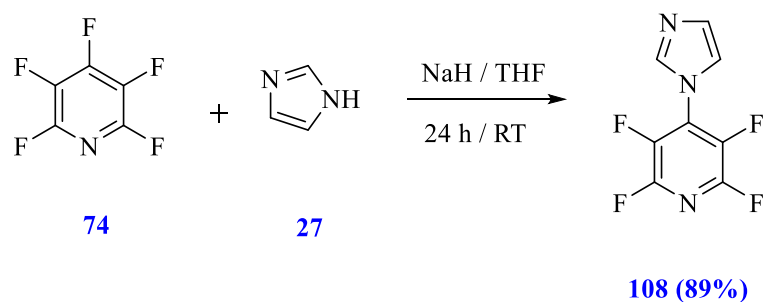
2.1.1. *Synthesis of perfluoro heterocyclic compounds*

The aim of this study was the synthesis of a range of perfluorobiheteroaryl compounds containing dissimilar heterocyclic rings in order to have possible interaction with DNA and potential biological activity. It was hoped that hetero atoms such as N or S could function as effective nucleophiles to promote S_NAr of the fluorine atoms in a perfluoroarene, and that this would provide an easy and flexible method to rapidly assemble linked multi-ring heterocycles as possible DNA binding agents.

2.1.1.1. *Reaction of pentafluoropyridine with imidazole*

The aim of this reaction (Scheme 25) was the synthesis of a biheteroaryl compound containing imidazole and a perfluoropyridine ring in order to develop scaffolds with potential to interact with DNA. It was hoped that nitrogen heterocycles such as imidazole could function as effective nucleophiles to promote S_NAr of the fluorine atoms in a perfluoropyridine. The reaction of pentafluoropyridine with imidazole in presence of NaH as base and THF as solvent did not successfully afford the desired product. TLC and NMR revealed that some starting materials were still present with several products formed. Optimization of reaction conditions showed that a large excess of pentafluoropyridine (3 equiv.) was essential to complete consumption of starting material and formation of 2,3,5,6-tetrafluoro-4-(1*H*-imidazol-1-yl)pyridine **108**. The structure of compound

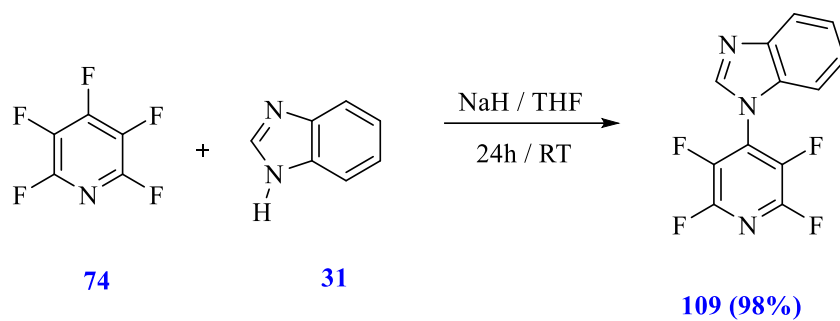
108, formed in 89% yield, was established by its ^1H NMR spectrum, with accurate mass measurement of m/z MS (ESI) (MH^+), 218.0335 matching $\text{C}_8\text{H}_3\text{F}_4\text{N}_3$. In addition the ^{19}F NMR spectrum showed signals for two pairs of fluorine atoms indicating that the tetrafluoropyridine ring was intact. Several crystallization methods were tried to crystallize the product but the compound did not crystallize, and remained as a yellow oily liquid.



Scheme 25. Reaction of pentafluoropyridine with imidazole.

2.1.1.2. Reaction of pentafluoropyridine with benzimidazole

Initial attempts to make compound **109** using benzimidazole instead of imidazole (Scheme 26) led to its formation in a moderate 55% yield. To try to improve the yield slow addition was investigated. The reaction of pentafluoropyridine with benzimidazole in presence of NaH as base and THF as solvent was completed in 24 h at room temperature using a syringe pump to add the benzimidazole slowly. TLC and ^1H NMR spectroscopy indicated the compound **109** was made successfully as a shiny solid in a much improved 98% yield with accurate mass measurement m/z of 268.0491 (MH^+) for $\text{C}_{12}\text{H}_5\text{F}_4\text{N}_3$. The ^{19}F NMR spectrum showed signals for two pairs of fluorine atoms. The m.p. of the crystals was found to be 138-143 °C and the structure confirmed by x-ray crystallography (Figure 22). Therefore the yield was then improved to 98% by use of a syringe pump allowing a more controlled addition.



Scheme 26. Reaction of pentafluoropyridine with benzimidazole.

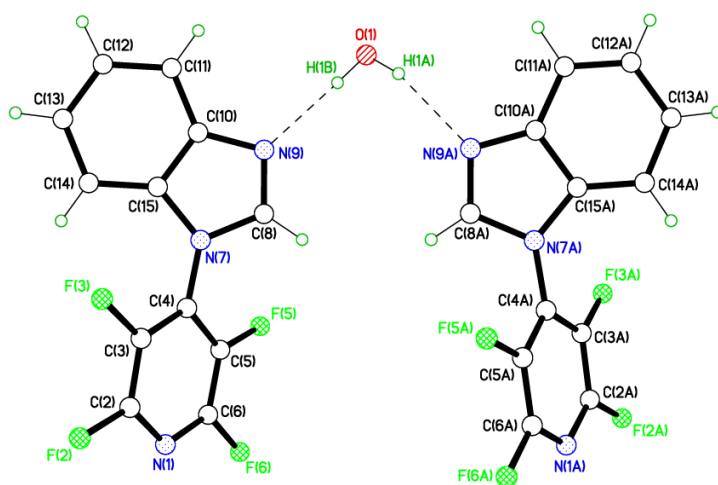
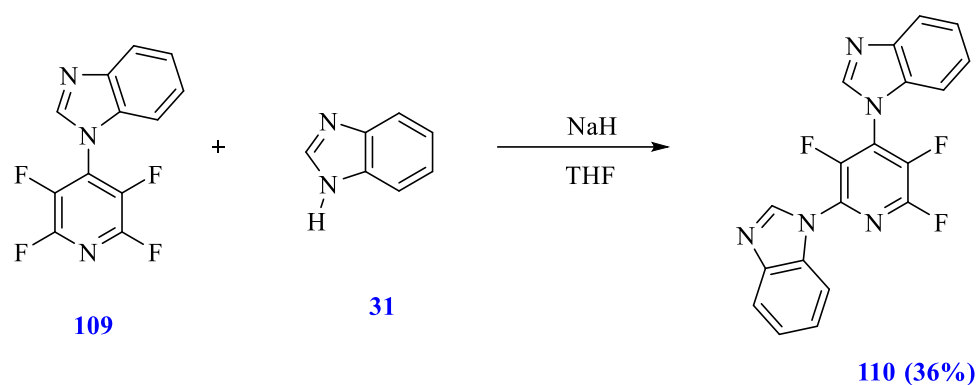


Figure 22. X-ray crystal structure of compound 109 which crystallises with one molecule of water with hydrogen bonds to the N-9 atoms of two benzimidazole rings.

2.1.1.3. Reaction of benzimidazolyltetrafluoropyridine derivative **109** with Benzimidazole

The aim of this reaction was formation of di-product **110** in order to form a linked three ring molecule with better potential as a groove binder for DNA (Scheme 27).



Scheme 27. Reaction of compound 109 with benzimidazole.

Therefore reaction of compound **109** (1 equiv.) with benzimidazole **31** (1 equiv.) was carried out under different conditions (Table 2)

Table 2. Different reaction conditions of compound 109 with benzimidazole

Entry	Reagents	Conditions	Results
1	NaH	THF, RT, 24 h. N ₂	Starting material, unknown compound and product 36%
2	NaH	DMF, RT, 24 h. N ₂	Starting material and product 30%
3	NaH	THF, reflux, 24 h. N ₂	Starting material, unknown compound and product 16%
3	NaH	Dioxane, reflux, 22 h. N ₂	Starting material, product 13%

As seen in table 2 entry 1, reaction in THF at room temperature indicated the best yield of target compound **110** which afforded by column chromatography. The structure was confirmed by ¹H NMR spectroscopy and accurate mass measurement (ESI) (MH⁺), m/z 366.0953 for C₁₂H₅F₄N₃ as expected.

The m.p. of the crystals was 186-190 °C. In addition the exact structure of compound **110** was confirmed by X-ray crystallography (Figure 23).

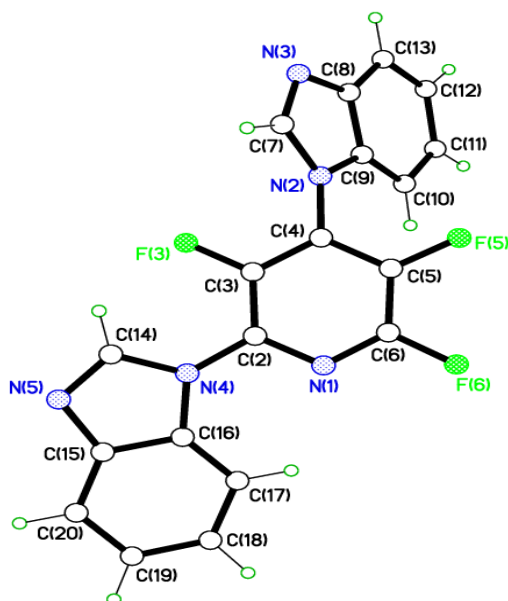
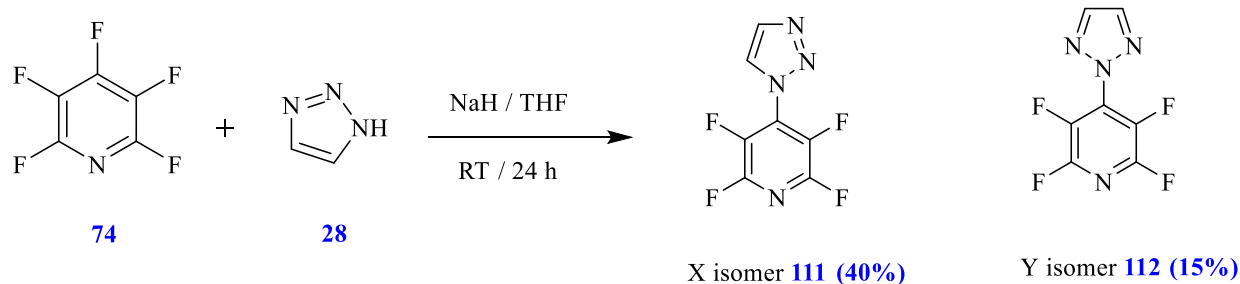


Figure 23. Crystal structure of compound. **110**.

2.1.1.4. Reaction of pentafluoropyridine with triazole

The aim of this reaction (Scheme 28) was to complete the synthesis of another biheteroaryl compound containing 1,2,3-triazole and a perfluoropyridine ring as a scaffold with possible interaction with DNA. The reaction of pentafluoropyridine with triazole (ratio 2:1) in presence of NaH as base and THF as solvent for 24 h at RT was carried out successfully. ^{19}F and ^1H NMR spectra indicated the presence of two different compounds in the product. The product mixture was purified by column chromatography using 6:4 light petrol:ethyl acetate as eluting solvent to give X isomer **111** as white shiny solid (40%) and 100% ethyl acetate to give Y isomer **112** as shiny light yellow solid (15%). The structures of both isomers were confirmed by ^1H NMR and ^{19}F NMR spectroscopy. The ^1H NMR perfectly proved the difference between each isomer as the ^1H NMR spectrum of isomer X **111** indicated two signals each integrating for 1H, whereas the spectrum of isomer Y **112** showed only 1 signal which integrated for 2H. Also accurate mass measurement of each isomer confirmed the correct structure. Isomer X **111** indicated MS (ESI) (MH^+), m/z 219.0287 for $\text{C}_7\text{H}_3\text{F}_4\text{N}_4$ and isomer Y **112** showed MS (ESI) (MH^+), m/z 219.0289 for $\text{C}_7\text{H}_3\text{F}_4\text{N}_4$ as expected. In addition the exact structure of compound **111** (X isomer) was confirmed by X-ray crystallography (Figure 24).



Scheme 28. Reaction of pentafluoropyridine with 1,2,3-triazole.

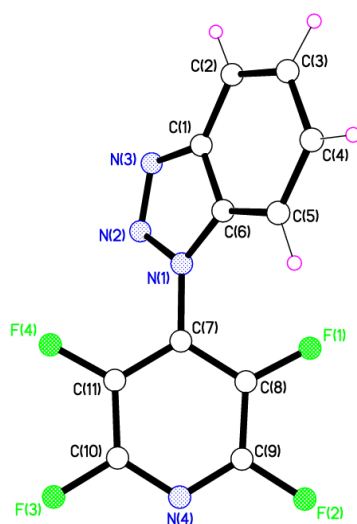
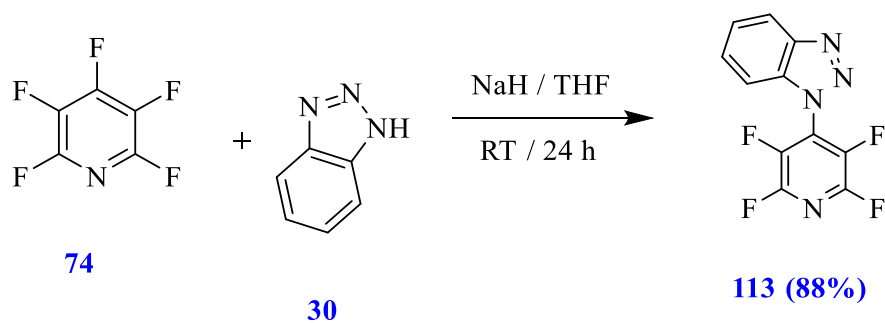


Figure 24. Crystal structure of compound 110.

2.1.1.5. Reaction of pentafluoropyridine with benzotriazole

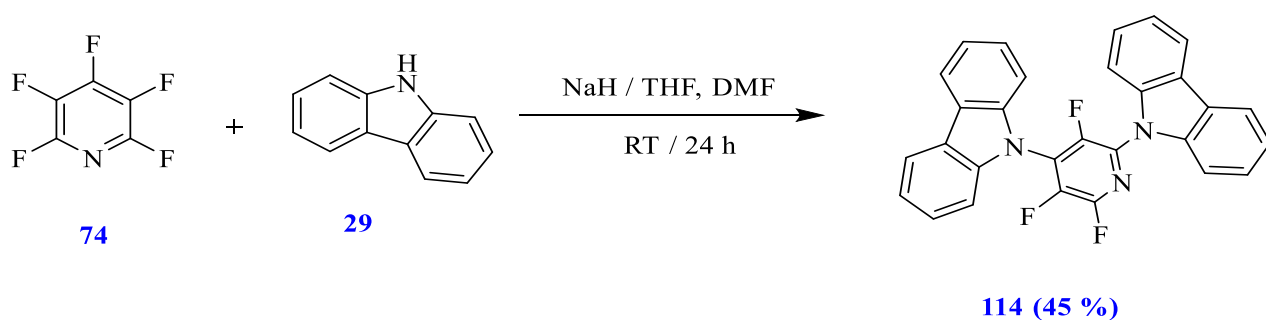
The aim of this reaction (Scheme 29) was to achieve the synthesis of another heteroaryl compound containing benzotriazole and a perfluoropyridine ring in order to have possible interaction with DNA and potential biological activity, as benzotriazole derivatives indicated useful activity in medicinal chemistry. The reaction of pentafluoropyridine with benzotriazole (ratio 2:1) in presence of NaH as base and THF as solvent for 24h at RT was carried out successfully. The target compound **113** was precipitated by adding the water to give a white solid in 88% yield. The structure was confirmed by the ^{19}F and ^1H NMR spectra with the ^{19}F NMR spectrum displaying two signals, each corresponding to 2 F as expected. Also accurate mass measurement (ESI) (MH^+), m/z 269.0443 confirmed the expected formula, $\text{C}_{12}\text{H}_5\text{F}_4\text{N}_4$.



Scheme 29. Reaction of pentafluoropyridine with benzotriazole.

2.1.1.6. Reaction of pentafluoropyridine with carbazole

Reaction of pentafluoropyridine **74** with carbazole **29** was carried out at RT in the presence of NaH as base and a mixture of THF and DMF as solvents (Scheme 30). TLC analysis showed the presence of the starting carbazole **29**, and column chromatography purification allowed us to get the target product **114** as white crystals in 45 % yield. ^1H NMR and ^{19}F NMR spectroscopy proved the presence of the compound **114** with the ^{19}F NMR spectrum displaying 3 signals, each corresponding to 1 F as expected. Also mass spectrometry found the expected mass of the compound MS (ESI) (MH^+), $\text{C}_{29}\text{H}_{17}\text{F}_3\text{N}_3$ requires m/z 464.1369 found m/z 464.1370. In addition the exact structure of compound **114** was confirmed by X-ray crystallography (Figure 25).



Scheme 30. Reaction of pentafluoropyridine with carbazole.

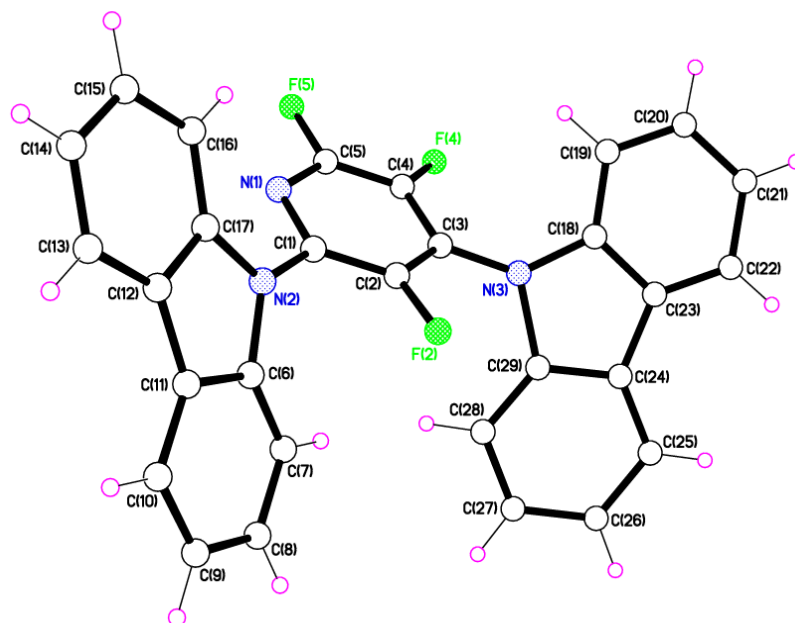
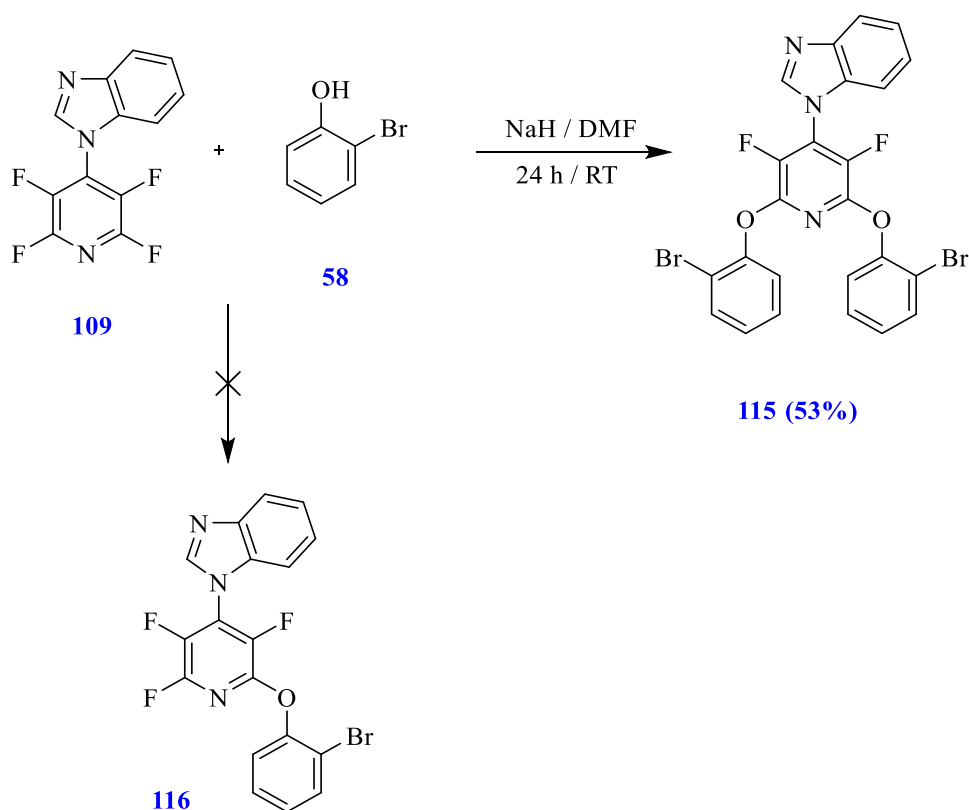


Figure 25. Crystal structure of compound 114.

2.1.1.7. Reaction of 2-bromophenol with compound 109

The aim of this reaction was the synthesis of polycyclic compounds with more than one heteroatom in their chemical structure in order to have potential interaction with DNA and useful biological activity. The reaction of compound **109** with 2-bromophenol in the presence of NaH as base and THF as solvent at room temperature for 24 h did not successfully afford the expected compound **116** (Scheme 31). The ^1H NMR and GC mass spectra did not show the product formed. Optimization of reaction condition showed that changing the solvent to DMF was essential to complete reaction and formation of product, although the TLC and NMR analysis showed presence of small quantity of impurity. After recrystallization, the product **115**, in which two molecules of bromophenol had added, was formed in 53% yield and confirmed by ^1H NMR spectroscopy and accurate mass measurement with m/z of 573.9383 for $\text{C}_{24}\text{H}_{15}\text{Br}_2\text{F}_2\text{N}_3\text{O}_2$. Moreover, the ^{19}F NMR spectrum showed one signal for one pair of fluorine atoms indicating that 2,6-disubstitution had occurred. Also product showed a m.p of 178-181 $^\circ\text{C}$.

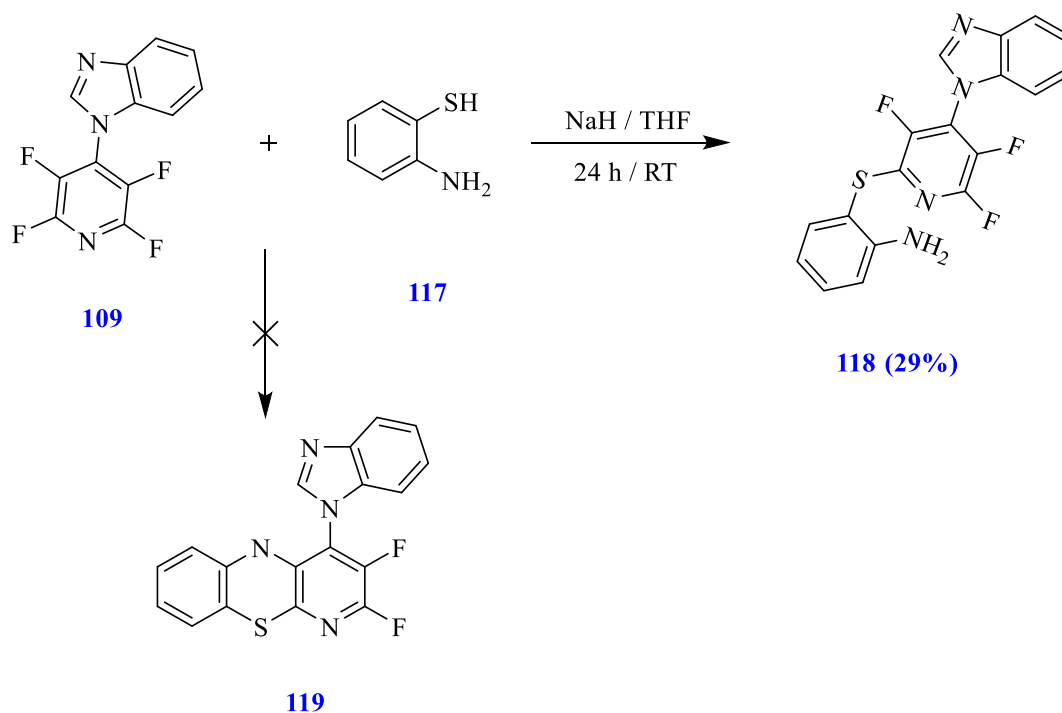


Scheme 31. Reaction of 2-bromophenol with compound 109.

2.1.1.8. Reaction of 2-aminothiophenol with compound 109

The aim of this reaction was synthesis of higher polycyclic compounds with more than one heteroatom in their chemical structure in order to have good interaction with DNA and enhance biological activity. The reaction of compound **109** with 2-aminothiophenol **117** in the presence of NaH as base and THF as solvent at room temperature for 24 h did not successfully afford the expected tricyclic compound **119** (Scheme 32). TLC revealed that some starting material was still present with two products being formed.

After column chromatographic purification the compound **118** was obtained in 29% yield as dark red solid which was confirmed by its ^1H NMR spectrum and high resolution mass spectrum (scheme 32). The accurate mass of 374.0728 matched the expected formula of $\text{C}_{18}\text{H}_{12}\text{F}_3\text{N}_4\text{S}$. While the ^{19}F NMR spectrum showed three signals for three fluorine atoms as expected. Also IR spectroscopy indicated the presence of a NH group by the signal at 3355 cm^{-1} .



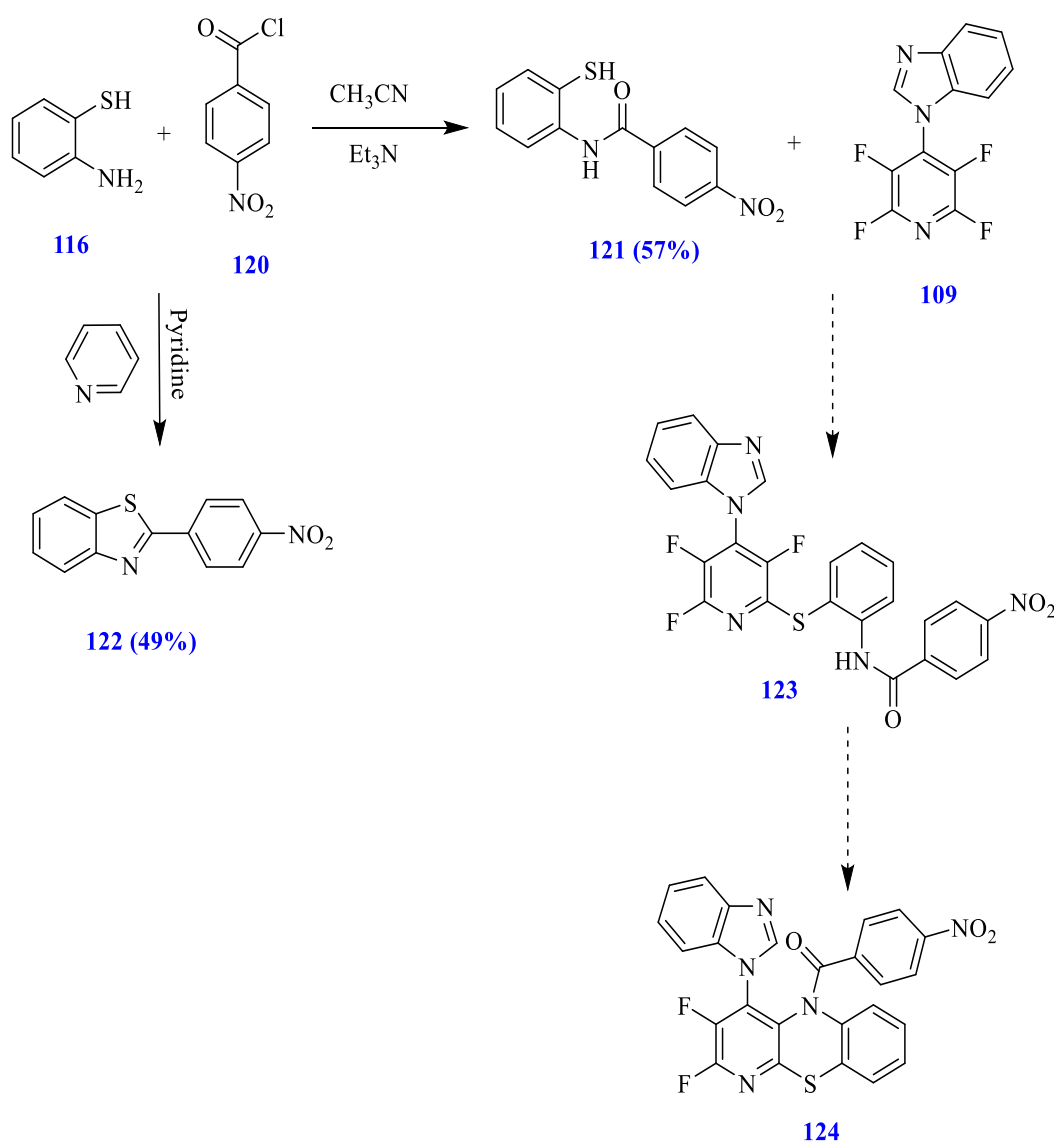
Scheme 32. Reaction of the 2-aminothiophenol with compound 109.

2.1.1.9. Reaction of 2-aminobenzenethiol with 4-nitrobenzoyl chloride

The aim of this reaction was the synthesis of target compound **121** as a starting compound for further reaction with pentafluoropyridine. It was hoped acylating the amino group would render the NH group more acidic and allow deprotonation to activate the nitrogen to nucleophilic attack leading to formation of the desired tricyclic thiazine derivative **124** (Scheme 33).

To synthesise target, *N*-(2-mercaptophenyl)benzamide **121**, 2-aminobenzenethiol was reacted with 4-nitrobenzoyl chloride **120** in the presence of Et₃N (base) and THF (solvent) at room temperature for 24 h. The ¹H NMR and mass analysis indicated some impurity and product was formed only in very low yield. Optimization of reaction conditions showed that changing the solvent to acetonitrile (CH₃CN) was essential to give complete reaction and formation of target product in 57% yield, which was confirmed by ¹H NMR spectroscopy and accurate mass measurement of 273.0339 for C₁₃H₁₀N₂O₃S. In addition the IR data proved the presence of NH and carbonyl groups with peaks at 3348.54 and 1681.98 cm⁻¹. Also the m.p. of the product was 178-181 °C. The thiol **121** was found to undergo easy oxidation in air to the disulfide. This then meant that an additional step to reduce the disulfide bond would be required for the proposed reactions with fluoroarenes.

2-(4-Nitrophenyl)benzothiazole **122** was formed when the reaction of 2-aminobenzenethiol with 4-nitrobenzoyl chloride was carried out in pyridine (as base and solvent) at room temperature for 24 h, showing it was unsuitable as a solvent to form **121** leading to dehydration and ring closure. The structure was confirmed by ^1H NMR spectroscopy and accurate mass measurement with m/z of 257.0377 for $\text{C}_{13}\text{H}_8\text{N}_2\text{O}_2\text{S}$. In addition in the IR spectrum, disappearance of the NH and carbonyl peaks at 3348.54 and 1681.98 cm^{-1} proved that cyclization of compound **121** had occurred, and compound **122** had formed. The m.p. of the product was 224-229 $^\circ\text{C}$. Due to the difficulty in preparing **121** and its easy aerial oxidation to the corresponding disulfide, it was not possible to study its reaction with **109** to make fused products such as **124**.



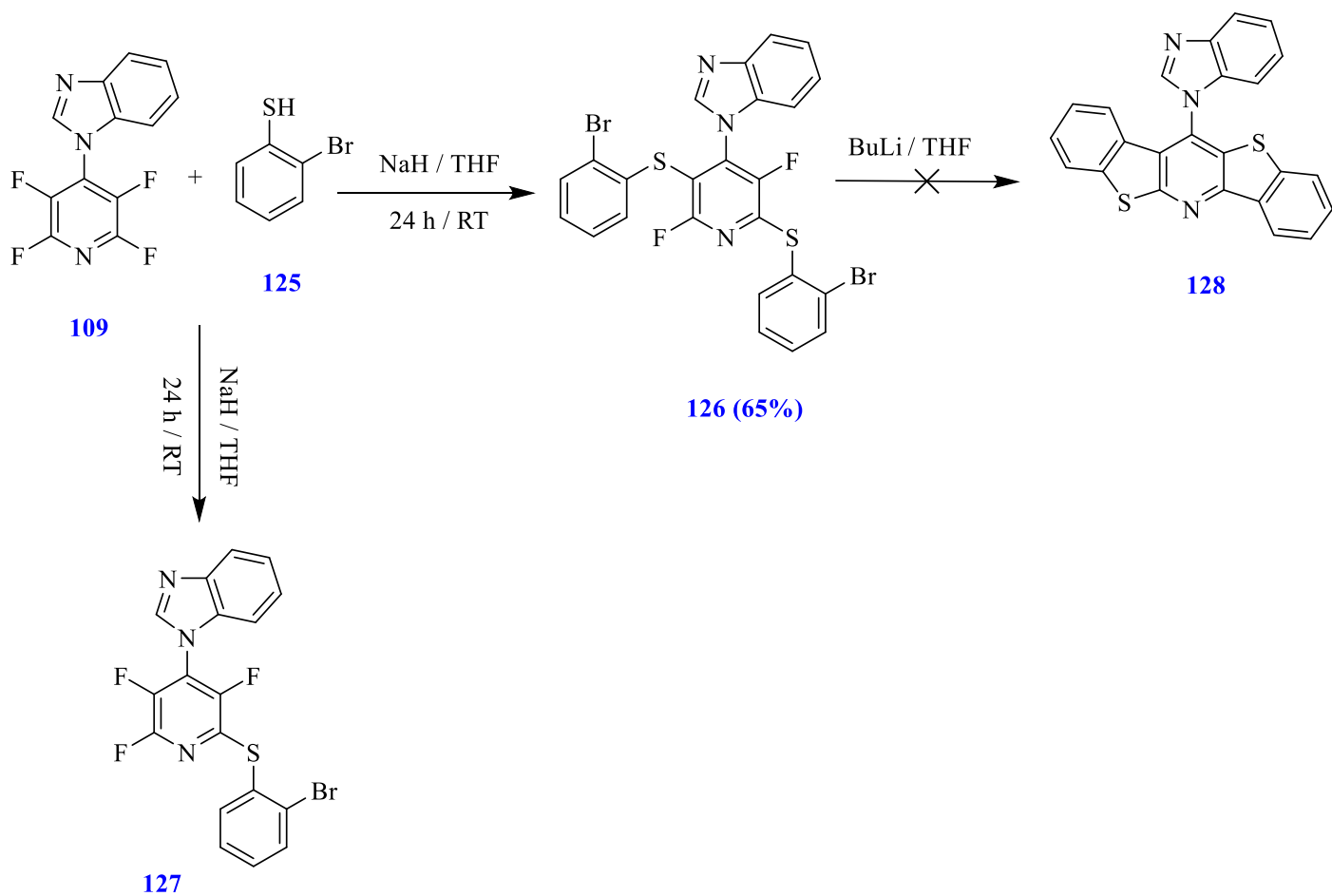
Scheme 33. Reaction of 2-aminobenzenethiol with 4-nitrobenzoyl chloride.

2.1.1.10. Reaction of 2-bromothiophenol with compound 109

The aim of this reaction was the synthesis of condensed polycyclic compounds which contain more than one electronegative atom such as nitrogen, fluorine, or sulphur in their chemical structure. Introduction of a 2-bromophenylthio- or 2-bromophenoxy-groups has been shown to be a viable method to effect fusion of a benzothiophene or benzofuran ring by bromine-lithium exchange, and intermolecular S_NAr reaction. The reaction of 2-bromothiophenol **125** with compound **109** in presence of NaH as base and THF as solvent was thus carried out over 24 h at room temperature. TLC and NMR revealed that some starting material (compound **109**) was still present. However after recrystallization from hot ethanol the formation of difluoropyridine derivative **126** in 65% yields was confirmed by 1H NMR spectroscopy and accurate mass measurement at 603.8952 for $C_{24}H_{13}Br_2F_2N_3S_2$. The ^{19}F NMR spectrum showed two signals for two fluorine atoms as expected for the 2,4,5 trisubstituted pyridine. Also the m.p. of the crystals was 166-170 °C. In addition the exact structure of **126** was confirmed by X-ray crystallography (Figure 26).

Cyclisation of dipyrindine derivative **126** (Scheme 34) was attempted with the hope of forming the bis-benzothiophenopyridine **128** but this could not be achieved by using BuLi to effect bromine-lithium exchange.

To minimize the formation of the difluoropyridine derivative **126** and encourage formation of target compound **127**, the reaction was repeated under different conditions. Increasing the amount of tetrafluoropyridine derivative **109** (2 equiv.), and decreasing the time of reaction at 0 °C was studied. The NMR spectra and accurate mass indicated that even under these conditions still compound **126** was still the main product and compound **127** did not form.



Scheme 34. Reaction of 2-bromothiophenol with compound 109.

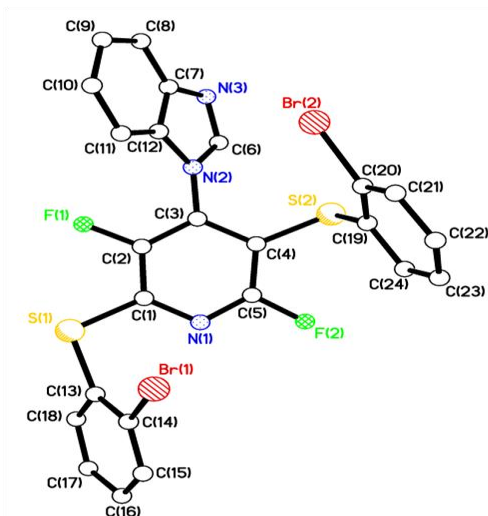
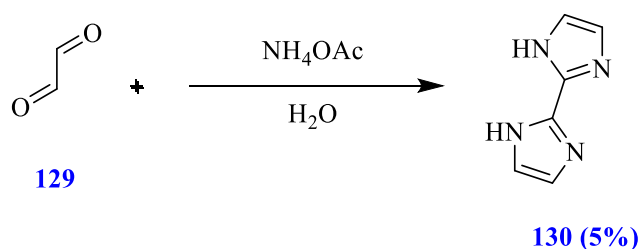


Figure 26. crystal structure of compound 126.

2.1.2. Synthesis of Bis N-heterocyclic compounds as starting materials for reaction with fluoroarenes

2.1.2.1. Reaction of glyoxal with ammonium acetate ¹²⁰

The aim of this reaction was synthesis of a bis-imidazole derivative by the condensation of glyoxal **129** (an α -dicarbonyl aldehyde compound) with two equivalents of ammonium acetate in order to use as starting material for further reaction with perfluorinated arenes.⁽²⁾ The known 1*H*,1'*H*-2,2'-biimidazole **130** was formed in a low 5% yield. The structure was confirmed by ¹H NMR spectroscopy and by its mass spectrum with *m/z* 135.0668 for C₆H₇N₄. Also IR spectroscopy indicated the present of a NH group by showing a signal in the region 3000-3500 cm⁻¹. Although the yield is low, the product was easy to isolate by simple filtration and the starting materials were cheap.



Scheme 35. Reaction of glyoxal with ammonium acetate

2.1.3. Synthesis of 2,2-(1,4-butanediyl)-bis-1*H*-imidazole and 2,2-(1,4-butanediyl)-bis-1*H*-benzimidazole

As the 1*H*,1'*H*-2,2'-biimidazole **130** did not dissolve in most organic solvents and showed low reactivity towards perfluorinated compounds, it was decided to prepare a linked bis-imidazole with a flexible spacer as such compounds were of interest as possible cross-linking agents. 2,2-(1,4-butanediyl)-bis-1*H*-imidazole, **132** with long chain hydrocarbon linker to increase their solubility were thus prepared.

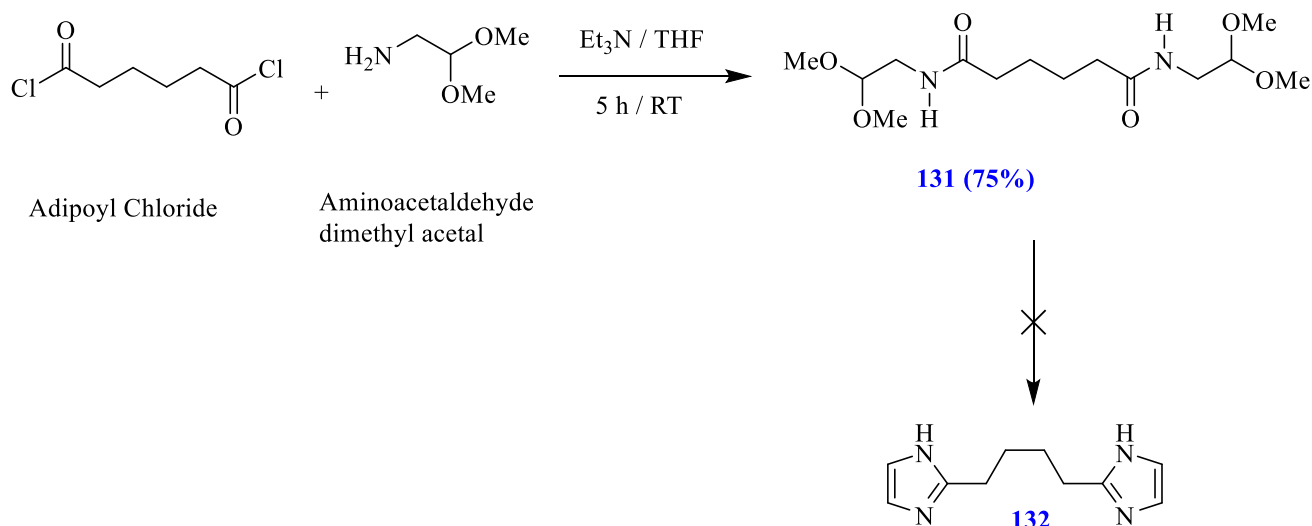
2.1.3.1. Reaction of adipoyl chloride with aminoacetaldehyde dimethyl acetal

The aim of this reaction was to synthesise intermediate compound **131** and to investigate cyclisation with acid to prepare target compound **132**. The reaction of adipoyl chloride with aminoacetaldehyde dimethyl acetal in the presence of Et₃N as base and THF as solvent for 5 h at room temperature

successfully afforded the desired product. The compound **131** was formed in 75% yield as white solid and its structure confirmed by its ^1H NMR spectrum and by its mass spectrum with m/z 321.2019 (MH^+) for $\text{C}_{14}\text{H}_{29}\text{O}_6\text{N}_2$. Also the IR spectrum indicated the present of NH group by showing the signal in area $3000\text{--}3500\text{ cm}^{-1}$ (broad peak). The compound **131** had an m.p of $93\text{--}95\text{ }^\circ\text{C}$. The reaction was followed by treating the successfully made compound **132** with different acid conditions (Table 3) with the aim of converting the acetyl groups to aldehydes and promoting cyclisation to the imidazole target compound **132**. Unfortunately the reactions were unsuccessful, and none of the conditions tried led to formation of target compound **132** as seen in (Scheme 36).

Table 3. different reaction conditions for cyclization of compound 132

Entry	Reagents	Conditions	Results
1	AcOH / NH_4OAc	$80\text{ }^\circ\text{C}$, 24 h. N_2	Unsuccessful
2	PPA / NH_4OAc	$80\text{ }^\circ\text{C}$, 24 h. N_2	Unsuccessful
3	$\text{H}_2\text{SO}_4/\text{AcOH}$ / NH_4OAc	$80\text{ }^\circ\text{C}$, 24 h. N_2	Unsuccessful



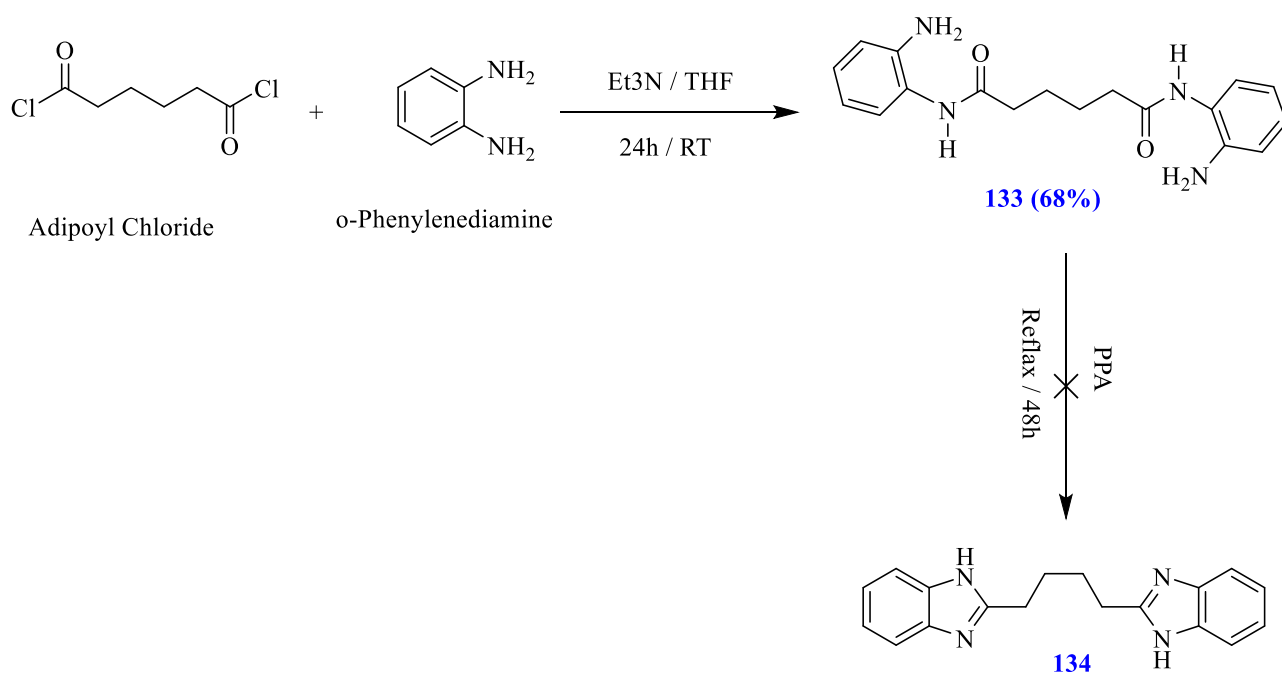
Scheme 36. Reaction of adipoyl chloride with aminoacetaldehyde dimethyl acetal

2.1.3.2. Reaction of adipoyl chloride with *o*-phenylenediamine

The aim this reaction was the synthesis of the linked bis-amide compound **133** and its cyclisation with acid to prepare the target linked benzimidazole **134**. The reaction of adipoyl chloride with *o*-phenylenediamine in the presence of Et_3N as base and THF as solvent for 24 h at room temperature

successfully afforded compound **133** which was formed in 68% yield as a white solid. The structure was confirmed by ^1H NMR spectroscopy and by its mass spectrum with m/z 327.1814 (MH^+) for $\text{C}_{18}\text{H}_{23}\text{O}_2\text{N}_4$. Also the IR spectrum indicated the presence of an NH group by signals in the area $3000\text{-}3500\text{ cm}^{-1}$ (broad peak). The compound **133** had a m.p. of $155\text{-}165\text{ }^\circ\text{C}$.

The reaction was followed by treating the compound **134** with polyphosphoric acid (PPA) at $85\text{ }^\circ\text{C}$ for 48 h. ^1H NMR spectroscopy indicated presence of both cyclised and non-cyclised compounds which unfortunately could not be separated to isolate the target compound due to the high polarity of both compounds.



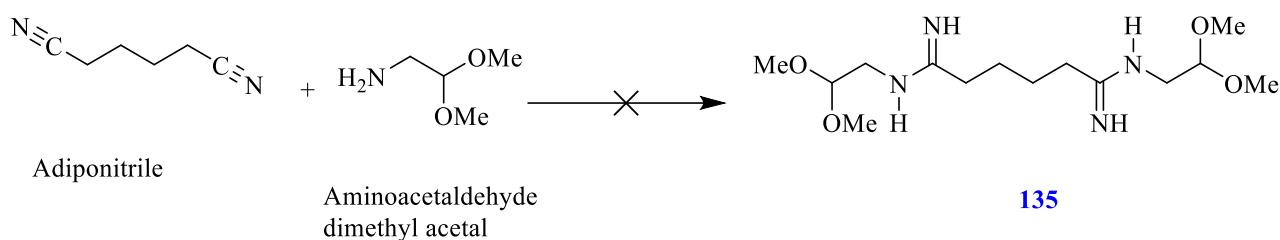
Scheme 37. Reaction of adipoyl chloride with aminoacetaldehyde methyl ester.

2.1.3.3. Reaction of adiponitrile with aminoacetaldehyde dimethyl acetal

As synthesis of compound **132** by using the adipoyl chloride was not successful as shown in scheme 36, it was decided to study the reaction of adiponitrile, to change the carbonyl group in compound **131** to an imine which might help cyclisation and allow preparation of target compound **132**. Therefore the reaction of adiponitrile with aminoacetaldehyde dimethyl acetal was carried out under different conditions (Table 4). However, the reactions did not work at all and ^1H NMR spectroscopy indicated only the presence of starting material (adiponitrile) and the target compound **135** did not formed. (Scheme 38).

Table 4. different reaction conditions attempted for the formation of compound 135.

Entry	Reagents	Conditions	Results
1	Cu(OTf) ₂	THF /reflux, 24 h, N ₂	no reaction
2	-	THF/reflax, 24 h, N ₂	no reaction
3	-	reflux, 24 h, N ₂	no reaction



Scheme 38. Reaction of adiponitrile with aminoacetaldehyde dimethyl acetal.

2.1.3.4. Synthesis of imidate and formation of the target compound **132** and **134**

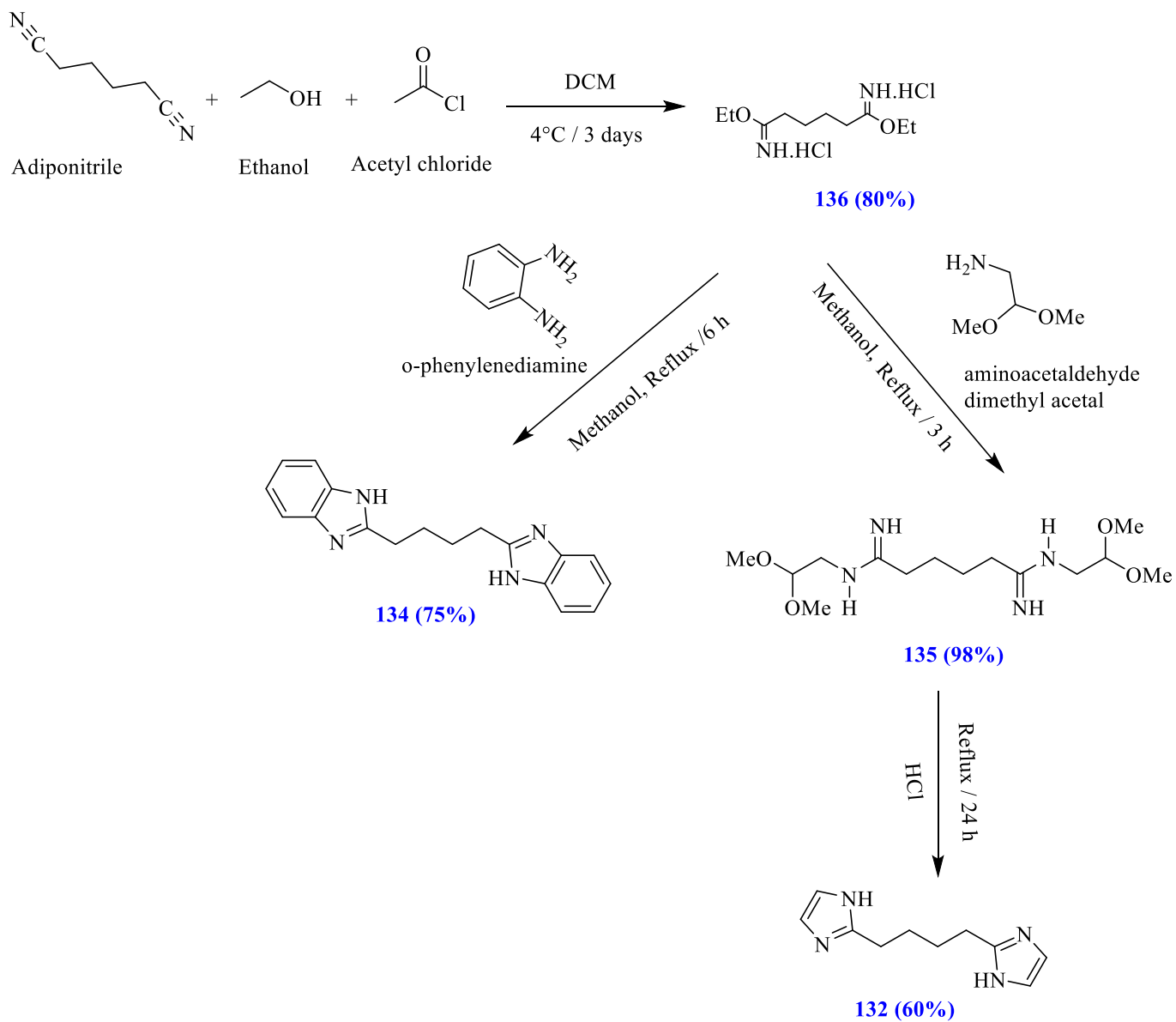
The aim of these reactions was formation of imidate **136** as starting material to react with aminoacetaldehyde dimethyl acetal and *o*-phenylenediamine to allow synthesis of target compounds **132** and **134** which could not be formed using the conditions above.

The reaction of adiponitrile with ethanol and acetyl chloride in DCM was completed in 3 days at 4 °C. The imidate salt **136** formed as white solid in 80% yield and was confirmed by ¹H NMR spectroscopy. Also the IR spectrum indicated the present of a NH group by showing a signal at 3000-3500 cm⁻¹. Compound **136** had a m.p. of 135-136 °C.

The intermediate compound **136** then reacted successfully with aminoacetaldehyde dimethyl acetal in methanol as solvent at 65 °C for 3 h. The compound **135** was formed as a yellow syrup in 98% yield, and was confirmed by its ¹H NMR spectrum and accurate mass measurement with *m/z* of 319.2315 (MH⁺) for C₁₄H₃₁O₄N₄. Also the IR spectrum indicated the present of the NH group with a signal at 3000-3500 cm⁻¹.

Compound **135** was treated successfully with 37% HCl at 65 °C for 24 h to synthesise target bis-imidazole **132** as a brown solid in 60% yield (Scheme 39). The structure was confirmed by ¹H NMR and ¹³C NMR spectroscopy. However, the ¹H NMR spectrum recorded in DMSO showed two singlet

signals at 6-7 ppm for 4H atoms and one singlet signal for NH at 12 ppm (Figure 27) whereas the ^1H NMR in methanol only indicated one singlet signal at 6.8 ppm for 4H atom and did not show any signal for NH (Figure 28), which could be caused by hydrogen exchange between two nitrogens in methanol. Accurate mass measurement confirmed the correct molecular formula with m/z of 191.1296 (MH^+) for $\text{C}_{10}\text{H}_{13}\text{N}_4$. The compound **132** failed to melt, but decomposed at 168 °C. Reaction of the imidate salt with o-phenylenediamine was carried out successfully in the presence of methanol for 6 h at 80 °C (Scheme 38). The linked benzimidazole **134** formed as a light yellow solid in 75% yield and was confirmed by ^1H NMR and ^{13}C NMR spectroscopy and accurate mass measurement with m/z of 291.1581 (MH^+) for $\text{C}_{18}\text{H}_{18}\text{N}_4$. Also IR spectrum indicated the presence of NH group with a signal in area 3000-3500 cm^{-1} . The compound **134** m.p. was 258-260 °C in agreement with the literature value of 258 °C.³¹ In addition the exact structure of **134** was confirmed by X-ray crystallography (Figure 29).



Scheme 39. Synthesis of bis-imidate to form linked imidazole and benzimidazoles 132 and 134.

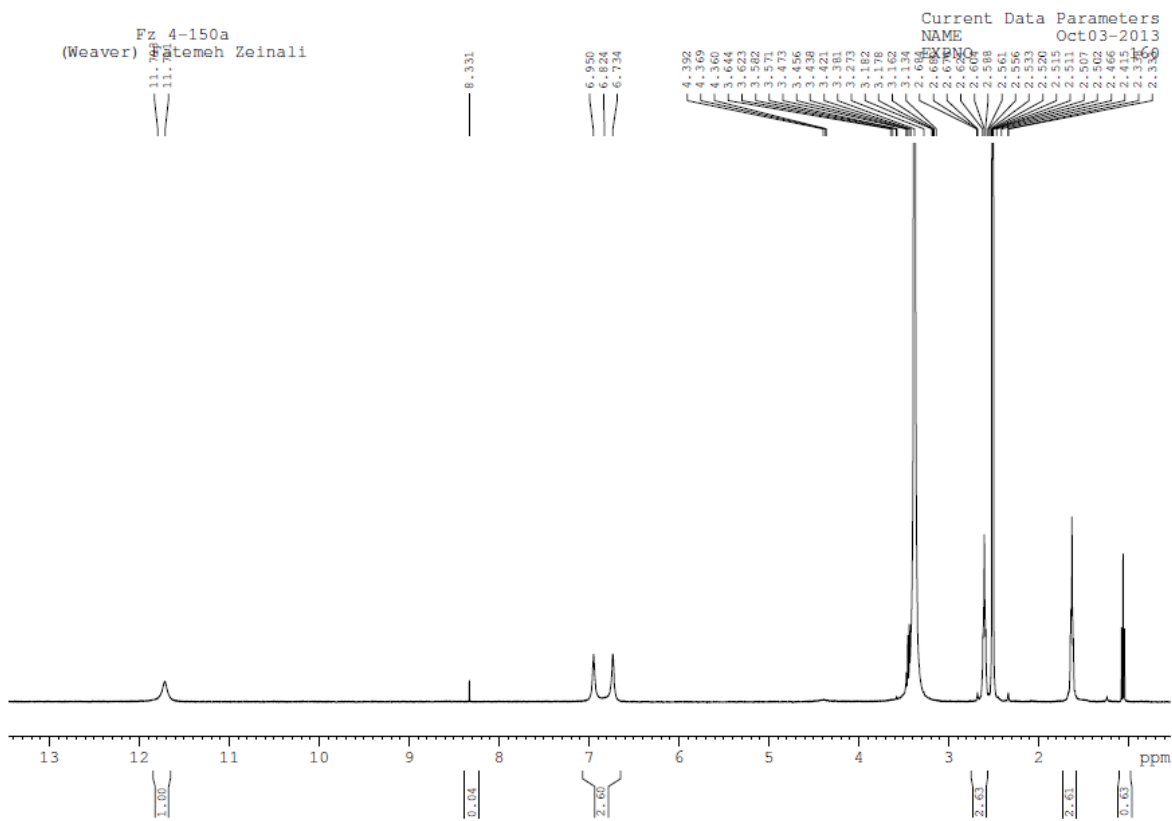


Figure 27. ^1H NMR (400 MHz, DMSO- d_6) spectrum of compound 132.

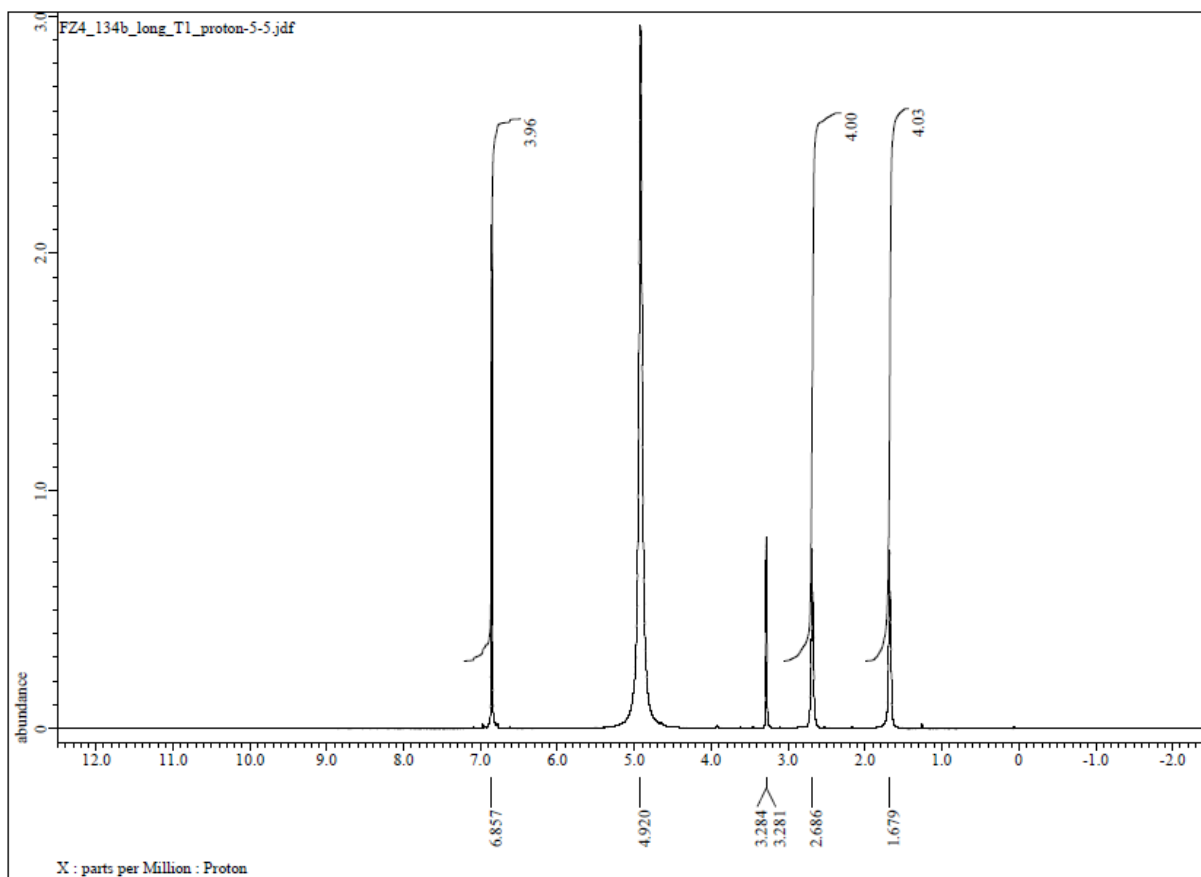


Figure 28. ^1H NMR (400 MHz, methanol- d_4) spectrum of compound 132.

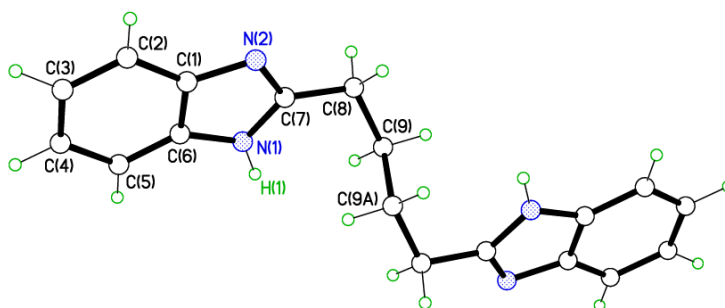


Figure 29. Crystal structure of compound 134.

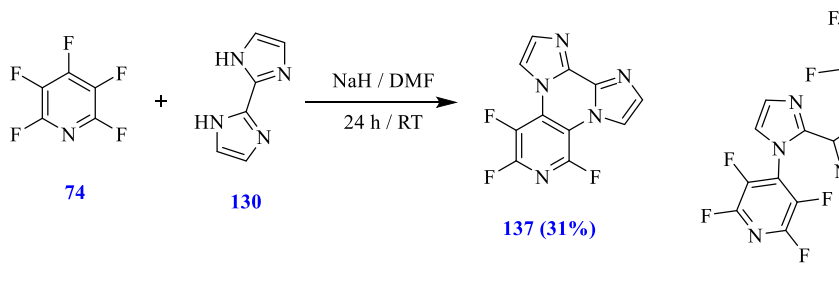
2.1.4. Synthesis of bis-imidazole and bis-benzimidazole containing perfluoro heterocyclic derivatives

Nitrogen containing heterocyclic aromatic compounds such as bis-imidazole and bis-benzimidazole are an important type of nitrogen containing heterocyclic aromatic substances in drug design and synthesis. Also they are of importance in medicinal chemistry due to their biological activity. Moreover, several functional groups are easily introduced into the structurally rigid of bis-imidazole and Bis-benzimidazole ring and alter the biological activities allowing using as cross linking agents for double-stranded DNA.³⁷

We planned to synthesize compounds which contain more than one bio labile constituent, namely bis-imidazole or bis-benzimidazole and fluorinated containing heterocyclic substances to provide a biologically active DNA binding structure as lead scaffolds.

2.1.4.1. Reaction of the pentafluoropyridine with 1H,1H-2,2'-biimidazole

The reaction of pentafluoropyridine **74** with 1H,1H-2,2'-biimidazole **130** in the presence of NaH as base and dry DMF as solvent was conducted over 24 h at room temperature. TLC revealed that two compounds formed and some starting material was still present. By adding water compound **138** (0.14 g, 33%) was precipitated and collected as white solid. After an extraction process compound **137** (0.08 g, 31%) was isolated. Their structures confirmed by ¹H NMR spectroscopy and accurate mass measurement with *m/z* of 264.0413 (MH⁺) for C₁₁H₅F₃N₅ for **137**, and 433.0441 (MH⁺) for C₁₆H₅F₈N₆ matching **138**. The ¹⁹F NMR spectra showed three signals (1 F for each signal) for compound **137** and 2 signals (4 F atom for each signal) for compound **138** as expected. Compound **137** had m.p. of 288-295 °C which is much higher than compound **138** (158-164 °C). The structure of **138** was confirmed by X-ray diffraction analysis (Figure 30).



Scheme 40. Reaction of the pentafluoropyridine with 1H,1H-2,2'-biimidazole.

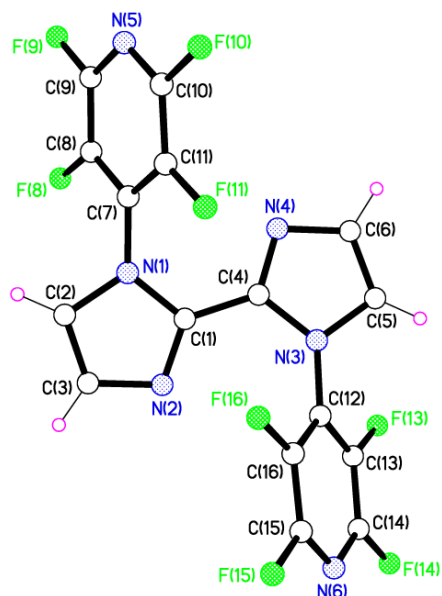
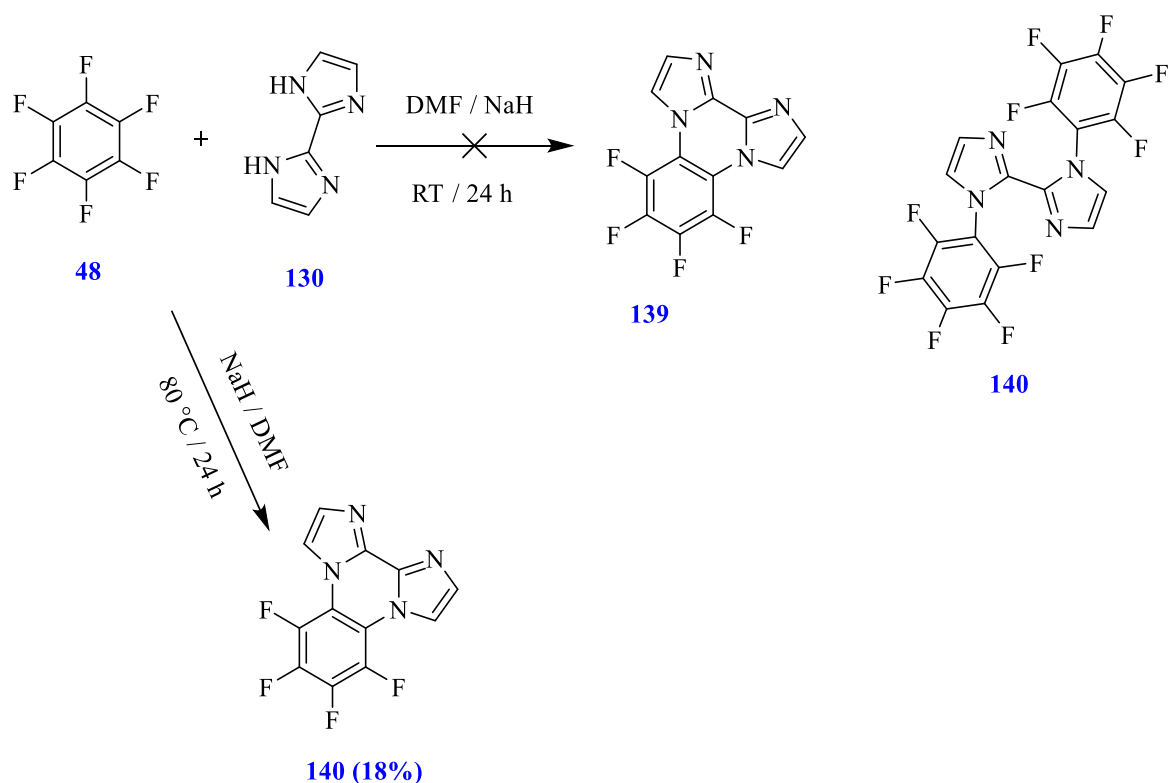


Figure 30. Crystal structure of compound 134.

2.1.4.2. Reaction of the hexafluorobenzene with 1*H*,1*H*-2,2'-biimidazole

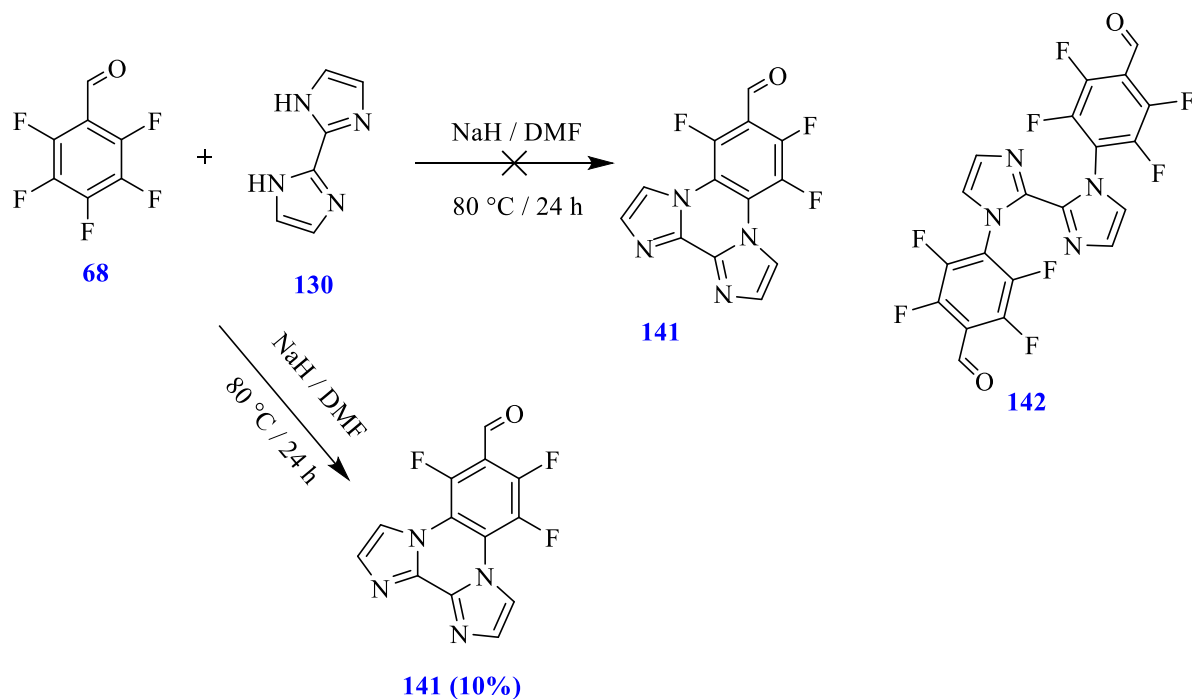
The reaction of hexafluorobenzene **48** (2 equiv.) with 1*H*,1*H*-2,2'-biimidazole **130** (1 equiv.) in the presence of NaH as base and dry DMF as solvent was conducted over 24 h at room temperature. According to the ^1H NMR spectrum and TLC the target compound did not form and starting material was present as the main compound. However, the reaction worked at 80 °C in the presence of NaH as base and dry DMF in 1:3 ratio of starting biimidazole and hexafluorobenzene. After recrystallization from hot ethanol the product **139** was obtained as a brown solid (18% yield) and the structure confirmed by ^1H NMR spectrum and accurate mass measurement with m/z of 281.0433 (MH^+) for $\text{C}_{12}\text{H}_5\text{F}_4\text{N}_4$. The ^{19}F NMR spectrum showed two signals (2F for each environment) as expected. No evidence for the formation of **140** was obtained.



Scheme 41. Reaction of the pentafluoropyridine with 1H,1H-2,2'-biimidazole.

2.1.4.3. Reaction of the pentafluorobenzaldehyde with 1H,1H-2,2'-biimidazole.

The reactions of pentafluorobenzaldehyde **68** with 1H,1H-2,2'-biimidazole **130** in 1:1 and 2:1 ratios were attempted with NaH as base and dry DMF as solvent and were conducted over 24 h at room temperature. TLC and NMR of both reactions revealed mixtures of different compound formed. Attempts to separate and purify the products by repeated recrystallization methods were unsuccessful. Attempts to isolate pure product by column chromatography afforded five fractions, but the ^1H NMR spectra of all fractions indicated they were still not pure. However, the reaction worked after heating the reactants in DMF at 80 °C for 24 h in the presence of NaH as base and in a 1:1 ratio. After recrystallization from DCM and light petrol the product **141** was obtained as a yellow solid in 10% yield, and the structure confirmed by ^1H NMR spectroscopy and accurate mass measurement with m/z of 291.476 (MH^+) for $\text{C}_{13}\text{H}_6\text{F}_3\text{N}_4$. The ^{19}F NMR spectrum showed three signals (1F for each signal) indicating cyclisation had occurred to form **141** rather than **142**.

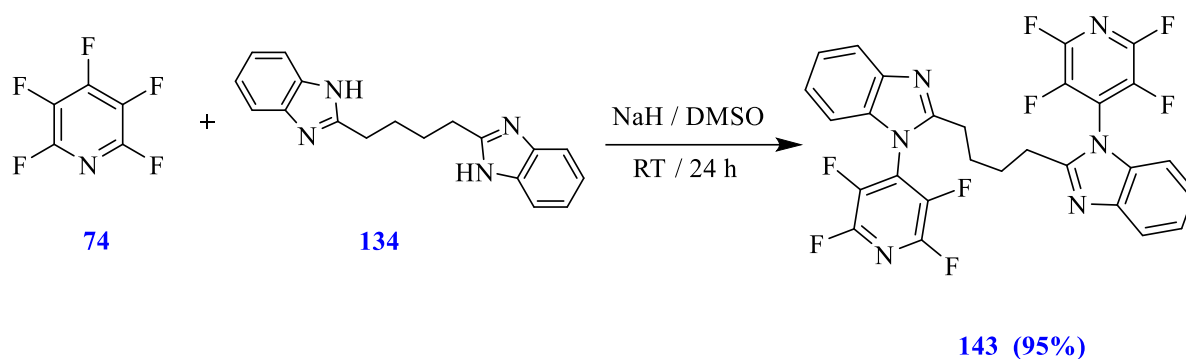


Scheme 42. Reaction of pentafluorobenzaldehyde with 1H,1H-2,2'-biimidazole.

2.1.4.4. Reaction of pentafluoropyridine with Bis-benzimidazole 134

The reaction of pentafluoropyridine **74** (3 equiv) with bis-benzimidazole **134** (1 equiv.) was studied under two conditions; the first was with NaH as base and dry DMF as solvent over 24 h at room temperature. TLC and ^1H NMR spectroscopy indicated a mixture of different compounds. Therefore different crystallization methods were tried to isolate pure product, but they were unsuccessful and the ^1H NMR spectrum of the product mixture was messy and complicated.

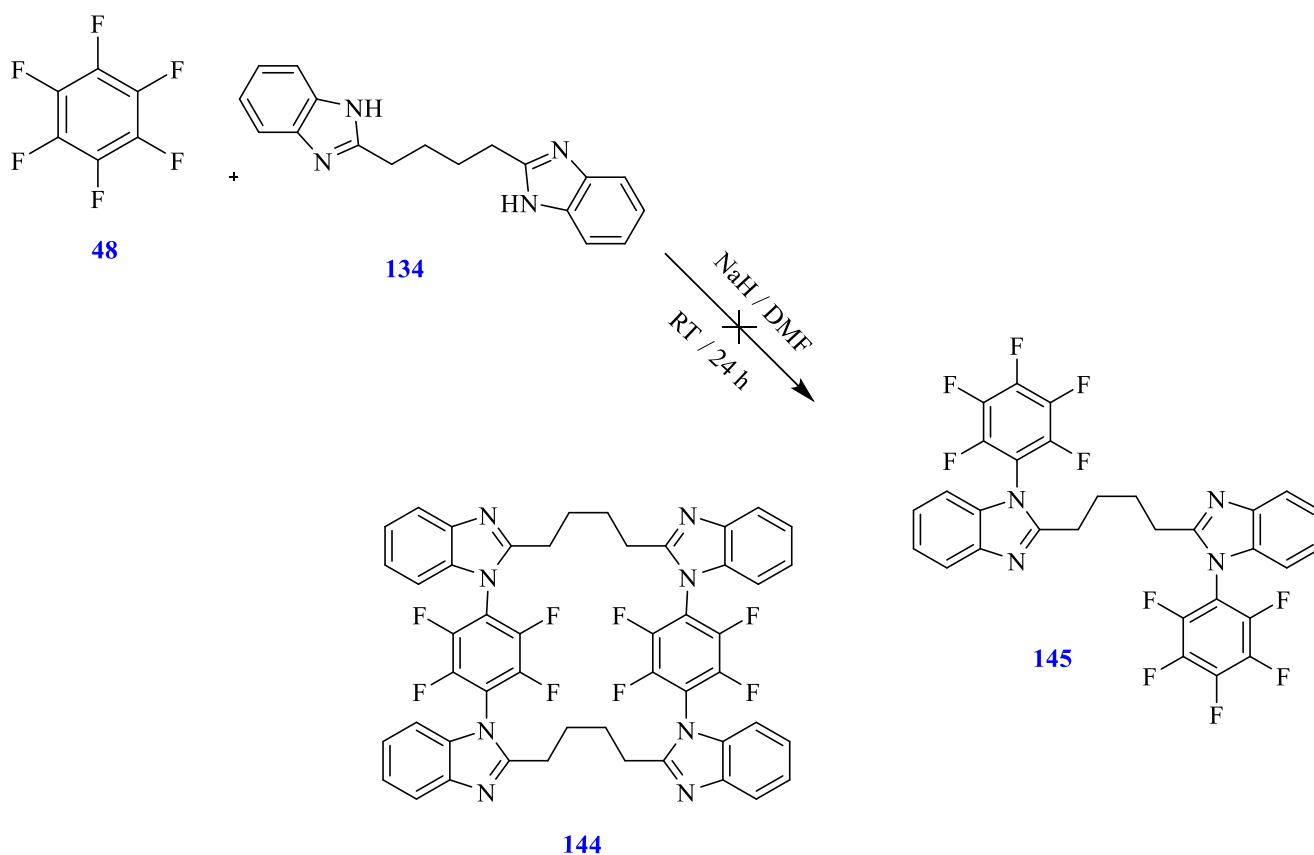
The second condition employed DMSO as solvent instead of DMF and bis-benzimidazole was added dropwise by syringe pump. TLC revealed one main compound formed with only a trace impurity. After recrystallization from hot toluene, the product **143** (95%) was obtained as a white solid, and the structure assigned by ^1H NMR spectroscopy and accurate mass measurement with m/z of 589.1376 (MH^+) for $\text{C}_{28}\text{H}_{17}\text{F}_8\text{N}_6$. The ^{19}F NMR spectrum showed 2 signals (4 F atom for each signal) as expected. Compound **143**, had a m.p of 197-198 $^\circ\text{C}$.



Scheme 43. Reaction of the pentafluoropyridine with bis-benzimidazole 134.

2.1.4.5. Reaction of the hexafluorobenzene with bis-benzimidazole 134

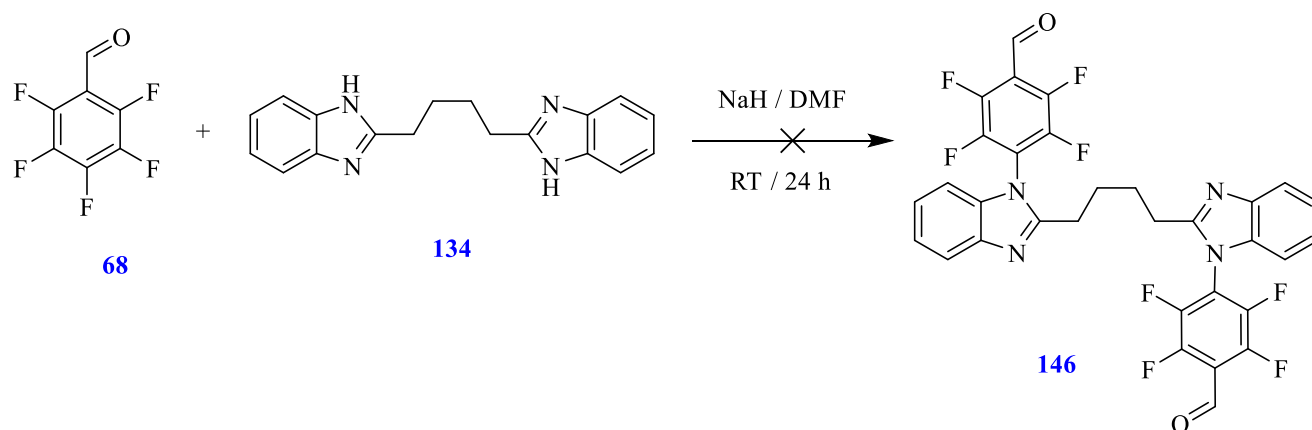
The reaction of hexafluorobenzene **48** with bis-benzimidazole **134** was tried under two conditions; firstly with NaH as base and dry DMF as solvent over 24 h at room temperature using a 10:1 ratio of hexafluorobenzene and bis-benzoimidazole. TLC indicated very polar products were formed and the ^1H NMR spectrum showed broad complex signals in the aromatic region. A different recrystallization method were tried but was unsuccessful and neither **144** nor **145** could be obtained. The second experiment used syringe pump addition of the bis-benzimidazole. This time TLC showed many spots which indicated many compounds formed. Recrystallization was attempted but was unsuccessful. Preparative TLC was then employed but only one component of the mixture was isolated pure, but proved to be in a negligible amount to characterise, while other spots were very close together and could not be separated. Also at the base line, preparative TLC showed a fluorescent compound formed, which was isolated but has not yet proved possible to identify.



Scheme 44. Reaction of the pentafluoropyridine with bis-benzimidazole 134.

2.1.4.6. Reaction of pentafluorobenzaldehyde with bis-benzimidazole 134

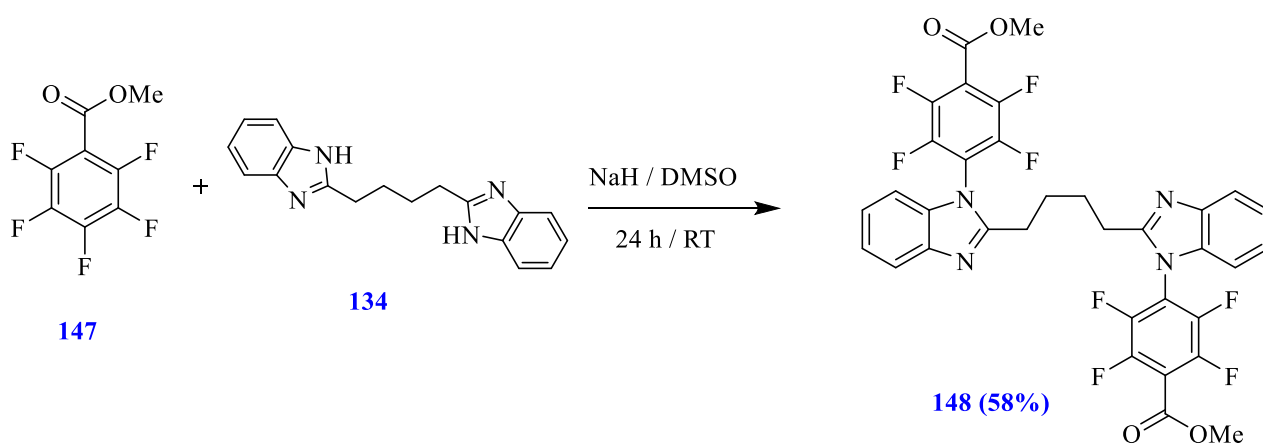
The reaction of pentafluorobenzaldehyde (2 equiv.) with bis-benzimidazole **134** (1 equiv.) was carried out in the presence of NaH as base and dry DMF as solvent over 24 h at room temperature using a syringe pump to ensure slow addition. The compound formed was a red solid which tailed on the TLC plate, and ^1H NMR spectroscopy showed only broad, messy peaks in the aromatic reaction. Attempts to isolate a pure product by recrystallization or chromatography were unsuccessful and no evidence for the formation of **146** could be obtained. (Scheme 45)



Scheme 45. Reaction of pentafluorobenzaldehyde with bis-benzimidazole 134.

2.1.4.7. Reaction of compound **134** with methyl pentafluorobenzoate

The reaction of methyl pentafluorobenzoate **147** (2 equiv.) with bis-benzimidazole **133** (1 equiv.) was carried out in presence of NaH as base and DMSO as solvent over 24 h at room temperature. TLC revealed one main compound formed with only a trace impurity. After recrystallization from hot ethanol, the product **148** (58%) was obtained as a white solid, and the structure assigned by ^1H NMR spectroscopy and accurate mass measurement with m/z of 703.1569 (MH^+) for $\text{C}_{34}\text{H}_{23}\text{F}_8\text{O}_4\text{N}_6$. The ^{19}F NMR spectrum showed 2 signals (4 F atoms for each signal) as expected. Compound **148**, had a m.p of 195-198 °C



Scheme 46. Reaction of compound 134 with methyl pentafluorobenzoate.

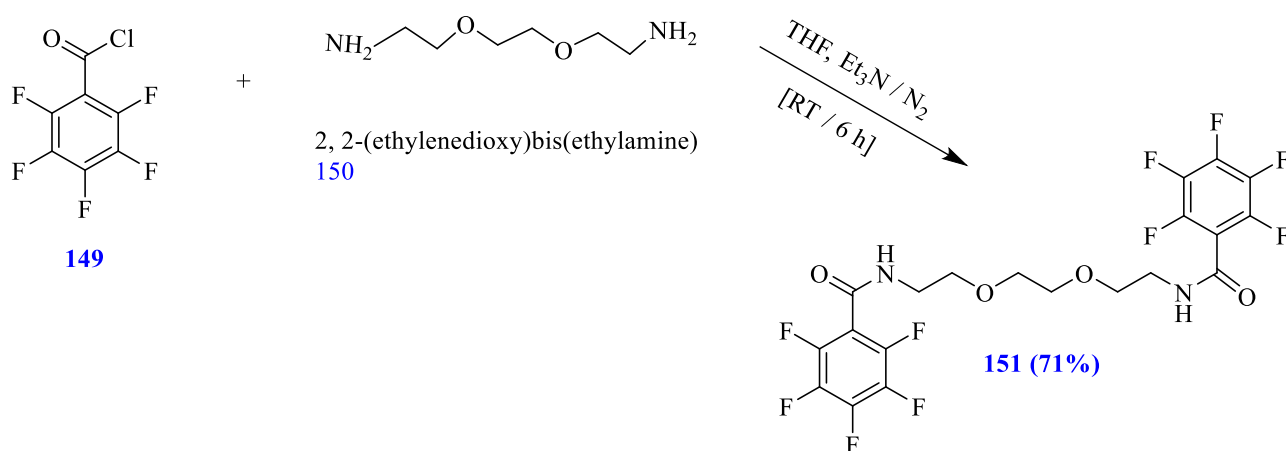
2.1.5. Synthesis of bis-linked binding agents via formation of an amide bond

Organic bis-linked binding agents are compounds that interact with double stranded DNA, usually reversibly. Bis-linked binding compounds contain two possible intercalating ring systems connected together by a linker. Bis-linked binding agents have higher DNA binding constants due to more than one intercalating unit and can exhibit sequence selectivity and show slower dissociation than mono compounds.

Therefore it was planned to exploit the reactivity of the acyl halide group in derivatives of pentafluorobenzoyl chloride towards di-amide formation by reaction with long chain diamines. It was hoped that diamide compounds would act as bis-nucleophiles and allow two potential binding compounds to be linked together to increase their DNA binding potency. The pentafluorophenyl benzamides could also be used as starting compounds for further functionalization to improve activity.

2.1.5.1. Reaction of pentafluorobenzoyl chloride with 2,2-(ethylenedioxy)bis(ethylamine)

In order to synthesise fluorinated bis-intercalating compounds, reaction of pentafluorobenzoylchloride **149** with the aliphatic amine 2, 2-(ethylenedioxy)bis(ethylamine) **150** was investigated in a 2:1 ratio at RT in THF as solvent and with Et₃N as base. The target compound **151** was afforded in 75% yield (Scheme 47). ¹⁹F NMR spectroscopy displayed the expected fluorine signals for the target compound, δ_F (376 MHz, CDCl₃) 21.14-21.22 (4F, m), 11.04-11.20 (2F, m), 1.79-1.81(4F, m) and mass spectrometry gave the mass of the expected compound **151**, MS (ESI) (MH⁺), C₂₀H₁₄O₄F₁₀N₂ requires m/z 537.0867, found m/z 537.0867. The structure of **151** was confirmed by X-ray diffraction analysis (Figure 31), m.p. 128 - 129 °C.



Scheme 47. Reaction of pentafluorobenzoyl chloride and 2,2-(ethylenedioxy)bis(ethylamine).

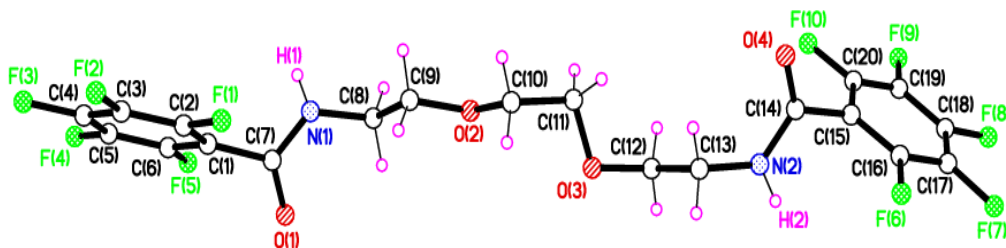


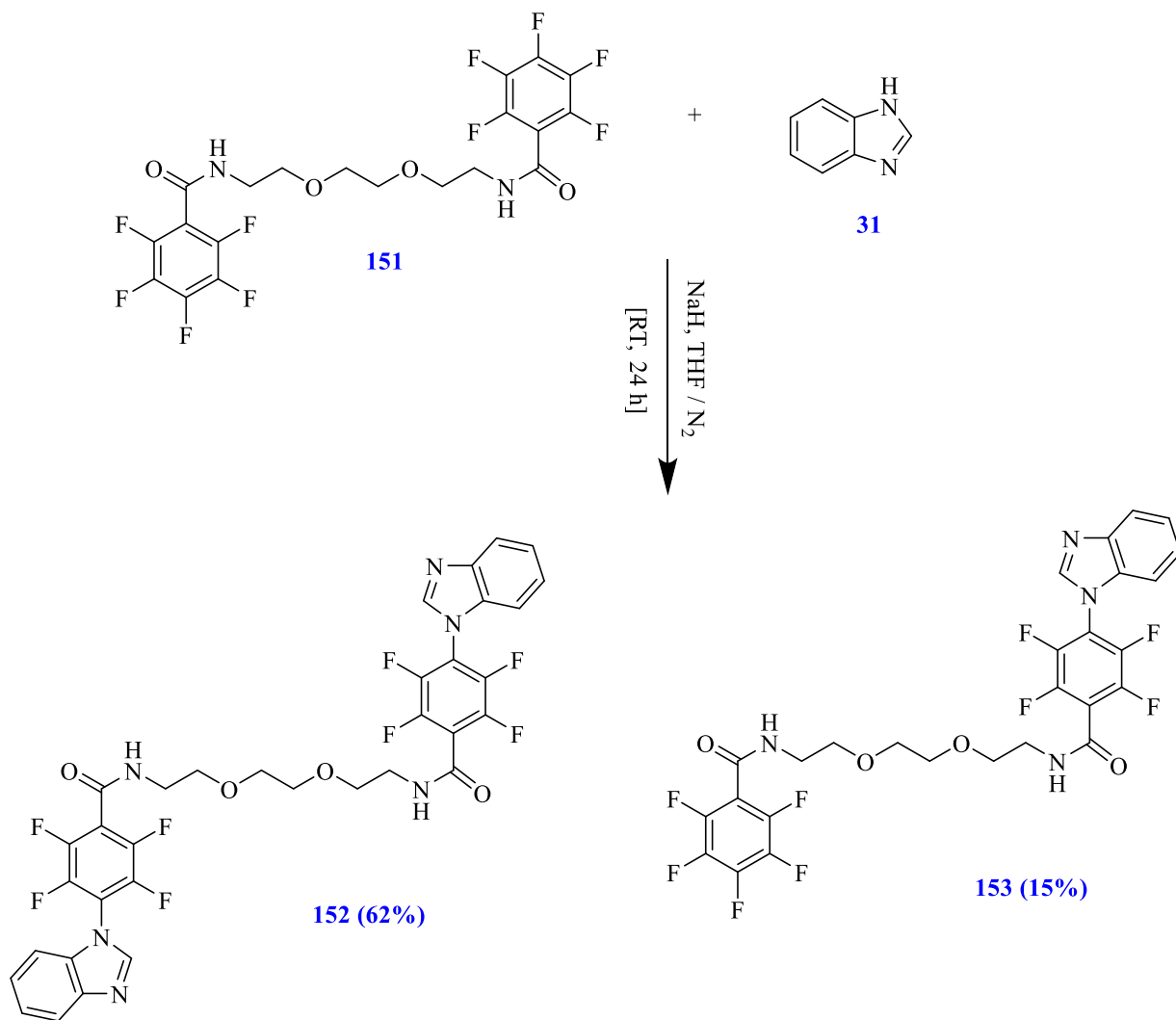
Figure 31. crystal structure of compound **151**.

2.1.5.2. Substitution reaction of benzimidazole **31** with fluorinated bis-linked scaffold **151**

After successful synthesis of the fluorinated bis-link binder **151** it was planned to investigate the possibility introducing different heterocyclic groups into the compound **151** by S_NAr reaction to make larger agents with increased surface area to interact with DNA as potential bis-intercalators. Therefore the reaction of benzimidazole **31** with compound **151** was carried out in a 2:1 ratio at RT in the THF as solvent and NaH as base. The workup procedure gave a white solid which TLC indicated to be a mixture of two compounds. Therefore column chromatography was used to separate the mixture to give target compound **152** (62%) and compound **153** (15%) (Scheme 44). ^{19}F NMR spectroscopy of the compound proved the di-substituted derivative **152** had formed by exhibiting two signals for eight fluorine atom each signal containing 4 F atoms.

and mass spectrometry was in accord with the expected formula, MS (ESI) (MH^-), $C_{34}H_{23}O_4F_8N_6$ requires m/z 731.1659, found m/z 731.1657. Similarly ^{19}F NMR spectroscopy of the compound **153** proved mono substitution had occurred in one ring only, by exhibiting five signals for nine fluorine atoms, δ_F (376 MHz, $CDCl_3$) 22.48 (2F, dd, J , 22.93, 11.65), 22.07-21.01 (2F, m), 16.59 (2F, dd, J , 23.31, 11.65), 11.1 (1F, t, J 20.3), 1.83-1.70 (2F, m).

The mass spectrum confirmed the required formula, MS (ESI) (MH^-), $C_{27}H_{18}O_4F_9N_4$ requires m/z 633.1190 found m/z 633.1192. Also the structure of **152** was confirmed by X-ray diffraction analysis (Figure 32).



Scheme 48. Reaction of benzimidazole with fluorinated bis-linked scaffold 151.

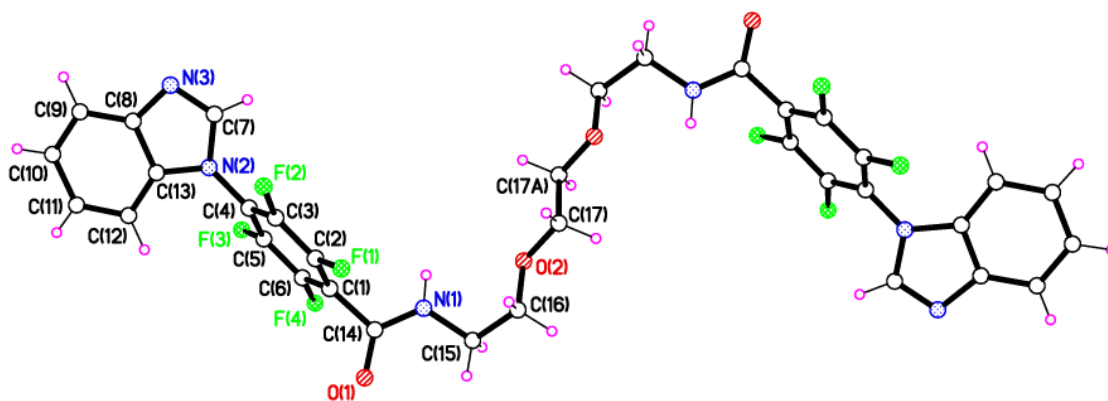


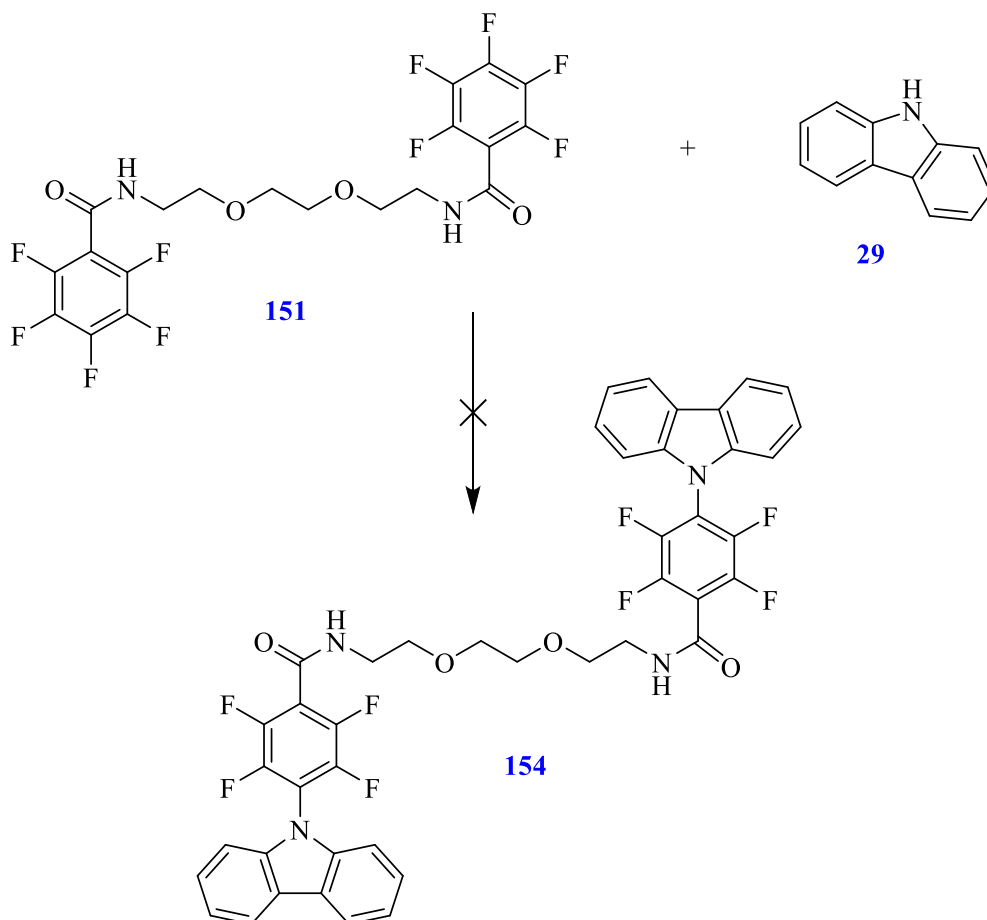
Figure 32. Crystal structure of compound 152.

2.1.5.3. Substitution reaction of carbazole with fluorinated bis-linked scaffold 151

The reaction of carbazole **29** with compound **151** was carried under different conditions as shown in table 5, hoping to displace the 4-position fluorine atom in compound **151** to form the target compound **154** by nucleophilic substitution reaction (Scheme 49). Unfortunately the reactions did not work and only the starting material was recover according to TLC and ^1H NMR spectroscopy, which showed only signals in the aromatic region.

Table 5. Different reaction conditions attempted for the of carbazole with Fluorinated bis-linked scaffold 151.

Entry	Reagents	Conditions	Results
1	NaH	THF, RT, 22 h. N ₂	Starting material
2	NaH	THF, 65 °C, 22 h. N ₂	Starting material
3	NaH	DMF, RT, 22 h. N ₂	Starting material
4	NaH	DMF, 85 °C, 22 h. N ₂	Starting material



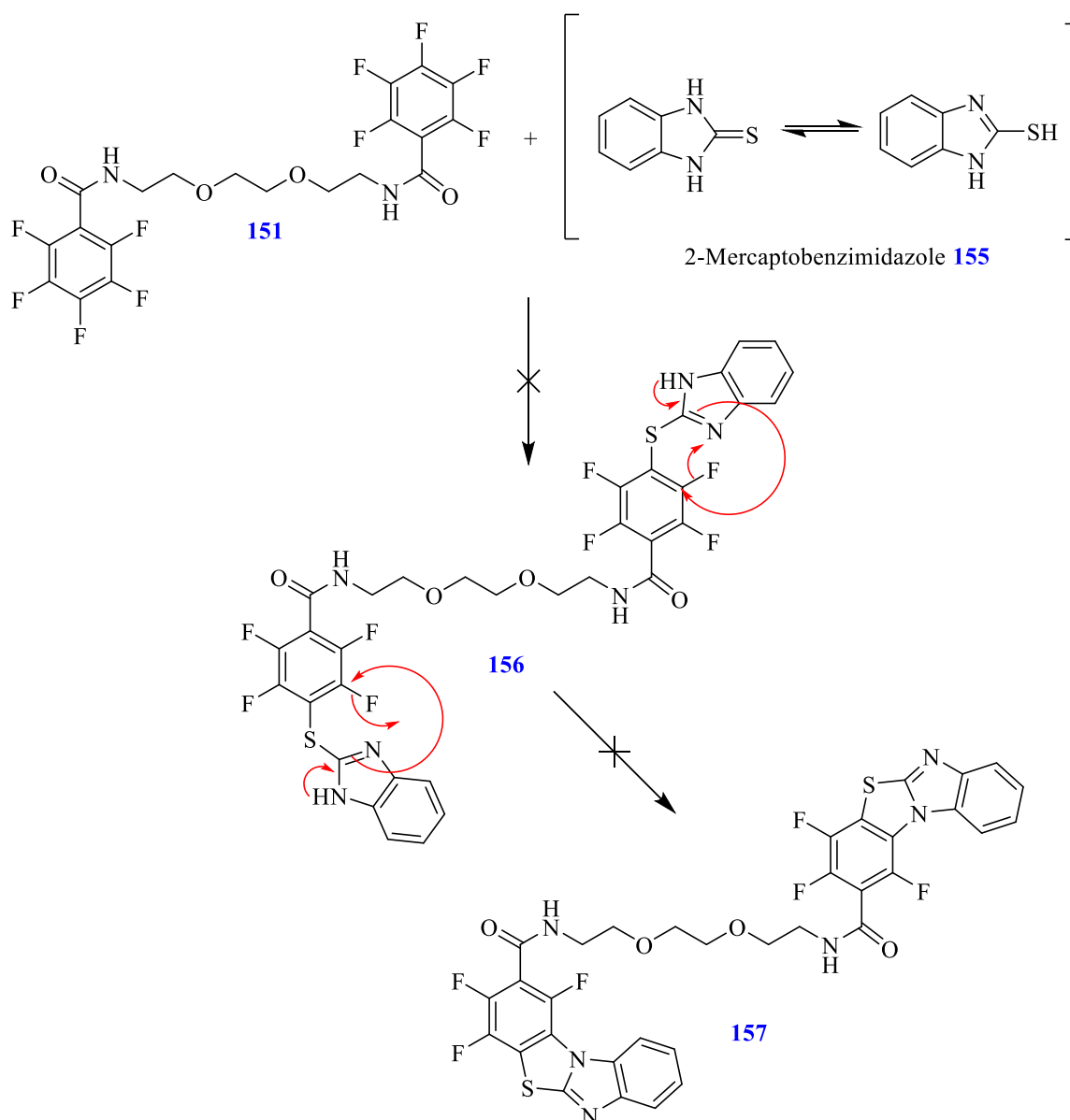
Scheme 49. Attempted reaction of carbazole with fluorinated bis-linked scaffold 151.

2.1.5.4. Substitution reaction of 2-mercaptobenzimidazole with fluorinated bis-linked scaffold 151

After the unsuccessful reaction of carbazole **29** with compound **151** the reaction of 2-mercaptobenzimidazole **155** with compound **151** was investigated using different conditions as shown in table 6, hoping to displace the 4-fluorine atom in compound **151** with formation of intermediate compound **156** by nucleophilic substitution reaction which may then cyclize to form the linked tetracyclic compound **157** (Scheme 50). Unfortunately the reactions did not work and only starting material was recovered according to TLC and ^1H and ^{19}F NMR spectroscopy. The ^1H spectroscopy did not show any signal at aromatic region and ^{19}F NMR spectroscopy indicated the same signals as compound **151**.

Table 6. Different reaction conditions of 2-mercaptobenzimidazole with fluorinated bis-linked scaffold 151

Entry	Reagents	Conditions	Results
1	NaH	THF, RT, 22 h. N ₂	Starting material
2	NaH	THF, Reflux (65 °C), 22 h, N ₂	Starting material
3	NaH	DMF, RT, 22 h, N ₂	Starting material
4	NaH	DMF, 85 °C, 22 h, N ₂	Starting material

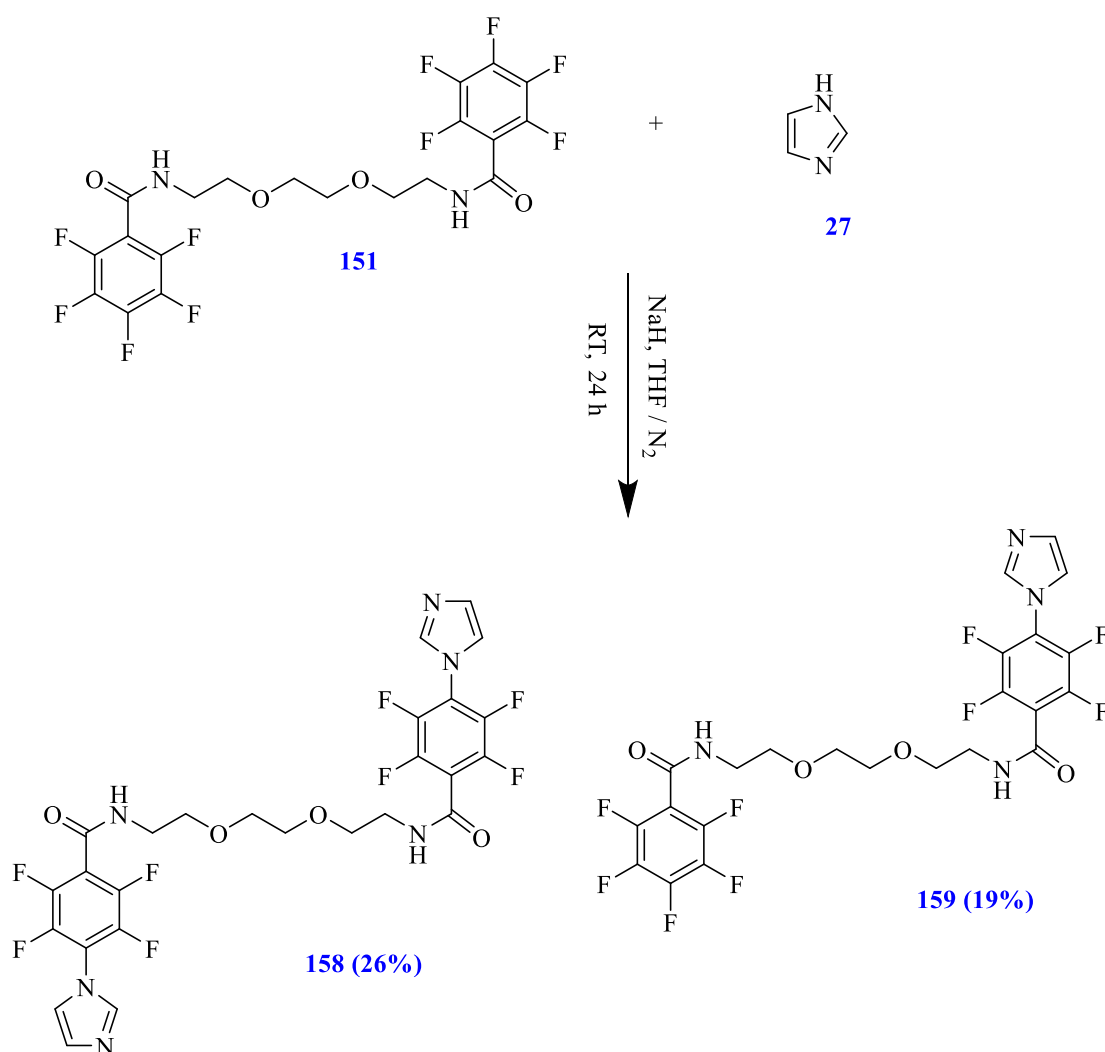


Scheme 50. Reaction of 2-mercaptobenzimidazole with fluorinated bis-linked scaffold 151.

2.1.5.5. Substitution reaction of imidazole with fluorinated bis-linked scaffold 151

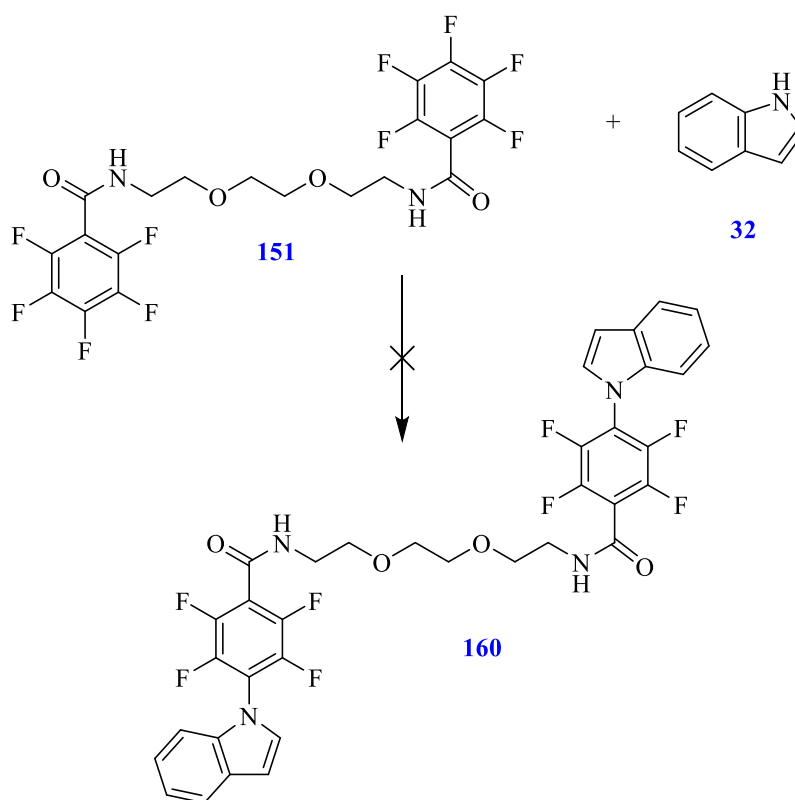
After the failed efforts to synthesis potential bis linked binding agents using carbazole or 2-mercaptobenzimidazole it was decided to try imidazole derivatives as nucleophiles as the benzimidazole had worked well before (section 2.1.5.2). Thus reaction of imidazole with synthesis compound **151** was carried out in 2:1 ratio at RT in THF as solvent and with NaH as base. The workup procedure gave an oily product and TLC indicated the presence of a mixture of two compounds plus some starting material. Therefore column chromatography purification was carried to give target compound **158** (26%) and compound **159** (19%) (Scheme 51). The ^{19}F NMR spectrum

of the compound proved di-substituent **158** had occurred by exhibiting two signals for eight fluorine atoms each signal containing 4F atoms. Also mass spectrometry confirmed the expected formula with (ESI)(MH⁺), C₂₆H₂₁F₈N₆O₄ requires m/z 633.1491, found m/z 633.1473. Also ¹⁹F NMR spectroscopy proved mono substitution **159** had occurred in by exhibiting five signals for nine fluorine atoms, δ_F (376 MHz, CDCl₃) 22.39-22.48 (2F, q, *J*, 12.03), 21.07-21.01 (2F, m), 16.59-16.67 (2F, q, *J*, 11.65), 11.1 (1F, t, *J* 20.3), 1.70-1.83 (2F, m). and mass spectrometry confirmed the formula, (ESI)(MH⁺), C₂₃H₁₆F₉N₄O₄ requires m/z 583.1033, found m/z 583.1040. it is worth mentioning that the benzimidazole show better reactivity than imidazole and gave much higher yields of mono and di-substituted products as seen in Scheme 44 with the same reaction conditions.



Scheme 51. Reaction of imidazole with fluorinated bis-linked scaffold 151.

2.1.5.6. Substitution reaction of indole with fluorinated bis-linked binding scaffold **151**



Scheme 52. Reaction of indole with fluorinated bis-linked binding scaffold **151**

The reaction of indole **32** with compound **151** (Scheme 52) was next carried out under the conditions shown in table 7 in a 2:1 ratio of reactants. Disappointingly again the reactions did not work and only the starting materials were identified as proved by TLC and NMR spectroscopy.

Table 7. Different reaction conditions for the attempted reaction of indole with fluorinated bis-linked scaffold **151**

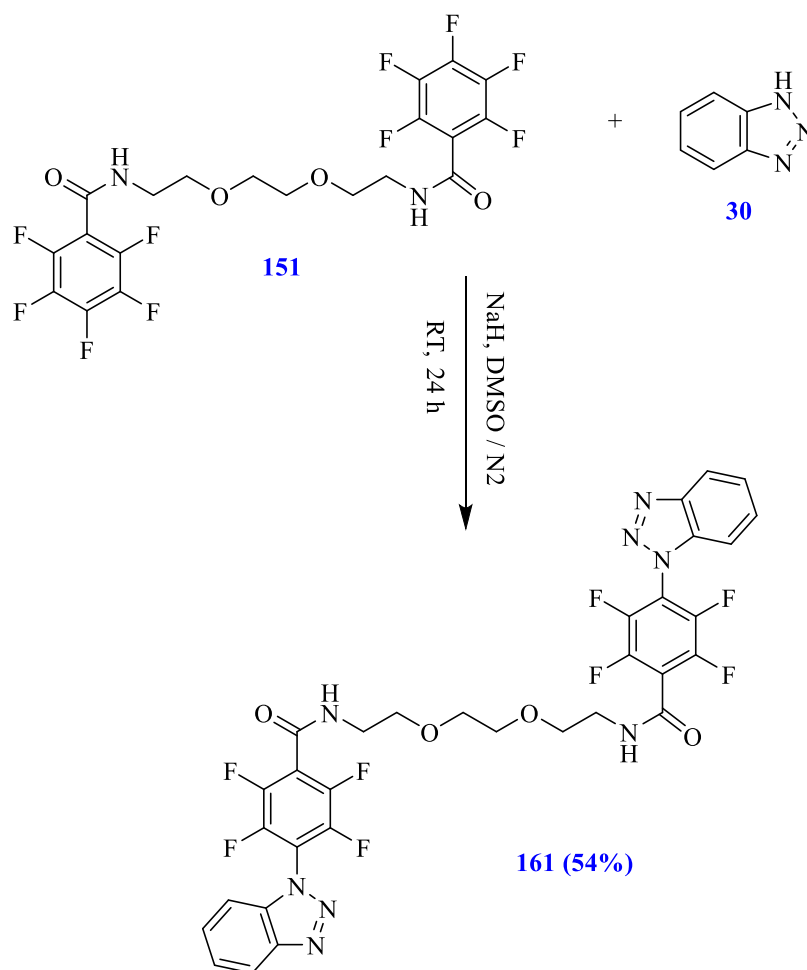
Entry	Reagents	Conditions	Results
1	NaH	THF, RT, 22 h, N ₂	Starting material
2	NaH	THF, Reflux (65 °C), 22 h, N ₂	Starting material
3	NaH	DMF, RT, 22 h, N ₂	Starting material

2.1.5.7. Substitution reaction of benzotriazole with fluorinated bis-intercalator scaffold **151**

After the failed effort to synthesis a potential bis-linked binding using indole and successful reaction of benzimidazole it was planned to attempt reaction with benzotriazole as it is known to be a good nucleophile. Thus reaction of benzotriazole **30** with compound **151** (Scheme 53) was carried out under different conditions as shown in table 8, of these the reaction which was carried in a 2:1 ratio at RT in DMSO as solvent and NaH as base indicated the highest yield of target compound (entry 3). The workup procedure gave a colourless oily product. The ¹H NMR spectrum indicated the presence of some impurities. Column chromatography purification was therefore carried to give target compound **161** (54 %) as a white solid. ¹⁹F NMR spectroscopy showed two signals (4 F for each signal) as expected for target compound **161** and mass spectrometry displayed the expected mass of the compound, MS (ESI) (MH⁺), C₃₂H₂₃F₈N₈O₄ requires m/z 735.1709, found m/z 735.1705.

Table 8. Different reaction conditions for the attempted reaction of benzotriazole with fluorinated bis-linked scaffold 151.

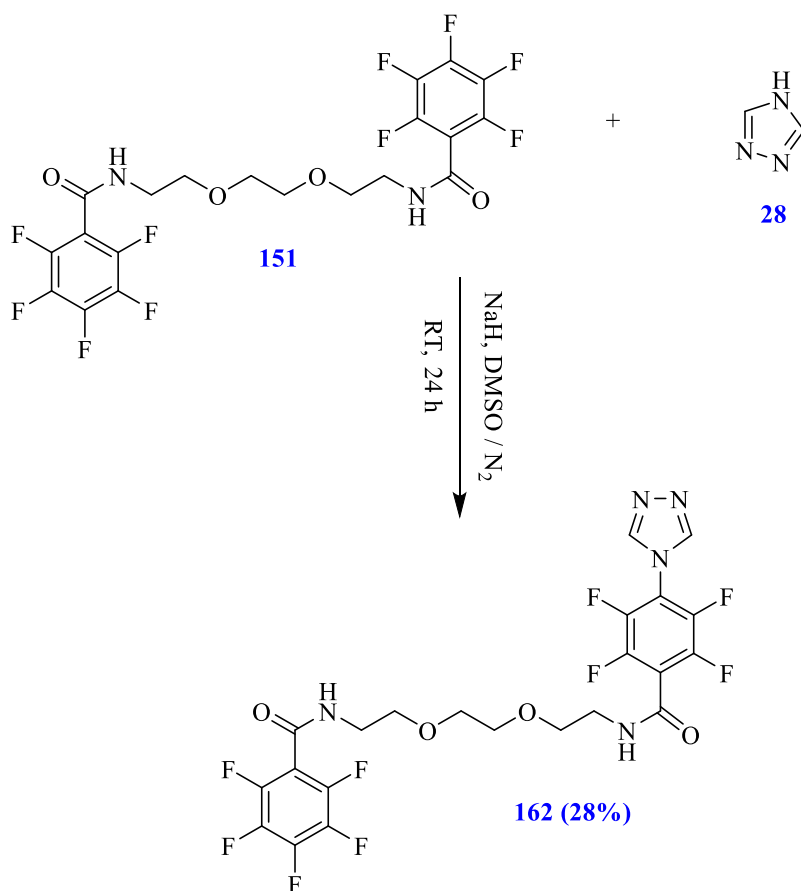
Entry	Reagents	Conditions	Results
1	NaH	THF, RT, 22 h, N ₂	Starting material
2	NaH	DMF, 65 °C, 22 h, N ₂	Starting material, product 161 (29%)
3	NaH	DMSO, RT, 22 h, N ₂	Starting material, product 161 (54%)



Scheme 53. Reaction of benzotriazole with fluorinated bis-intercalator scaffold 159.

2.1.5.8. Substitution reaction of 1,2,4-triazole with fluorinated bis-intercalator scaffold 151

After the successful effort to synthesis a potential bis intercalator using benzotriazole it was planned to attempt to make the 1,2,4-triazole derivative. Thus reaction of 1,2,4-triazole **28** with synthesised compound **151** was carried out in a 2:1 ratio at RT in DMSO as solvent and NaH as base. The workup procedure gave colourless oily product. The ^1H NMR spectrum indicated the presence of some starting material. Therefore column chromatographic purification was carried to give target compound **162** (28 %) as white solid (Scheme 54). ^{19}F NMR spectroscopy showed the expected fluorine signals for the target compound, δ_{F} (376 MHz, CDCl_3) 22.74-22.64 (2F, q, J , 11.65), 21.15-21.05 (2F, m), 14.49-14.40 (2F, q, J , 11.28), 11.4 (1F, t, J 20.68), 1.95-1.81 (2F, m). Mass spectrometry displayed the expected mass of the compound, MS (ESI) (MH^+), $\text{C}_{22}\text{H}_{15}\text{F}_9\text{N}_5\text{O}_4$ requires m/z 584.0986, found m/z 584.0994



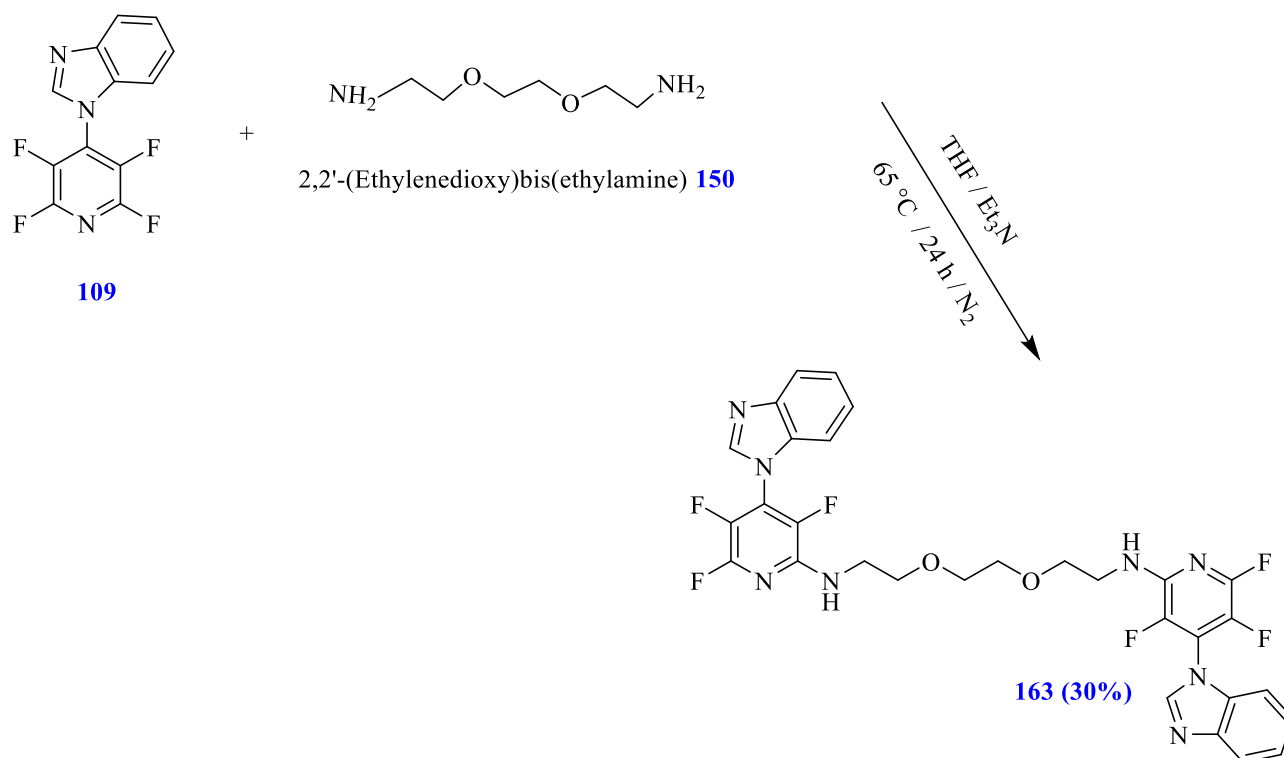
Scheme 54. reaction of 1,2,4-triazole with fluorinated bis-intercalator scaffold 151.

2.1.6. Synthesis of bis-linked binding agents by introducing of aliphatic hydrophilic link to synthesised fluorinated heterocyclic compounds.

In this part of the investigation we planned to make another series of novel bis-linked binding agent by introducing an aliphatic hydrophilic link to synthesised fluorinated heterocyclic compounds with better water solubility, and to investigate their DNA binding properties.

2.1.6.1. Reaction of compound 109 with 2,2-(ethylenedioxy)bis(ethylamine).

The aim of this reaction was formation of compound 163 by replacement of the 2-fluorine atom in compound 109 with 2,2'-(ethylenedioxy)bis(ethylamine) to make another bis-linked binding agent by formation of an aryl amine bond by S_NAr reaction (Scheme 55).



Scheme 55. Reaction of compound 109 with 2,2'-(ethylenedioxy)bis(ethylamine).

Therefore reactions of compound **109** (2 equiv.) with 2,2'-(ethylenedioxy)bis(ethylamine) **150** (1 equiv.) were carried with the different conditions shown in table 9. However the reaction which was carried in the presence of THF as solvent and Et₃N as base under reflux (65 °C) for 24 h indicated highest yield of target compound (entry 3).

Table 9. Different methods for synthesising target compound 163.

Entry	Reagents	Conditions	Results
1	None	THF, RT, 24 h, N ₂	Starting material
2	None	THF, Reflux (65 °C), 24 h, N ₂	Starting material, product 163 (31%)
3	Et ₃ N	THF, Reflux (65 °C), 22 h, N ₂	Starting material, product 163 (55%)

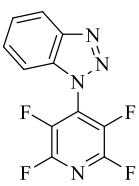
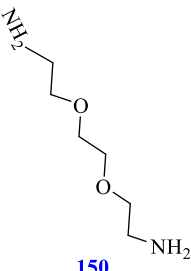
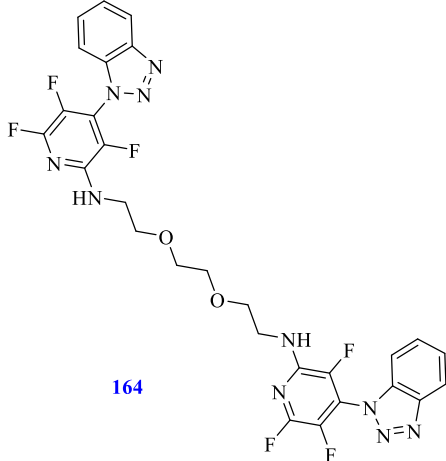
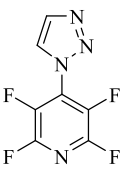
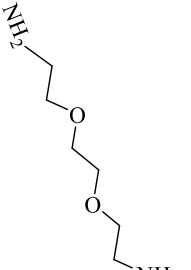
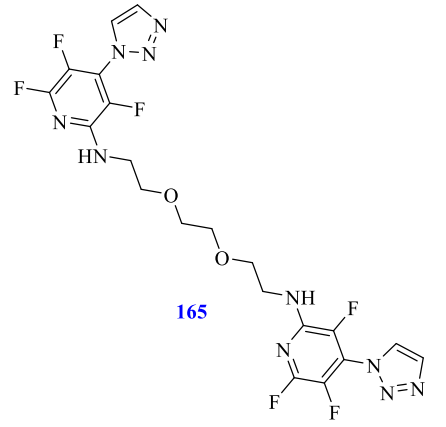
TLC revealed a mixture of two polar compounds one of which only just moved with ethyl acetate as eluent, while the other remained on the base line. Also some starting material was still present. After column chromatography purification processes the target product **163** was obtained in 55% yield and the structure was confirmed by its ¹H NMR spectrum and accurate mass measurement with *m/z* of 641.1845 (MH⁺) for C₃₀ H₂₃ F₆ N₈ O₂. The ¹⁹F NMR spectrum showed three signals (2F for each

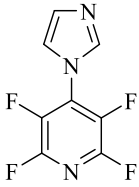
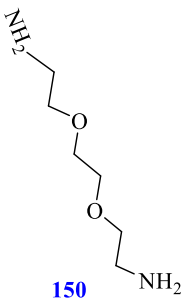
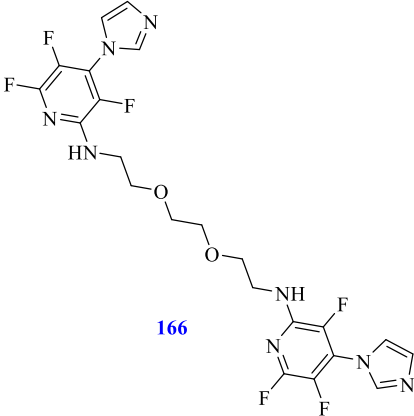
signal) as expected. Also IR spectroscopy indicated the presence of an NH group by a signal in the region 3000-3500 cm^{-1} .

2.1.6.2. Reaction of further perfluoropyridine derivatives with 2,2'-(ethylenedioxy)bis(ethylamine)

After optimizing the conditions for the reaction of 1-(perfluoropyridin-4-yl)-1*H*-benzo[*d*]imidazole **109** with 2,2'-(ethylenedioxy)bis(ethylamine), we were decided to try different perfluoropyridine derivatives to synthesise a series of more polar fluorinated heterocyclic compounds using 2,2'-(ethylenedioxy)bis(ethylamine) as aliphatic hydrophilic linker as shown in Table 10.

Table 10. Reaction of different perfluoropyridine derivatives with 2,2'-(ethylenedioxy)bis(ethylamine).

Reactant	Reactant	Conditions	Expected product	Yield%
 <p>113</p>	 <p>150</p>	THF as solvent, Et ₃ N as base, Reflux (65 °C), 22 h, N ₂	 <p>164</p>	70%
 <p>111</p>	 <p>150</p>	THF as solvent, Et ₃ N as base, Reflux (65 °C), 22 h, N ₂	 <p>165</p>	30%

 <p style="text-align: center;">108</p>	 <p style="text-align: center;">150</p>	<p>THF as solvent, Et₃N as base, Reflux (65 °C), 22 h, N₂</p>	 <p style="text-align: center;">166</p>	<p style="text-align: center;">65%</p>
---	---	---	--	--

As seen in table 10 reaction of compound **113** with 2,2'-(ethylenedioxy)bis(ethylamine) in THF as solvent, and Et₃N as base under reflux (65 °C) for 22 h worked well and the target compound **164** was afforded in 70% yield. The ¹⁹F NMR spectrum showed three signals (2F for each signal) as expected. Also mass spectrometry confirmed the expected mass for the target product **164**, MS (ESI) (MH⁺), C₂₈H₂₃F₆N₁₀O₂ requires m/z 645.1904, found m/z 645.1908.

Compound **111** was reacted with 2,2'-(ethylenedioxy)bis(ethylamine) under the same conditions as for the preparation of compound **164** (table 10) but the desired compound **165** was afforded in only 30% yield which is much less than compound **164** therefore the benzotriazolyl perfluoropyridine derivative appears more reactive than the triazolyl perfluoropyridine. ¹⁹F spectroscopy proved the presence of six fluorine atoms in the product by detecting three signals which each signal contain 2 F as expected. In addition mass spectrometry found the expected mass for target product **165**, MS (ESI)(MH⁺), C₂₀H₂₉F₆N₁₀O₂ requires m/z 545.1591, found m/z 545.1576.

Also target compound **166** was afforded (65% yield) in a similar way (Table 10). The ¹⁹F spectrum proved the product was formed and displayed three signals (2F atoms for each signal as expected). Moreover the mass spectrum displayed a signal for the expected molecular formula for the target compound **166**, MS (ESI) (MH⁺), C₂₂H₂₁F₆N₈O₂ requires m/z 543.1686, found m/z 543.1686

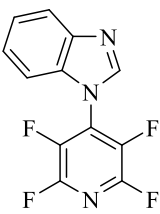
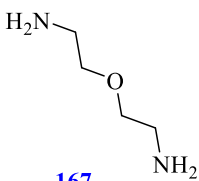
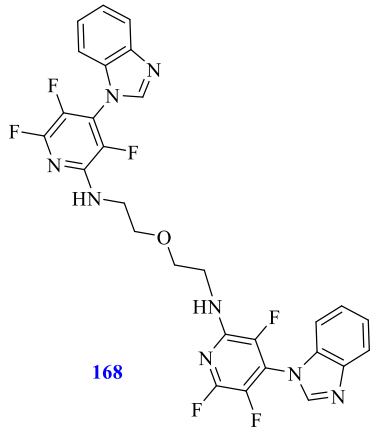
2.1.6.3. Reaction of different perfluoropyridine derivatives with 2-(2-aminoethoxy) ethylamine

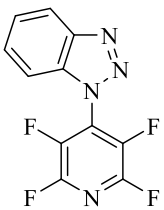
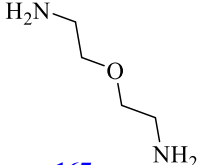
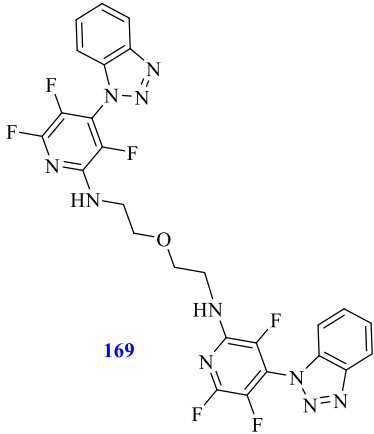
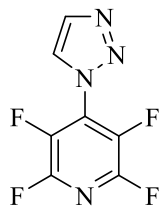
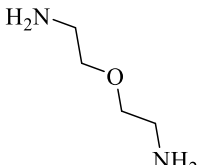
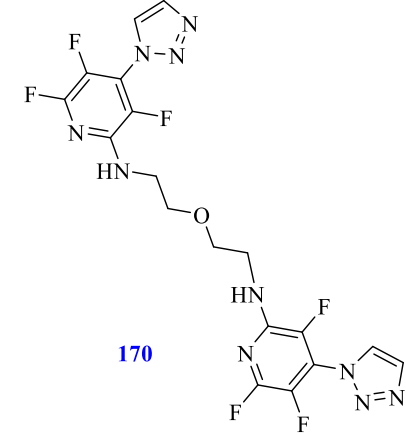
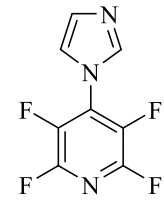
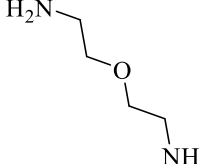
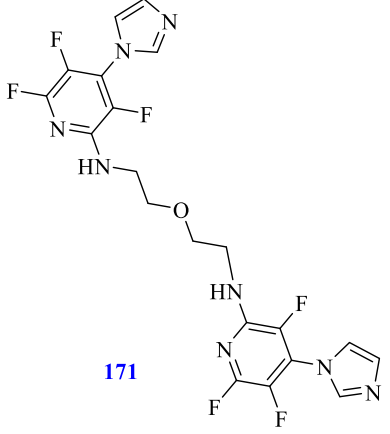
The aim of these reactions was formation of an alternative series of polar fluorinated heterocyclic novel compounds with a shorter linker. Varying the length of the linker could allow different binding modes with duplex DNA to be probed. Replace most of a fluorine atom in perfluoropyridine derivatives with 2-(2-aminoethoxy) ethylamine was expected again to proceed readily by S_NAr reaction.

After optimization of the conditions for reaction with 2,2'-(ethylenedioxy)bis(ethylamine) **148** (section 2.1.6.2), we were decided to test the same conditions for reactions of perfluoropyridine derivatives with 2-(2-aminoethoxy)ethylamine **165** as an alternative aliphatic hydrophilic linker (Table 11).

But as can be seen in table 11 reaction of compound **109** and **113** with 2-(2-aminoethoxy)ethylamine **165** resulted in lower yields compared to reactions with 2,2'-(ethylenedioxy)bis(ethylamine) **148** in table 10 Therefore was decided to try reaction of compound **111** with 2-(2-aminoethoxy)ethylamine in the more polar DMF instead of THF as solvent. The result indicated the reaction worked much better in DMF by showing higher % yield of product. Thus, reaction of compound **108** with 2-(2-aminoethoxy) ethylamine was also carried out in DMF.

Table 11. Reaction of different perfluoropyridine derivatives with 2-(2-aminoethoxy) ethylamine.

Reactant	Reactant	Conditions	Expected product	Yield
 109	 167	THF as solvent, Et ₃ N as base, Reflux (65 °C), 22 h, N ₂	 168	23%

 <p>113</p>	 <p>167</p>	<p>THF as solvent, Et₃N as base, Reflux (65 °C), 22h. N₂</p>	 <p>169</p>	<p>15%</p>
 <p>111</p>	 <p>167</p>	<p>DMF as solvent, Et₃N as base, 65 °C, 22 h, N₂</p>	 <p>170</p>	<p>55%</p>
 <p>108</p>	 <p>167</p>	<p>DMF as solvent, Et₃N as base, 65 °C, 22 h, N₂</p>	 <p>171</p>	<p>50%</p>

As seen in table 11, reaction of compound **109** with 2-(2-aminoethoxy) ethylamine in THF as solvent, and Et₃N as base under reflux (65 °C) for 22 h worked and the target compound **168** was afforded in 23% yield. The ¹⁹F NMR spectrum showed three signals (2F for each signal) as expected.

Also mass spectrometry showed the expected mass for target product **168**, MS (ESI) (MH⁺), C₂₈H₂₁F₆N₈O₁ requires *m/z* 599.1737, found *m/z* 599.1720

Compound **113** was reacted with 2-(2-aminoethoxy)ethylamine under the same conditions as for compound **109** (Table 11) and target compound **169** was afforded in 15% yield. ¹⁹F spectroscopy proved the product formed by detecting three signals (2F atoms for each signal as expected).. Also mass spectrometry found the expected mass for target product **169**, MS (ESI) (MH⁺), C₂₆H₁₉F₆N₁₀O₁ requires *m/z* 601.1642, found *m/z* 601.1637

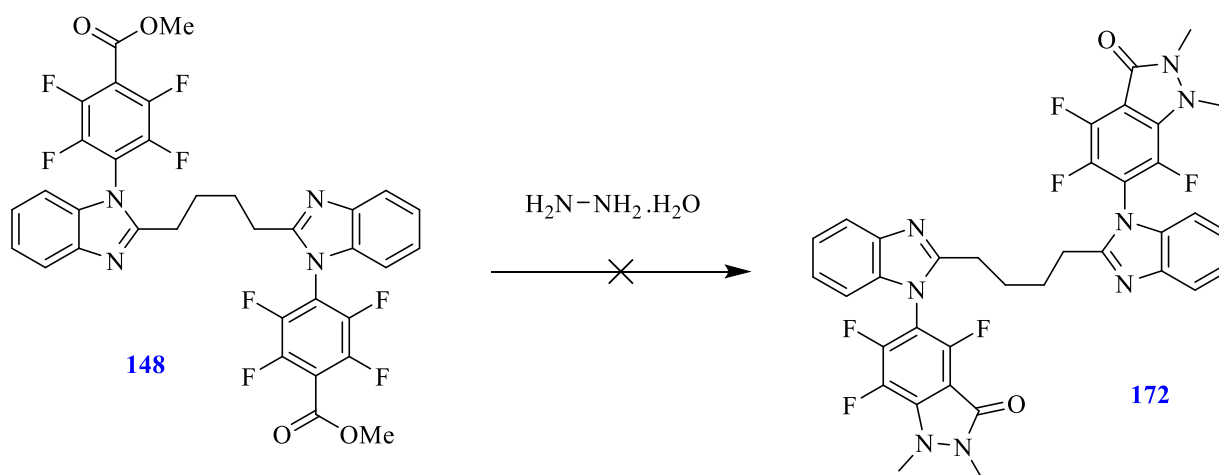
Due to the low yield of compounds **168** and **169**, reaction of compound **111** with 2-(2-aminoethoxy)ethylamine was carried out in DMF as solvent, using Et₃N as base but at the same temperature (65 °C) for 22 h. The reaction was successful affording the target compound **170** in 55% yields. ¹⁹F spectroscopy proved the product formed by detecting three signals (2F atoms for each signal as expected). Also mass spectrometry found the expected mass for the target compound **170**, MS (ESI) (MH⁺), C₁₈H₁₅F₆N₁₀O₁ requires *m/z* 501.1329, found *m/z* 501.1320.

In addition target compound **171** was afforded (50% yield) in similar conditions as for compound **170** (Table 11), and its structure proved by ¹⁹F spectroscopy which found three signals (2F atoms for each signal as expected). Mass spectrometry showed the expected mass for target compound **171**, MS (ESI) (MH⁺), C₂₀H₁₇F₆N₈O₁ requires *m/z* 499.1424, found *m/z* 499.1409.

2.1.7. Further functionalization to make bis-linked binding agent

Another approach taken was the design and synthesis of a series of potentially fluorinated bis-intercalating compounds involving potential cyclization of ester derivatives to make bi- or tri-cyclic bis-intercalators.

2.1.7.1. Reaction of compound 148 with hydrazine



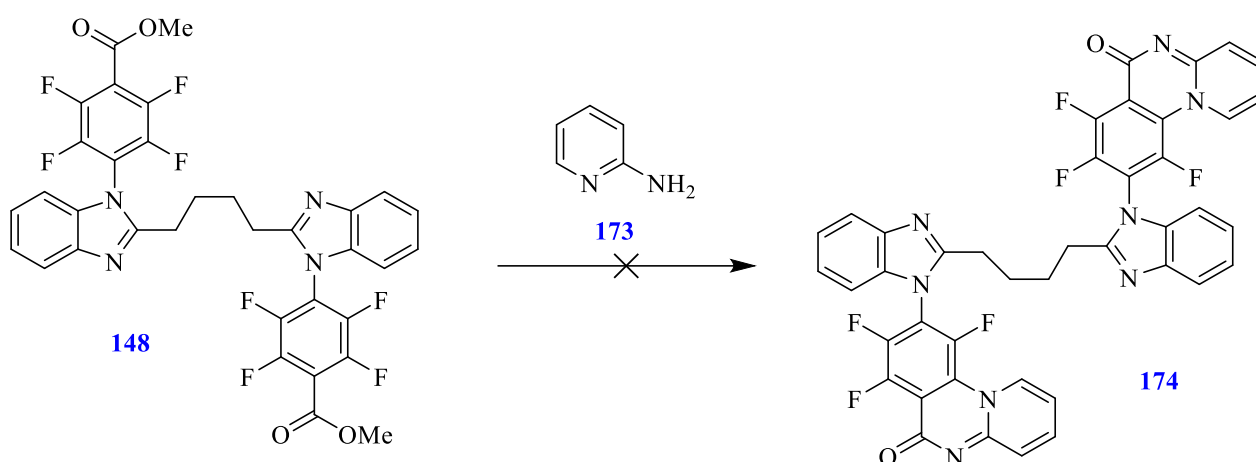
Scheme 56. Reaction of compound 148 with hydrazine.

The reaction of hydrazine with compound 148 (Scheme 56) was carried out under different conditions as shown in table 12 in a 4:1 ratio of reactants. As in entry 1 the hydrazine hydrate did not dissolve very well in THF and only starting material was recovered. Therefore in entry 2, methanol was added to dissolve the hydrazine and form a homogeneous reaction mixture. Unfortunately the reactions did not work and only the starting materials were recovered. Only in entry 3 did the ^{19}F NMR spectrum indicate reaction had occurred but it was such a complex spectrum and nothing was recovered, even after several different purification methods.

Table 12. Different condition attempted for synthesising target compound 172.

Entry	Reagents	Conditions	Results
1	None	THF, RT, 22 h, N ₂	Starting material
2	None	THF and 2 ml of methanol, RT, 22 h, N ₂	Starting material
3	None	methanol, 1 h, 65 °C and RT, 22 h, N ₂	Starting material, unknown compounds formed

2.1.7.2. Reaction of compound **148** with 2-aminopyridine



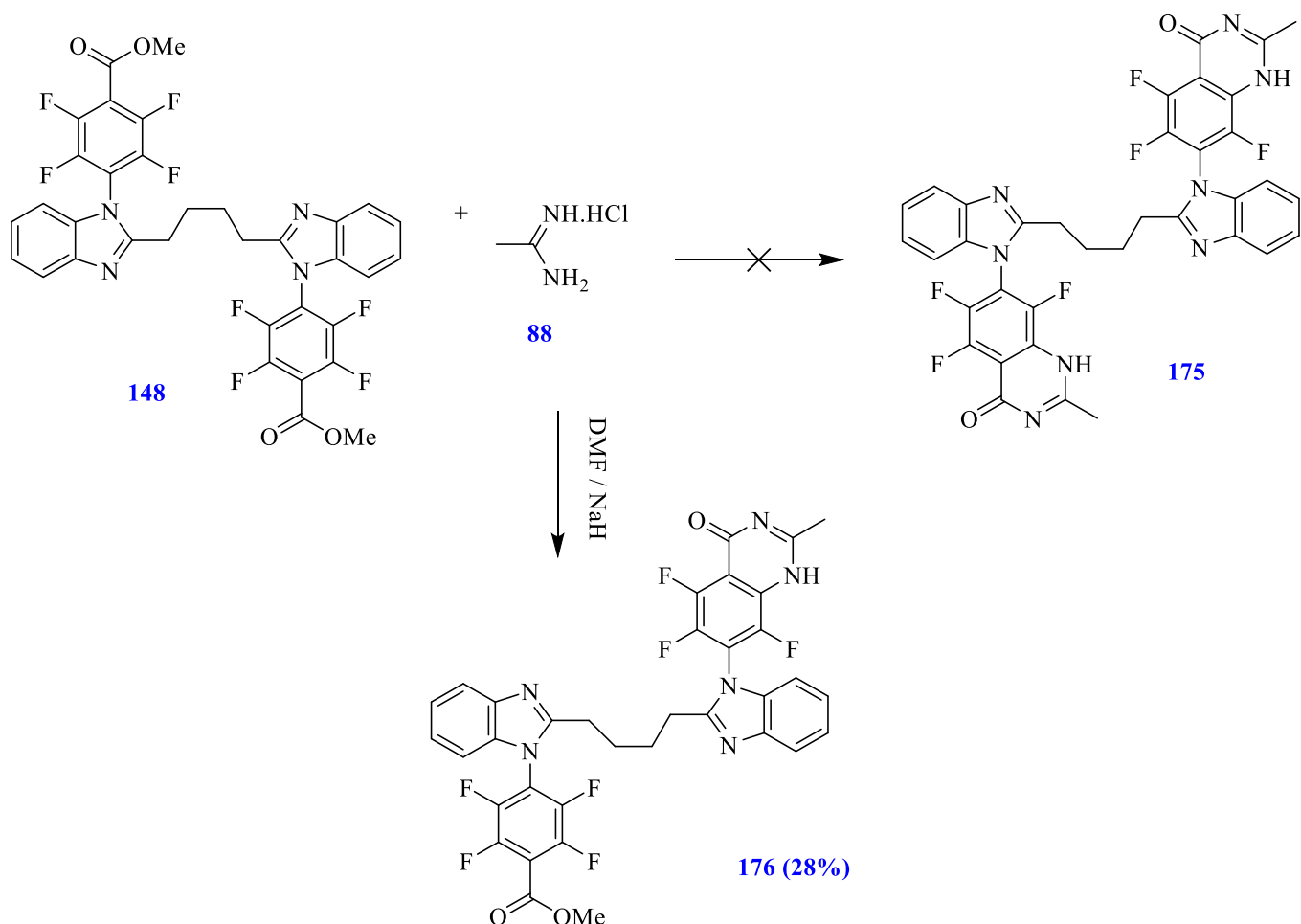
Scheme 57. Reaction of compound **148 with 2-aminopyridine.**

After the unsuccessful reaction of hydrazine with ester compound **148** and the poor solubility of hydrazine in nonpolar solvents, it was decided to try 2-aminopyridine as a nucleophilic reagent which might form both an amide bond to the ester in **148** and cyclise by effecting S_NAr reaction of the adjacent fluorine to form tricyclic compound **174** (Scheme 57). Reactions of 2-aminopyridine with the successfully synthesised ester compound **148** were conducted with a higher ratio of 2-aminopyridine (4:1) under different conditions as shown in table 12. Unfortunately all the reactions did not work and only starting materials were recovered.

Table 13. Different conditions attempted for synthesising target compound **174.**

Entry	Reagents	Conditions	Results
1	NaH	THF, RT, 22 h, N ₂	Starting material
2	None	Dioxane, 10 h, RT and 10 h 80 °C, 22 h, N ₂	Starting material,
3	None	Acetic acid, 24 h, 100 °C and RT, 22 h. N ₂	Starting material

2.1.7.3. Reaction of ester compound **148** with acetamidine hydrochloride



Scheme 58. Reaction of ester compound **148 with acetamidine hydrochloride.**

After unsuccessful reaction of 2-aminopyridine with compound **148** it was decided to try another more reactive nucleophile like acetamidine (Scheme 58). The reactions of ester compound **148** and acetamidine hydrochloride were carried in a 1:2 ratio as shown in table 14, As seen in entry 4 the reaction which was carried at 85°C, in DMF as solvent and NaH as base indicated highest yield of target compound **176** (entry 3). The workup procedure gave yellow solid product. The ^1H NMR indicated the presence of some impurities. Therefore column chromatography purification was carried out to give compound **176** (28%) as a white solid. ^{19}F and ^1H NMR spectroscopy indicated that the acetamidine had added and cyclised on only one of the fluoroarene rings, leaving the ester intact on the other as seen in (Scheme 58). Also mass spectrometry displayed the expected mass of the compound **176**, MS (ESI) (MH^+), $\text{C}_{35}\text{H}_{24}\text{F}_7\text{N}_6\text{O}_3$ requires m/z 709.1793 found m/z 709.1775. The

formation of **176** showed the reaction to be viable, and further investigation to effect reaction on both rings should be continued.

Table 14. Different condition for synthesising target compound 176.

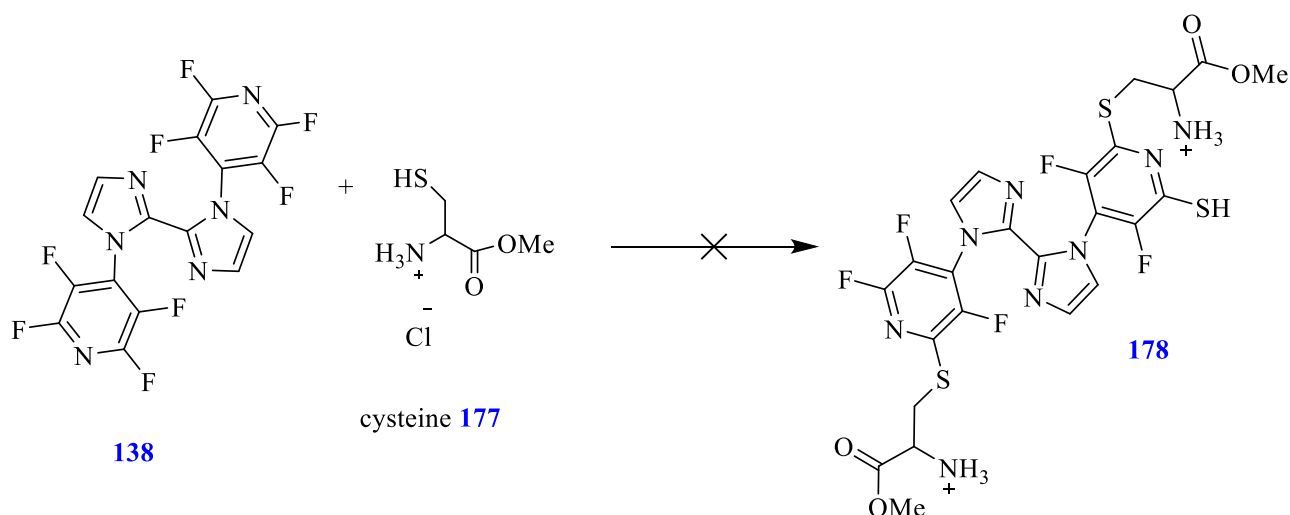
Entry	Reagents	Conditions	Results
1	None	Pyridine and 1 ml of methanol, 80 °C, 22 h, N ₂	Starting material
2	Sodium acetate	Methanol, reflux, 24 h, N ₂	Starting material
3	NaH	THF, RT, 22 h, N ₂	Starting material,
4	NaH	DMF, RT, 22 h, N ₂	Starting material, product 176 (10%)
5	NaH	DMF, 85°C, 22 h, N ₂	Starting material, product 176 (28%)
6	NaH	DMSO, RT, 22 h, N ₂	Starting material, complex NMR spectrum of unknown compound.

2.1.8. Addition of hydrophilic side chains to the successfully synthesised fluorinated heterocyclic compounds.

Throughout the biological assays it had been found that some of synthesised compounds had poor solubility in the buffers employed. For the purpose of improving the water solubility of the novel synthesised compounds it was planned to introduce hydrophilic side chains to the compounds. Therefore the aim of these reactions is to replace a fluorine atom in the successfully prepared fluorinated heterocycles with different side chains by an aromatic nucleophilic substitution reaction. Hopefully the aliphatic side chain bearing polar groups should make the compound more water-soluble and could improve DNA binding activity.

2.1.8.1. Reaction of compound 138 with cysteine

The aim of this reaction was to increase the water solubility and improve DNA binding activity of compound **138** by adding the amino acid cysteine **177** (protected as its methyl ester) as a side chain through reaction of its thiol side group. (Scheme 59)



Scheme 59. Reaction of the compound **138** with cysteine.

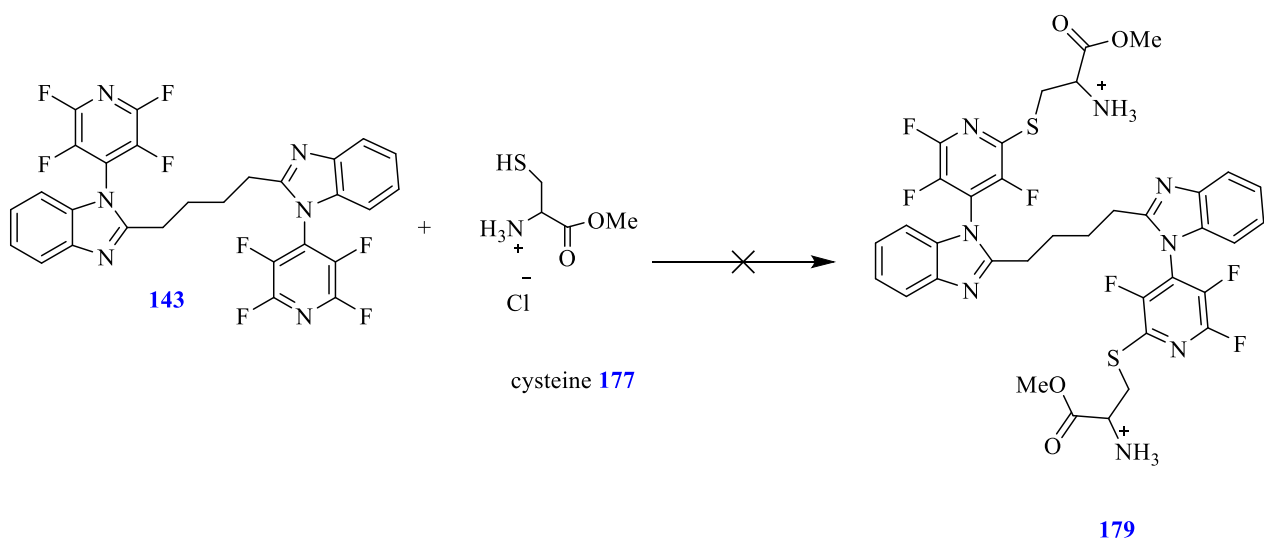
Therefore reaction of compound **138** (1 equiv) with methyl cysteine **177** (2 equiv) was carried under different conditions as shown in table 15. TLC and mp point indicated only the presence of compound **138** as starting material. The reaction had not worked and the target compound **178** was not formed.

Table 15. different reaction conditions for compound **138** with cysteine.

Entry	Reagents	Conditions	Results
1	Et ₃ N	THF, RT, 22 h, N ₂	Starting material
2	Et ₃ N	DMF, RT, 22 h, N ₂	Starting material
3	Et ₃ N	DMF and THF, RT, 22 h, N ₂	Starting material

2.1.8.2. Reaction of the compound **143** with cysteine

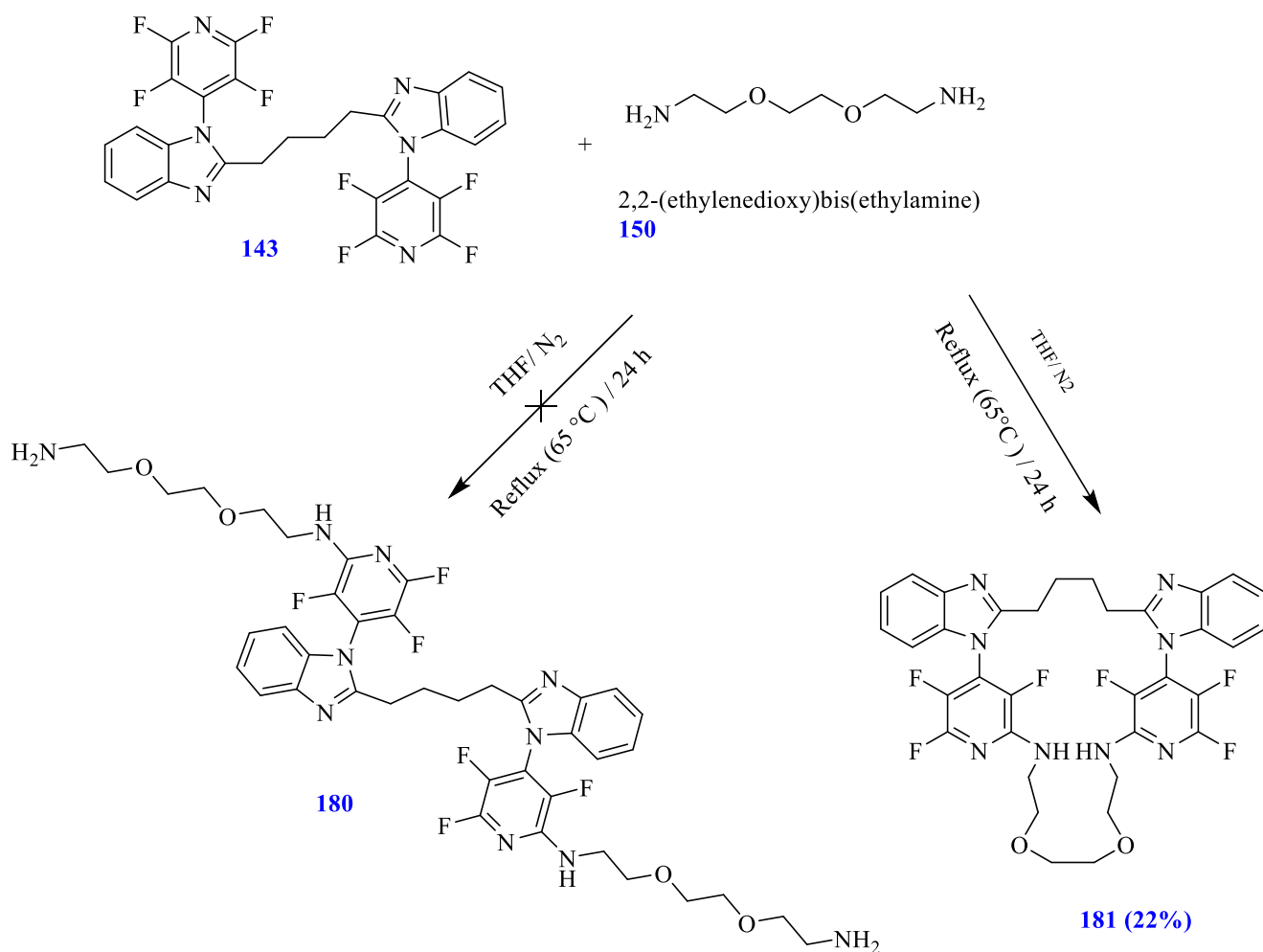
As the successfully synthesised compound **143** did show positive activity against some cancer cell lines, but had low water solubility, we decided to use this compound as a core biological agent and introduce different hydrophilic side chains by replacing the F atoms with further nucleophiles. It was hoped to synthesise a set of more water soluble fluorinated heterocycles with potential biological activity using this strategy. Therefore reaction of compound **143** with cysteine **177** was carried out in ratio 1:2 in the presence of Et₃N as base and DMF as solvent was carried out for 24 h at room temperature under N₂ in an attempt to form target compound **179**. Unfortunately NMR spectroscopy indicated only the presence of starting material and the target compound was not afforded.



2.1.8.3. Study of the reaction of compound 143 with 2,2-(ethylenedioxy)bis(ethylamine)

The aim of this reaction is improve the biological activity of compound **143** by replacement of two fluorine atoms of compound **143** with two amine chains and hopefully synthesising target compound **180** as a possible DNA groove binding agent. (Scheme 61)

The reaction of compound **143** (1 equiv.) with 2,2-(ethylenedioxy)bis(ethylamine) **150** (2 equiv.) in THF as solvent was conducted over 24 h at 65 °C under N₂. TLC revealed a mixture of starting material and a new compound. Therefore column chromatographic purification was carried out affording the interesting and unexpected macro-cyclized compound **181** in 22% yields, instead of the target compound **180**. The structure was confirmed by ¹H and ¹³C NMR spectroscopy and accurate mass measurement with *m/z* of 697.2469 (MH⁺) for C₃₄H₃₁F₆N₈O₂. The ¹⁹F NMR spectrum showed three signals (2F for each signal) as expected. Also the structure of **181** was confirmed by X-ray diffraction analysis (Figure 33).



Scheme 61. Reaction of compound **143** with 2,2-(ethylenedioxy)bis(ethylamine).

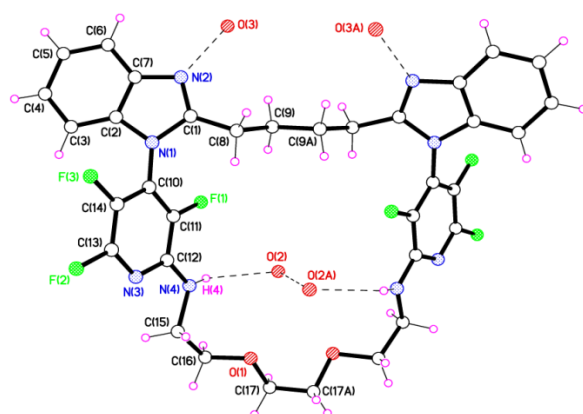
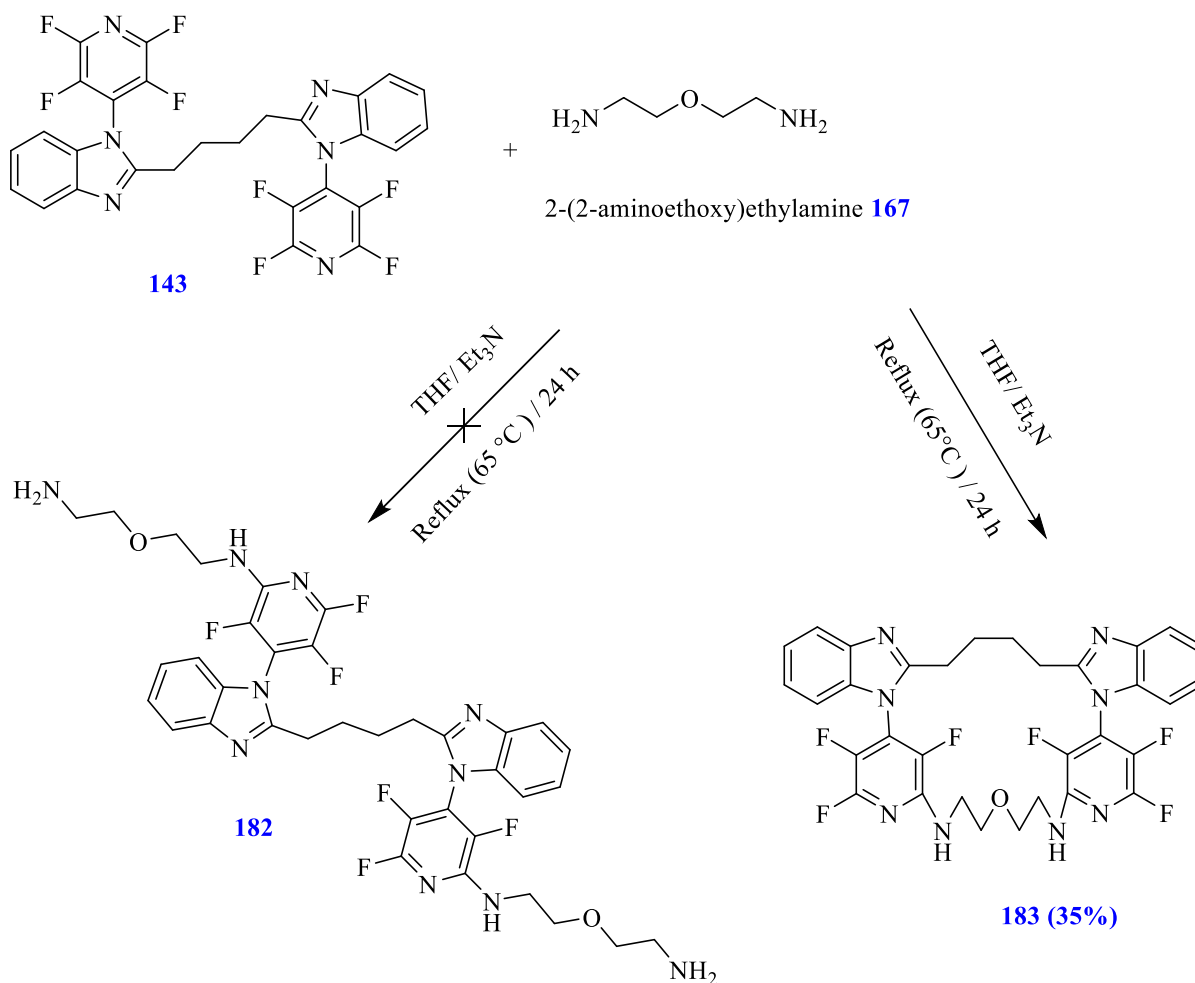


Figure 33. X-ray crystal structure of **181·2½H₂O** showing the 24-membered macrocycle with 2½ hydrogen bonded water molecules. The molecule lies on a 2-fold axis. O(3) and O(3A) are each ¼ occupied.

2.1.8.4. Investigation of the Reaction of compound **143** with 2-(2-Aminoethoxy)ethylamine

After synthesis of the unexpected macro cyclized compound **181** it was planned to try the shorter linker 2-(2-aminoethoxy)ethylamine to find out if this would still lead to a cyclized compound. Therefore reaction of compound **143** (1 equiv) with 2-(2-aminoethoxy)ethylamine **167** (2 equiv) in THF as solvent and with Et₃N as base was conducted over 24 h at 65°C under N₂ (scheme 62) TLC revealed a mixture of starting material and a new compound. After column chromatographic purification the macro cyclized compound **183** was obtained in 35% yield. As seen, even with a shorter linker macrocyclisation occurred, and target compound **182** was not formed. Compound **183** was confirmed by ¹H, ¹⁹F and ¹³C NMR spectroscopy and accurate mass measurement with *m/z* of 653.2207 (MH⁺) for C₃₂H₂₆F₆N₈O. The ¹⁹F NMR spectrum showed three signals (2 F for each signal) as expected. Also the structure of **183** was confirmed by X-ray diffraction analysis (Figure 34).



Scheme 62. Reaction of compound **143** with 2-(2-aminoethoxy)ethylamine.

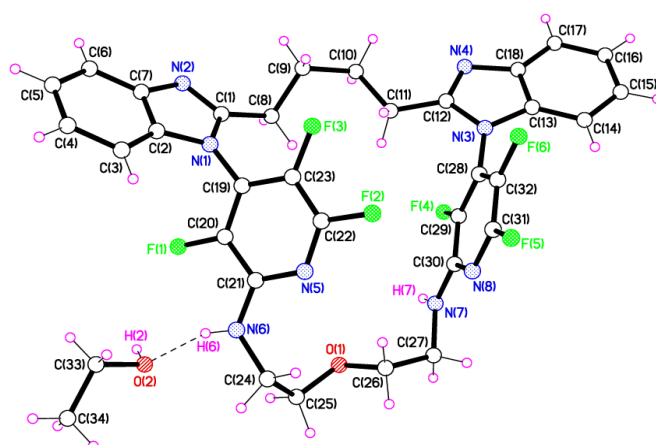
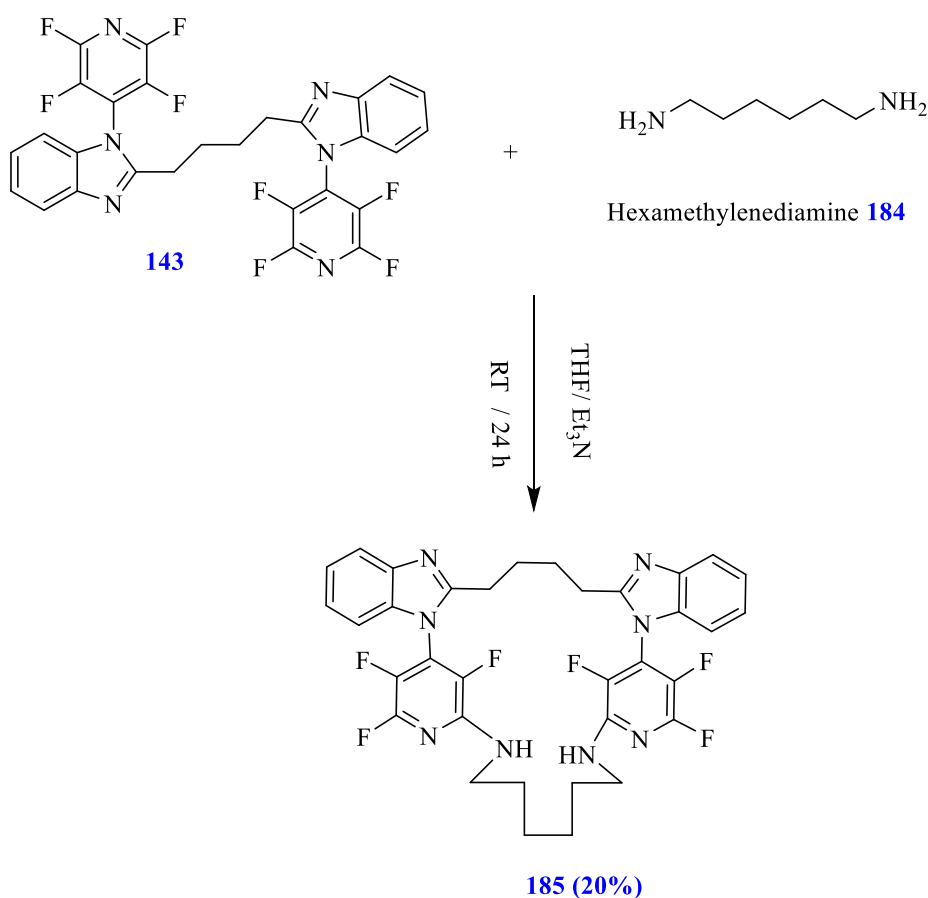


Figure 34. X-ray crystal structure of **183** showing the 21-membered macrocycle with a hydrogen-bonded ethanol solvate molecule.

2.1.8.5. Study of the reaction of perfluoro bis-benzimidazole derivative **143** with hexamethylenediamine

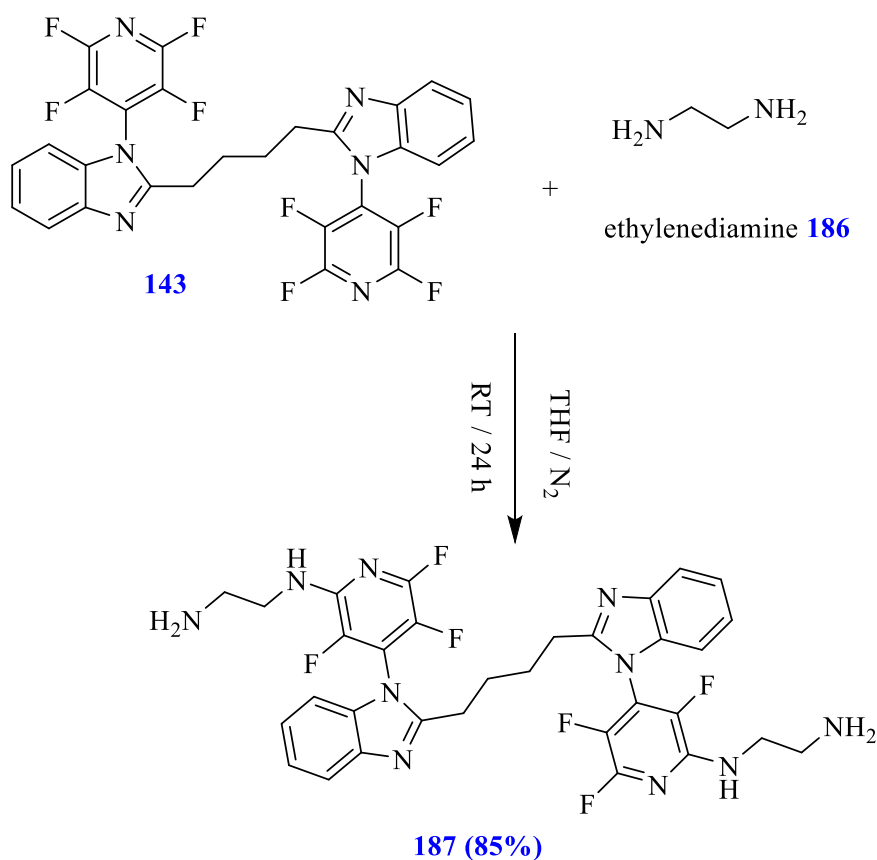
After successfully synthesising macro cyclized compounds **181** and **183** it was decided to try hexamethylenediamine in order to make further examples of such macro cycles. Thus reaction of perfluoro bis-benzimidazole derivative **143** with hexamethylenediamine **184** in 1:1 ratios was carried out in THF as solvent and in the presence of Et₃N as base at RT for 24 h (scheme 63). After purification the target macro cyclized compound **185** was again afforded in 20% yield. The structure was confirmed by ¹H, ¹⁹F and ¹³C NMR spectroscopy and accurate mass measurement with *m/z* of 655.2570 (MH⁺) for C₃₄H₃₁F₆N₈. The ¹⁹F NMR spectrum showed three signals (2 F for each signal) as expected. Formation of a 22-membered ring in this case, confirms the relative ease of macrocycle formation in these systems, which is likely due to the hindered rotation of the aryl benzimidazole groups increasing the probability of the final amino group encountering the other fluoropyridine ring, rather than reacting with a second molecule to form oligomers or polymers.



Scheme 63. reaction of perfluoro bis-benzimidazole derivative **143** with hexamethylenediamine.

2.1.8.6. Study of the reaction of compound **143** with ethylenediamine

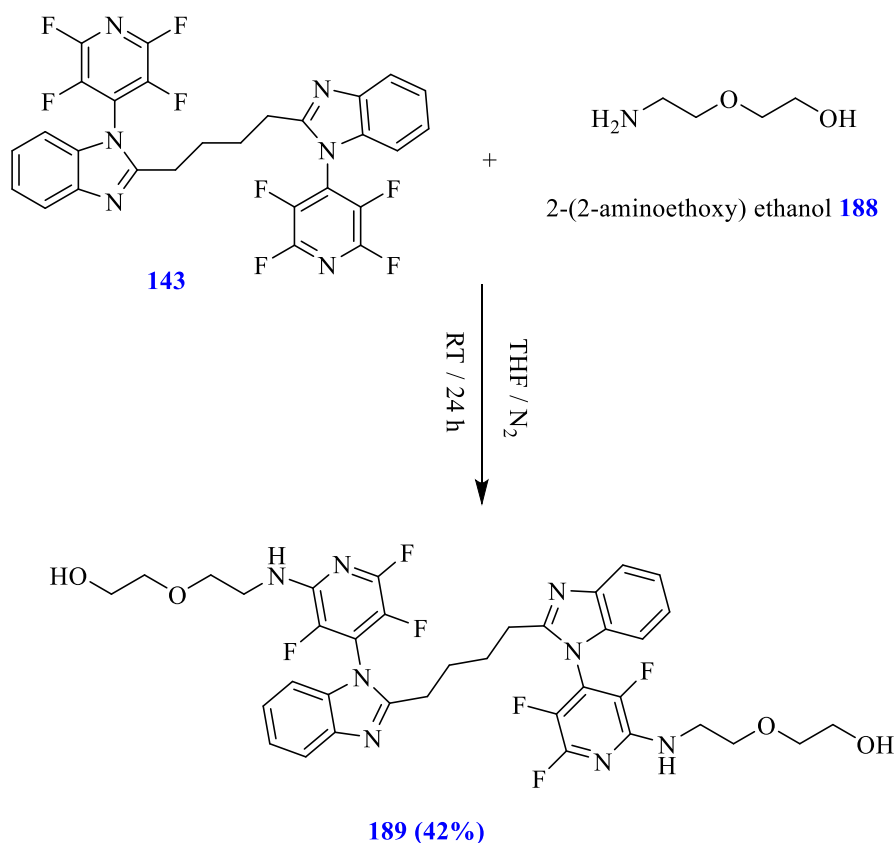
Next it was planned to study the possibility of adding two molecules of ethylenediamine **186** perfluoro bis-benzimidazole derivative **143** by treating it with two equivalents of ethylenediamine **186** in THF at RT for 24 h (Scheme 64). The target compound **187** was afforded easily by addition of water to the reaction mixture in 85% yield. The structure was confirmed by its ^1H NMR spectrum and accurate mass measurement with m/z of 669.2632 (MH) for $\text{C}_{32}\text{H}_{31}\text{F}_6\text{N}_{10}$. The ^{19}F NMR spectrum showed three signals (2F for each signal) as expected.



Scheme 64. Reaction of compound **143** with ethylenediamine.

2.1.8.7. Investigation of the reaction of compound **143** with 2-(2-aminoethoxy) ethanol

Two equivalents of 2-(2-aminoethoxy) ethanol **188** were then reacted with one equivalent of compound **143** in order to form a further target compound **189** that might possess potential biological activity or DNA binding activity. The reaction was carried out in THF at RT for 24 h. The target compound **189** was afforded in 42% by recrystallization from DCM and light petroleum (scheme 65). The structure was confirmed by its ^1H NMR spectrum and accurate mass measurement with m/z of 759.2836 (MH^+) for $\text{C}_{36}\text{H}_{37}\text{F}_6\text{N}_8\text{O}_2$. The ^{19}F NMR spectrum showed three signals (2 F for each signal) as expected. Elemental analysis fitted with the expected composition for a molecular formula of $\text{C}_{36}\text{H}_{36}\text{F}_6\text{N}_8\text{O}_2 \cdot 3\text{H}_2\text{O}$ (785).



Scheme 65. Reaction of compound **188** with 2-(2-aminoethoxy)ethanol.

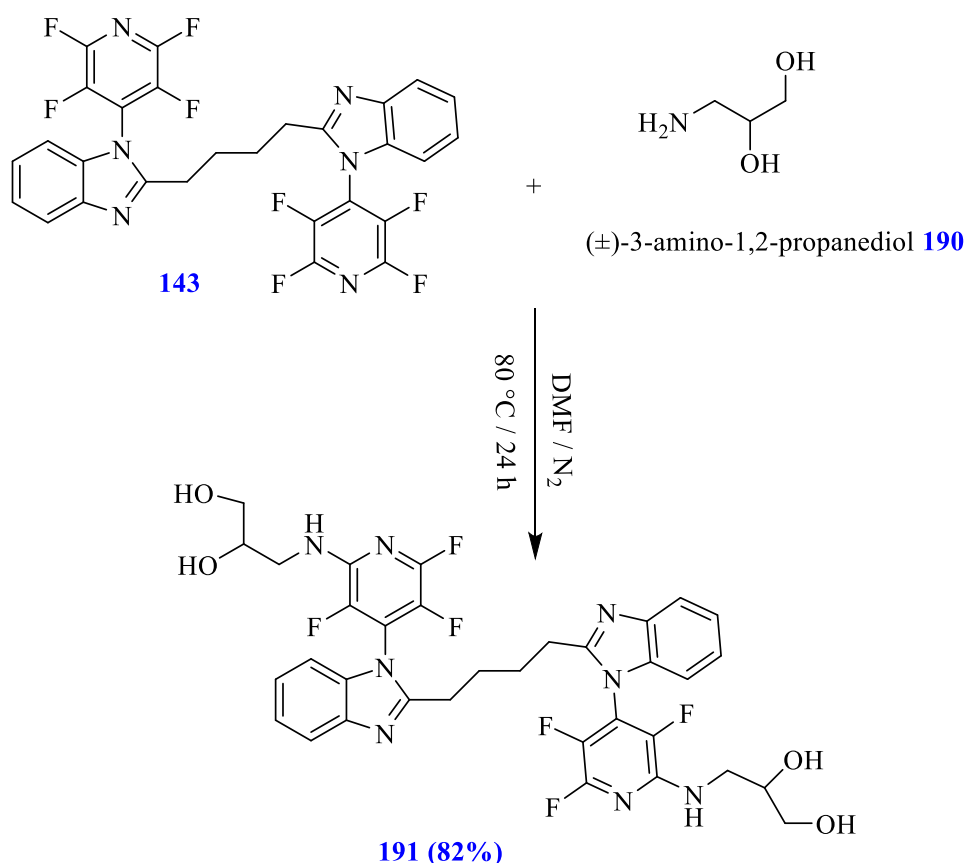
2.1.8.8. Investigation of the reaction of compound **143** with (\pm)-3-amino-1,2-propanediol

Reaction of two equivalents (\pm)-3-amino-1,2-propanediol **190** with one equivalent of compound **143** was tried in THF at RT similar to previous reactions. Unfortunately this time the reaction did not work well and different conditions were therefore studied (Table 16).

Table 16. different reaction conditions for compound 143 with (\pm)-3-amino-1,2-propanediol.

Entry	Reagents	Conditions	Results
1	None	THF, RT, 24 h. N ₂	Starting material
2	None	DMF, RT, 24 h. N ₂	Starting material and product (30%)
3	None	DMF, 80 °C, 24 h. N ₂	Product (82%)

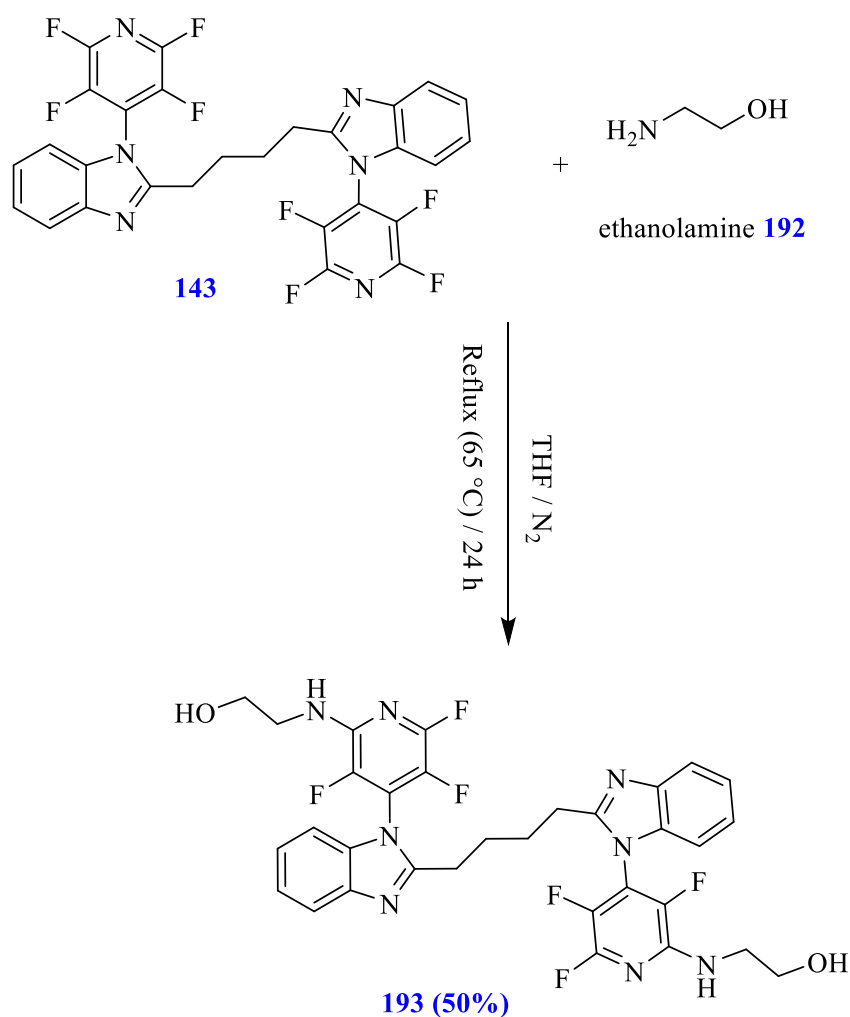
As seen in table 16, the reaction worked very well in DMF at 80 °C and target compound **191** was afforded in 82% (Scheme 66). The structure was confirmed by NMR spectroscopy. The ¹⁹F NMR spectrum showed three signals (2 F for each signal) as expected. In addition accurate mass measurement gave m/z of 731.2523 (MH⁺) for C₃₄H₃₃F₆N₈O₈



Scheme 66. Reaction of compound 143 with (±)-3-amino-1,2-propanediol.

2.1.8.9. Reaction of compound 143 with ethanolamine

In order to extend the number of novel hydrophilic fluorinated heterocyclic compounds as potential biological agents, two equivalents of ethanolamine **192** were reacted with one equivalent of compound **143** in order to form the target **193** (Scheme 67). The reaction was carried out in boiling THF at RT for 24 h and compound **193** was afforded in 50% after recrystallization from hot ethanol. The structure was confirmed by its ^1H NMR spectrum and accurate mass measurement with m/z of 669.2161 (MH^+) for $\text{C}_{34}\text{H}_{27}\text{F}_6\text{O}_2\text{N}_8$. The ^{19}F NMR spectrum showed three signals (2F for each signal) as expected.

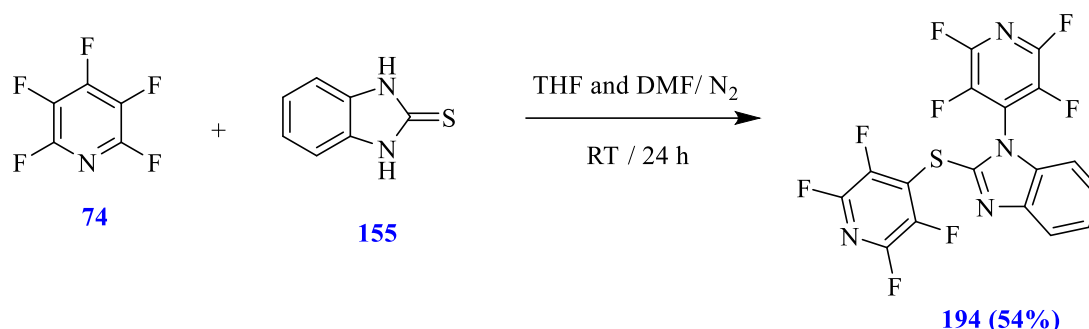


Scheme 67. Reaction of compound **143** with ethanolamine.

2.1.8.10. Reaction of pentafluoropyridine **74** with 2-mercaptobenzimidazole

As scaffold **194** showed positive activity against Trypanosoma parasites¹²⁷ and as this scaffold would have potential for further modification to allow synthesis of diverse libraries of molecules that can be screened for biological activity, we decided to synthesise this scaffold again, and also attempt to improve the yield by modifying the existing method as the reported yield¹²⁸ was very low. Therefore reaction of pentafluoropyridine **74** with 1,3-dihydro-2*H*-benzimidazole-2-thione **155** was carried out in a mixture of DMF and THF as solvent, and with NaH as base, but in this case the solution of 2-mercaptobenzimidazole in DMF : THF (3:10) was added by slow addition to a stirred

mixture of NaH and pentafluoropyridine in THF using a syringe pump to control the rate of addition. This helped to improve the reaction by increasing the yield from 27% to 54%.

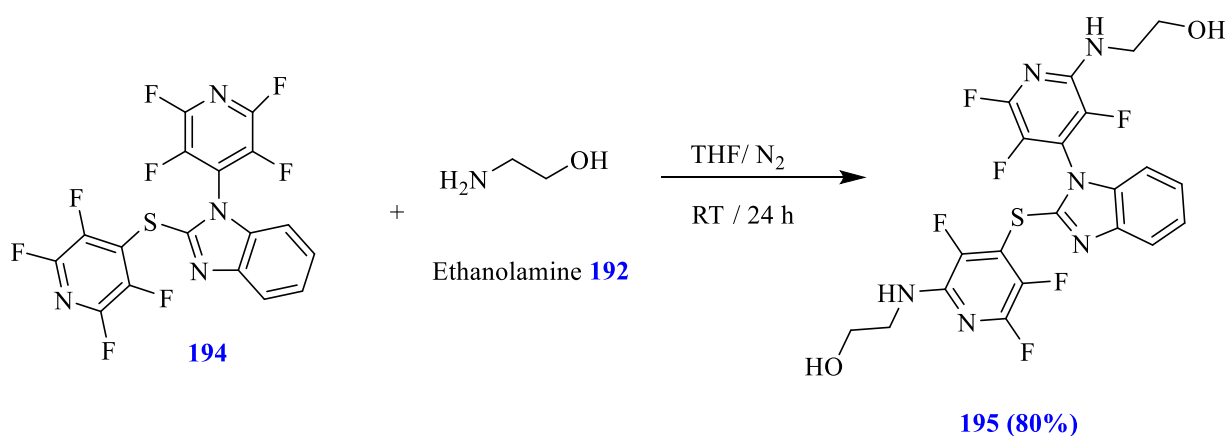


Scheme 68. Reaction of pentafluoropyridine with 2-mercaptobenzimidazole.

2.1.8.11. Investigation of further substitution of fluorine in scaffold **194** by ethanolamine

As mentioned above the bis-tetrafluoropyridyl benzimidazole derivative **194** had shown positive activity against Trypanosoma parasites¹²¹ it was therefore decided take this compound on for further modification, and to add hydrophilic side chains to improve water solubility and biological activity, by further S_NAr reaction.

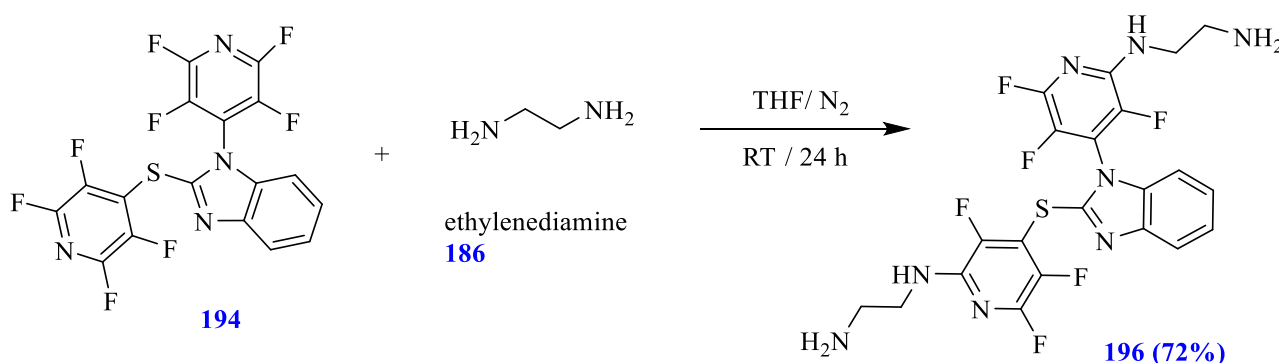
Thus, ethanolamine **192** was chosen as the first nucleophile to be investigated, and two equivalents were reacted with one equivalent of compound **194** in an approach to form the target compound **195** (Scheme 69). The reaction was carried out in THF as solvent and Et_3N as base for 24 h, at RT and the desired compound **195** was afforded in 80% after extraction as a shiny white sugary solid. The structure was confirmed by the 1H NMR spectrum and accurate mass measurement with m/z of 531.1028 (MH^+) for $C_{21}H_{17}F_6N_6O_2S$. The ^{19}F NMR spectrum showed six signals (1F for each signal) as expected.



Scheme 69. Reaction of scaffold **194** with ethanolamine.

2.1.8.12. Substitution reaction of scaffold **194** with ethylenediamine

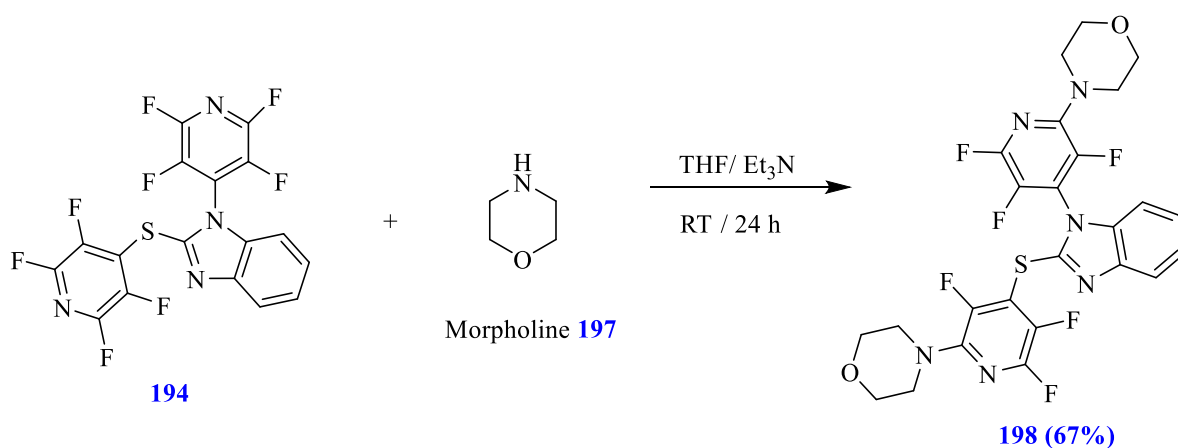
Reaction of two equivalents of ethylenediamine **186** with one equivalent of scaffold **194** was next tried with the same conditions (Scheme 70). The target compound **196** was afforded in 72% as a yellow sugary solid. The structure was confirmed by ^1H NMR spectroscopy and accurate mass measurement with m/z of 529.1350 (MH^+) for $\text{C}_{21}\text{H}_{19}\text{F}_6\text{N}_8\text{S}$. The ^{19}F NMR spectrum showed six signals (1F for each signal) as expected.



Scheme 70. Reaction of scaffold **194** with ethylenediamine.

2.1.8.13. Substitution Reaction of scaffold **194** with morpholine

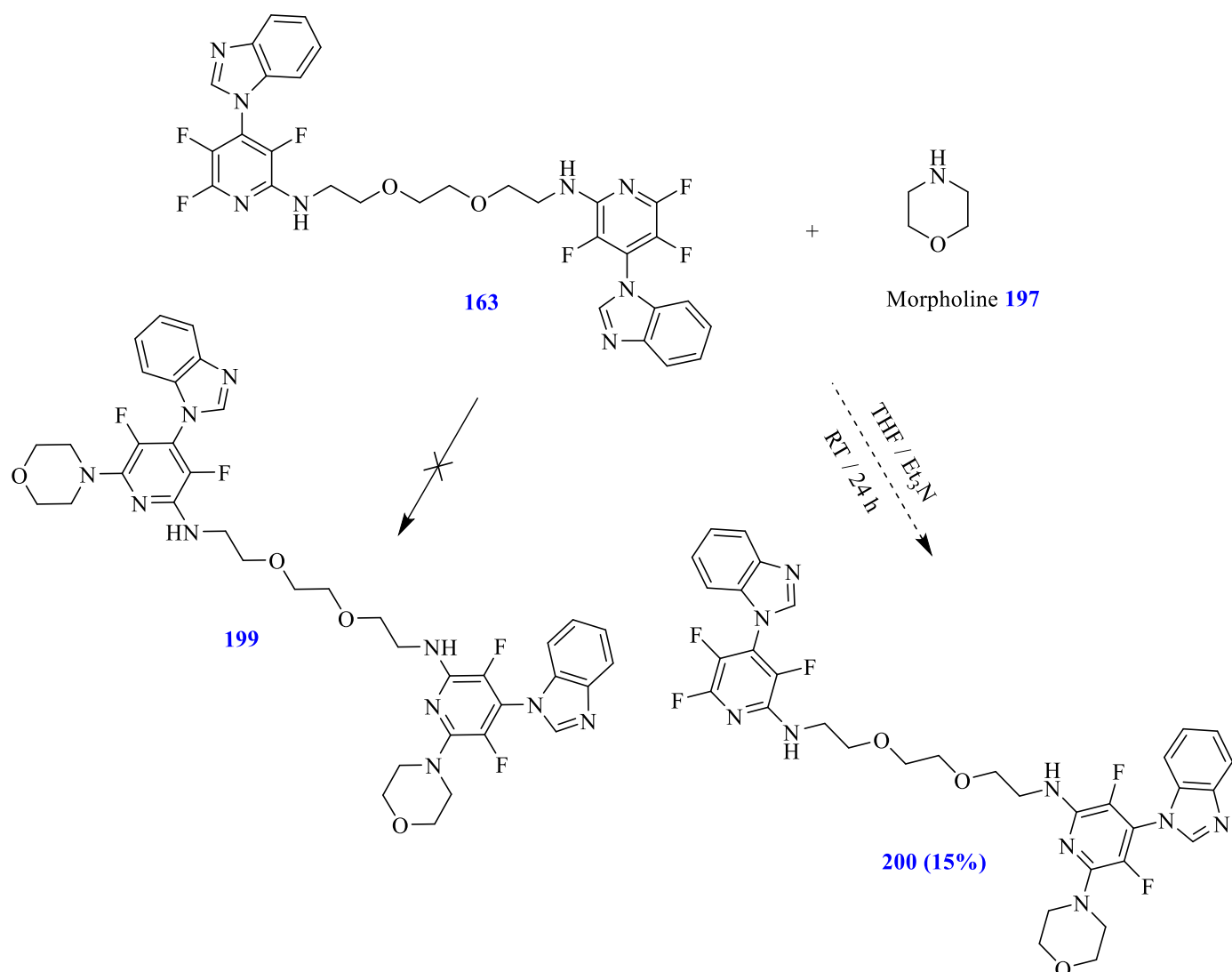
Similarly reaction of morpholine **197** with compound **194** in ratio 2:1 was investigated in THF as solvent and Et_3N as base at RT for 24 h. pleasingly the target compound **198** was again afforded in good yield (67%) after chromatographic purification. The structure was confirmed by NMR spectroscopy and accurate mass measurement with m/z of 583.1345 (MH^+) for $\text{C}_{25}\text{H}_{21}\text{F}_6\text{N}_6\text{O}_2\text{S}_1$. The ^{19}F NMR spectrum showed six signals (1F for each signal) as expected for the two differently substituted trifluoropyridine rings.



Scheme 71. Reaction of scaffold 194 with Morpholine.

2.1.8.14. Investigation of reaction of morpholine with the tethered bis-benzimidazolyl pyridine 163

After successful substitution of fluorine by morpholine 197 in compound 194 and synthesis of tethered compound 198 it was decided to try reaction of compound 163 with morpholine 197 in the hope of replacing a third fluorine in the pyridyl rings to form compound 199. Therefore reaction of morpholine with compound 163 in ratio 2:1 was undertaken in THF as solvent and Et₃N as base at RT for 24 h. After separation by column chromatography the compound 200 was afforded in 15% yield. However compound 199 was not afforded as shown in (Scheme 72), and in this reaction morpholine had added to only one of the pyridine rings and mono-substitution occurred. The structure of compound 200 was confirmed by ¹H NMR and ¹⁹F NMR spectroscopy with tiny impurity which could not be more purify due to lack of the time and polarity of the compound. The ¹⁹F NMR spectrum showed five signals (1F for each signal) as expected. Reaction at only one pyridine ring illustrates the decreasing reactivity of the remaining fluorines on increasing substitution, particularly with electron donating groups such as amines. Reaction at higher temperature may lead to morpholine adding to both pyridine end groups to form the symmetrical compound 199.



Scheme 72. Reaction of morpholine with tethered compound 163.

2.1.9. Investigation of reaction of perfluoroarenes with aliphatic side chains which contain thiol

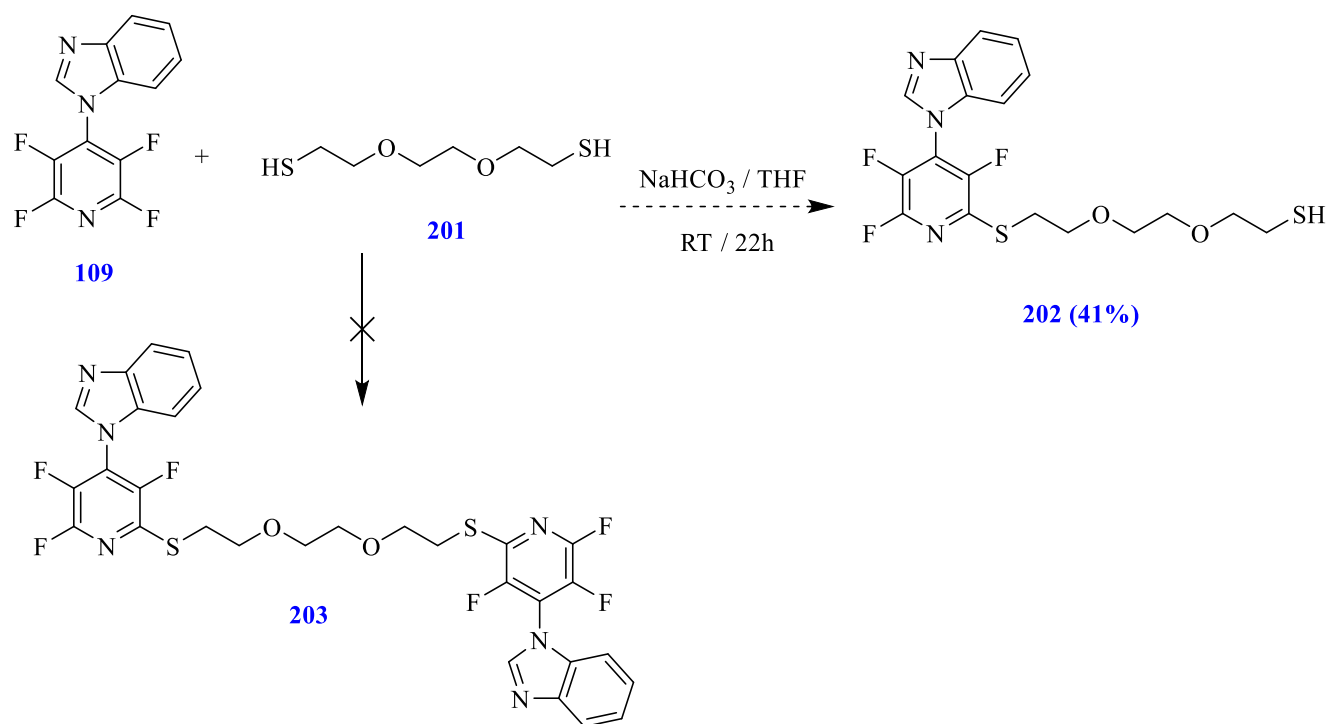
After successfully reaction of perfluoroarenes with aliphatic containing hydrophilic amino and make series of novel linked and fused heterocyclic scaffolds containing amine group. We was decided to try another aliphatic side chain which contain thiol to make series of novel linked and fused heterocyclic scaffolds containing thiol group and compare the biological activity of each series.

2.1.9.1. Reaction of compound **109** with 3,6-dioxa-1,8-octanedithiol

To start we decided try to react compound **109** with **201** to make bis-linked binding agent containing sulphur group therefore reaction of compound **109** (2 equiv.) with 3,6-dioxa-1,8-octanedithiol **201** (1equiv.) was carried under different conditions. As seen in table 17, the reactions did not work well and only the reaction which was carried at 65 °C, in THF as solvent and NaHCO₃ as base indicated presence of compound **202** which was afforded by column chromatography as white solid in 41 % yield (entry 5). However the ¹H NMR spectrum was not completely clean and still showed some impurity, and the compound could therefore not be fully characterised. Although ¹⁹F NMR spectroscopy showed 3 signals as expected, each signal contained 1 F atom. Also mass spectrometry displayed the expected mass of the compound **202**. MS (ESI) (MH⁺), C₁₈H₁₉F₃N₃O₂S₂ requires m/z 430.0871 found m/z 430.0869. Although the target bis linked intercalator compound **203** not formed, the formation of compound **202** showed the reaction to be viable and further investigation to effect reaction on both rings should be continued.

Table 17. different reaction conditions for compound 109 with 3,6-dioxa-1,8-octanedithiol.

Entry	Reagents	Conditions	Results
1	Et ₃ N	THF, reflux (65 °C), 22 h. N ₂	Complex NMR spectrum of unknown compound.
2	Et ₃ N	THF, RT, 22 h. N ₂	Still complex NMR spectrum
3	No base	THF, RT. 22 h. N ₂	Starting material
4	NaHCO ₃	THF, RT, 22 h, N ₂	Starting material
5	NaHCO ₃	THF, 65 °C, 22 h, N ₂	Starting material and compound 202



Scheme 72. Reaction of compound 109 with 3,6-dioxa-1,8-octanedithiol.

2.2. DNA binding studies

2.2.1. UV absorption spectroscopy experiment

The interaction of the synthetic compounds prepared with DNA was determined by a UV absorption spectroscopy which is a simple and useful method for analysing binding. In the UV absorption assay the change in the absorbance of the test compound with and without SS-DNA gives an idea about the interaction of the substance with DNA. Known compounds, Actinomycin D (an intercalator) and naproxen (a groove binder) were used as controls. Compounds binding with DNA through intercalation usually result in hypochromism and bathochromism (red shift). As the intercalative mode involving a stacking interaction between an aromatic chromophore and the base pair of DNA, the extent of the hypochromism is usually consistent with the strength of intercalative interaction.⁴⁴ In the case of electrostatic attraction between the compound and DNA, a hyperchromic effect is observed that reflects the corresponding changes of DNA in its conformation and structure after the complex–DNA interaction has occurred. The hyperchromic effect is the noticeable increase in absorbance of DNA upon denaturation.

All spectral characteristics indicated some change which were caused by change in conformation and structure of DNA after the compounds binds to it. Also the association/ binding constants of all DNA-complexes were determined by Benesi-Hildebrand equation, Eq. (1)

$$\frac{A_0}{A-A_0} = \frac{\epsilon_G}{\epsilon_{H-G}-\epsilon_G} + \frac{\epsilon_G}{\epsilon_{H-G}-\epsilon_G} \times \frac{1}{K[DNA]} \quad (1)$$

Where K is the binding constant, A_0 is absorbance of drug without any DNA, and A is absorbance of the DNA-Drug complex. ϵ_G and ϵ_{H-G} are the absorption coefficients of the drug and DNA-Drug complex, respectively. The K value was determined from the intercept-to-slope ratio of $A_0/A-A_0$ vs. $1/[DNA]$ plot.

In addition the Gibbs free energy (ΔG) was used to calculate for each complex using Eq. (2)

$$\Delta G = -RT \ln K \quad (2)$$

Where R is general gas constant ($8.314 \text{ JK}^{-1}\text{mol}^{-1}$) and T is room temperature (298 K).

2.2.1.1. UV-visible spectroscopy of ACTD as known intercalate agent and naproxen as known groove binder

ACTD is a known DNA-interacting transcription blocker with anti-cancer activity. It interferes with both DNA replication and transcription by intercalation between bases. Also it acts as a cytotoxic inducer of apoptosis in tumour cells. Therefore it was used as reference in this study (Figure 35)

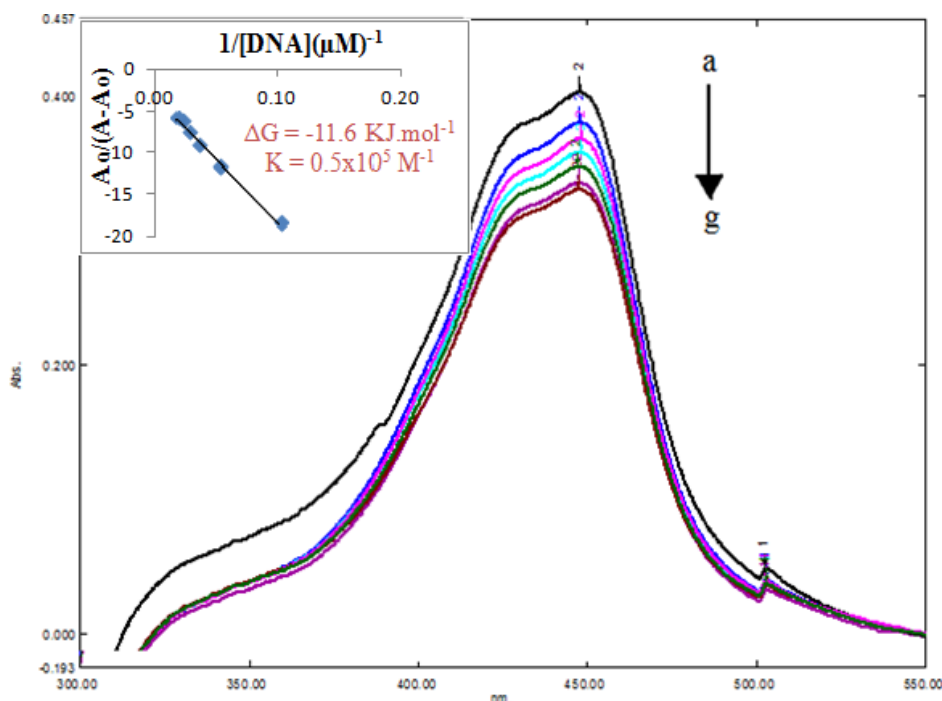


Figure 35. Absorption spectra of 1×10^{-5} M ACTD in absence (a) and presence of 9.6 μ M (b), 18 μ M (c), 27 μ M (d), 35 μ M (e), 43 μ M (f) and 50 μ M (g) of DNA.

The arrow shows increasing DNA concentration. Inside graph is plot of $A_0/(A-A_0)$ vs. $1/[DNA]$ for determination of binding constant (K) and Gibbs free energy (ΔG) of ACTD. ($R^2 = 0.9926$ for six point)

According to Figure 35, the ACTD as known intercalator control showed strong absorption in the region (440-460 nm) which is accredited to the long-living triplet excited state of aromatic system. Also the spectra indicated that by increasing concentration of DNA, the absorption bands of the complex were decreased which resulting in the tendency of hypochromism as expected due to the intercalation of ACTD with DNA. Hypochromism is caused by contraction of DNA helix, as well as from conformational change of DNA. The binding constant value for ACTD is $0.5 \times 10^5 \text{ M}^{-1}$ which

indicated strong affinity of the drug to SS-DNA. The Gibbs free energy is -11.6 kJmol^{-1} . The negative value of ΔG shows a spontaneous process in this interaction.

Naproxen is another known DNA binding agent which was used as possible groove binder control. As seen in (Figure 36) it showed strong absorption at 300 nm. The spectra indicated that by increasing concentration of DNA, the absorption decreased therefore in the case of groove binding still we have the hypochromism as well as the intercalation interaction. The K value ($1 \times 10^5 \text{ M}^{-1}$) and the Gibbs free energy (-12.3 kJmol^{-1}) of naproxen was higher than the K value and the Gibbs free energy of ACTD (figure 14) which indicated that naproxen has higher affinities to SS-DNA than AD. The negative value of ΔG shows a spontaneous process.

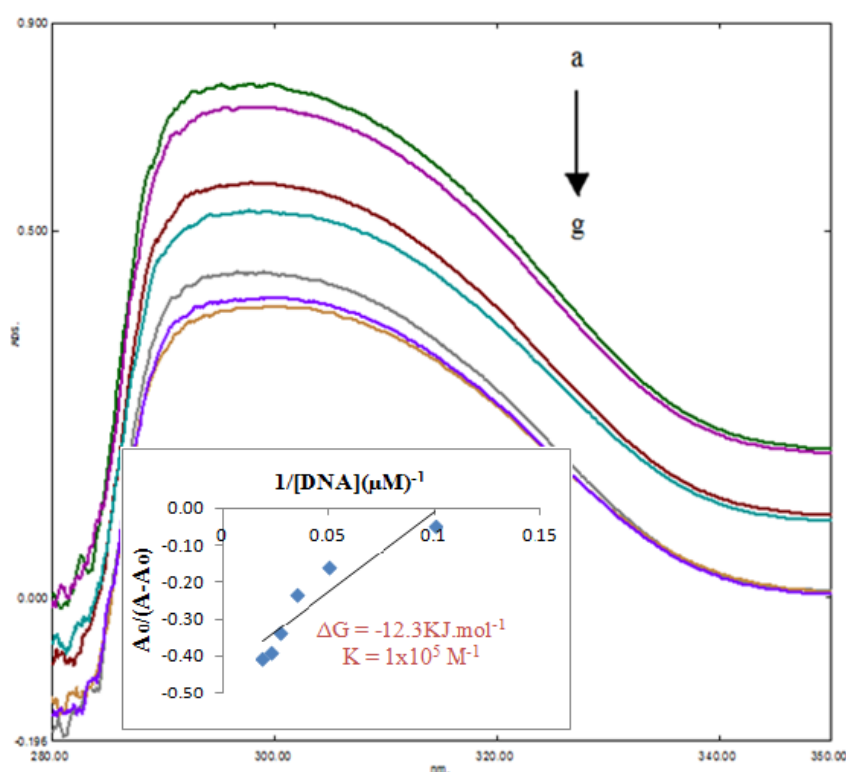


Figure 36. Absorption spectra of $1 \times 10^{-5} \text{ M}$ of naproxen in absence (a) and presence of $9.6 \mu\text{M}$ (b), $18 \mu\text{M}$ (c), $27 \mu\text{M}$ (d), $35 \mu\text{M}$ (e), $43 \mu\text{M}$ (f) and $50 \mu\text{M}$ (g) DNA.

The arrow shows increasing of DNA concentration. Inside graph is plot of $A_0/(A-A_0)$ vs. $1/[DNA]$ for determination of binding constant (K) and Gibbs free energy (ΔG) of naproxen ($R^2 = 0.8614$ for six points)

2.2.1.2. *Studies of UV absorption results and cooperation of binding constant data*

Table 18. Absorption changes caused by synthesised compounds intraction with DNA.

Compounds	Absorption	K value (M^{-1})
108	Decrease (hypochromism)	0.5×10^4
111	Decrease (hypochromism)	2.9×10^4
113	Decrease (hypochromism)	1.1×10^5
114	Decrease (hypochromism)	1.5×10^5
137	Decrease (hypochromism)	0.1×10^5
138	Decrease (hypochromism)	0.3×10^4
143	Decrease (hypochromism)	0.6×10^5
151	Decrease (hypochromism)	4.7×10^4
152	Decrease (hypochromism)	1.4×10^5
161	Decrease (hypochromism)	6.9×10^4
162	Decrease (hypochromism)	2.5×10^4
163	Decrease (hypochromism)	0.8×10^4
164	Decrease (hypochromism)	1.5×10^3
165	Increase (hyperchromic effect)	1.5×10^5
166	Decrease (hypochromism)	8.9×10^4
169	Decrease (hypochromism)	4.4×10^4
170	Decrease (hypochromism)	9.8×10^4
171	Decrease (hypochromism)	8.8×10^4
181	Decrease (hypochromism)	1.1×10^5
183	Decrease (hypochromism)	7.6×10^4
187	Decrease (hypochromism)	4.4×10^4
189	Decrease (hypochromism)	1×10^5
191	Decrease (hypochromism)	3×10^4
195	Decrease (hypochromism)	2.4×10^5
196	Decrease (hypochromism)	1.8×10^5
198	Increase (hyperchromic effect)	2.1×10^5

According to the above table the K values (bonding constant) more than 1×10^{-5} indicates good binding affinity, the K values between $1 \times 10^{-4} - 1 \times 10^{-5}$ indicate moderate binding affinity and the K values below 1×10^{-4} indicate poor binding affinity. Also most of the compounds on adding the DNA in different concentrations showed a decrease in the absorption which indicated a hypochromic effect due to the intercalative interaction. Only compounds **165** and **198** showed an increase in the absorption due to a hypochromic effect which can be result of electrostatic attraction between the compounds and DNA.

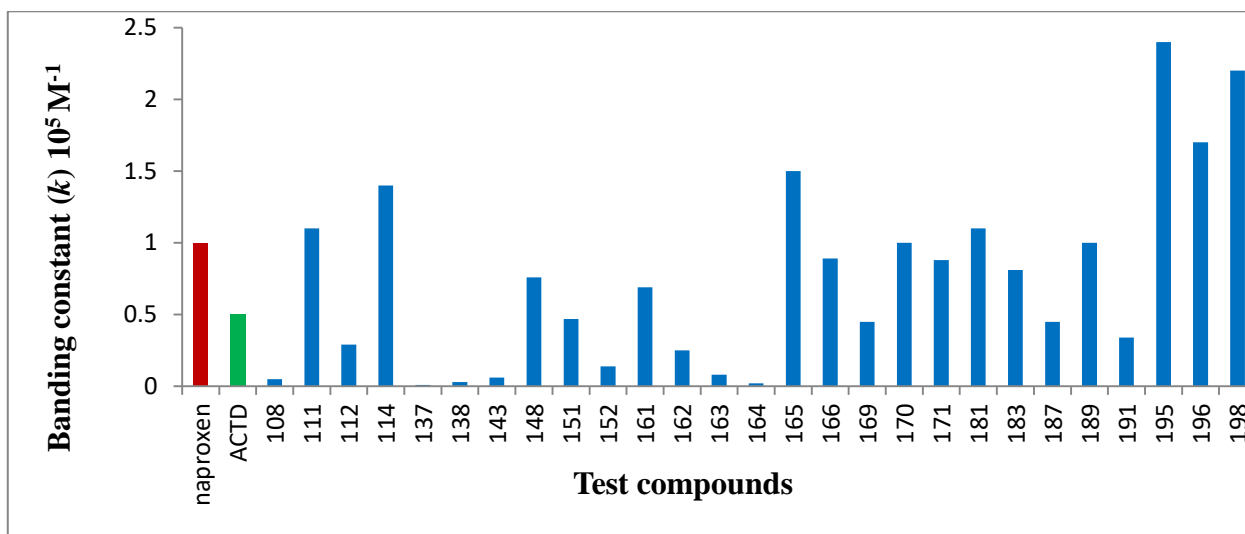
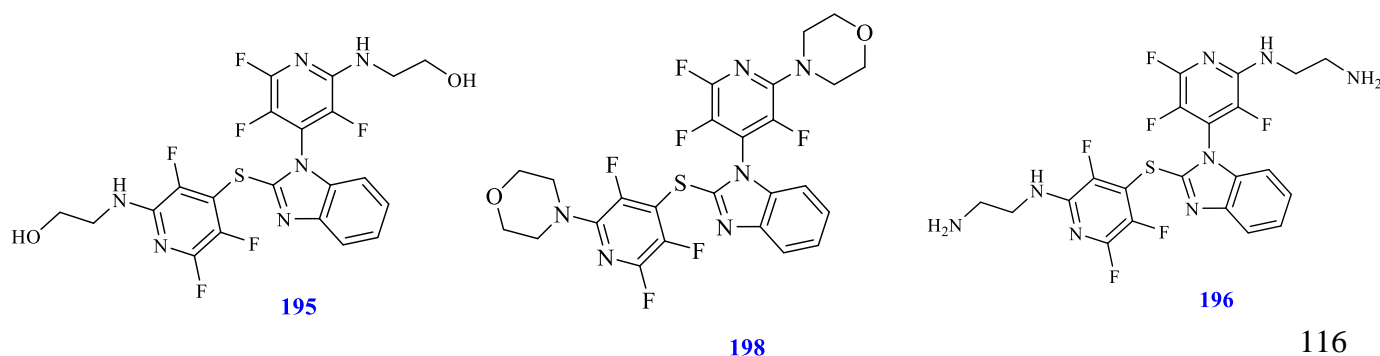


Figure 37. UV absorption of synthesised compounds with different concentrations of DNA. Each bar in this graph represents the binding constant of different synthesised compounds.

According to figure 37, all of the synthesised compounds showed some affinity to SS-DNA in the UV absorption assay, although in comparison to the reference compounds and each other, binding is very different. Interestingly compounds **165**, **196** and **198** showed the greatest *k* values compared to the other compounds and even references which indicated highest bonding affinity to SS-DNA than other synthesised compounds. In addition compound **195** and **198** showed closest and higher binding constants in comparison to **196** which might be because of presence of oxygen in both structure, as seen in below.



Compounds **114** and **165** have the second largest binding constant values which are still higher than reference's K value. Compounds **113**, **170**, **181** and **189** indicated very similar K values to naproxen. Along with the K value of compounds **169** and **187**, which was very close to ACTD, compounds **108**, **112**, **137**, **143**, **162**, **163**, **164**, and **191**, showed very weak DNA binding affinity compared to the reference and the other compounds.

2.2.2. Ethidium bromide (EB) fluorescence displacement experiment

Ethidium bromide (EB) fluorescence displacement assay was another useful method for studying the interaction of the synthetic compounds prepared with DNA. In this method the EB fluorescence intensity will increase in the presence of DNA by intercalation of EB into the double helix (Figure 38). It is quenched by addition of another compound as the quencher then displaces EB from DNA. Therefore if the fluorescence intensity decreased on adding the compound it means that the test compound binds to the DNA and displaces the EB. If no change in intensity occurs it does not mean the compound does not bind to DNA as it may bind in another non-intercalating way.

The linear Stern-Volmer quenching constant K_{sv} was calculated from the linear Stern-Volmer equation (3), by considering the quenching of EB bound to DNA by different concentration of quencher or compound.

$$I_0/I = 1 + K_{sv}[Q] \quad (3)$$

Where I_0 and I represent the fluorescence intensities in absence and presence of the compound and Q is the concentration of the compound. K_{sv} values were calculated from the slope of the regression line in the derived plot of I_0/I vs compound concentration.

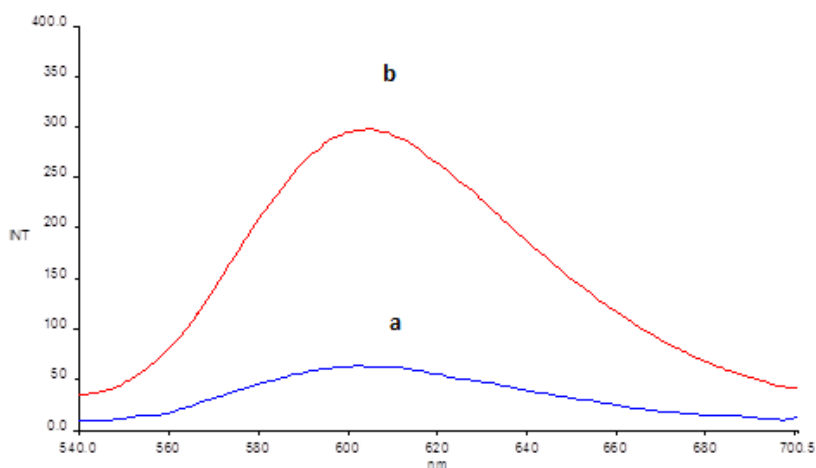


Figure 38.) Emission spectra of EB 1×10^{-6} M in the absence of DNA and b) Emission spectra in presence of DNA 3.17×10^{-5} M

2.2.2.1. EB fluorescence displacement assay of Actinomycin D as intercalating agent

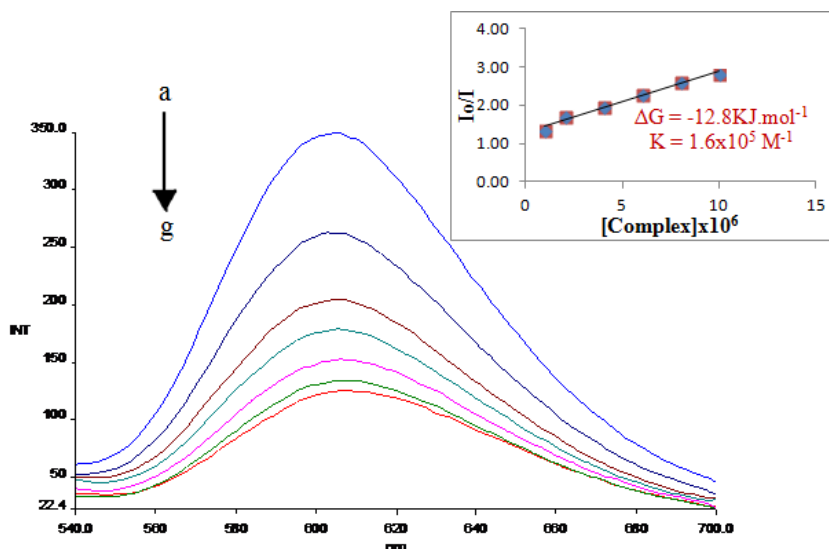


Figure 39. Emission spectra of SS-DNA-EB in tris-HCl buffer on titration of ACTD. $K_{ex} = 480$ nm; [EB] = 1×10^{-6} M; [DNA] = 3.17×10^{-5} M; [ACTD] (a) 0.0, (b) 1×10^{-6} , (c) 2×10^{-6} , (d) 4×10^{-6} , (e) 6×10^{-6} , (f) 8×10^{-6} , (g) 10×10^{-6} M. The arrow shows the increase of the complex concentration. Inside graph is plot of I_0/I vs. [DNA] for determination of K and ΔG values. ($R^2 = 0.9782$ for six points)

According to figure 39, by increasing of the ACTD concentration, the fluorescence intensity at 605 nm decreased significantly, which indicated the ACTD had displaced the EB completely and bound to DNA by intercalation interaction as expected. Also the K_{vs} value for ACTD complex was found to be 1.6×10^5 which indicated a very strong affinity of ACTD complex to SS-DNA. The Gibbs free energy is $-12.8 \text{ kJ.mol}^{-1}$. The negative value of ΔG shows a spontaneous process in this interaction.

2.2.2.2. EB fluorescence displacement assay of naproxen as groove binding agent reference.

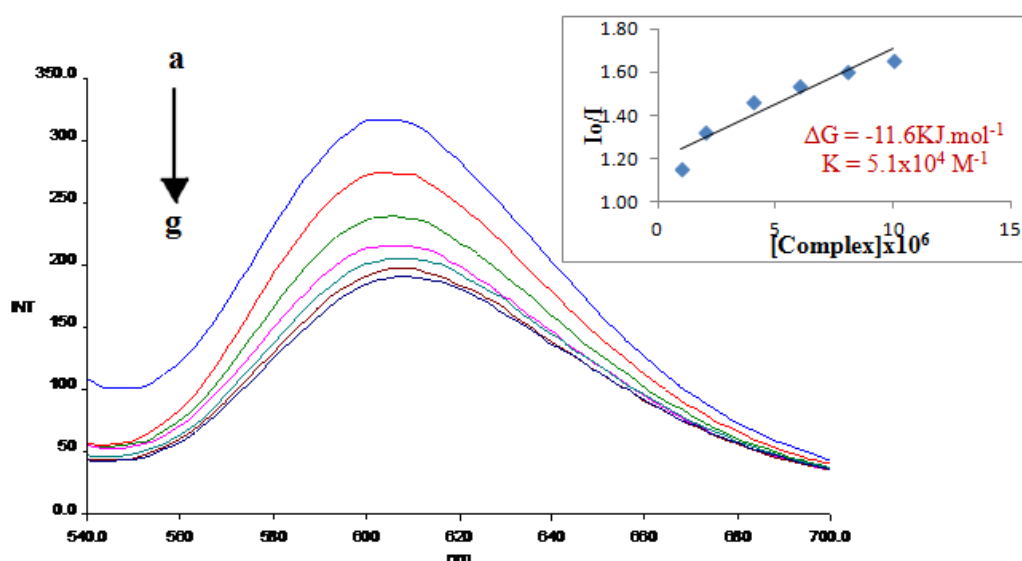


Figure 40. Emission spectra of SS-DNA-EB in tris-HCl buffer on titration of naproxen.

$K_{ex} = 480 \text{ nm}$; $[\text{EB}] = 1 \times 10^{-6} \text{ M}$; $[\text{DNA}] = 3.17 \times 10^{-5} \text{ M}$; $[\text{AD}]$ (a) 0.0, (b) 1×10^{-6} , (c) 2×10^{-6} , (d) 4×10^{-6} , (e) 6×10^{-6} , (f) 8×10^{-6} , (g) $10 \times 10^{-6} \text{ M}$. The arrow shows the increase of the complex concentration. Inside graph is plot of I_0 / I vs. $[\text{DNA}]$ for determination K and ΔG values. ($R^2 = 0.9782$ for six points)

According to Figure 40, by increasing of the naproxen concentration the fluorescence intensity decreased which indicated naproxen complex interact with DNA as groove binder and releasing some EB from EB-DNA system. Another possibility is naproxen binds to DNA in different binding sites and changes the conformation of DNA which causes a decrease in the fluorescence intensity. Also the K_{vs} value for naproxen complex was found to be $5.1 \times 10^4 \text{ M}^{-1}$ which indicated affinity of naproxen complex to compete at binding site of SS-DNA which EB binds as an intercalating agent is much less than ACTD (Figure 39) as expected. The Gibbs free energy is $-12.8 \text{ kJ. mol}^{-1}$. The negative value of ΔG again shows a spontaneous process.

2.2.2.3. Binding constant comparison of synthesis compound using EB quenching assay

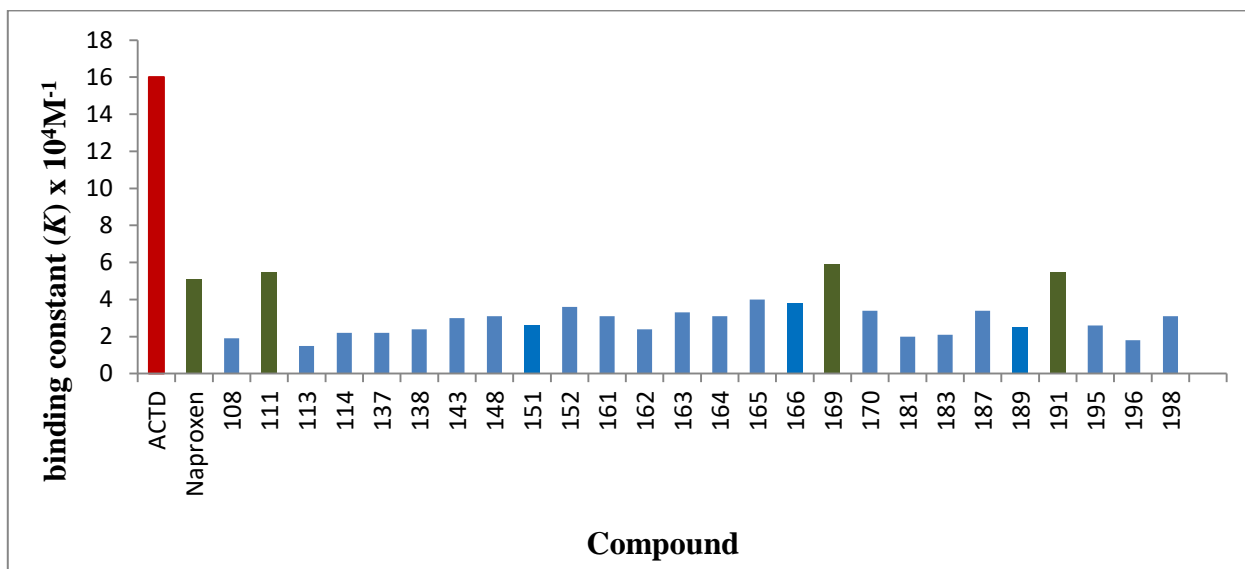
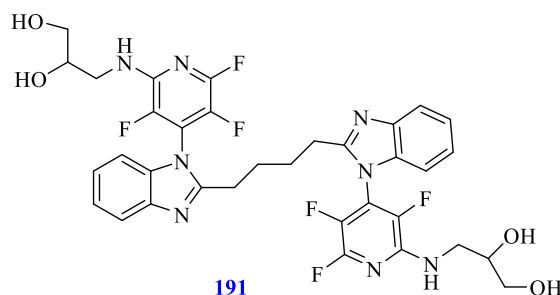
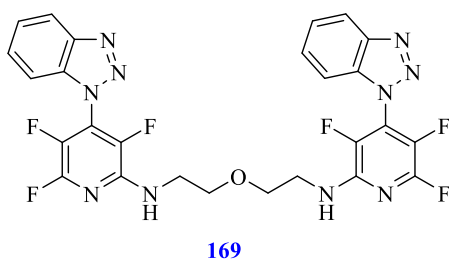
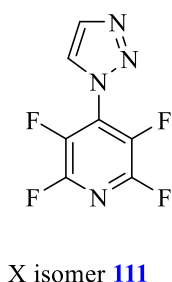


Figure 41. EB displacement assay of synthesis compound. Each bar in this graph represents binding constant of different synthesised compounds. ACTD and naproxen were used as references.

According to Figure 41, all the synthesised compounds showed some affinity to SS-DNA in this assay, although in comparison to the intercalating reference compound ACTD binding was very weak. Compounds **111**, **169**, and **191**, indicated the greater K values compared to others. Therefore these compound showed stronger affinity to SS-DNA than other synthesised compound and their K_{vs} values are closest to the K_{vs} value of naproxen.



2.3. Anticancer activity in vitro

The anticancer activities of synthesis compounds (**143**, **148**, **151**, **152**, **181**, **183**, **187**, **189**, **191**, **193** and **194**) were determined against breast carcinoma MCF-7 and leukemia K562 cell lines after 72 h of incubation using the Calcein assay, and the CDK inhibitor, roscovitine, as a control compound. The results obtained (Table 19), show that compounds **143**, **187**, **183** and **194** display cytotoxicity in which IC₅₀ values reached low micromolar ranges.

Table 19. Cytotoxicity of fluoroarylbenzimidazole derivatives

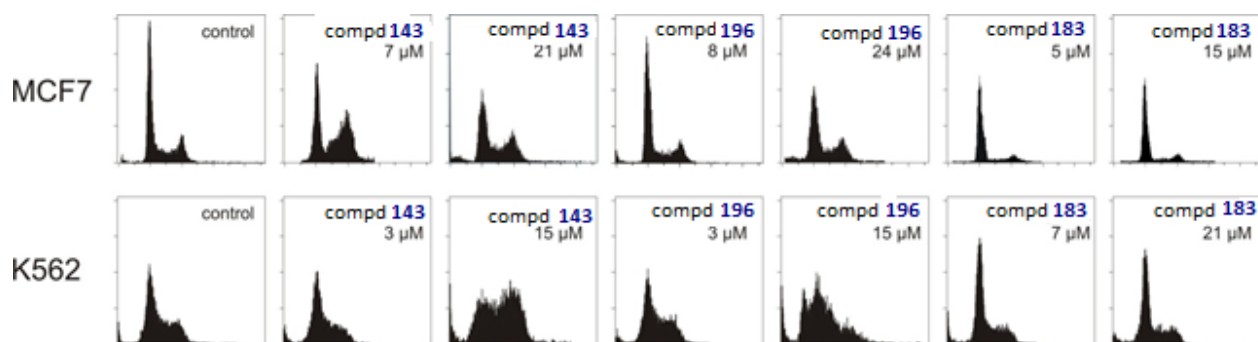
.Compound	Cell line IC ₅₀ (μM)	
	K-562	MCF-7
143	2.8 ± 0.4	7.8 ± 2.0
148	>12.5	>12.5
152	>12.5	>12.5
183	7.2 ± 1.5	4.8 ± 0.4
187	3.4 ± 0.1	8.0 ± 2.6
189	>12.5	>12.5
191	>12.5	>12.5
193	>12.5	>12.5
194	13.2 ± 1.3	>25
Roscovitine	42 ± 3	11 ± 1

These four compounds were further screened by collaborating partners against melanoma G361 and osteosarcoma HOS cell lines to expand information about selectivity towards various types of cancers (Table 20). Concentration-dependent activity it was observed in all cases with these four compounds. Three of the active compounds contained the tetramethylene bis-benzimidazole linker group **134** with tri- or tetrafluorinated pyridine rings, whilst the smaller molecule **194** also contains two fluorinated pyridine rings, separated by the benzimidazole ring. This suggests that two fluorinated pyridine rings separated by 4-6 Å is desirable for activity. However the mechanism of the activity is not yet clear.

Table 20. Cytotoxicity of lead derivatives.

Compound	IC50 (μM)	
	G361	HOS
143	2.0 ± 0.1	1.8 ± 0.1
183	6.0 ± 0.1	8.3 ± 2.0
187	19.9 ± 1.2	16.3 ± 3.0
194	4.4 ± 0.6	2.5 ± 0.9
Roscovitine	22.4 ± 0.2	24.3 ± 0.2

Further experiments were conducted to gain information about the mechanism underlying the observed cytotoxicity. Firstly, the effect of compounds **183**, **187** and **194** on the cell cycle of K562 and MCF-7 cells was analysed. Asynchronously growing cells were treated for 24 h with compounds in two doses, corresponding to $1\times$ and $3\times$ IC_{50} values, followed by analysis by flow cytometry. As shown in Figure 42, the compounds markedly influenced cell cycle profiles in both cell lines although each compound demonstrated this effect in a different way. Treatment of MCF-7 cells with a low dose of **143** led to a decrease in the S phase, whilst a higher dose significantly decreased G1-phase population and increased sub-G1 population in both K562 and MCF-7 cell lines. Compound **187** had no effect at the lower dose used, but the higher dose significantly increased G2/M population in MCF-7 cells. Interestingly, treated K562 cells completely altered the profile, with apparent block of S phase. Macrocytic compound **183** markedly reduced S and G2/M phases in MCF7 cells, while the cell cycle profile in K562 was not changed at all.

**Figure 42. Effect of studied compounds on the cell cycle of MCF7 and K562 cells treated for 24 h.**

Flow cytometric analysis revealed that some compounds increase sub-G1 population, which is a well accepted indicator of ongoing apoptotic cell death. We therefore analyzed treated K562 cells for activity of caspases 3 and 7, proteases that are activated during apoptotic cell death. (Figure 43) shows the results of biochemical assay of caspase 3/7 activity in cells treated for 24 h with the studied compounds at doses corresponding to 1× and 3× IC₅₀ values. While **187** was inactive in the assay, compounds **183** and **194** significantly stimulated activation of the caspases, with the increase in activity more than twenty-fold, and five-fold, over untreated control cells respectively. Based on flow cytometric results and biochemical assay of caspases we conclude that **183** and **194** induce apoptosis in treated cells. However, the flow cytometric experiments suggest that the active compounds exhibit their toxicity through different cellular targets. Further work is ongoing to identify the mode of action of these fluorinated compounds.

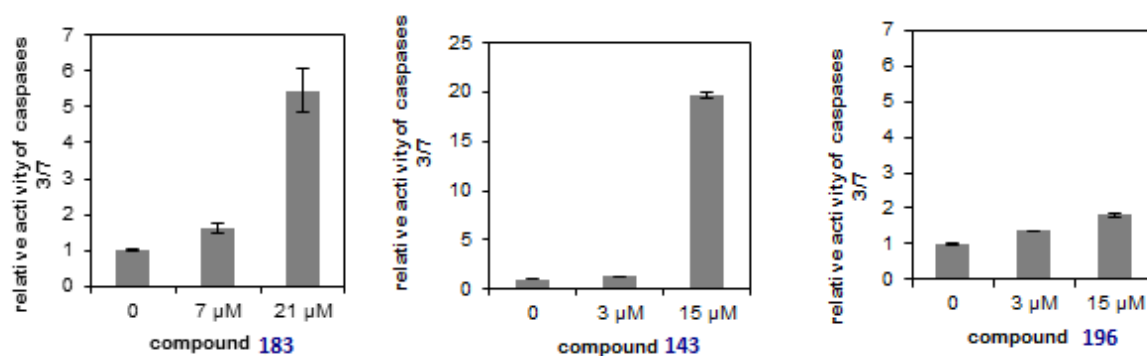


Figure 43. Fluorimetric caspase activity assay. K562 cells treated with studied compounds for 24 h were lysed and the activities of caspases were measured using the fluorogenic substrate Ac-DEVD-AMC and normalised to untreated control.

2.4. Antibacterial activity of synthesised compounds

The synthesised compounds were examined against a gram positive (*Staphylococcus aureus*) and a gram negative (*Escherichia coli*) bacterium *in vitro* by using the disc diffusion method with each experiment performed in triplicate. Amoxicillin was used as reference antibiotic in this assay. Criteria for activity is based on the diameter of the inhibition zone (mm); an inhibition zone more than 20 mm indicates significant activity, for 18-20 mm inhibition is good, 15-17 mm is low, and below 11-14 mm is non-significant activity.^{35, 66} The following compounds at 10⁻³ M were tested, **108, 114, 137, 138, 143, 148, 161, 162, 163, 164, 165, 171, 181, 183, 198**, but showed no zone

inhibition at all. Compounds **111**, **113**, **251**, **252**, **166**, **169**, **170**, **187**, **189**, **191**, **195** and **196** showed an inhibition zone and reading of the zone inhibition represents the mean value of these readings, which are shown in Table 21.

Unfortunately the antibacterial activity assay confirmed that the tested compounds showed non-significant activity against the bacteria, because the inhibition zones were below 11-14 mm. As the high concentration 10^{-3} M did not show a significant inhibition we did not study any lower concentrations of the compounds. Although the compound **191** showed highest activity against *E. coli* and compound **187** showed the highest activity against *S. aureus*. Therefore the fluorinated synthesized compounds in the present study did not show good antibacterial activity against either *Escherichia coli* or *Staphylococcus aureus* strains, despite the evidence for DNA binding. Further studies would be required to understand the exact interaction of the compounds with bacterial cells.

Table 21. Antimicrobial activity of some fluorinated synthesized compounds

Compound	Average zone of inhibition (mm)	
	<i>Escherichia coli</i>	<i>Staphylococcus aureus</i>
Amoxicillin	19	40
111	9	0
113	9	0
151	11	0
152	10	7
166	10	8
169	7	9
170	9	0
187	0	14
189	10	0
191	12	0
195	0	7
196	0	9

2.5. Hanging drop DNA crystallization

In DNA crystallization assay a piece of melting point tube was used to hold a drop of DNA-compound mixture in a cacodylate buffer solution. This was attached to wall of sample vial above

cotton wool wetted with the more concentrated buffer solution to help to absorb solvent from the drop to concentrate it, leading to crystallisation. The sample tube containing the drop was left at RT for a prolonged time to form crystals. Cacodylate buffer was used to dissolve the short synthetic oligonucleotide CGCGAATTCGCG by adding 600 μ l of the buffer to DNA to prepare conc. 0.5 mM of DNA. Synthesised compounds were dissolved in DMSO (0.01 mol, 10 ml) in separate vials and the drop was made by mixing 2 μ l of each compound stock solution with 20 μ l of CGCGAATTCGCG DNA. Unfortunately to date no crystals have formed and this method has given no information about the DNA-compound complexes formed.

3. Conclusions and future work

Over fifty new composite, linked and fused heterocyclic scaffolds have been successfully synthesised using S_NAr substitution reactions of perfluorinated arene building blocks including pentafluoropyridine, hexafluorobenzene, and methyl pentafluorobenzoate with different nucleophile heteroarenes such as imidazole, triazole, benzimidazole, benzotriazole, and carbazole. Furthermore, these scaffolds would have potential for further modification by introducing different water solubilising side chains to allow synthesis of diverse libraries of molecules which are more water soluble and have improved potential for biological activity. X-ray crystal structures of ten compounds were obtained including those of two macrocyclic compounds **181** and **183** containing 24- and 21-membered rings.

Cyclization of ester derivative **148** to make bi- or tri-cyclic bis-intercalators by using different nucleophiles reagent such as hydrazine, 2-aminopyridine and acetamidine did not prove successful. Only compound **176** cyclised on just one of the fluoroarene rings, leaving the ester intact on the other, by using acetamidine which was a more reactive nucleophile than the other reagents tested.

A number of compounds synthesised have been shown to bind to DNA by a combination of UV absorption and fluorescence measurement, although the exact nature of binding has not been determined.

From UV absorption most of the test compounds showed decrease in the absorption which indicated a hypochromic effect due to the intercalative interaction. Only compounds **195** and **168** showed a hypochromic effect by an increase in the UV absorption, which can be result of electrostatic attraction between the compound and DNA.

In addition, interestingly compounds **195**, **196** and **198** showed the greatest K values in binding constant compared to the other compounds and known references which indicated higher bonding

affinity to SS-DNA than other synthesised compounds. Compounds **113**, **170**, **181** and **189** indicated very similar K values to naproxen. Along with K value of compounds **169** and **187** was very close to ACTD.

In terms of fluorescence assay, only compounds **191**, **169** and **112** indicated greater K values compared to other scaffolds, which showed stronger affinity to SS-DNA than the other synthesised compounds, although in comparison to the K value of intercalating reference compound ACTD are still much lower.

For anticancer activity of the test compounds, only three compounds **143**, **183** and **187** demonstrated micromolar inhibition against K-562 and MCF-7 cell lines. These compounds, in addition to **194**, also demonstrated micromolar inhibition against G361 and HOS cell lines. Compounds **143** and **183** were found to activate caspases leading to apoptosis.

Attempts to co-crystallize the compounds with a synthetic oligonucleotide to allow X-ray diffraction studies to determine binding were unsuccessful. Also studies on the antimicrobial activity of a range of the new compounds indicated non-significant activity against the bacteria because the inhibition zones were below 11-14 mm. However, compound **187** showed the highest activity against of *S. aureus* and compound **191** showed highest activity against *E. coli*.

The synthetic work has generated several areas where additional study would be desirable. The formation of **176** showed the cyclization of ester derivatives to make bi- or tri-cyclic bis-intercalators to be viable, and further investigation to effect reaction on both rings should be continued. Also cyclization of ester derivative using more reactive nucleophiles reagents could be explored. Further development of methods to foresee and control the stepwise addition of nucleophiles to perfluoroarenes should be undertaken to study the orientation effects of the added groups, and to improve reactivity as the number of available fluorine atoms falls with progressive substitution. To improve biological activity of the compounds further work could be carried out to replace the remaining fluorine atoms in the ring systems synthesised with alternative aromatic or aliphatic containing hydrophilic amino, hydroxyl and thiol groups. Also synthesis of positively charged derivatives should be undertaken to improve binding to DNA.

Additional attempts to co-crystallize the products synthesised with the DNA strands of known composition should be carried out, to allow a more detailed understanding of the molecular interaction involved in binding activity. A number of the successfully synthesised compounds in this work are being taken forward in a further project to test for anticancer and anti-parasitic activity.

4. Experimental

4.1. *General*

All starting materials and solvents were obtained commercially. THF was distilled under a nitrogen atmosphere from sodium/benzophenone ketyl radical. Anhydrous conditions were obtained by using oven/flame-dried glassware purged with nitrogen prior to the addition of chemical reagents. A nitrogen atmosphere was maintained throughout reactions where necessary through the use of a nitrogen balloon. NMR spectra were recorded on a Bruker DPX 400 operating instrument or a Jeol ECS-400 at 400 MHz for ^1H or 376 MHz for ^{19}F NMR spectra or 100 MHz for ^{13}C spectra were recorded in CDCl_3 , DMSO-d_6 or methanol- d_4 . Chemical shifts are given in parts per million (ppm) and coupling constants are recorded in hertz. Tetramethylsilane was used as internal standard for ^1H and ^{13}C spectra. ^{19}F NMR spectra re referenced to hexafluorobenzene. DEPT was used to assign environment (CH , CH_2 , and CH_3) to each carbon atom in the ^{13}C spectra. Mass spectra were recorded on a Thermo Scientific Exactive (Orbi) ESI (Ethanol) via nanomate (Advion) or were recorded at the EPSRC National mass Spectrometry Facility. The solvent used for all samples was methanol. GC-MS was performed on a Fisons 8060 with a DB5MS column of 30 m length and splitless injection.

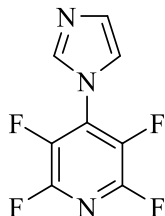
IR spectra were obtained using a Perkin-Elmer spectrum 65 FT-IR spectrophotometer. Sodium chloride plates were used to acquire thin film spectra, or samples were recorded as KBr discs. Melting points were recorded using an Electrothermal-IA 9100 melting point instrument and are uncorrected. Elemental analysis was determined using a Perkin-Elmer 2400 analyser.

The reactions were checked using thin layer chromatography (TLC) on Merck TLC silica gel 60 F254 aluminum backed plates. UV radiation at a wavelength of 254 nm using a U.V.P chromate-vue cabinet model CC-60 used to visualise TLC plates. Column chromatography was carried out on Merck Kiesel 60 silica gel.

For biological activity assays salmon sperm (SS) DNA, naproxen, ACTD and EB were purchased from Sigma. A Spectra UV-2550 instrument was used for UV absorption assay and a Perkin Elmer Luminescence Spectrometer S50B was used for fluorescence assay. For DNA crystallization experiments the DNA sequence CGCGAATTCGCG was purchased from Sigma. Cacodylate buffer was pH 6.5; 50 mM-isopropanol 15% solution. Gram-positive *Staphylococcus aureus* and Gram-negative *Escherichia coli* strains were used for antibacterial studies. Muller Hinton agar, petri dish 90 × 14 mm (diameter and height respectively) and Townson + Mercer incubator was used to incubate the bacteria in anti-microbial activity studies.

4.2. Organic synthesis

4.2.1. 2,3,5,6-Tetrafluoro-4-(1H-imidazol-1-yl)pyridine **108**¹²⁹

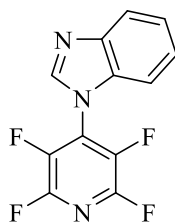


108 (89%)

A solution of imidazole **27** (2 mmol, 0.136 g) in THF (4 mL) was added dropwise to a stirred suspension of sodium hydride NaH (60% dispersion in mineral oil) (2.5 mmol, 0.1 g) in THF (5 mL). The mixture was reacted at room temperature for 30 min. A solution of pentafluoropyridine **74** (6 mmol, 0.7 mL) in THF (3 mL) was added dropwise to the mixture and the reaction left to stir at room temperature overnight. The solvent was evaporated and water (20 mL) was added to the residue. The reaction mixture was extracted with DCM (25 mL \times 3) and the combined organic layers dried over MgSO₄, filtered and evaporated to give compound **108** (0.39g, 89%) as yellow oil.

ν_{max} /cm⁻¹ (film) 2986, 1645, 1479, 1265, 1189, 1078, 968, 832, 738 ; MS (ESI) (MH⁺), C₈H₃F₄N₃ requires m/z 218.0328; found m/z 218.0335; δ_H (400 MHz, CDCl₃) 8.01 (1H, s), 7.43 (1H, t, J 1.6 Hz), 7.32 (1H, s); δ_F (376 MHz, CDCl₃) 175.54-75.70 (2F, BB'), 13.13-13.23 (2F, AA')

4.2.2. 1-(Perfluoropyridin-4-yl)-1H-benzo[d]imidazole **109**¹³⁰



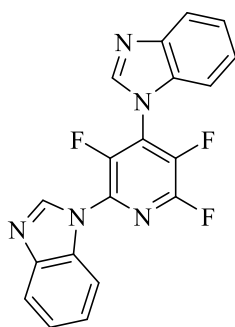
109 (98%)

A solution of pentafluoropyridine **74** (10 mmol, 1.1 mL) in THF (3 mL) was added dropwise to a stirred suspension of sodium hydride NaH (60% dispersion in mineral oil) (15 mmol, 0.6g) in THF (10 mL). A solution of benzimidazole **31** (10 mmol, 1.2 g) in THF (15 mL) was added dropwise to the mixture by using a syringe pump and the reaction left to stir at room temperature for 24 h under

N₂. The solvent was evaporated and water (20 mL) was added to the residue. The reaction mixture was extracted with DCM (25 mL × 3) and the combined organic layers dried over MgSO₄, filtered and evaporated to give compound **109** (2.62g, 98%) as a shiny, creamy solid.

m.p. 136-140°C; ν_{max} /cm⁻¹ (film) 2988, 1712, 1478, 1265, 1222, 969, 896, 748; MS (ESI) (MH⁺), C₁₂H₅F₄N₃ requires m/z 268.0469 found m/z 268.0491; δ_H (400 MHz, CDCl₃) 8.11 (1H, s), 7.94-7.90 (1H, m), 7.47-7.44 (2H, q, J , 7.2, 4.4) 7.34-7.33 (1H, m); δ_F (376 MHz, CDCl₃) 75.98-76.14 (2F, BB'), 16.34-16.15 (2F, AA'); δ_C (100 MHz, CDCl₃) 144.3 (td, J , 240, 11, C-F), 143.2 (Cq), 141.1 (N-CH=N), 136.9 (dd, J , 270, 37, C-F), 132.3 (Cq), 127.0-127.2 (m, Cq-N), 125.2 (CH), 124.4 (CH), 121.3 (CH), 110.9 (CH).

4.2.3. 1,1'-(3,5,6-Trifluoropyridine-2,4-diyl)bis(1H-benzo[d]imidazole) **110**

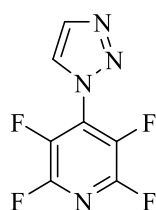


110 (36%)

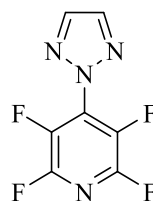
A solution of tetrafluoropyridine derivative **109** (2 mmol, 0.53 g) in THF (5 mL) was added dropwise to the stirred suspension of sodium hydride NaH (60% dispersion in mineral oil) (2.5 mmol, 0.1 g) in THF (5 mL). A solution of benzimidazole **31** (2 mmol, 0.24 g) in THF (5 mL) was added dropwise to the mixture using pressure compensating dropping funnel and the reaction left to stir at room temperature overnight. The solvent was evaporated and water (20 mL) was added to the residue. The reaction mixture was extracted with DCM (25 mL × 3) and the combined organic layers dried over MgSO₄, filtered and evaporated to give brown sticky solid (0.6 g). Purification was carried out by column chromatography and 1-(2-(benzo[d]imidazol-1-yl)-3,5,6-trifluoropyridin-4-yl)-1H-benzo[d]imidazole **110** was obtained as a brown solid (0.08 g, 36%).

m.p. 186-190 °C ; MS (ESI) (MH⁺), C₁₂H₅F₄N₃ requires m/z 366.0953; found m/z 366.0960; δ_H (400 MHz, CDCl₃) 8.43 (1H, d, J 2.8), 8.11 (1H, t, J 2), 8.01 (2H, d, J 7.6), 7.90-7.88 (1H, m), 7.85-7.83 (1H, m), 7.41-7.38 (4H, m), 7.33 -7.31 (1H, m); δ_F (376 MHz, CDCl₃) 79.3 (1F, t, J 23.3), 27.8 (1F, d, J 28.9), 18.4 (1F, d, J 23.3).

4.2.4. 2,3,5,6-Tetrafluoro-4-(1H-1,2,3-triazol-1-yl)pyridine 111 and 2,3,5,6-tetrafluoro-4-(2H-1,2,3-triazol-2-yl)pyridine 112



X isomer **111** (40%)



Y isomer **112** (15%)

A solution of pentafluoropyridine **74** (40 mmol, 4.4 mL) in THF (4 mL) was added dropwise to a stirred suspension of sodium hydride NaH (60% dispersion in mineral oil) (30 mmol, 1.2 g) in THF (10 mL). A solution of 1,2,3-triazole **28** (20 mmol, 1.38 g) in THF (15 mL) was added dropwise to the mixture and the reaction left to stir at room temperature for 24 h under N₂. The solvent was evaporated and water (20 mL) was added to the residue. The reaction mixture was extracted with DCM (25 mL × 3) and the combined organic layers dried over MgSO₄, filtered and evaporated to give oily semi solid compound (3.5 g). ¹⁹F and ¹H NMR spectra indicated the presence of two different compounds in the product. The mixture was separated by column chromatography using 6:4 light petrol: ethyl acetate as eluting solvent to give isomer X **111** as a shiny white solid (1.72 g, 40%) and 100% ethyl acetate to give isomer Y **112** as shiny light yellow solid (0.66 g, 15%).

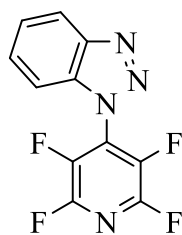
X isomer 111:

m.p. 63-65 °C; ν_{max}/cm^{-1} (film) 1643, 1465, 1257, 1180, 956, 848, 671. MS (ESI) (MH⁺), C₇H₃F₄N₄ requires m/z 219.0288 found m/z 219.0287; δ_H (400 MHz, CDCl₃) 8.61 (1H, s), 8.28 (1H, s); δ_F (376 MHz, CDCl₃) 77.48-77.32 (2F, BB'), 14.41-14.25 (2F, AA'); δ_C (100 MHz, CDCl₃) 154.5 (CH), 145.2 (CH), 144.1 (td, J 270, 23, C-F), 136.7 (dd, J 210, 30 C-F), 127.15-127.98 (m, Cq-N); Analysis (%) for C₇H₂F₄N₄ (218) required: C, 38.55; H, 0.92; N, 25.69 Found: C, 38.34; H, 0.83; N, 25.08.

Y isomer 112:

m.p. 150-152°C; ν_{max}/cm^{-1} (film) 1651, 1427, 1265, 1057, 956, 833; MS (ESI) (MH⁺), C₇H₃F₄N₄ requires m/z 219.0288 found m/z 219.0289; δ_H (400 MHz, CDCl₃) 8.64 (2H, t, J 2); δ_F (376 MHz, CDCl₃) 76.14-75.68 (2F, BB'), 15.00-18.84 (2F, AA'); δ_C (100 MHz, CDCl₃) 144.5 (td, J 190, 11 C-F), 141.0 (t, J , 4 CH), 135.3 (dd, J 200, 10, C-F), 124.5-124.7 (m, Cq-N); Analysis (%) for C₇H₂F₄N₄ (218) required: C, 38.55; H, 0.92; N, 25.69 Found: C, 38.37; H, 0.85; N, 25.04

4.2.5. 1-(Perfluoropyridin-4-yl)-1H-benzo[d][1,2,3]triazole **113**¹³¹

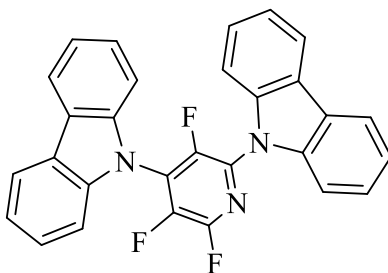


113 (88%)

A solution of pentafluoropyridine **74** (40 mmol, 4.4 mL) in THF (5 mL) was added dropwise to a stirred suspension of sodium hydride NaH (60% dispersion in mineral oil) (30 mmol, 1.2 g) in THF (10 mL). A solution of benzotriazole **30** (20 mmol, 2.4 g) in THF (15 mL) was added dropwise to the mixture by syringe pump and the reaction left to stir at room temperature for 24 h under N₂. The solvent was evaporated and distilled water (10 mL) was added to the residue. A white solid was precipitated and was collected by suction filtration to give compound **113** (4.72 g, 88%) as white solid.

m.p. 135-138°C; ν_{max} /cm⁻¹ (film) 2924, 2854, 1695, 1473, 1249, 1041, 956, 840, 624; MS (ESI) (MH⁺); C₁₂H₅F₄N₄ requires m/z 269.0445 found m/z 269.0443; δ_H (400 MHz, CDCl₃) 8.22 (1H, d, J 8.4), 7.67 (1H, t, J 7.2), 7.56-7.48 (2H, m); δ_F (376 MHz, CDCl₃) 75.99-75.76 (2F, BB'), 17.24-17.04 (2F, AA'); δ_C (100 MHz, CDCl₃) 145.6 (Cq), 144.2 (dt, J 230, 14, C-F), 136.7 (dd, J 270, 37, C-F), 132.6 (Cq), 127.0-127.1 (m, Cq-N), 125.9 (CH), 130.0 (CH), 109.8 (CH), 121.0 (CH).

4.2.6. 9,9'-(3,4,6-Trifluoropyridine-2,5-diyl)bis(9H-carbazole) **114**



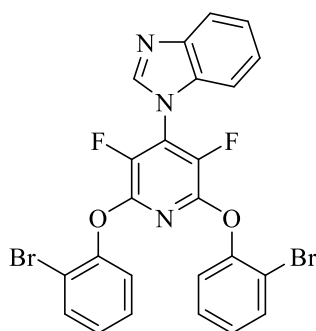
114 (45 %)

A solution of pentafluoropyridine **74** (50 mmol, 8.85 g) in THF (3 mL) was added dropwise to a stirred suspension of NaH (60% dispersion in mineral oil) (20 mmol, 0.8 g) in THF (5 mL). A solution of carbazole **29** (10 mmol, 1.67 g) in THF (10 mL) and DMF (2 mL) was added dropwise to

reaction mixture under N₂ and left to stir at RT for 24 h. The solvent was evaporated and water (20 mL) was added to the residue. a yellow solid precipitated and was filtered (3.47 g). The product was purified by column chromatography using 8:2 light petrol:diethyl ether eluting solvent to give compound **114** (4.1g, 45%) as white crystals.

m.p. 203-205 °C; ν_{max} /cm⁻¹ (film) 1597, 1419, 1118, 972, 856; MS (ESI) (MH⁺), C₂₉H₁₇F₃N₃ requires m/z 464.1369 found m/z 464.1370; δ_H (400 MHz, CDCl₃) 8.15 (1H, d, *J* 8), 8.11 (1H, d, *J* 7.6), 7.54-7.45 (3H, m), 7.41-7.31 (3H, m); δ_F (376 MHz, CDCl₃) 77.89 (1F, t, 28.95), 38.30 (1F, d, *J* 30.01), 22.84 (1F, d, *J* 26.32); δ_C (100 MHz, CDCl₃), 147.28 (dd, *J* 250, 20, C-F), 146.0 (dd, *J* 260, 10, C-F), 139.2 (Cq), 139.0 (Cq), 139.8 (dd, *J* 220, 31, C-F), 132.01-132.85 (m, Cq-N), 127.45-128.05 (m, Cq-N), 126.8 (CH), 126.5 (CH), 124.7 (Cq), 124.6 (Cq), 122.1 (CH), 121.8 (CH), 120.8 (CH), 120.5 (CH), 110.9 (d, *J* 2.8, C-H), 110.3 (C-H); Analysis (%) for C₂₉H₁₆F₃N₃. (445) required: C, 75.16; H, 3.48; N, 9.07 Found: C, 74.93; H, 3.35; N, 9.02.

4.2.7. 1-(2,6-bis(2-Bromophenoxy)-3,5-difluoropyridin-4-yl)-1H-benzo[d]imidazole **115**



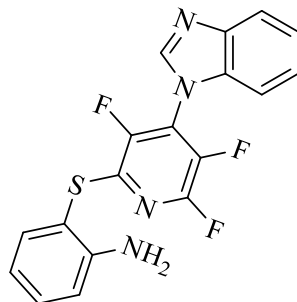
115 (53%)

A solution of 2-bromophenol **58** (1 mmol, 0.11 mL) in THF (3 mL) was added dropwise to a stirred suspension of sodium hydride NaH (60% dispersion in mineral oil) (1.5 mmol, 0.06 g) in THF (5 mL) and left 30 min at room temperature. A solution of tetrafluoropyridine derivative **109** (1 mmol, 0.267 g) in THF (5 mL) and was added dropwise to the reaction mixture and the reaction left to stir at room temperature overnight. The solvent was evaporated and water (20 mL) was added to the residue. The reaction mixture was extracted with DCM (3 × 25 mL) and the combined organic layers dried over MgSO₄, filtered and evaporated to give cream colour solid (0.53 g). Recrystallization from DCM and hexane gave shiny white crystals of 1-(2,6-bis(2-bromophenoxy)-3,5-difluoropyridine-4-yl)-1H-benzo[d]imidazole **115** as shiny white crystals (0.31 g, 53%).

m.p. 178-181 °C; ν_{max} /cm⁻¹ (film): 1712, 1635, 1519, 1435, 1350, 1287, 1080, 979, 871, 732;

MS (ESI) (MH^+), $C_{24}H_{16}^{79}Br_2F_2N_3O_2$ requires m/z 573.9387; found m/z 573.9383; δ_H (400 MHz, $CDCl_3$) 8.23 (1H, t, J 2), 7.85 (1H, dt, J 6, 1.6), 7.48-7.46 (5H, m), 7.17 (2H, dt, J 8, 1.2), 7.06-7.02 (4H, m); δ_F (376 MHz, $CDCl_3$) 14.9 (2F, s).

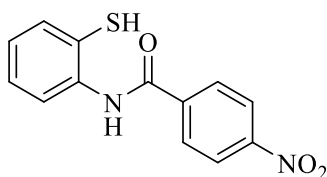
4.2.8. 2-((4-(1H-benzo[d]imidazol-1-yl)-3,5,6-trifluoropyridin-2-yl)thio)aniline **118**



118 (29%)

A solution of tetrafluoropyridine derivative **109** (1 mmol, 0.267 g) in THF (3 mL) was added dropwise to a stirred suspension of sodium hydride NaH (60% dispersion in mineral oil) (1.3 mmol, 0.05 g) in THF (5 mL). 2-aminothiophenol **117** (1 mmol, 0.11 mL) was mixed with sodium borohydride (1 mmol, 0.038 g) in THF (5 mL) and was added dropwise to the mixture using a pressure compensating dropping funnel, and the reaction left to stir at room temperature overnight. The reaction was quenched with a few drops of methanol. Distilled water (10 mL) was added, and the mixture was extracted with DCM (3×20 mL). The organic extract was washed with aqueous sodium chloride and dried over $MgSO_4$, filtrated and evaporated to give dark yellow sticky solid (0.41 g). Purification was carried out by column chromatography giving 2-((4-(1H-benzo[d]imidazol-1-yl)-3,5,6-trifluoropyridine-2 yl)thiol)aniline **118** as dark red solid (0.11 g, 29%). m.p. 60-64 °C; ν_{max}/cm^{-1} (film) 3333 (broad, N-H), 1612, 1512, 1435, 1303, 1257, 802, 740 ; MS (ESI) (MH^+), $C_{18}H_{11}F_3N_4S$ requires m/z 374.0729, found m/z 374.0728; δ_H (400 MHz, $CDCl_3$) 8.01 (1H, s), 7.86-7.82 (1H, m), 7.41-7.39 (1H, dd, J 7.6, 1.2), 7.36-7.32 (2H, m), 7.25-7.21 (2H, m), 6.78 (2H, dd J 8, 1.2), 4.27 (2H, s, N-H); δ_F (376 MHz, $CDCl_3$) 78.5 (1F, t, J 24), 35.1 (1F, d, J 29), 14.9 (1F, d, J 24).

4.2.9. *N*-(2-Mercaptophenyl)-4-nitrobenzamide **121**

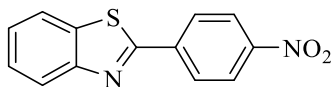


121 (57%)

2-Aminothiophenol **116** (2 mmol, 0.22 mL) was mixed with sodium borohydride (2 mmol, 0.08 g) in CH₃CN (5 mL) and was added dropwise to a stirred solution of Et₃N (2 mmol, 0.28 mL) in CH₃CN (4 mL). A solution of 4-nitrobenzoyl chloride **120** (2 mmol, 0.371 g) in CH₃CN (5 mL) and was added dropwise to the reaction mixture and the reaction left to stir at room temperature overnight. After distilled water (10 mL) was added solid precipitated and was collected by suction filtration to give yellow solid (0.095 g). Recrystallization from hot ethanol gave shiny yellow crystals of *N*-(2-mercaptophenyl)-4-nitrobenzamide **121** (0.31 g, 57%).

m.p. 178-181 °C ; ν_{max} /cm⁻¹ (film) 3348 (N-H), 1681 (C=O), 1581 and 1519 (NO₂), 1311, 1249, 1103, 1010, 833, 756, 632, 540; MS (ESI) (MH⁻), C₁₃H₁₀N₂O₃S requires m/z 273.0348; found m/z 273.0339; δ_H (400 MHz, CDCl₃,) 8.91 (1H, s, N-H), 8.43 (1H, d, *J* 8.0), 8.34-8.31 (2H, m), 7.93 (1H, d, *J*, 8.8), 7.81 (1H, dd, *J* 2.4, 6.8), 7.56 (1H, dd *J* 7.6, 1.2), 7.33-7.30(1H, m), 7.05 (1H, t *J* 6), 4.25 (1H, s, SH).

4.2.10. 2-(4-Nitrophenyl)benzo[d]thiazole **122**



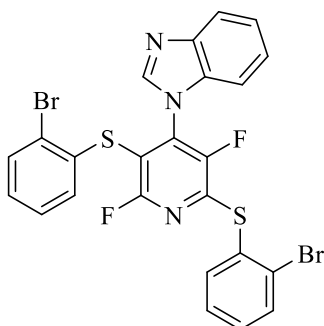
122 (49%)

2-Aminothiophenol **116** (2 mmol, 0.22 mL) was mixed with sodium borohydride (2 mmol, 0.076 g) in pyridine (5 mL) and left to stir at room temperature for 30 min. A solution of 4-nitrobenzoyl chloride **120** (2 mmol, 0.371 g) in pyridine (5 mL) and was added dropwise to the reaction mixture and the reaction left to stir at room temperature overnight. The solvent was evaporated and water (20 mL) was added to the residue. The reaction mixture was extracted with DCM (3 × 25 mL) and the combined organic layers dried over MgSO₄, filtered and evaporated to give yellow sticky solid

(0.54 g). The compound was washed with cold ethanol and collected by suction filtration to give compound **122** (0.25 g, 49%) as a shiny yellow solid.

m.p. 224-229 °C; ν_{max}/cm^{-1} (film) : 1597 and 1519 (NO₂), 1342, 1219, 1111, 972, 848, 763, 732, 686; MS (ESI) (MH⁺), C₁₃H₉N₂O₂S requires m/z 257.0371; found m/z 257.0377; δ_{H} (400 MHz, CDCl₃) 8.4 (2H, d, *J* 2), 8.29 (2H, d, *J* 8.8), 8.16 (1H, d, *J* 8.4), 7.99 (1H, d, *J* 8), 7.58(1H, t, *J* 7.6), 7.49 (1H, d, *J* 7.2).

4.2.11. 1-(2,5-bis((2-Bromophenyl)thio)-3,6-difluoropyridin-4-yl)-1H-benzo[d]imidazole **126**

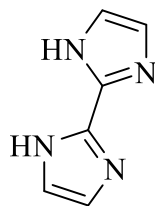


126 (65%)

A solution of 2-bromothiophenol **125** (1 mmol, 0.12 mL) in THF (3 mL) was added dropwise to stirred suspension of sodium hydride NaH (60% dispersion in mineral oil) (1.5 mmol, 0.05 g) in THF (5 mL). A solution of tetrafluoropyridine derivative **109** (1 mmol, 0.267 g) in THF (5 mL) added dropwise to the reaction mixture and left to stir at room temperature overnight. The solvent was evaporated and water (20 mL) was added to the residue. The reaction mixture was extracted with DCM (3 × 25 mL) and the combined organic layers dried over MgSO₄, filtered and evaporated to give creamy solid (0.4 g). Recrystallization from hot ethanol gave shiny white crystals of 1-[2,6-bis-(2-bromo-phenylsulfanyl)-3,5-difluoro-pyridin-4-yl]-1H-benzoimidazole **126** (0.39 g, 65%).

m.p. 162-165 °C; ν_{max}/cm^{-1} (film): 1581, 1450, 1333, 1149, 1018, 1080, 884, 740; MS (ESI) (MH⁺), C₂₄H₁₄Br₂F₂N₃S₂ requires m/z 603.8973; found m/z 603.8952; δ_{H} (400 MHz, CDCl₃) 7.79 (1H, s), 7.72-7.67 (3H, m), 7.35 (1H, t, *J* 1.2), 7.28 (1H, dd, *J* 6, 2), 7.26-7.22 (3H, m), 7.03 (1H, d, *J* 4.8), 6.83-6.81 (2H, m), 6.73-6.71 (1H, m); δ_{F} (376 MHz, CDCl₃) 101.9 (1F, d, *J* 27), 33.30 (1F, d, *J* 27).

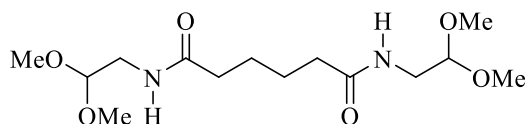
4.2.12. 1*H*,1'*H*-2,2'-Biimidazole **130**¹²⁰



130 (5%)

Aqueous glyoxal **129** (50%, 0.1 mol, 11.5 mL) was added dropwise to a stirred solution of ammonium acetate (0.26 mol, 20 g) in water (10 mL) and the reaction left to stir at room temperature overnight. The dark brown solid formed (0.71 g) was collected by suction filtration and washed with water (3 × 10 mL) and acetone (3 × 10 mL) to give 1*H*,1'*H*-2,2'-biimidazole **130** (0.7 g, 5%) m.p. 347-350 °C (literature value : > 300 °C)⁽²⁷⁾; MS (ESI) (MH⁺), C₆H₆N₄ requires *m/z* 135.0668; found *m/z* 135.0662; ν_{max}/cm^{-1} (film) 3368 (broad peak, H₂O), 2922 and 2852 (2 N-H), 1651, 1402, 1329, 1102, 937, 745; δ_{H} (400 MHz, DMSO-*d*₆) 12.85 (2H, s, N-H), 7.18 (2H, s), 7.06 (2H, s).

4.2.13. *N1,N6-bis(2,2-Dimethoxyethyl)adipamide 131*

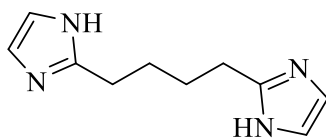


131 (75%)

A solution aminoacetaldehyde dimethyl acetal (4 mmol, 0.46 g) in THF (2 mL) was added dropwise to a stirred solution of triethylamine (4 mmol, 0.61 mL) in THF (3 mL). The mixture was stirred at room temperature for 30 min. A solution of adipoyl chloride (2 mmol, 0.29 mL) in THF (2 mL) was added dropwise to the mixture and the reaction left to stir at room temperature overnight under N₂. The reaction was quenched with distilled water (10 mL), and the mixture was extracted with DCM (3×20 mL). The organic extract was dried over MgSO₄, filtered and evaporated to give compound **131** (0.48 g, 75%) as a white solid.

m.p. 93-95°C; ν_{max}/cm^{-1} (film) 3315-3284 (broad peak) NH group, 1649 (C=O), 1423, 1384, 1138, 1199, 966, 832, 738, 607; MS (ESI) (MH⁺), C₁₄H₂₉N₂O₆ requires *m/z* 321.2020; found *m/z* 321.2019; δ_{H} (400 MHz, CDCl₃) 5.88 (2H, s), 4.38 (2H, t, *J* 5.2), 3.39-3.41(16H, m), 2.21-2.26 (4H, m), 1.64-1.68 (4H, m).

4.2.14. 1,4-di(1H-imidazol-2-yl)butane **132**



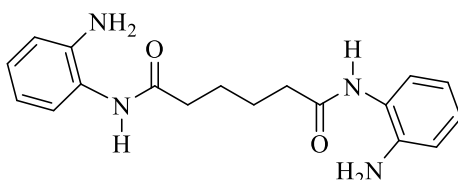
132 (60%)

The intermediate compound **135** (8.3 mmol, 1.58 g) was treated with HCl (40 mmol, 6 mL) and the mixture heated at 65 °C for 24 h under N₂. After 24 h the reaction mixture was cooled and neutralized with dry sodium carbonate (Na₂CO₃). Addition of water precipitated the target compound **132** (0.79 g, 50%) which was filtered as a light brown solid.

mp: decomposed at 168 °C; ν_{max}/cm^{-1} (film) 3000-3450 (broad peak, NH), 1639, 1577, 1423, 1342, 1153, 1103, 991, 887, 763, 675; MS (ESI) (MH⁺), C₁₀H₁₅N₄ requires m/z 191.1291 found m/z 191.1296; MS (ESI) (MH⁻), C₁₀H₁₃N₄ requires m/z 189.1146, found m/z 189.1147

δ_H (400 MHz, DMSO-d₆) 11.79 (2H, s), 6.95 (2H, s), 6.73 (2H, s), 2.57-2.54 (4H, m), 1.61-1.56 (4H, m); δ_H (400 MHz, Methanol-d₄) 6.85 (4H, s), 2.66-2.70 (4H, m), 1.69-1.67 (4H, m); δ_C (100 MHz, Methanol-d₄) 149.9 (Ar Cq), 120.1 (Ar CH), 27.6 (CH₂), 27.3 (CH₂).

4.2.15. N1,N6-bis(2-Aminophenyl)adipamide **133**

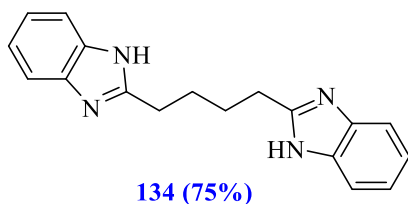


133 (68%)

A solution of *o*-phenylenediamine (4 mmol, 0.47 g) in THF (4 mL) was added dropwise to a stirred solution of triethylamine (4 mmol, 0.6 mL) in THF (3 mL). The mixture was stirred at room temperature for 30 min. A solution of adipoyl chloride (2 mmol, 0.29 mL) in THF (2 mL) was added dropwise to the mixture and the reaction left to stir at room temperature overnight under N₂. The solvent was evaporated and water (20 mL) was added to the residue. A yellow solid precipitated and was filtered to give compound **133** (0.49 g, 75%) as white solid.

m.p. 155-165°C; ν_{max}/cm^{-1} (film) 3250 (broad peak) NH group, 1658 (C=O), 1643, 1512, 1481, 1290, 1136, 1068, 966, 832, 752, 607; MS (ESI) (MH⁺), C₁₈H₂₂N₄O₂ requires m/z 327.1815 found m/z 327.1814; δ_H (400 MHz, DMSO-d₆) 9.34 (1H, s), 9.15 (1H, s), 7.15 (2H, d, *J* 8), 6.89 (2H, t, *J* 7.2) 6.70 (2 H, t, *J* 7.6), 6.54 (2 H, t, *J* 7.6), 4.32 (2H, s), 2.34-2.33- (4H, m), 1.64-1.63 (4H, m).

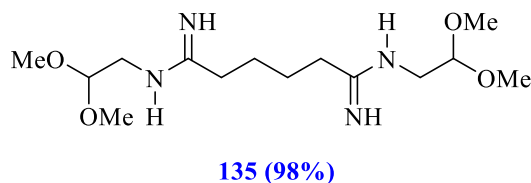
4.2.16. 1,4-bis(1H-benzo[d]imidazol-2-yl)butane 134



A solution of *o*-phenylenediamine (4 mmol, 0.43 g) in methanol (6 mL) was added to a suspension of compound **18** (2 mmol, 0.55 g) in methanol (3 mL). The mixture was refluxed for 3 h under N₂. After 3 h the reaction was stopped and treated with water (20 mL). Compound **134** precipitated and was collected by suction filtration as shiny light yellow solid (0.44 g, 75%). m.p. 258-260°C; ν_{max}/cm^{-1} (film) 3441-3163 (broad, NH), 1620, 1535, 1415, 1141, 1006, 840, 744; MS (ESI) (MH⁺), C₁₈H₁₉N₄ requires m/z 291.1592, found m/z 291.1581

MS (ESI) (MH⁺), C₁₈H₁₇N₄ requires m/z 289.1549 found m/z 289.1559; δ_{H} (400 MHz, DMSO-d₆), 12.2 (2H, s), 7.44 (4H, dd, J 6, 2.8), 7.16 (4H, dd, J 6, 3.2), 2.96-2.89 (4H, m), 1.85-1.77 (4H, m). δ_{C} (100 MHz, DMSO-d₆) 155.5 (Ar Cq), 138.8 (broad Ar Cq), 127.14-127.7 (m, N-Cq=N), 114.5 (Ar CH), 120.4 (Ar CH), 28.7 (CH₂), 27.5 (CH₂).

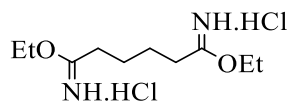
4.2.17. N1,N6-bis(2,2-Dimethoxyethyl)adipimidamide 135



A solution of aminoacetaldehyde dimethyl acetal (0.0045 mol, 0.47 g) in methanol (3 mL) was added to stirred suspension of compound **136** (0.002 mol, 0.48 g) in methanol (3 mL). The reaction mixture was heated under reflux for 3 h. The solvent was evaporated to give intermediate compound **135** (0.6 g, 95%) as a yellow syrup.

MS (ESI) (MH⁺), C₁₄H₃₁N₄O₄ requires m/z 319.2341 found m/z 319.2315; ν_{max}/cm^{-1} (film) 3483, 3051 (NH), 1656, 1452, 1502, 1237, 1195, 1066, 798, 742; δ_{H} (400 MHz, Methanol-d₄) 4.54 (2H, t, J 4.8 Hz), 3.44 (16H, m), 2.53 (4H, m), 1.74 (4H, m).

4.2.18. Diethyl adipimidate dihydrochloride **136**

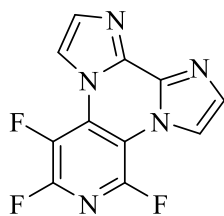


136 (80%)

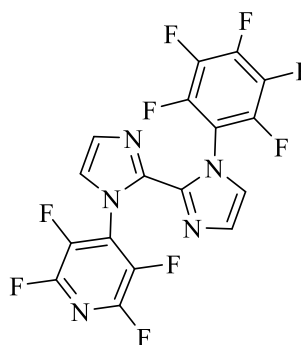
Ethanol (0.4 mol, 18.4 g) and acetyl chloride (0.25 mol, 17.8 mL) were added to a solution of adiponitrile (0.1 mol, 10.8 g) in DCM (10 mL). The mixture was stirred for 30 min then left at 4 °C for 3 days. After this time, compound **136** had precipitated and was collected as white solid by suction filtration (23 g, 80%).

m.p. 135-136°C; ν_{max} /cm⁻¹ (film) 3383 (broad peak) NH group, 1651, 1462, 1377, 1215, 1114, 879, 777; δ_H (400 MHz, D₂O) 4.66 (4H, q, *J* 6) 2.37-2.35 (4H, m), 1.58-1.59 (4H, m), 1.20 (6H, t, *J* 5.6 Hz). (N-H, peak not detected)

4.2.19. 5,7,8-Trifluorodiimidazo[1,2-*a*:2',1'-*c*]pyrido[3,4-*e*]pyrazine **137** and 1-(perfluorophenyl)-1'-(perfluoropyridin-4-yl)-1*H*,1'*H*-2,2'-biimidazole **138**



137 (31%)



138 (33%)

A solution of pentafluoropyridine **74** (2 mmol, 0.22 g) in THF (5 mL) was added dropwise to stirred suspension of sodium hydride NaH (60 % dispersion in mineral oil) (2.5 mmol, 0.1 g) in THF (5 mL). A solution of 1*H*,1'*H*-2,2'-biimidazole **130** (1 mmol, 0.134 g) in THF (5 mL) and was added dropwise at room temperature and the mixture stirred overnight. The reaction was quenched with a few drops of methanol. After distilled water (10 mL) was added some solid formed and was collected by suction filtration to give compound **138** (0.14 g, 33%) as a white solid. The aqueous filtrate was extracted with DCM (3×20 mL). The organic extract was dried over MgSO₄, filtered and evaporated to give dark yellow sticky solid which recrystallized from hot ethanol to give the pure compound **137** (0.08 g, 31%) as yellow solid.

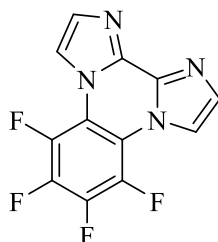
Compound **137**

m.p. 288-295 °C; ν_{max} /cm⁻¹ (film), 1681, 1243, 1187, 957, 787; MS (ESI) (MH⁺), C₁₁H₅F₃N₅ requires m/z 264.0483; found m/z 264.0413; δ_H (400 MHz, DMSO-d₆) 8.42-8.33 (2H, dd, *J*, 32, 1.2), 7.74-7.69 (2H, dd, *J* 1.6, 18.4); δ_F (376 MHz, CDCl₃) 8.31 (1F, dt, *J* 23.3, 2.6), 69.31 (1F, q, *J* 11.7), 86.90 (1F, dq, *J* 13.5, 3.0).

Compound **138**

m.p. 158-164 °C; ν_{max} /cm⁻¹ (film), 1651, 1203, 1087, 927, 717; MS (ESI) (MH⁺), C₁₆H₅F₈N₆ requires m/z 433.0434; found m/z 433.0441; δ_H (400 MHz, CDCl₃) 8.13-8.08 (2H, m), 7.68-7.66 (4H, dd, *J* 10.4, 1.2); δ_F (376 MHz, CDCl₃) 74.70-74.53 (4F, BB'), 16.03-15.77 (4F, AA').

4.2.20. 5,6,7,8-Tetrafluorodiimidazo[1,2-a:2',1'-c]quinoxaline **140**



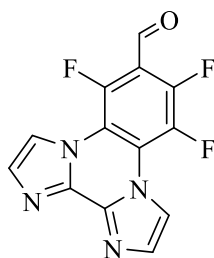
140 (18%)

A solution of hexafluorobenzene **48** (2 mmol, 0.37 g) in DMF (3 mL) was added dropwise to a stirred suspension of sodium hydride NaH (60% dispersion in mineral oil) (2.5 mmol, 0.1 g) in DMF (5 mL). 1*H*,1*H*-2,2'-biimidazole **130** (1 mmol, 0.134 g) in DMF (3 mL) and was added dropwise to the mixture. The mixture was heated at 80°C overnight under N₂. The solvent was evaporated and water (20 mL) was added to the residue. Some yellow solid precipitated and was filtered to give a brown solid which after recrystallization from ethanol afforded compound **140** (0.05 g, 18%) as a brown solid. m.p. decomposed at 240 °C

ν_{max} /cm⁻¹ (film), 29.33, 1631, 1223, 1187, 957, 787; MS (ESI) (MH⁺), C₁₂H₅F₅N₄ requires m/z 281.0445 found m/z 281.0433; δ_H (400 MHz, CDCl₃) 8.16 (2H, d, *J* 1), 7.67 (2H, d, *J* 1);

δ_F (376 MHz, CDCl₃) 14.04-13.94 (2F, BB'), 4.57-4.54 (2F, AA').

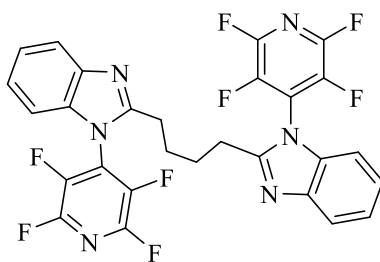
4.2.21. 5,7,8-Trifluorodiimidazo[1,2-a:2',1'-c]quinoxaline-6-carbaldehyde 141



141 (10%)

A solution of pentafluorobenzaldehyde **68** (1 mmol, 0.19 g) in DMF (3 mL) was added dropwise to a stirred suspension of sodium hydride NaH (60% dispersion in mineral oil) (1.5 mmol, 0.06 g) in DMF (5 mL). 1*H*,1*H*-2,2'-biimidazole **130** (1 mmol, 0.134 g) in DMF (3 mL) and was added dropwise to the mixture. The mixture was heated at 80 °C overnight under N₂. The solvent was evaporated and distilled water (10 mL) was added. Solid formed which was collected by suction filtration to give impure brown solid after recrystelazaion by DCM and light petrol compound **141** (10%) was isolated as yellow solid. ν_{max}/cm^{-1} (film), 2923, 1709, 1646, 1500, 1260, 10.91, 796, 682; MS (ESI) (MH⁺), C₁₃H₆F₃N₅O requires m/z 291.0488 found m/z 291.0476; δ_{H} (400 MHz, CDCl₃,) 10.46 (1H, s), 8.22 (2H, d, J 1.2), 7.69 (2H, d, J 1.6) ; δ_{F} (376 MHz, CDCl₃) 13.21-13.11 (1F, m), 20.16 (1F, d, J 21.8), 32.91 (1F, d, J 18.4).

4.2.22. 1,4-bis-1-Tetrafluoropyrid-4-yl-1*H*-benzimidazol-2-ylbutane 143



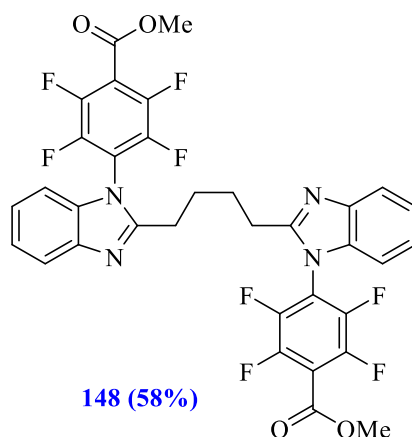
143 (95%)

A solution of pentafluoropyridine **74** (1.5 mmol, 0.25 g) in DMSO (2 mL) was added dropwise to stirred suspension of sodium hydride NaH (60 % dispersion in mineral oil) (1.5 mmol, 0.06 g) in DMSO (2 mL). Compound **133** (0.5 mmol, 0.15 g) in DMSO (4 mL) and was added dropwise by syringe pump and the reaction mixture left for 24 h at room temperature under N₂. The solvent was

evaporated and water (20 mL) was added to the residue. Solid precipitated and was collected by suction filtration to give compound **143** (0.28 g, 95%) as a white shiny solid.

m.p. 195-198 °C; ν_{max}/cm^{-1} (film), 2924, 1642, 1471, 1255, 1136, 972, 743; MS (ESI) (MH^+), $C_{28}H_{17}F_8N_6$ requires m/z 589.1381 found m/z 589.1376; δ_H (400 MHz, $CDCl_3$) 7.81 (2H, d, J 7.6), 7.36 (4H, m), 7.07 (2H, d, J 7.6), 2.87 (4H, m), 2.06 (4H, m); δ_F (376 MHz, $CDCl_3$) 76.4-76.1 (4F, m), 18.2-17.9 (4F, m); δ_C (100 MHz, $CDCl_3$) 153 (Ar N-Cq=N), 144.2 (dd, J 230, 26, C-F), 142.8 (Ar Cq), 136.8 (dd, J 267, 36, C-F), 134.2 (Ar Cq), 128.1-127.2 (m, Cq-N), 124.2 (Ar CH), 124.0 (Ar CH), 120.1 (Ar CH), 109.4 (Ar CH), 29.8 ($CH_2-C=N$), 26.4 ($CH_2-CH_2-CH_2$); Analysis (%) for $C_{28}H_{16}F_8N_6 \cdot \frac{1}{2}H_2O$ (597) requires: C, 56.28; H, 2.85; N, 14.07, found: C, 56.38; H, 3.01; N, 13.86.

4.2.23. 1,4-bis-1-(4-Methoxycarbonyl-2,3,5,6-tetrafluorophenyl)-1H-benzimidazol-2-ylbutane 148



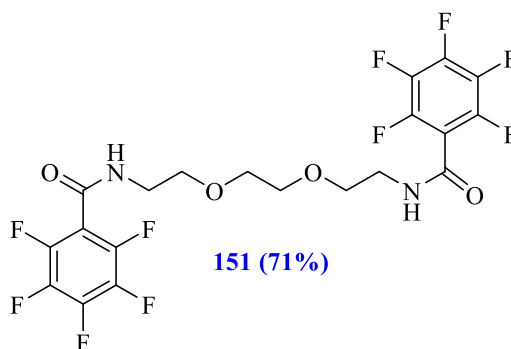
A solution of methyl pentafluorobenzoate **147** (2 mmol, 0.45 g) in DMSO (3 mL) was added dropwise to stirred suspension of sodium hydride NaH (60% dispersion in mineral oil) (2 mmol, 0.08 g) in DMSO (3 mL). Compound **134** (1 mmol, 0.3 g) in DMSO (4 mL) was added dropwise to the reaction mixture after 30 min by syringe pump and it left 24 h at room temperature under a N_2 atmosphere. By adding distilled water (10 mL) to the mixture light yellow solid (0.8 g) precipitated and was collected by suction filtration which was recrystallized from hot ethanol to give compound **148** (0.4 g, 58%) as white shiny crystals.

m.p. 195-198 °C; ν_{max}/cm^{-1} (film), 2924, 1642, 1471, 1255, 1136, 972, 743

MS (ESI) (MH^+), $C_{34}H_{23}F_8N_6O_4$ requires m/z 703.1586 found m/z 703.1569; δ_H (400 MHz, $CDCl_3$) 7.81 (2H, d, J 7.6), 7.30-7.38 (m, 4H), 7.04 (2H, d, J 8.0), 4.09 (6H, 2), 2.87 (4H, m), 2.06 (4H, m); δ_F (376 MHz, $CDCl_3$) 25.3-25.2 (4F, m), 19.3-19.2 (4F, m); δ_C (100 MHz, $CDCl_3$) 159.3 (C=O), 154.0 (Ar N -Cq=N), 145.4 (dd, J 180, 21, C-F), 142.9 (Ar Cq), 142.8 (dd, J 170, 13, C-F), 135.0

(Ar Cq), 123.8 (Ar CH), 123.5 (Ar CH), 119.9 (Ar CH), 114.1 (t, J 17, Ar Cq-C=O), 109.3 (Ar CH), 53.8 (CH₃), 27.1 (CH₂-C=N), 26.5 (CH₂-CH₂-CH₂), (1 ArF Cq not detected).

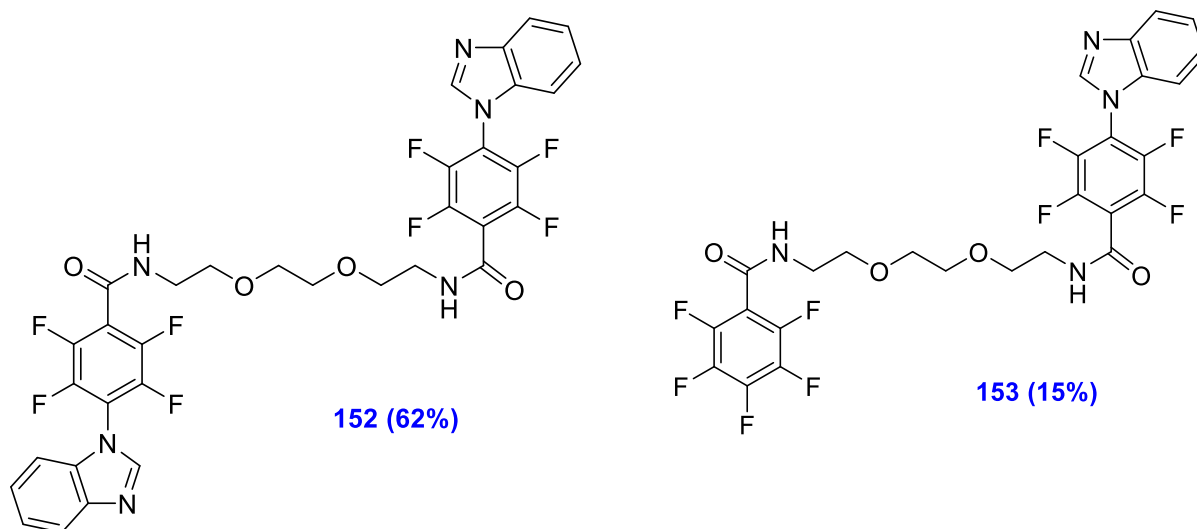
4.2.24. 2,2-(Ethylenedioxy)-bis-ethyl pentafluorobenzamide **151**



A solution of 2,2-(ethylenedioxy)bis(ethylamine) **150** (1 mmol, 0.15 g) in THF (2 mL) was added dropwise to stirred solution of triethylamine (2 mmol, 0.20 g) in THF (2 mL). A solution of pentafluorobenzoyl chloride **149** (2 mmol, 0.46 g) in THF (2 mL) and was added dropwise to the reaction mixture and left for 24 h at room temperature under N₂. The solvent was evaporated and water (10 mL) was added to the residue. Yellow orange solid precipitated, and was filtered (0.5 g). Recrystallization using DCM and light petroleum gave compound **151** (0.38 g, 71%) as white shiny crystals.

m.p. 128-129 °C; ν_{max}/cm^{-1} (film), 3279 (N-H), 2872, 1658 (C=O), 1501, 1135, 1119, 992, 731; MS (ESI) (MH⁺), C₂₀H₁₄O₄F₁₀N₂ requires m/z 537.0867, found m/z 537.0867; δ_H (400 MHz, CDCl₃) 6.55 (2H, s, NH), 3.70-3.66 (8H, m), 2.87 (4H, m); δ_F (376 MHz, CDCl₃) 21.2-21.1 (4F, m), 11.26 (2F, t, J 20.3), 1.74-1.90 (4F, m); δ_C (100 MHz, CDCl₃) 157.6 (C=O), 144.2 (dd, J 255, 12, C-F), 142.3 (dd, J 260, 25, C-F), 137.5 (dd, J 230, 32, C-F), 111.5 (t, J 30, Ar Cq-C=O), 70.8 (CH₂-O), 69.8 (CH₂-O), 40.1 (CH₂-N). Analysis (%) for C₂₀H₁₄F₁₀N₂O₄ (536) required: C, 44.79; H, 2.63; N, 5.22 Found: C, 44.78; H, 2.44; N, 5.25.

4.2.25. 2,2'-(Ethylenedioxy)-bis-ethyl 4-benzimidazol-1-yltetrafluorobenzamide 152 and N-(2-(2-(4-(1H-benzo[d]imidazol-1-yl)-2,3,5,6-tetrafluorobenzamido)ethoxy)ethoxyethyl)-2,3,4,5,6-pentafluorobenzamide 151



A solution of benzimidazole **31** (2 mmol, 0.24 g) in THF (3 mL) was added dropwise to stirred suspension of sodium hydride NaH (60% dispersion in mineral oil) (2 mmol, 0.08 g) in THF (3 mL) after 30 min. A solution of compound **151** (1 mmol, 0.54 g) in THF (3 mL) was added dropwise to the reaction mixture. The reaction mixture was left to stir for 24 h at room temperature under N₂. Distilled water (10 mL) was added to the reaction mixture and it was extracted with DCM (3×25 mL). The organic extract was dried over MgSO₄, filtered and evaporated to give white solid (0.65 g). TLC indicated presence of mixture of two compounds and traces of starting material in the product. Thus further purification was carried out by column chromatography. Compound **153** (0.1 g, 15%) was afforded by using 99:1 ethyl acetate and methanol eluting as a colourless oil. Compound **152** (0.45 g, 62%) was eluted using 90:10 ethyl acetate and methanol to afford the compound **153** as a shiny white solid.

ν_{max} /cm⁻¹ (film) 3279 (broad N-H), 2831, 1665 (C=O), 1496, 1280, 1211, 1118, 987, 740

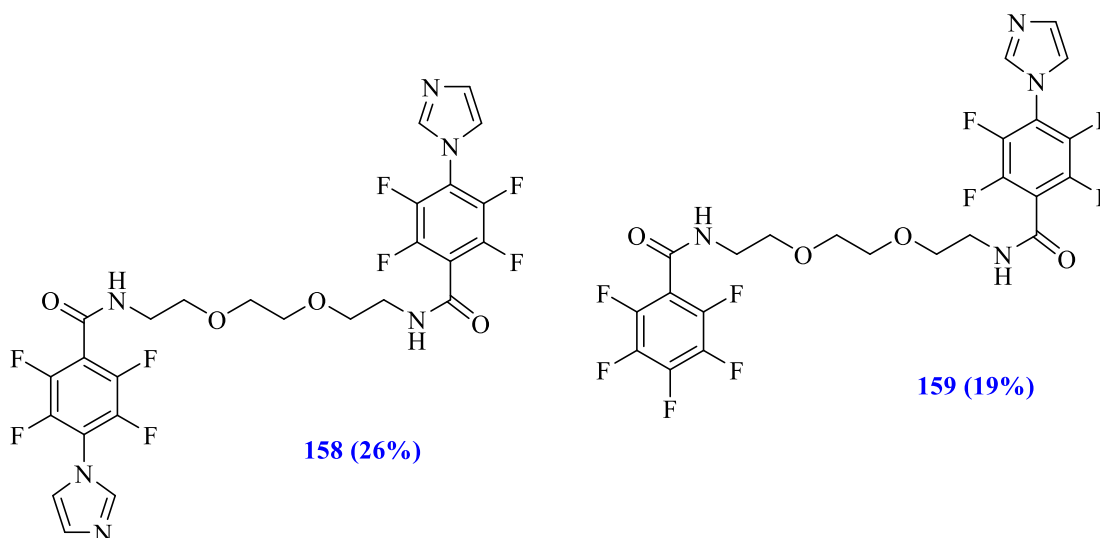
MS (ESI) (MH⁺), C₂₇H₁₈F₉N₄O₄ requires m/z 633.1190 found m/z 633.1192; δ_H (400 MHz, CDCl₃) 8.04 (1H, s), 7.88 (1H, d, J 3.6), 7.42-7.40 (2H, m), 7.23-7.22 (1H, m), 7.12 (1H, s, NH), 6.82 (1H, s, NH), 3.75-3.64 (12H, m); δ_F (376 MHz, CDCl₃) 22.48 (2F, dd, J 22.93, 11.65), 22.07-21.01 (2F, m), 16.59 (2F, dd, J 23.31, 11.65), 11.1 (1F, t, J 20.3), 1.83-1.70 (2F, m).

Compound **152**

m.p. 115-117 °C; ν_{max} /cm⁻¹ (film) 3194 (N-H), 2877, 1666 (C=O), 1550, 1418, 1280, 1134, 987, 710, 748; MS (ESI) (MH⁺), C₃₄H₂₃F₈N₆O₄ requires m/z 731.1659 found m/z 731.1657;

δ_H (400 MHz, $CDCl_3$) 8.03 (2H, s), 7.91-7.89 (2H, m), 7.43-7.38 (4H, m), 7.22 (2H, d, J 6), 7.00 (2H, s), 3.75-3.73 (12H, m); δ_F (376 MHz, $CDCl_3$) 22.6-22.5 (4F, m), 17.8-17.7 (4F, m); δ_C (100 MHz, $CDCl_3$) 157.5 (C=O), 142.9 (Ar CH=N), 141.1 (Ar Cq), 133.0 (Ar Cq), 124.9 (Ar CH), 123.9 (Ar CH), 120.9 (Ar CH), 110.4 (Ar CH), 70.5 (CH₂-O), 69.4 (CH₂-O), 40.2 (CH₂-N) (C-F and C-N could not be detected); Analysis (%) for C₃₄H₂₄F₈N₆O₄ (732) required: C, 55.74; H, 3.30; N, 11.47 Found: C, 55.59; H, 3.37; N, 11.16.

4.2.26. *N,N'*-((Ethane-1,2-diylbis(oxy))bis(ethane-2,1-diyl))bis(2,3,5,6-tetrafluoro-4-(1H-imidazol-1-yl)benzamide) 158 and 2,3,4,5,6-pentafluoro-N-(2-(2-(2-(2,3,5,6-tetrafluoro-4-(1H-imidazol-1-yl)benzamido)ethoxy)ethoxy)ethyl)benzamide 159



A solution of imidazole **27** (1 mmol, 0.07 g) in THF (3 mL) was added dropwise to stirred suspension of sodium hydride NaH (60 % dispersion in mineral oil) (2 mmol, 0.08 g) in THF (3 mL). The reaction mixture was left to stir for 30 min at RT then a solution of compound **151** (0.5 mmol, 0.26 g) in THF (3 mL) was added dropwise to the reaction mixture. The reaction mixture was left to stir for 24 h at room temperature under N₂. Distilled water (10 mL) was added to the reaction mixture and it was extracted with DCM (3×25 mL). The organic extract was dried over MgSO₄, filtered and evaporated to give colourless oil (0.3 g). TLC indicated the presence of mixture of two compounds and traces of starting material in the product. Thus further purification was carried out by column chromatography. Compound **158** (0.076 g, 26%) was afforded, after elution with 100% ethyl acetate, as a white oil. Compound **159** (0.05 g, 19%) was afforded using 99:1 ethyl acetate and methanol as eluent as a colourless oil.

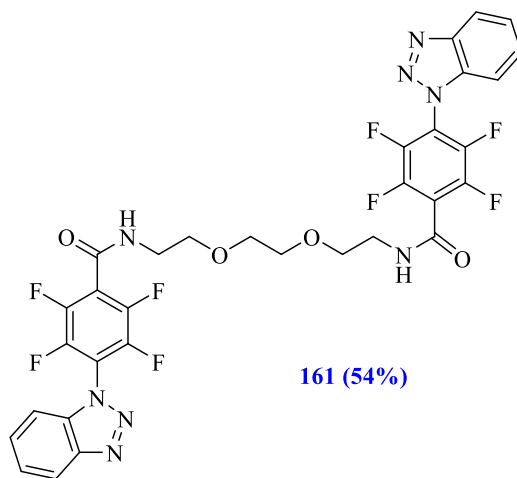
Compound **159**

ν_{max} /cm⁻¹ (film) 3252 (NH), 2931, 1678 (C=O), 1498, 1349, 1294, 1118, 978, 746; MS (ESI) (MH⁺), C₂₃H₁₆F₉N₄O₄ requires m/z 583.1033 found m/z 583.1040; δ_H (400 MHz, CDCl₃) 7.80 (1H, s), 7.27 (2H, d, J 9.6), 6.99 (1H, s, NH), 6.82 (1H, s, NH), 3.75-3.64 (12H, m); δ_F (376 MHz, CDCl₃) 22.39-22.48 (2F, q, J 12.03), 21.07-21.01 (2F, m), 16.59-16.67 (2F, q, J 11.65), 11.1 (1F, t, J 20.3), 1.70-1.83 (2F, m).

Compound **158**

ν_{max} /cm⁻¹ (film) 3192 (NH), 2881, 1668 (C=O), 1481, 1309, 1138, 978, 810; MS (ESI) (MH⁺), C₂₆H₂₁F₈N₆O₄ requires m/z 633.1491 found m/z 633.1473; δ_H (400 MHz, CDCl₃) 7.77 (2H, s), 7.26 (4H, d, J 11.6), 3.74-3.65 (12H, m), 1.90 (2H, s, N-H); δ_F (376 MHz, CDCl₃) 22.30-22.39 (4F, q, J 11.65), 14.52-14.60 (4F, q, J 9.0); δ_C (100 MHz, CDCl₃) 157.5 (C=O), 137.4 (Ar CH), 130.2 (Ar CH), 119.9 (Ar CH), 115.6 (Ar Cq-C=O), 70.4 (CH₂-O), 69.3 (CH₂-O), 40.1 (CH₂-N), (C-F and C-N could not be detected).

4.2.27. *N,N'*-((Ethane-1,2-diylbis(oxy))bis(ethane-2,1-diyl))bis(4-(1H-benzotriazol-1-yl)-2,3,5,6-tetrafluorobenzamide) **161**



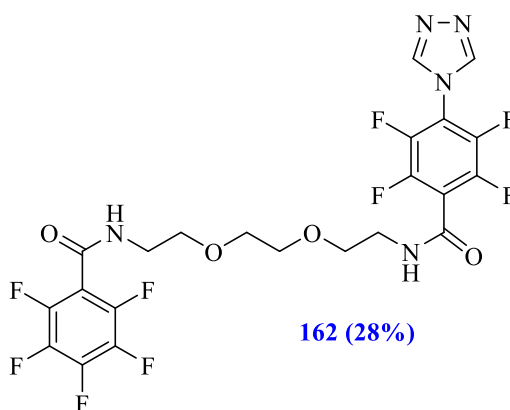
A solution of benzotriazole **30** (0.2 mmol, 0.02 g) in DMSO (2 mL) was added dropwise to stirred suspension of sodium hydride NaH (60 % dispersion in mineral oil) (0.2 mmol, 0.02 g) in DMSO (2 mL) and after 30 min a solution of compound **151** (0.1 mmol, 0.05 g) in DMSO (2 mL) was added dropwise to the reaction mixture. The reaction mixture was left to stir for 24 h at room temperature under a N₂ atmosphere.

Distilled water (10 mL) was added to the reaction mixture and it was extracted with DCM (3×25 mL). The organic extract was washed with aqueous sodium chloride and dried over MgSO₄, filtered and evaporated to give white oil (0.06 g). TLC indicated the presence of some impurity in the

product. Thus further purification was carried out by column chromatography. Compound **161** was afforded after elution with 6:4 ethyl acetate and petrol followed by recrystallization from DCM and petrol to give a shiny white solid (0.041 g, 54%). m.p. 206-208 °C

ν_{max} /cm⁻¹ (film) 3248 (N-H), 2877, 1658 (C=O), 1489, 1280,1041,979, 740; MS (ESI) (MH⁺), C₃₂H₂₃F₈N₈O₄ requires m/z 735.1709 found m/z 735.1705; δ_H (400 MHz, CDCl₃,) 8.21 (2H, d, J 8.4), 7.64 (2H, td, J 6.8, 0.8), 7.52 (2H, td, J 6, 0.8), 7.42 (2H, d, J 8), 7.13 (2H, s, NH), 3.76-3.68 (12H, m); δ_F (376 MHz, CDCl₃) 22.70-22.61 (4F, q, J 11.28), 18.52-18.42 (4F, q, J 11.25,); δ_C (100 MHz, CDCl₃) 157.5 (C=O), 145 (Ar Cq), 133.4 (Ar Cq), 129.6 (Ar CH), 125.9 (Ar CH), 120.6 (Ar CH), 109.6 (Ar CH), 70.6 (CH₂-O), 69.4 (CH₂-O), 40.3 (CH₂-N) (C-F and C-N could not be detected); Analysis (%) for C₃₂H₂₂F₈N₈O₄.1/2H₂O (743) required: C, 51.68; H, 3.09; N, 15.07 Found: C, 51.99; H, 3.08; N, 14.86.

4.2.28. 2,3,4,5,6-Pentafluoro-N-(2-(2-(2-(2,3,5,6-tetrafluoro-4-(4H-1,2,4-triazol-4-yl)benzamido)ethoxy)ethoxy)ethyl)benzamide 162

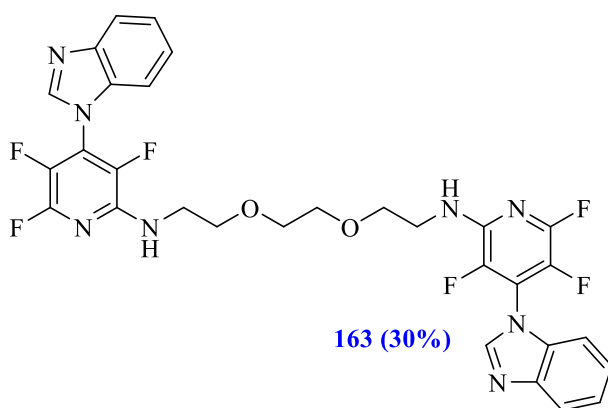


A solution of 1,2,4-triazole **28** (1 mmol, 0.07 g) in DMSO (3 mL) was added dropwise to stirred suspension of sodium hydride NaH (60% dispersion in mineral oil) (2 mmol, 0.08 g) in DMSO (3 mL). The reaction mixture was left to stir for 30 min at RT then a solution of compound **151** (0.5 mmol, 0.26 g) in DMSO (3 mL) was added dropwise. The reaction mixture was left to stir for 24 h at room temperature under a N₂ atmosphere.

Distilled water (10 mL) was added to the reaction mixture and it was extracted with ethyl acetate (3×25 mL). The organic extract was washed with aqueous sodium chloride and dried over MgSO₄, filtered and evaporated to give colourless oil (0.15 g). Purification was carried out by column chromatography, eluting with 9:1 ethyl acetate and petrol. Recrystallization from DCM and petrol then gave compound **162** (0.08 g, 28%) as a white solid.

m.p. 92-94 °C; ν_{max}/cm^{-1} (film) 3282 (NH), 2921, 1662 (C=O), 1503, 1519, 1323, 1131, 990, 739; MS (ESI) (MH⁺), C₂₂H₁₅F₉N₅O₄ requires m/z 584.0986 found m/z 584.0994; δ_H (400 MHz, CDCl₃) 8.47 (1H, s), 8.26 (1H, s), 6.90 (1H, s, NH), 3.71-3.65 (12H, m); δ_F (376 MHz, CDCl₃) 22.69 (2F, q, J 11.65), 21.15-21.05 (2F, m), 14.45 (2F, q, J 11.28), 11.4 (1F, t, J 20.68), 1.95-1.81 (2F, m); Analysis (%) for C₂₂H₁₆F₉N₅O₄ (743) required: C, 45.14; H, 2.75; N, 11.96 Found: C, 45.05; H, 2.98; N, 11.37.

4.2.29. *N,N'*-((Ethane-1,2-diylbis(oxy))bis(ethane-2,1-diyl))bis(4-(1*H*-benzo[*d*]imidazol-1-yl)-3,5,6-trifluoropyridin-2-amine) 163

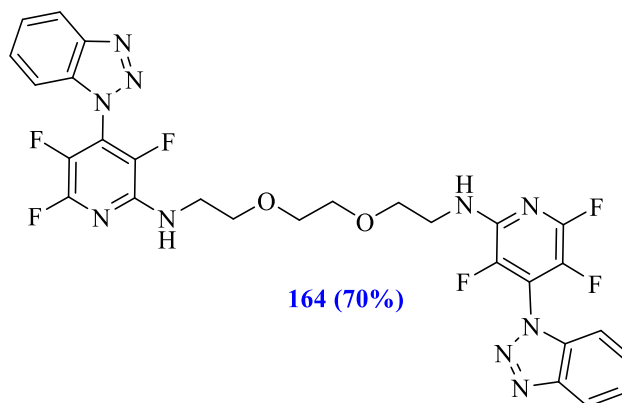


A solution of compound **109** (2 mmol, 0.53 g) in THF (3 mL) was added dropwise to a stirred solution of 2,2-(ethylenedioxy)bis(ethylamine) **150** (1 mmol, 0.15 g) in THF (3 mL). The reaction mixture was refluxed at 65 °C for 24 h under N₂. The solvent was evaporated and distilled water (10 mL) was added to residue. The mixture was extracted with DCM (3×20 mL). The organic extract was dried over MgSO₄, filtrated and evaporated to give a sugary shiny solid (0.4 g). ¹⁹F and ¹H NMR spectrum indicated the presence of some impurities in the product. Therefore further purification was carried out by column chromatography and compound **163** (0.19 g, 30%) was afforded as shiny solid using 100% ethyl acetate as eluting solvent.

m.p. 258-260 °C; ν_{max}/cm^{-1} (film) 3302 (N-H), 2921, 1653, 1513, 1206, 744; MS (ESI) (MH⁺), C₃₀H₂₅F₆N₈O₂ requires m/z 643.1999 found m/z 643.1953; MS (ESI) (MH⁺), C₃₀H₂₃F₆N₈O₂ requires m/z 641.1843 found m/z 641.1845; δ_H (400 MHz, CDCl₃) 8.02 (2H, s), 7.89 (2H, d, J 6.8), 7.38-7.32 (4H, m), 7.28-7.26 (2H, m), 5.25 (2H, s), 3.72-3.64 (12H, m); δ_F (376 MHz, CDCl₃) 72.11 (2F, t, J 29), 11.2 (2F, dd, J 29, 9), 2.04 (2F, dd, J 23, 11); δ_C (100 MHz, CDCl₃) 146.4 (dd, J 230, 11, C-F), 143.1 (Ar CH=N), 142.5 (t, J , 15, Ar Cq-NH), 142.1 (Ar Cq), 136.5 (dd, J 260, 7, C-F), 132.8 (Ar Cq), 129.6 (dd, J 260, 21, C-F), 124.5 (Ar CH), 123.7 (Ar CH), 123.1-122.9 (m, Cq-N), 120.8 (Ar

CH), 111.1 (Ar CH), 70.3 (CH₂-O), 69.5 (CH₂-O), 40.9 (CH₂-N); Analysis (%) for C₃₀H₂₄F₆N₈O₂ (642) required: C, 56.08; H, 3.76; N, 17.44 Found: C, 56.09; H, 3.91; N, 17.35.

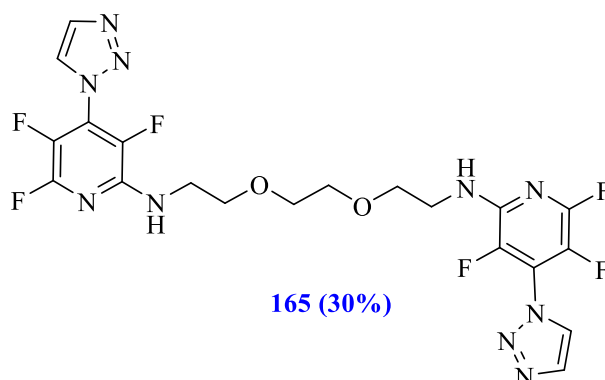
4.2.30. *N,N'*-((Ethane-1,2-diylbis(oxy))bis(ethane-2,1-diyl))bis(4-(1*H*-benzo[*d*][1,2,3]triazol-1-yl)-3,5,6-trifluoropyridin-2-amine) 164



A solution of compound **113** (6 mmol, 1.6 g) in THF (6 mL) and DMF (2 mL) was added dropwise to a stirred solution of triethylamine (6 mmol, 0.8 mL) in THF (3 mL). A solution of 2,2-(ethylenedioxy)bis(ethylamine) **150** (3 mmol, 0.437 g) in THF (6 mL) was added dropwise to the mixture and the reaction left to stir at room temperature overnight under N₂. The solvent was evaporated and water (10 mL) was added to the residue to give a sugary solid precipitate (1.56 g). TLC indicated the presence of some starting material in the product. Therefore further purification was carried out by column chromatography. Compound **164** (1.36 g, 70%) was afforded after elution with 1:1 ethyl acetate and petroleum ether as a white solid.

m.p. 162-164 °C; ν_{max} /cm⁻¹ (film) 3394 (NH), 2921, 1651, 1427, 1257, 1057, 979, 740; MS (ESI) (MH⁺), C₂₈H₂₃F₆N₁₀O₂ requires m/z 645.1904 found m/z 645.1908; δ_H (400 MHz, CDCl₃) 8.16 (2H, d, J 8), 7.58 (1H, t, J 7.2), 7.48-7.43 (4H, m), 5.25 (2H, s), 3.72-3.68 (12H, m); δ_F (376 MHz, CDCl₃) 72.11 (2F, td, J 23, 7), 12.08 (2F, dd, J 29, 10), 1.51 (2F, dd, J 22, 9); δ_C (100 MHz, CDCl₃) 145.5 (Ar Cq), 133.1 (Ar Cq), 129.3 (Ar CH), 125.0 (Ar CH), 120.5 (Ar CH), 110.1 (Ar CH), 70.3 (CH₂-O), 69.5 (CH₂-O), 40.9 (CH₂-N), (C-F and C-N could not be detected); Analysis (%) for C₂₈H₂₂F₆N₁₀O₂ (644) required: C, 52.18; H, 3.44; N, 21.73 Found: C, 52.21; H, 3.30; N, 21.94.

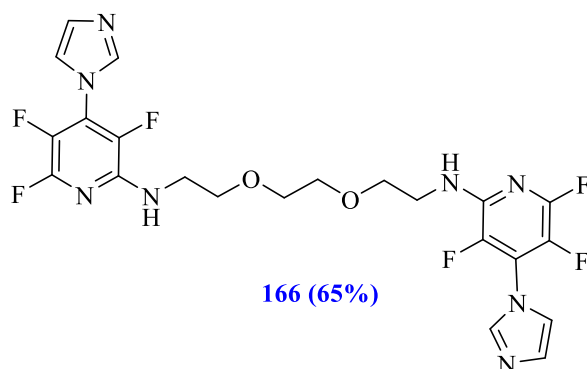
4.2.31. *N,N'*-((Ethane-1,2-diylbis(oxy))bis(ethane-2,1-diyl))bis(3,5,6-trifluoro-4-(1*H*-1,2,3-triazol-1-yl)pyridin-2-amine) **165**



A solution of compound **111** (1 mmol, 0.218 g) in THF (3 mL) was added dropwise to a stirred solution of triethylamine (1 mmol, 0.13 mL) in THF (3 mL). A solution of 2,2-(ethylenedioxy)bis(ethylamine) **150** (0.5 mmol, 0.07 g) in THF (3 mL) was added dropwise to the mixture and the reaction left to stir at room temperature overnight under N₂. The solvent was evaporated and distilled water (10 mL) was added. The mixture was extracted with DCM (3×20 mL). The organic extract was dried over MgSO₄, filtrated and evaporated to give sugary solid (0.3 g) which was purified by column chromatography. Compound **165** (0.08 g, 30%) was afforded after elution with 100% ethyl acetate as a white solid.

m.p. 111-113 °C; ν_{max}/cm^{-1} (film) 3279 (NH), 2924, 1643, 1504, 1419, 1350, 1257, 1064, 927, 740 ; MS (ESI) (MH⁺), C₂₀H₂₉F₆N₁₀O₂ requires m/z 545.1591 found m/z 545.1576; δ_{H} (400 MHz, CDCl₃) 8.52 (2H, s), 8.24 (2H, s), 5.29 (2H, s), 3.69-3.62 (12H, m); δ_{F} (376 MHz, CDCl₃) 71.26 (2F, t, J 28.9), 10.13 (2F, dd, J 28.9, 11.6), 4.02 (2F, d, J 21.1); δ_{C} (100 MHz, CDCl₃) 154.2 (Ar CH), 146.2 (dd, J 240, 11, C-F), 145.3 (Ar CH), 142 (t, J 13, C_q-NH), 135.5 (d, J 260, C-F), 128.3 (dd, J , 280, 33, C-F), 124.2-123.8 (m, C_q-N), 70.3 (CH₂-O), 69.6 (CH₂-O), 40.9 (CH₂-N).

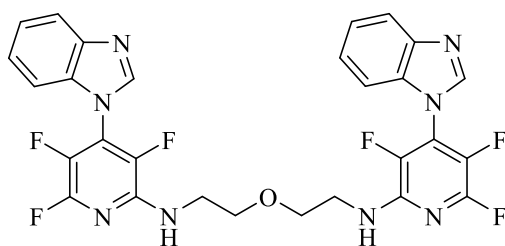
4.2.32. *N,N'*-((Ethane-1,2-diylbis(oxy))bis(ethane-2,1-diyl))bis(3,5,6-trifluoro-4-(1*H*-imidazol-1-yl)pyridin-2-amine) **166**



A solution of compound **108** (6 mmol, 1.3 g) in THF (6 mL) was added dropwise to a stirred solution of triethylamine (6 mmol, 0.8 mL) in THF (3mL). A solution of 2,2-(ethylenedioxy)bis(ethylamine) **150** (3 mmol, 0.44 g) in THF (6 mL) was added dropwise to the mixture and the reaction left to stir at room temperature overnight under the N₂.The solvent was evaporated and distilled water (10 mL) was added to the residue. The mixture was extracted with DCM (3×20 mL). The organic extract was dried over MgSO₄, filtrated and evaporated to give sugary shiny solid (1.26 g). Purification was carried out by column chromatography. The compound **166** (1.05 g, 65%) was afforded by using 50 % Ethyl acetate and 50% Petroleum ether which washed with diethyl ether as creamy shiny solid.

m.p.117-120°C; ν_{max}/cm^{-1} (film) 3217, 31.24 (N-H), 2931, 1655, 1419, 1350, 1273, 1087, 927, 740, 601; MS (ESI) (MH⁺), C₂₂H₂₁F₆N₈O₂ requires m/z 543.1686 found m/z 543.1686; δ_{H} (400 MHz, CDCl₃,) 7.89 (2H, s), 7.38 (4H, d, J 10.8), 5.28 (2H, s), 3.61-3.72 (12H, m); δ_{F} (376 MHz, CDCl₃) 71.62 (2F, t, J 24.4), 8.11 (2F, dd, J 7.14, 27.44), 4.68 (2F, dd, J 8.64 , 24.8); δ_{C} (100 MHz, CDCl₃) 146.6 (dd, J 180, 8.7 C-F), 142.2 (t, J 11, Ar Cq-NH), 137.4 (Ar N-CH=N), 135.1 (ddd, J 200, 4.6, 1.7, C-F), 130.1 (Ar CH), 128.5 (dd, J 200, 26.3 C-F), 124.1-123.9 (M, Cq-N), 111.1 (Ar CH), 119.5 (Ar CH), 69.6 (CH₂-O), 70.2 (CH₂-O),40.8 (CH₂-N); Analysis (%) for C₂₂H₂₀F₆N₈O₂ (542) required: C, 48.71; H, 3.72; N, 20.66 Found: C, 48.80; H, 3.75; N, 20.05.

4.2.33. *N,N'*-(Oxybis(ethane-2,1-diyl))bis(4-(1*H*-benzo[*d*]imidazol-1-yl)-3,5,6-trifluoropyridin-2-amine) **168**



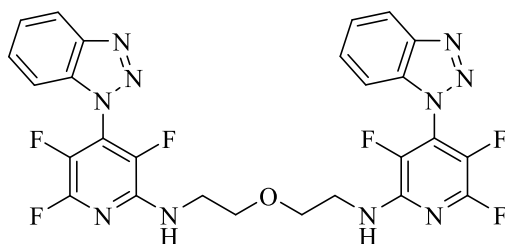
168 (23%)

A solution of compound **109** (2 mmol, 0.43 g) in THF (3 mL) was added dropwise to a stirred solution of triethylamine (4 mmol, 0.52 mL) in THF (3 mL). A solution of 2-(2-aminoethoxy)ethylamine) **167** (1 mmol, 0.178 g) in THF (3 mL) was added dropwise to the mixture and the reaction left to stir at room temperature overnight under N₂. The solvent was evaporated and distilled water (10 mL) added to residue. The mixture was extracted with DCM (3×20 mL). The organic extract was dried over MgSO₄, filtrated and evaporated to give a creamy solid (0.35 g) which was purified by column chromatography. Compound **168** (0.013 g, 23%) was afforded after elution with 100% ethyl acetate and recrystallization from DCM and petrol as a shiny white solid.

m.p. 140-141 °C; ν_{max}/cm^{-1} (film) 3299 (NH), 2941, 1681, 1532, 1459, 1226, 1157, 962, 695

MS (ESI) (MH⁺), C₂₈H₂₁F₆N₈O₁ requires m/z 599.1737 found m/z 599.1720; δ_H (400 MHz, CDCl₃,) 8.01 (2H, s), 7.89 (2H, d, J 7.2), 7.38-7.33 (4H, m), 7.28-7.24 (2H, m), 5.14 (2H, s), 3.75-3.70 (8H, m); δ_F (376 MHz, CDCl₃) 72.11 (2F, t, J 23), 12.14 (2F, dd, J 30, 9), 1.16 (2F, dd, J 23, 9); δ_C (100 MHz, CDCl₃) 155.1 (Ar N-CH =N), 142.0 (Ar Cq), 136.5 (Ar Cq), 124.6 (Ar CH), 123.8 (Ar CH), 120.5 (Ar CH), 111.0 (Ar CH), 69.5 (CH₂-O), 41.9 (CH₂-N), (C-F, C-NH and C-N could not be detected).

4.2.34. *N,N'*-(Oxybis(ethane-2,1-diyl))bis(4-(1*H*-benzo[*d*][1,2,3]triazol-1-yl)-3,5,6-trifluoropyridin-2-amine) **169**

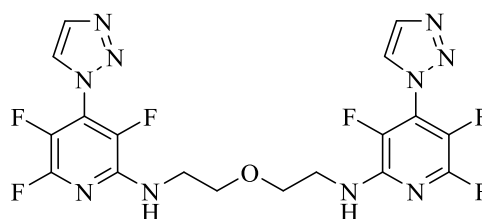


169 (15%)

A solution of compound **113** (2 mmol, 0.54 g) in THF (3 mL) was added dropwise to a stirred solution of triethylamine (4 mmol, 0.52 mL) in THF (3 mL). A solution of 2-(2-aminoethoxy)ethylamine) **167** (1 mmol, 0.18 g) in THF (3 mL) was added dropwise to the mixture and the reaction left to stir at room temperature overnight under N₂. The solvent was evaporated and distilled water (10 mL) was added precipitating a creamy solid (0.43 g). Purification was carried out by column chromatography. Compound **169** was afforded as a white solid (0.09g, 15%) using 1:1 ethyl acetate and petroleum ether as eluent followed by recrystallized from DCM and petrol. m.p. 157-159 °C; ν_{max} /cm⁻¹ (film) 3279 (NH), 2931, 1651, 1512, 1419, 1265, 1057, 972, 617; MS (ESI) (MH⁺), C₂₆H₁₉F₆N₁₀O requires *m/z* 601.1642 found *m/z* 601.1637; δ_H (400 MHz, CDCl₃,) 8.14 (2H, d, *J*, 8), 7.56 (2H, t, *J* 8), 7.50-7.41 (4H, m), 5.15 (2H, s), 3.76-3.69 (8H, m); δ_F (376 MHz, CDCl₃) 72.11 (2F, t, *J* 23), 11.29 (2F, dd, *J* 28, 7), 1.62 (2F, dd, *J* 23, 8); δ_C (100 MHz, CDCl₃) 155.1 (Ar CH), 146.3 (dd, *J* 240, 18, C-F), 145.5 (Ar Cq), 142.3 (t, *J* 13, Cq-NH), 136.5 (d, *J*, 260, C-F), 133.0 (Ar Cq), 129.8 (dd, *J* 230, 21, C-F), 129.3 (Ar CH), 125.0 (Ar CH), 123.7-122.7 (m, Cq-N), 120.5 (Ar CH), 111.0 (Ar CH), 69.5 (CH₂-O), 40.9 (CH₂-N); Analysis (%) for C₂₆H₁₈F₆N₁₀O_{1.5}H₂O (609) required: C, 51.23; H, 3.11; N, 22.98 Found: C, 51.29; H, 2.81; N, 22.35.

4.2.35. *N,N'*-(Oxybis(ethane-2,1-diyl))bis(3,5,6-trifluoro-4-(1H-1,2,3-triazol-1-yl)pyridin-2-amine)

170

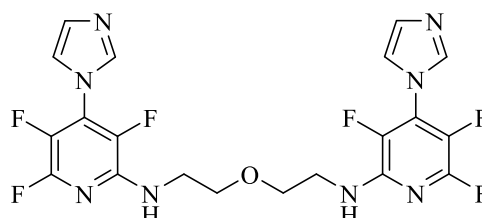


170 (55%)

A solution of compound **111** (1 mmol, 0.22 g) in DMF (3 mL) was added dropwise to a stirred solution of triethylamine (2 mmol, 0.26 mL) in THF (3 mL). A solution of 2-(2-aminoethoxy)ethylamine) **167** (0.5 mmol, 0.18 g) in THF (3 mL) was added dropwise to the mixture and the reaction was refluxed at 65 °C for 24 h, under N₂. The solvent was evaporated and distilled water (10 mL) was added to give a cream solid (0.37 g) which was filtrated by suction filtration. The TLC plate indicated the presence of some starting material in the product. Thus the product was recrystallized by hot ethanol to cover compound **170** (0.138 g, 55%) as white solid. m.p. 127-129°C; ν_{max}/cm^{-1} (film) 3363, 3132 (N-H), 2947, 1658, 1519, 14350, 1265, 1126, 979, 67; MS (ESI) (MH⁺), C₁₈H₁₅F₆N₁₀O₁ requires m/z 501.1329 found m/z 501.1320; δ_{H} (400 MHz, CDCl₃) 8.50 (2H, s), 8.22 (2H, s), 5.12 (2H, s), 3.73-3.62 (8H, m); δ_{F} (376 MHz, CDCl₃) 72.11(2F, t, J 29), 10.10 (2F, dd, J 29, 11), 3.66 (2F, dd, J 23, 11); δ_{C} (100 MHz, CDCl₃) 153.2 (Ar CH), 146.2 (dd, J 230, 21, C-F), 145.3 (Ar CH), 142.3 (t, J 16, Cq-NH), 135.4 (d, J 250, C-F), 128.4 (dd, J 240, 33, C-F), 123.8-12.31 (m, Cq-N), 69.4 (CH₂-O), 40.9 (CH₂-N); Analysis (%) for C₁₈H₁₄F₆N₁₀O₁. (500) required: C, 43.21; H, 2.82; N, 27.99 Found: C, 43.15; H, 2.65; N, 26.93.

4.2.36. *N,N'*-(Oxybis(ethane-2,1-diyl))bis(3,5,6-trifluoro-4-(1H-imidazol-1-yl)pyridin-2-amine)

171



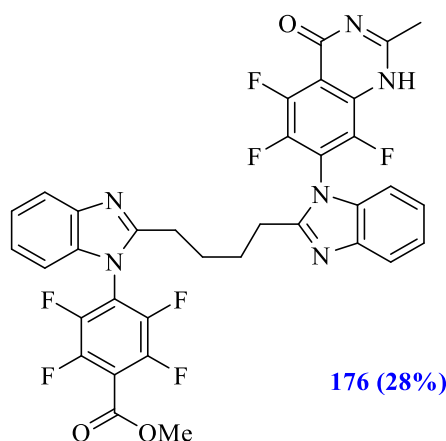
171 (50 %)

A solution of compound **108** (1 mmol, 0.22 g) in DMF (3 mL) was added dropwise to a stirred solution of triethylamine (2 mmol, 0.26 mL) in THF (3 mL). A solution of 2-(2-aminoethoxy) ethylamine) **167** (0.5 mmol, 0.12 g) in THF (3 mL) was added dropwise to the mixture and the reaction was heated at 65 °C for 24 h, under N₂. The solvent was evaporated and distilled water (10 mL) was added to the residue. The mixture was extracted with DCM (3×20 mL). The organic extract was dried over MgSO₄, filtered and evaporated to give yellow sticky oil (0.31 g). The product was triturated with diethyl ether to recover a white solid (0.16 g). TLC indicated the presence of some starting material in the product. Therefore the product was recrystallized from hot ethanol to give compound **171** (0.12 g, 50%) as a shiny white solid.

m.p. 144-145 °C; ν_{max}/cm^{-1} (film) 3333, 3225 (N-H), 2931, 1651, 1519, 1350, 1280, 1080, 979, 748, 671; MS (ESI) (MH⁺), C₂₀H₁₇F₆N₈O₁ requires m/z 499.1424 found m/z 499.1409

δ_H (400 MHz, CDCl₃) 7.89 (2H, s), 8.29 (4H, d, J 20), 5.08 (2H, s), 3.73-3.64 (8H, m); δ_F (376 MHz, CDCl₃) 72.11(2F, t, 22.93), 8.14 (2F,d, J 28.95), 4.36 (2F,d, J 23.31); δ_C (100 MHz, CDCl₃) 144.5 (Ar N-CH=N), 153.2 (Ar C-H), 133.5 (Ar CH), 120.3 (Ar CH), 69.5 (CH₂-O), 40.9 (CH₂-N). (C-F, C-N and C-NH could not be detected); Analysis (%) for C₂₀H₁₆F₆N₈O₁. (498) required: C, 48.20; H, 3.24; N, 22.48 Found: C, 48.27; H, 3.20; N, 21.84.

4.2.37. Methyl2,3,5,6-tetrafluoro-4-(2-(4-(1-(5,6,8-trifluoro-2-methyl-4-oxo-1,4-dihydroquinazolin-7-yl)-1H-benzo[d]imidazol-2-yl)butyl)-1H-benzo[d]imidazol-1-yl)benzoate 176

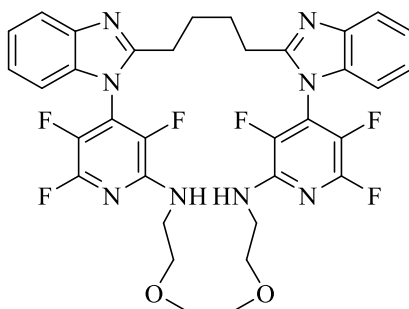


A solution of acetamide hydrochloride **88** (0.2 mmol, 0.02 g) in DMF (3 mL) was added dropwise to a stirred suspension of sodium hydride NaH (60% dispersion in mineral oil) (0.3 mmol, 0.012 g) in DMF (3 mL). A solution of compound **148** (0.1 mmol, 2.38 g) in DMF (3 mL) was added dropwise to the reaction mixture after 30 min by syringe pump and the reaction was refluxed at

85 °C for 24 h under a N₂ atmosphere. The solvent was evaporated and distilled water (10 mL) was added. The yellow solid partials precipitated and were collected by suction filtration (0.07 g). TLC plate indicated the presence of some starting material and impurity in the product therefore further purification was carried out by column chromatography. Compound **176** (0.02 g, 28%) as white crystal was afforded using 7:3 ethyl acetate: light petrol eluting solvent which was recrystallized from DCM and petrol.

m.p. 203-205 °C; ν_{\max} /cm⁻¹ (film) 3394 (N-H), 2931, 1705 (C=O), 1620, 1489, 1280, 1157, 1003, 748, 624; MS (ESI) (MH⁺), C₃₅H₂₄F₇N₆O₃ requires m/z 709.1793 found m/z 709.1775; δ_{H} (400 MHz, CDCl₃,) 11.24 (1H, s, NH), 7.78 (2H, dd, J 7.6, 16.4), 7.28-7.21 (4H, m), 7.02 (2H, t, J 8.4), 3.71 (3H, s, CH₃), 2.81-2.71 (4H, m), 2.61 (3H, s, CH₃), 1.85-2.03 (4H, m); δ_{F} (376 MHz, CDC13) 28.25 (1F, d, J 15.04), 24.57-24.46 (2H, m), 20.60 (1F, t, J 22.56), 15.72-15.66 (2F, m), 14.97 (1F, d, J 18.8).

4.2.38. Reaction of 1,4-bis-1-tetrafluoropyrid-4-yl-1H-benzimidazol-2-ylbutane 143 with 2,2-(ethylenedioxy)bis(ethylamine): macrocycle 181



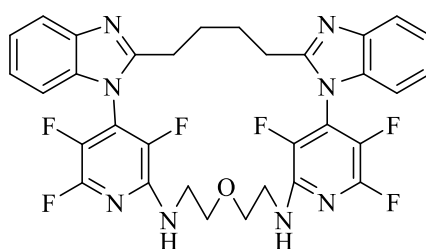
181 (22%)

A solution of 2,2-(ethylenedioxy)bis(ethylamine) **150** (0.4 mmol, 0.06 g) in THF (3 mL) was added dropwise to stirred solution of compound **143** (0.4 mmol, 0.24 g) in THF (5 mL). The reaction mixture was refluxed at 65°C for 24 h under N₂. The solvent was evaporated and distilled water (10 mL) added to residue. The mixture was extracted with DCM (3×20 mL). The organic extract was dried over MgSO₄, filtered and evaporated to give a white sugary solid (0.23 g). Column chromatography purification was carried using 1:1 ethyl acetate and light petroleum as eluting solvent give compound **181** (0.06 g, 22%) as white crystals.

m.p. 133-135 °C; ν_{\max} /cm⁻¹ (film) 3311 (N-H), 2925, 2840, 1652, 1508,1454,1263,1097, 990, 744; MS (ESI) (MH⁺), C₃₄H₃₁F₆N₈O₂ requires m/z 697.2469 found m/z 697.2462; δ_{H} (400 MHz, CDCl₃) 7.79 (2H, d, J 7.6), 7.37-7.33 (2H, td, 7.2, 0.8), 7.30-7.26 (2H, td, J 8.0, 1.2), 7.04 (2H, d, J 7.6), 5.37

(2H, t, *J* 4.8), 3.83-3.59 (12H, m), 2.82-2.63 (4H, m), 2.03-1.87 (4H, m); δ_F (376 MHz, CDCl₃) 72.9 (2F, t, *J* 29.0), 11.95 (2F, d, *J* 35.0), -0.74 (2F, dd, *J* 19.9, 5.6); δ_C (100 MHz, CDCl₃) 153.9 (Ar N-Cq=N), 142.6 (Ar Cq), 134.7 (Ar Cq), 123.6 (Ar CH), 123.3 (Ar CH), 119.7 (Ar CH), 109.4 (Ar CH), 69.9 (CH₂-O), 69.0 (CH₂-O), 40.7 (CH₂-N) 26.9 (CH₂-C=N), 26.2 (CH₂-CH₂-CH₂), (C-F and C-N could not be detected). Analysis (%) for C₃₀H₃₀F₆N₈O₂·2H₂O (732) requires: C, 55.74; H, 4.64; N, 15.30, found: C, 55.88; H, 4.37; N, 14.91.

4.2.39. Reaction of 1,4-bis-1-tetrafluoropyrid-4-yl-1H-benzimidazol-2-ylbutane 143 with 2-(2-aminoethoxy)ethylamine: macrocycle 183



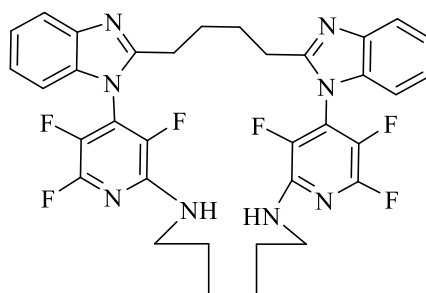
183 (35%)

A solution of 2-(2-aminoethoxy)ethylamine **167** (0.4 mmol, 0.07 g) in THF (3 mL) was added to stirred solution of triethylamine (0.8 mmol, 0.08 g) in THF (2 mL). After 15 min a solution of compound **143** (0.2 mmol, 0.12 g) in THF (3 mL) was added dropwise to the reaction mixture. The reaction mixture was heated at 65 °C for 24 h under N₂.

The solvent was evaporated and water (10 mL) was added to the residue. A yellow orange solid precipitated, and was filtered (0.12 g). Column chromatography purification using 9:1 ethyl acetate and light petroleum as eluting solvent gave compound **183** (0.04 g, 35%) as white sugary crystals.

m.p. 203-205 °C; ν_{max} /cm⁻¹ (film) 3434 (NH), 2099, 1648, 1550, 1453, 1260, 1126, 1011, 744; MS (ESI) (MH⁺), C₃₂H₂₆F₆N₈O requires *m/z* 653.2207 found *m/z* 653.2196; δ_H (400 MHz, CDCl₃) 7.75 (2H, d, *J* 8.0), 7.29-7.18 (4H, m), 6.99 (2H, d, *J* 8.4), 5.28 (2H, s), 4.05-4.00 (2H, m), 3.81-3.73 (4H, m), 3.45-3.39 (2H, m), 2.93-2.82 (2H, m), 2.68-2.63 (2H, m), 2.04-1.87 (4H, m); δ_F (376 MHz, CDCl₃) 72.6 (2F, t, *J* 29.0), 11.7 (2F, d, *J* 29.0), 0.55 (2F, d, *J* 17.3); δ_C (100 MHz, CDCl₃) 153.8 (Ar N-Cq=N), 142.8 (Ar Cq), 142.1 (t, *J*, 14 Ar Cq-NH), 138.0 (dd, *J*, 290, 11, C-F), 134.8 (Ar Cq), 130.9 (dd, *J*, 250, 30, C-F), 123.5 (Ar CH), 123.3 (Ar CH), 123.5-123.0 (m Ar Cq-N), 119.9 (Ar CH), 109.4 (Ar CH), 68.6 (CH₂-O), 40.6 (CH₂-N), 27.0 (CH₂-C=N), 26.0 (CH₂-CH₂-CH₂), (1 ArFCq not detected); Analysis (%) for C₃₂H₂₆F₆N₈O·H₂O (670) requires: C, 57.31; H, 4.17; N, 16.72, found: C, 57.38 H, 4.18; N, 16.41.

4.2.40. Reaction of 1,4-bis-1-tetrafluoropyrid-4-yl-1H-benzimidazol-2-ylbutane 143 with 2-(2-aminoethoxy)ethylamine : macrocycle 185

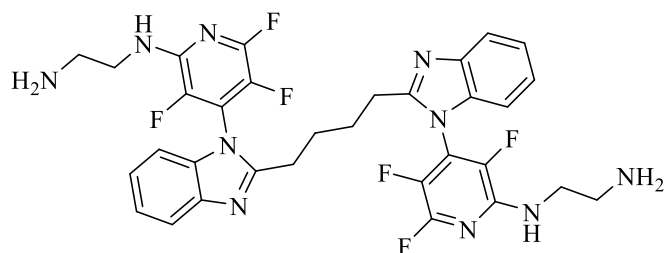


185 (20%)

A solution of hexamethylenediamine **184** (0.5 mmol, 0.06 g) in THF (3 mL) was added to a stirred solution of triethylamine (1 mmol, 0.1 g) in THF (2 mL) after 15 min solution of compound **143** (0.2 mmol, 0.12 g) in THF (3 mL) was added dropwise to the reaction mixture. The reaction mixture was refluxed at 65 °C for 24 h under N₂. The solvent was evaporated and water (10 mL) was added to the residue. A yellow orange solid precipitated and was filtered (0.3 g). Column chromatography purification using 8:2 light petrol and ethyl acetate eluting solvent gave compound **185** as yellow sugary crystals (0.03 g, 20 %).

Decomposed at 180°C; ν_{\max} /cm⁻¹ (film) 3279 (broad peak, NH), 2924, 1651, 1512, 1427, 1257, 964,833; MS (ESI) (MH⁺), C₃₄H₃₁F₆N₈ requires m/z 655.2570 found m/z 655.2569; δ H (400 MHz, CDCl₃) 7.72 (2H, d, *J* 8), 7.31-7.19 (4H, m), 6.98 (2H, d, *J* 8), 5.36 (2H, s), 3.82-3.72 (8H, m), 3.65-3.51 (4H, m), 2.84-2.66 (4H, m), 2.02-2.15 (4H, m); δ F (376 MHz, CDCl₃) 72.32 (2F, t, *J* 25.56), 12.71 (2F, dd, *J* 7.5, 30.08), 1.29 (2F, dd, *J* 8.6, 21.43) δ C (100 MHz, CDCl₃) 153.8 (Ar N-Cq=N), 142.9 (Ar Cq), 134.8 (Ar Cq), 123.4 (Ar CH), 123.3 (Ar CH), 119.9 (Ar CH), 109.4 (Ar CH), 70.8 (CH₂-CH₂-CH₂), 69.6. (CH₂-CH₂-CH₂), 40.6 (CH₂-N), 27.0 (CH₂-C=N), 26.0 (CH₂-CH₂-CH₂), (C-F, C-NH and C-N could not be detected).

4.2.41. 1,4-bis-1-[2-(2-Aminoethylamino)-trifluoropyrid-4-yl]-1H-benzimidazol-2-ylbutane 187

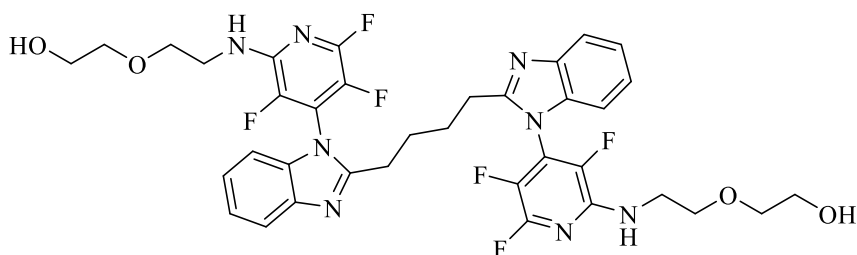


187 (85%)

A solution of ethylenediamine **186** (0.4 mmol, 0.025 g) in THF (2 mL) was added dropwise to a stirred solution of compound **143** (0.2 mmol, 0.12 g) in THF (3 mL) and the mixture stirred at room temperature for 24 h under N₂. Distilled water (10 mL) was added and the mixture extracted with DCM (3×20 mL). The organic extract was dried over MgSO₄, filtered and evaporated to give compound **187** (0.11 g, 85%) as a white shiny solid.

m.p. 195-198 °C; ν_{max}/cm^{-1} (film), 3400 (broad, NH), 2095, 1647, 1509, 1453, 1388, 1264; MS (ESI) (MH⁺), C₃₂H₃₁F₆N₁₀ requires m/z 669.2632, found m/z 669.2621; δ_H (400 MHz, CDCl₃) 7.80 (2H, d, J 7.6), 7.35-7.29 (4H, m), 7.11 (2H, d, J , 7.6), 5.50-5.38 (2H, td, J 8.4, 5.4), 3.57 (4H, dd, J 11.2, 5.2), 3.05 (4H, t, J 5.6), 2.81 (4H, s), 1.99-1.95 (4H, m); δ_F (376 MHz, CDCl₃) 72.3 (2F, m), 13.09 (2F, dd, J 23.3, 8.6), 1.44 (2F, dd, J 23.3, 8.6).

4.2.42. 1,4-bis-1-[2-[2-(2-Hydroxyethoxy)ethylamino]-trifluoropyrid-4-yl]-1H-benzimidazol-2-ylbutane 189

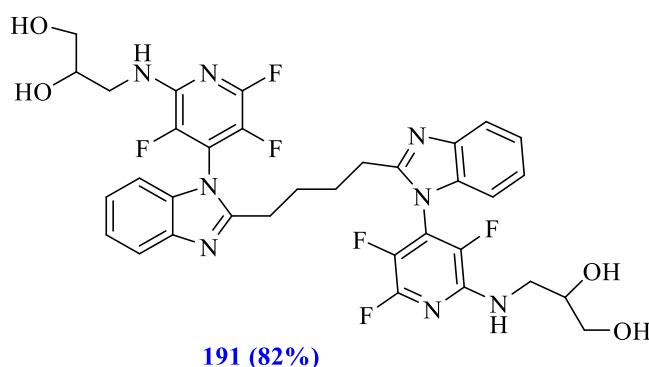


189 (42%)

A solution of 2-(2-aminoethoxy)ethanol **188** (0.2 mmol, 0.02 g) in THF (4 mL) was added dropwise to stirred solution of compound **143** (0.1 mmol, 0.06 g) in THF (4 mL) and the mixture stirred at room temperature for 24 h under N₂. Distilled water (10 mL) was added to reaction mixture and it was extracted with ethyl acetate (3×25 mL). The organic extract was dried over MgSO₄, filtered and evaporated to give white oily product (0.07 g) which was recrystallized from DCM and light petroleum to give compound **189** (0.03 g, 42%) as colourless shiny crystals.

m.p. 168-170 °C; ν_{max}/cm^{-1} (film), 3333 (N-H), 2870,1651,1512, 1427, 1388, 1273, 1118, 1072, 987, 740; MS (ESI) (MH⁺), C₃₆H₃₇F₆N₈O₂ requires m/z 759.2836 found m/z 759.2829; δ_H (400 MHz, (CD₃)₂CO) 7.67 (2H, d, *J* 8.0), 7.46 (2H, s), 7.33-7.24 (6H, m), 4.68 (2H, t, *J* 4.8), 3.61 (8H, t, *J* 5.6), 3.54-3.47 (8H, m (overlap with water peak)), 2.78 (4H, m), 1.84 (4H, m); δ_F (376 MHz, CDCl₃) 72.2 (2F, t, 11.7), 13.6-13.3 (2F, m), -1.93-(-1.46) (2F, m); Analysis (%) for C₃₆H₃₆F₆N₈O₂·3H₂O (785) required: C, 55.03; H, 4.96; N, 14.26 Found: C, 55.37; H, 4.67; N, 13.87.

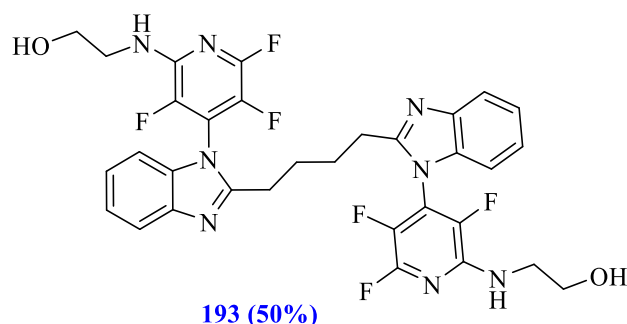
**4.2.43. 1,4-bis-1-[2-(2,3-Dihydroxypropylamino)-trifluoropyrid-4-yl]-1H-benzimidazol-2-ylbutane
191**



A solution of (±)-3-amino-1,2-propanediol **190** (0.2 mmol, 0.018 g) in DMF (3 mL) was added dropwise to a stirred solution of compound **143** (0.1 mmol, 0.058 g) in DMF (mL) and the mixture heated at 80 °C for 24 h under N₂. Distilled water (10 mL) was added and some solid formed which collected by suction filtration to give compound **191** (0.08 g, 82%) as a white solid.

m.p. 123-126 °C; ν_{max}/cm^{-1} (film), 3417 (broad N-H), 2931, 1651,1427, 1257, 1057, 979,748; MS (ESI) (MH⁺), C₃₄H₃₃F₆N₈O₈ requires m/z 731.2523 found m/z 731.2516; δ_H (400 MHz, CDCl₃) 1.92-1.86 (4H, m), 2.90-2.75 (4H, m), 3.47-3.42 (2H, m), 3.84 -3.56 (6H, m), 3.90 (4H, m), 4.25 (2H, s), 7.28-7.18 (6H, m), 7.64 (2H, d, *J* 7.6); δ_F (376 MHz, CDCl₃) 72.53 (2F, t, *J* 25.9), 14.02 (2F, dd, *J* 29.0, 8.6), 5.09 (2F, dd, *J* 25.9, 8.6); δ_C (100 MHz, CDCl₃) 154.6 (Ar N -Cq=N), 142.9 (Ar Cq), 135.1 (Ar Cq), 123.8 (Ar CH), 123.7 (Ar CH), 123.4(Ar CH), 119.5 (Ar CH), 110.7 (Ar CH), 70.0 (CH-O), 64.5 (CH₂-O), 44.8 (CH₂-N), 26.6 (CH₂-C=N), 26.4 (CH₂-CH₂-CH₂), (Ar C-F and C-N could not be detected).

4.2.44. 1,4-bis-1-[2-(2-Hydroxyethylamino)-trifluoropyrid-4-yl]-1H-benzimidazol-2-ylbutane 193



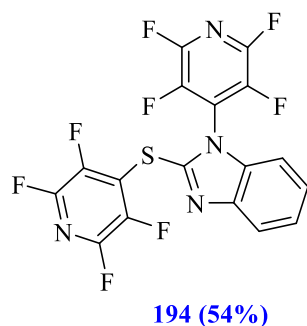
A solution of ethanolamine **192** (0.4 mmol, 0.024 g) in THF (4 mL) was added dropwise to stirred solution of synthesis compound **143** (0.2 mmol, 0.108 g) in THF (4 mL) at 80 °C for 24 h under a N₂ atmosphere. Distilled water (10 mL) was added and the mixture extracted with DCM (3×20 mL). The organic extract was dried over MgSO₄, filtered and evaporated to give a white solid (0.14 g) which was recrystallized from hot ethanol to give the pure compound **193** (0.06, 50%) as white shiny crystals.

m.p. 175-178 °C; ν_{max}/cm^{-1} (film), 3425 (broad N-H), 2947, 1651, 1512, 1427, 1149, 1057, 987, 748.

MS (ESI) (MH⁺), C₃₄H₂₇F₆N₈ O₂ requires m/z 669.2161 found m/z 669.2175;

δ_{H} (400 MHz, (CD₃)₂CO) 7.71-7.68 (2H, dd, J , 8.3, 1.6), 7.32-7.25 (4H, m), 6.60 (2H, s), 4.12 (2H, broad s), 3.78 (4H, t, J 11.2), 3.60-3.58 (4H, m), 2.88 (4H, m), 1.99 (4H, m); δ_{F} (376 MHz, CDCl₃) 72.5 (2F, t, J 14.7), 13.9 (2F, dd, J 29.0, 11.7), 5.1 (2F, dd, J 22.9, 8.6).

4.2.45. 1-Tetrafluoropyrid-4-yl-2-tetrafluoropyrid-4-ylsulfanyl-1H-benzimidazole 194



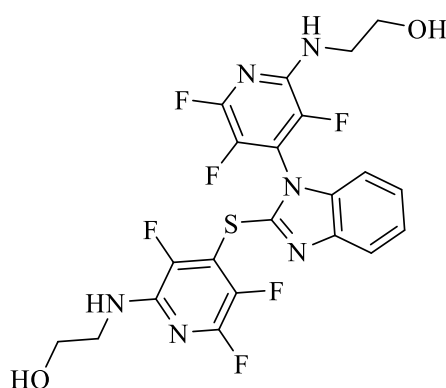
A solution of pentafluoropyridine **74** (100 mmol, 16.9 g) in THF (3 mL) and was added dropwise to a stirred suspension of NaH (60 % dispersion in mineral oil) (40 mmol, 1.6 g) in THF (4 mL). A solution of 2-mercaptobenzimidazole **155** (20 mmol, 3.0 g) in DMF (3 mL) and THF (10 mL) was added to reaction mixture dropwise using a syringe pump under N₂ atmosphere and left to stir at RT

for 24 h. The solvent was evaporated and water (20 mL) was added to the residue. The reaction mixture was extracted with DCM (3x25 mL) and organic extract was dried over MgSO₄, filtered and evaporated to give compound **194** (4.8 g, 54%) as creamy white crystals.

m.p. 113-115 °C

ν_{\max} /cm⁻¹(film) 1630, 1474, 1246, 975, 952; MS (ESI) (MH⁻), C₁₇H₃F₈N₄S found *m/z* 446.9962 requires *m/z* 446.9956; δ_{H} (400 MHz, CDCl₃) 7.85-7.80 (1H, m), 7.49-7.47 (2H, m), 7.23-7.19 (1H, m); δ_{F} (376 MHz, CDCl₃) 77.42-77.05 (2F, m), 74.37-73.97 (2F, m), 19.26-19.12 (2F, m), 27.03-26.87 (2F, m); δ_{C} (125 MHz, CDCl₃) 144.1 (dtd, *J* 248, 15, 4), 143.5 (dddd, *J* 247, 18, 13, 3), 143.4, 142.0, 141.2 (dm, *J* 260), 138.1 (dm, *J* 266), 135.0, 126.1, 126.0 (tt, *J* 13, 5), 125.0, 124.9 (tt, *J* 18, 3), 120.7, 110.1; Analysis (%) calculated for C₁₇H₄F₈N₄S (448): C, 45.55; H, 0.90; N, 12.50. Found C, 45.41; H, 0.92; N, 12.00

4.2.46. 2-((3,5,6-Trifluoro-4-((1-(2,3,5-trifluoro-6-((2-hydroxyethyl)amino)pyridin-4-yl)-1H-benzo[d]imidazol-2-yl)thio)pyridin-2-yl)amino)ethan-1-ol 195



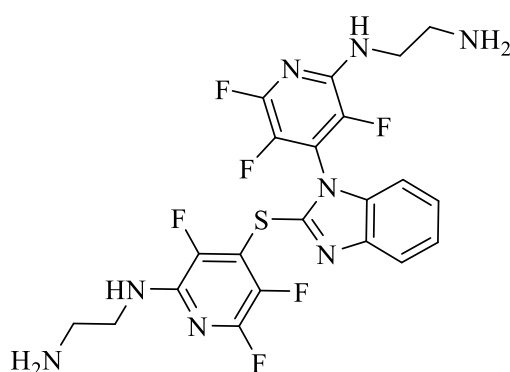
195 (80%)

A solution of ethanolamine **192** (1 mmol, 0.06 mL) in THF (4 mL) was added dropwise to stirred solution triethylamine (1 mmol, 0.14 mL) in THF (3 mL). A solution of scaffold **194** (0.5 mmol, 0.22 g) in THF (6 mL) was added dropwise to the mixture and the reaction left to stir at room temperature overnight under a N₂ atmosphere. Distilled water (10 mL) was added to the mixture and it was extracted with ethyl acetate (3x20 mL). The organic extract was washed with aqueous sodium chloride and dried over MgSO₄, filtrated and evaporated to give compound **195** (0.21 g, 80%) as white shiny solid.

m.p. 94-97 °C; ν_{\max} /cm⁻¹ (film), 3295 (NH), 2924, 2355, 2160, 1651, 1519, 1427, 1265, 1111, 964; 671. MS (ESI) (MH⁺), C₂₁H₁₇F₆N₆O₂S₁ requires *m/z* 531.1032 found *m/z* 531.1028

δ_{H} (400 MHz, CDCl_3) 7.80 (1H, dd, J 6, 2), 7.34-7.37 (2H, m), 7.11 (1H, d, J 7.6), 5.36 (2H broad s), 5.28 (2H, broad s) 3.91-3.75 (4H, m), 3.72-3.47 (4H, m); δ_{F} (376 MHz, CDCl_3) 72.54 (1F, t, J 23.3), 69.59 (1F, t, J 22.9), 23.99 (1F, dd, J 29.9, 7.1), 14.27 (1F, dd, J 30.8, 10.2), 8.33 (1F, dd, J 22.9, 7.1), 0.27 (1F, dd, J 23.3, 7.7); δ_{C} (100 MHz, CDCl_3) 143.2 (Ar Cq), 135.6 (Ar Cq), 123.2 (Ar CH), 120.4 (Ar CH), 110.0 (Ar CH), 61.7 ($\text{CH}_2\text{-O}$), 61.5 ($\text{CH}_2\text{-O}$), 53.5 ($\text{CH}_2\text{-N}$), 43.4 ($\text{CH}_2\text{-N}$), (C-F, C-S and C-N could not be detected).

4.2.47. *N*1-(4-((1-(2-((2-Aminoethyl)amino)-3,5,6-trifluoropyridin-4-yl)-1H-benzod[jimidazol-2-yl)thio)-3,5,6-trifluoropyridin-2-yl)ethane-1,2-diamine 196

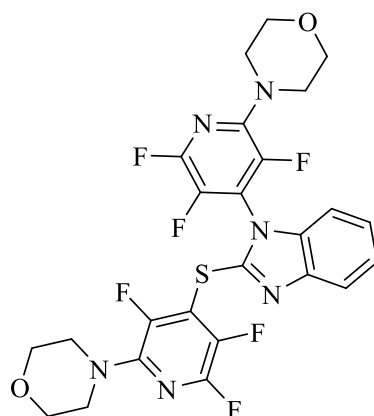


196 (72%)

A solution of ethylenediamine **186** (1 mmol, 0.06 g) in THF (5 mL) was added dropwise to a stirred solution triethylamine (1 mmol, 0.14 mL) in THF (3 mL). A solution of scaffold **194** (0.5 mmol, 0.22 g) in THF (8 mL) was added dropwise to the mixture and the reaction left to stir at room temperature overnight under a N_2 atmosphere. Distilled water (10 mL) was added to reaction mixture and it was extracted with ethyl acetate (3×20 mL). The organic extract was washed with aqueous sodium chloride and dried over MgSO_4 , filtrated and evaporated to give yellow sugary solid **196** (0.19 g, 72%).

Decomposed at 119 °C; $\nu_{\text{max}}/\text{cm}^{-1}$ (film), 3464 (NH), 3232 (N-H), 2893, 1651, 1427, 1257, 1072, 972, 810, 663; MS (ESI) (MH^+), $\text{C}_{21}\text{H}_{19}\text{F}_6\text{N}_8\text{S}_1$ requires m/z 529.1352 found m/z 529.1350; δ_{H} (400 MHz, CDCl_3) 7.78 (1H, dd, J 2.4, 5.2), 7.31-7.32 (2H, m), 7.14 (1H, d, J 6.8), 5.45 (1H, s, N-H), 5.08 (1H, s, N-H), 3.73-3.38 (4H, m), 3.01-2.87 (4H,m), 1.23 (4H, s, N-H); δ_{F} (376 MHz, CDCl_3) 75.38 (1F, t, J 23.3), 69.62 (1F, t, J 24.4), 23.60 (1F, dd, J 5.6, 28.5), 13.91 (1F, dd, J 8.6, 28.9), 7.76 (1F, dd, J 4.5, 23.3), 0.94 (1F, dd J 10.1, 23.3).

4.2.48. 4-(3,5,6-Trifluoro-4-((1-(2,3,5-trifluoro-6-morpholinopyridin-4-yl)-1H-benzo[d]imidazol-2-yl)thio)pyridin-2-yl)morpholine 198

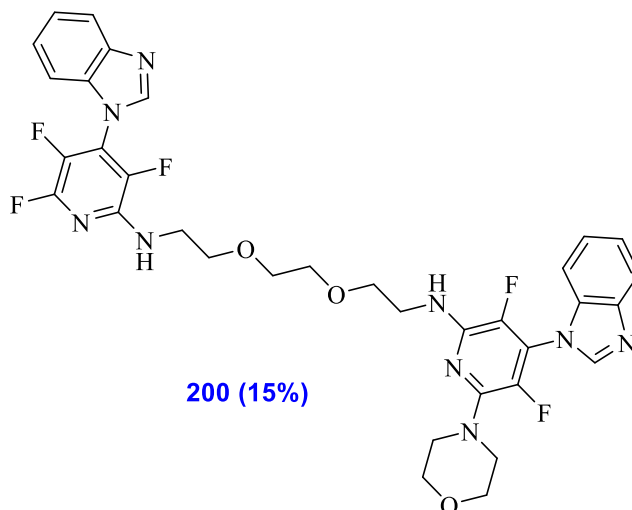


198 (67%)

A solution of morpholine **197** (1 mmol, 0.086 mL) in THF (4 mL) was added dropwise to a stirred solution triethylamine (1 mmol, 0.14 mL) in THF (3 mL). A solution of scaffold **194** (0.5 mmol, 0.22 g) in THF (6 mL) was added dropwise to the mixture and the reaction left to stir at room temperature overnight under N₂. The solvent was evaporated and water (10 mL) was added to the residue. A white solid precipitated, and was filtered (0.3 g). Column chromatography purification using eluting solvent 80% ethyl acetate and 20% light petroleum gave white sugary **198** (0.2 g, 67%).

m.p. 99-102 °C; ν_{max}/cm^{-1} (film) 2854, 1620, 1442, 1257, 1116, 972, 740; MS (ESI) (MH⁺), C₂₅H₂₁F₆N₆O₂S₁ requires m/z 583.1345 found m/z 583.1345; δ_H (400 MHz, CDCl₃) 7.77 (1H, dd, J 2.4, 8), 7.37-7.33 (2H, m), 7.11 (1H, d, J 8), 3.83 (4H, t, J 4.4), 3.75 (4H, t, J 4.4), 3.54 (4H, t, J 4), 3.39 (4H, t, J 4.4), δ_F (376 MHz, CDCl₃) 75.18 (1F, t, J 26.3), 72.28 (1F, t, J 24.4), 36.32 (1F, d, J 30.4), 25.26 (1F, d, J 31.5), 15.53 (1F, dd, J 5.6, 25.9), 5.96 (1F, d, J 24.4); δ_C (100 MHz, CDCl₃) 143.6 (Ar Cq), 135.5 (Ar Cq), 125.1 (Ar CH), 124.2 (Ar CH), 120.3 (Ar CH), 109.9 (Ar CH), 66.62 (d, J 4, CH₂-O), 47.8 (d, J 5.7, CH₂-N), 47.6 (d, J 5.7, CH₂-N), (C-F, C-S and C-N could not be detected); Analysis (%) for C₂₅H₂₁F₆N₆O₂S₁ (582) required: C, 51.55; H, 3.46; N, 14.43 Found: C, 51.63; H, 3.30; N, 13.94.

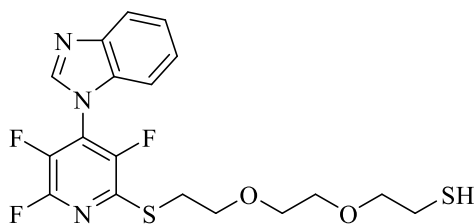
4.2.49. N-(2-(2-(2-((4-(1H-benzo[d]imidazol-1-yl)-3,5,6-trifluoropyridin-2-yl)amino)ethoxy)ethoxy)ethyl)-4-(1H-benzo[d]imidazol-1-yl)-3,5-difluoro-6-morpholinopyridin-2-amine 200



A solution of morpholine **197** (1 mmol, 0.086 mL) in dioxane (4 mL) was added dropwise to a stirred solution of scaffold **163** (0.5 mmol, 0.32 g) in dioxane (6 mL). The reaction left to stir at room temperature overnight under N₂. The solvent was evaporated and water (10 mL) was added to the residue. A white solid precipitated, and was filtered (0.35 g). Column chromatography purification using eluting solvent 95% ethyl acetate and 5% light petroleum gave **200** as white sugary solid (0.05 g, 15%). Only partial data available due to lack of time, and the polarity of compound which made purification difficult.

δ_{H} (400 MHz, CDCl₃) 8.06 (1H, s), 8.03 (1H, s), 7.92-7.88 (2H, m), 7.42-7.30 (6H, m), 5.28-5.27 (1H, m), 5.0-4.98 (1H, m), 3.83 (4H, t, *J* 3.6), 3.78-3.68 (12H, m), 3.46 (2H, t, *J* 2.8), 2.92 (2H, t, *J* 3.6); δ_{F} (376 MHz, CDCl₃) 75.16 (1F, dt, *J* 18.8, 3.8), 14.21 (1F, dd, *J* 22.5, 7.5), 11.49 (1F, dd, *J* 18.8, 8.2), 5.37 (1F, d, *J* 7.53), 1.13-1.01 (1F, m).

4.2.50. 2-(2-(2-((4-(1H-benzod[*i*]imidazol-1-yl)-3,5,6-trifluoropyridin-2-yl)thio)ethoxy)ethoxy)ethane-1-thiol **202**



202 (41%)

A solution of 3,6-dioxa-1,8-octanedithiol **201** (1mmol, 0.18 g) in THF (3 mL) was added dropwise to stirred solution of NaHCO₃ (2 mmol, 0.17 g) in THF (3 mL). A solution of compound **109** (2 mmol, 0.56 g) in THF (6 mL) was added dropwise to the mixture and the reaction mixture was refluxed at 65 °C for 24 h under N₂. The solvent was evaporated and distilled water (10 mL) added to residue. The mixture was extracted with DCM (3×20 mL). The organic extract was dried over MgSO₄, filtered and evaporated to give a white solid (0.67 g). Column chromatography purification using 45% ethyl acetate and 55% light petroleum as eluting solvent gave compound **202** (0.18 g, 41%) as white oil with some impurity which could not be purified further due to lack of time, therefore only partial data are available.

MS (ESI) (MH⁺), C₁₈H₁₉F₃N₃O₂S₂ requires *m/z* 430.0871 found *m/z* 430.0869; δ_F (376 MHz, CDCl₃) 72.20 (1F, t, *J* 23.1), 33.24 (1F, d, *J* 28.9), 11.54 (1F, d, *J* 23.3).

4.3. Biological activity studies

4.3.1. Preparation of Trisma base buffer

Trisma base (0.30 g) was dissolved into distilled water (500 ml) to make 2.5×10^{-3} M trisma base buffer. The pH was adjusted to 7.55 by adding 0.1 M HCl.

4.3.2. Preparation of DNA stock solution

SS-DNA (50 mg) was purchased from Sigma and was dissolved by stirring overnight in double deionized water (pH 7.0) and kept at 4 °C. A solution of (SS-DNA) in the trisma buffer gave a ratio of UV absorbance at 260 and 280 nm (A_{260}/A_{280}) of ca. ~ 1.8 , showing the DNA was free from any protein. SS-DNA concentration was found from absorption spectroscopy using molar absorption coefficient of $6600 \text{ M}^{-1}\text{cm}^{-1}$ (260 nm).

4.3.3. Preparation of synthesis and references compounds solution

Each synthesised compound or reference compound (ACTD and naproxen) was weighed and dissolved in DMSO to make 10^{-2} M stock solutions of each substance. Further dilutions were performed with DMSO to prepare different concentrations of each compound (10^{-3} – 10^{-6} mol.dm⁻³).

4.3.4. Method of UV absorption assay

The UV absorption assay for each synthesis and references compound was carry out by keeping the fixed concentration of each compound while varying SS-DNA concentration. In this method, different amounts of SS-DNA solution were added to samples containing fixed concentrations of each compound. The mixtures were shaken well and were allowed to incubate for 30 min at room temperature to measure the absorption. Absorption spectra were recorded using cuvettes of 1 cm path length at room temperature (25 ± 1 °C).

4.3.5. Method of fluorescence displacement assay

In this method 0.3 mL of EB solution (10^{-4} M) in trisma was added to 0.3 mL of SS-DNA solution then each test compound solution (30, 60, 120, 180, 240, 300 μL of 10^{-6} M) was titrated into the DNA/EB mixture. Each mixture were diluted up to 3 mL with trisma buffer, making the solutions

with varied concentration of (10^{-6} , 2×10^{-6} , 4×10^{-6} , 6×10^{-6} , 8×10^{-6} and 10^{-5} M) each compound to SS-DNA. The mixtures were shaken and incubated at room temperature for 30 min. The fluorescence spectra of EB bound to SS-DNA were recorded at an emission wavelength of 605 nm with excitation of 480 nm.

4.3.6. Hanging drop DNA crystallization method

4.3.6.1. Preparation of DNA solution

Cacodylate buffer (pH 6.5); 50 mM isopropanol 15% was used to prepare a stock buffer solution containing MgCl_2 (10 mM) by adding MgCl_2 (9 mg) to cacodylate buffer (10 ml). DNA solution (0.5 mM) was prepared by adding (600 μl) of buffer stock solution to CGCGAATTCGCG DNA vial which contained (314 nmol).

4.3.6.2. Preparation of the DNA-compound complex sample

In hanging drop DNA crystallization method a sample vial and a piece of glass melting point tube to hold the drop were used. In order to make the drop, 20 μL of DNA solution was added to 2 μL of compound solution (0.01 M). The drop was held in the m.p. tube which was streaked to a sample vial which containing cotton wool wetted with buffer in the bottom. The sample vial was left at RT until the drops partially evaporated and crystals appeared.

4.3.7. Antimicrobial activity studies

The synthesized compounds at 10^{-2} and 10^{-3} M concentration were tested against two bacterial strains Gram-positive strain (*Escherichia coli*) and Gram-negative strain (*Staphylococcus aureus*). The disk diffusion method was used for the determination of antibacterial activity. The bacteria (100 μL) were added to Muller-Hinton agar media (25 mL), mixed well and poured into 90 \times 14 mm petri plate (diameter and height respectively) and the media was allowed to solidify. Sterilized disks (6 mm in diameter) were saturated with the compound solution and placed gently on the inoculated agar plates. Each plate contained a blank disk, which was saturated with DMSO, the compound-containing disk and a control disk containing the antibiotic penicillin. The petri plates were incubated at 37 $^{\circ}\text{C}$ for 48 h.

5. References

- 1 Fadeyi, O.O., Adamson, S.T., Myles, E.L. and Okoro, C.O. Novel fluorinated acridone derivatives. Part 1: synthesis and evaluation as potential anticancer agents. *Bioorg. Med. Chem. Lett.* **18**, 4172–6 (2008).
- 2 Zhu, Y., Hu, J., Hu, Y. and Liu, W. Targeting DNA repair pathways: a novel approach to reduce cancer therapeutic resistance. *Cancer. Treat. Rev.* **35**, 590–6 (2009).
- 3 Rajendran, A. and Nair, B.U. Unprecedented dual binding behaviour of acridine group of dye: a combined experimental and theoretical investigation for the development of anticancer chemotherapeutic agents. *Biochimica et biophysica acta.* **1760**, 1794–801 (2006).
- 4 Rauf, S., Gooding, J.J., Akhtar, K., Ghauri, M.A., Rahman, M., Anwar, M.A, and Khalid, A.M. Electrochemical approach of anticancer drugs-DNA interaction. *J. Pharm. Biomed. Anal.* **37**, 205–17 (2005).
- 5 Pazos, E., Mosquera, J., Vazquez, E.M., and Mascarenas, L.J. DNA Recognition by Synthetic Constructs. *ChemBioChem.* **12**, 1958-1973 (2001).
- 6 Chang Y.M., Chen, C K.-M. and Hou, M.H. Conformational changes in DNA upon ligand binding monitored by circular dichroism. *Int. J. Mol. Sci.* **13**, 3394–413 (2012)
- 7 Cai, X., Gray, P.J. and Von Hoff, D.D. DNA minor groove binders: back in the groove. *Cancer. Treat. Rev.* **35**, 437–50 (2009).
- 8 Reddy, B.S., Sondhi, S.M. and Lown, J.W. Synthetic DNA minor groove-binding drugs. *Pharmacol. Ther.* **84**, 1–111 (1999).
- 9 Nelson, S.M., Ferguson, L.R. and Denny, W.A. Non-covalent ligand/DNA interactions: minor groove binding agents. *Mutat. Res.* **623**, 24–40 (2007).
- 10 Rescifina, A., Chiacchio, U., Corsaro, A., Piperno, A. and Romeo, R. Isoxazolidinyl polycyclic aromatic hydrocarbons as DNA-intercalating antitumor agents. *European journal of medicinal chemistry.* **46**, 129–36 (2011).
- 11 Kirk, K.L. Fluorine in medicinal chemistry: Recent therapeutic applications of fluorinated small molecules. *J. Fluorine Chem.* **127**, 1013–1029 (2006).
- 12 Bégué, J.P. and Bonnet-Delpon, D. Recent advances (1995–2005) in fluorinated pharmaceuticals based on natural products. *J. Fluorine Chem.* **127**, 992–1012 (2006).
- 13 Goslinski, T. and Piskorz, J. Fluorinated porphyrinoids and their biomedical applications. *Journal of Photochemistry and Photobiology C: Photochem. Rev.* **12**, 304–321 (2011).

- 14 Ponce González, J., Edgar, M., Elsegood, M.R.J. and Weaver, G.W. Synthesis of fluorinated fused benzofurans and benzothiophenes: Smiles-type rearrangement and cyclisation of perfluoro(het)aryl ethers and sulfides. *Org. Biomol. Chem.* **9**, 2294–305 (2011).
- 15 Colgin, N., Tatum, N.J., Pohl, E., Cobb, S L. and Sandford, G. Synthesis and molecular structure of a perfluorinatedpyridylcarbanion. *J. Fluor. Chem.* **133**, 33–37 (2012).
- 16 Hargreaves, C.A., Sandford, G., Slater, R., Yufit, D.S., Howard, J.A.K., and Vong, A. Synthesis of tetrahydropyrido[2,3-b]pyrazine scaffolds from 2,3,5,6-tetrafluoropyridine derivatives. *Tetrahedron.* **63**, 5204–5211 (2007).
- 17 Chambers, R.D., Martin, P.A., Sandford, G. and Williams, D.L.H. Mechanisms of reactions of halogenated compounds. *J. Fluorine Chem.* **129**, 998–1002 (2008)
- 18 Kopka, M., Goodsell, G., Han, G., Chiu T, Lown J. and Dickerson R. Defining GC-specificity in the minor groove: side-by-side binding of the di-imidazole lexitropsin to C-A-T-G-G-C-C-A-T-G. *Structure (London).* **5**, 1033–46 (1997).
- 19 Filler, R. and Saha, R. Fluorine in medicinal chemistry: a century of progress and a 60-year retrospective of selected highlights. *Future Med. Chem.* **1**, 777–91 (2009).
- 20 Prasanna Kumar, B.N., Mohana, K.N. and Mallesha, L. Synthesis and antiproliferative activity of some new fluorinated Schiff bases derived from 1,2,4-triazoles. *J. Fluorine Chem.* **156**, 15–20 (2013).
- 21 Ranjbar-Karimi, R., Danesteh, R. and Beiki-Shoraki, K. Synthesis of some fluorinated thiazolopyridine from pentafluoropyridine and 4-phenylsulfonyl tetrafluoropyridine. *Arab. J. Chem.* **5**, 59 (2015).
- 21b Bansal, Y. & Silakari, O. The therapeutic journey of benzimidazoles: a review. *Bioorg. Med. Chem.* **20**, 6208–36 (2012).
- 22 Jespersen C., Soragni E., James Chou C., Arora P.S., Dervan P.B., and Gottesfeld J.M. Chromatin structure determines accessibility of a hairpin polyamide-chlorambucil conjugate at histone H4 genes in pancreatic cancer cells. *Bioorg. Med. Chem. Lett.* **22**, 4068–71 (2012).
- 23 Haq, I. Thermodynamics of drug-DNA interactions. *Arch. Biochem. Biophys.* **403**, 1–15 (2002).
- 24 Reichenbacher, K., Suss, I., and Hulliger, H.J. Fluorine in crystal engineering- the little atom that could. *Chem. Soc. Rev.* **34**, 22-30 (2005)
- 25 Earl, J. and Kirkpatrick, P. Ezetimibe. *Nat. Rev. Drug Discov.* **2**, 97-98 (2003)
- 26 Khalafi-Nezhad, A, Soltani Rad, M. N., Mohabatkar, H., Asrari, Z. & Hemmateenejad, B. Design, synthesis, antibacterial and QSAR studies of benzimidazole and imidazole chloroaryloxyalkyl derivatives. *Bioorg. Med. Chem.* **13**, 1931–8 (2005).

- 27 Shalini, K., Sharma, P.K. and Kumar, N. A review on Imidazole and its biological activities : *Der Chem Sin.* **1**, 36–47 (2010).
- 28 Buckley, B.R., Yohan Chan, Y., Dreyfus, N., Elliott, C., Marken, F. and Bulman-Page, P.C. Harnessing Applied Potential to Oxidation in Water. *Green Chem.* **14**, 2221-2225 (2012).
- 29 Auvil, T. and Mattson, A. Internal Lewis Acid Assisted Benzoic Acid Catalysis. *Synthesis.* **44**, 2173–2180 (2012).
- 30 Mukhopadhyay, C., Ghosh, S. and Butcher, R.J. An efficient and versatile synthesis of 2,2'-(alkanediylo)-bis-1H-benzimidazoles employing aqueous fluoroboric acid as catalyst: Density Functional Theory calculations and fluorescence studies. *ARKIVOC*, (**ix**), 75–96 (2010).
- 31 Sirajuddin, M., Ali, S. and Badshah, A. Drug-DNA interactions and their study by UV-Visible, fluorescence and cyclic voltametry. *J. Photochem. Photobiol. B.* **124**, 1–19 (2013). spectroscopies
- 32 Sirajuddin, M., Ali, S., Shah, N.A., Khan, M.R. and Tahir, M.N. Synthesis, characterization, biological screenings and interaction with calf thymus DNA of a novel azomethine 3-((3,5-dimethylphenylimino)methyl)benzene-1,2-diol. *Spectrochim. Acta. A. Mol. Biomol. Spectrosc.* **94**, 134–42 (2012).
- 33 Dey, S., Sarkar, S., Paul, H., Zangrando, E. and Chattopadhyay, P. Copper(II) complex with tridentate N donor ligand: Synthesis, crystal structure, reactivity and DNA binding study. *Polyhedron.* **29**, 1583–1587 (2010).
- 34 Dey, S., Sarkar, S., Zangrando, E., Evans, H.S., Sutter, J.P. and Chattopadhyay, P. An oxamato bridged trinuclear copper(II) complex: Synthesis, crystal structure, reactivity, DNA binding study and magnetic properties. *Inorg. Chim. Acta* **376**, 129–135 (2011).
- 35 Ducruix, A. and Giege, R (eds). *Crystallization of nucleic acids and proteins: A practical approach.* IRL press, Oxford University, 1–331 (1992).
- 36 Mcpherson, A and Gavira, J.A. Introduction to protein crystallization. *Acta Crystallogr Sect F Struct Biol Cryst Commun.* **70**, 2–20 (2014)
- 37 Kruczynski, A., and Hill, B. Vinflunine, the latest Vinca alkaloid in clinical development. A review of its preclinical anticancer properties. *Critical reviews in oncology/hematology.* **40**, 159–73 (2001).
- 38 Estévez L., Alvarez I., Tusquets I., Seguí M.A., Muñoz M., Fernández Y. and Lluch A. Finding the right dose of fulvestrant in breast cancer. *Cancer. Treat. Rev.* **39**, 136-41 (2013).
- 39 Bohm H.J., Banner D., Bendels S., Kansy M., Kuhn B., Muller K., Obst-Sander U. and Stahl M. Fluorine in medicinal chemistry. *Chem.Bio.Chem.* **5**, 637–643 (2004).

- 40 Van Heek, M., France, C.F., Compton, D.S., McLeod, R.L., Yumibe, N.P., Alton, K.B., Sybertz, E.J. and Davis, HR Jr. In vivo metabolism-based discovery of a potent cholesterol absorption inhibitor, SCH58235, in the rat and rhesus monkey through the identification of the active metabolites of SCH48461. *J. Pharmacol. Exp. Ther.* **283**, 157–163 (1997).
- 41 Clader, J.W. The discovery of ezetimibe: a view from outside the receptor *J. Med. Chem.* **47**, 1-9 (2004).
- 42 Penning, T.D., Talley, J.J., Bertenshaw, S.R., Carter, J.S., Collins, P.W., Docter, S., Graneto, M. J., Lee, L.F., Malecha, J.W., Miyashiro, J M., Rogers, R.S., Rogier, D.J., Yu, S.S., Anderson, G. D., Burton, E.G., Cogburn J.N., Gregory, S.A., Koboldt, C.M., Perkins, W.E, Seibert, K, Veenhuizen, A.W, Zhang, Y.Y. and Isakson, P.C. Synthesis and biological evaluation of the 1,5-diarylpyrazole class of cyclooxygenase-2 inhibitors: identification of 4-[5-(4-methylphenyl)-3-(trifluoromethyl)-1H-pyrazol-1-yl]benzenesulfonamide (SC-58635, celecoxib). *J. Med. Chem.* **40**, 1347, (1997).
- 43 Smith, D.H., van de Waterbeemd, H. and Walker, D.K, *Pharmacokinetics and Metabolism in Drug Design, Methods and Principles in Medicinal Chemistry.* **13**, (2001).
- 44 Sun. A, Lankin D.C., Hardcastle. K. and Snyder J.P. 3-Fluoropiperidines and N-Methyl-3-fluoropiperidinium Salts: The Persistence of Axial Fluorine. *Chem. Eur. J.* 11:1579–1591(2005)
- 45 Jensen, H.H., Lyngbye, L., Jensen A. and Bols M. Stereoelectronic substituent effects in polyhydroxylated piperidines and hexahydropyridazines. *Chem–Eur. J.* **8**, 1218-1226 (2002).
- 46 van Niel, M.B., Collins, I., Beer, M.S., Broughton, H.B., Cheng, S.K.F., Goodacre, S. C., Heald, A., Locker, K.L., MacLeod, A.M., Morrison, D., Moyes., C.R.O., Connor, D., Pike, A., Rowley, M., Russel, M.G.N., Sohal, B., Stanton , J.A., Thomas, S., Verrier, H., Watt, A.P. and Castro, J.L., Fluorination of 3-(3-(piperidin-1-yl)propyl)indoles and 3-(3-(piperazin-1-yl)propyl)indoles gives selective human 5-HT_{1D} receptor ligands with improved pharmacokinetic profiles. *J. Med. Chem.* **42**, 2087–2104 (1999).
- 47 Swain, C.and. Rupniak, N.M.J. Progress in the development of neurokinin antagonist. *Ann. Rep. Med. Chem.* **34**, 51 – 60 (1999)
- 48 Wildman, S. and Crippen, G. Prediction of Physicochemical Parameters by Atomic Contributions. *J. Chem. Inf. Model.* 39, 868–873 (1999).
- 49 Ingle, R.G. and Magar, D.D. Heterocyclic Chemistry of Benzimidazoles and Potential Activities of Derivatives. *Int. J. Drug Res. Tech.* **1(1)**, 26–32 (2011).
- 50 Saini, M.S., Kumar, A., Dwivedi, J. and Singh, R. a Review : Biological Significances of Heterocyclic Compounds . *Int. J. Pharma. Sci. Res.* **4**, 66–77 (2013).

- 51 Zhang, L., Peng, X.M., Damu, G.L.V, Geng, R.X. and Zhou, C.H. Comprehensive review in current developments of imidazole-based medicinal chemistry. *Med. Res. Rev.* **34**, 340–437 (2014).
- 52 Aleksandrova, E.V., Kravchenko, A.N. and Kochergin, P.M., Properties of haloimidazoles. *Chem Heterocycl. Compd.* **47**, 261–289 (2011).
- 53 Narasimhan, B., Sharma, D. and Kumar, P. Biological importance of imidazole nucleus in the new millennium. *Med. Chem. Res.* **20**, 1119–1140 (2011).
- 54 Bhatnagar, A., Sharma, P.K. and Kumar, N. A review on “Imidazoles”: Their chemistry and pharmacological potentials. *Int. J. Pharm.Tech. Res.* **3**:268–282 (2011).
- 55 Steinman, R.A., Brufsky, A.M. and Oesterreich, S. Zoledronic acid effectiveness against breast cancer metastases A role for estrogen in the microenvironment? *Breast Cancer Res.* **14**, 213 (2012).
- 56 Burnier, M. and Wuerzner, G. Pharmacokinetic evaluation of losartan. *Expert Opin Drug Metab Toxicol.* **7**, 643–64 (2011).
- 57 Baroniya, S., Anwer, Z., Sharma, P.K., Dudhe, R. and Kumar, N., Recent advancement in imidazole as anticancer agents: A review. *Pharm Sinica.* **1**, 172–182 (2010).
- 58 Zhou, C.H. and Hassner, A. Synthesis and anticancer activity of novel chiral glucose derived bis-imidazoles and their analogs. *Carbohydr Res.* **333**, 313–326 (2001).
- 59 Babita, G. and Arvind, K S. Pharmacological activities of benzimidazole derivatives- Overview. *IJSID*, **2 (1)**, 121-136 (2012).
- 60 Wright, J.B. The chemistry of the benzimidazoles. *Chem. Rev.* **48**, 397-541 (1951).
- 61 Kalidhar, U. and Kaur, An Overview on Some Benzimidazole and Sulfonamide Derivatives with Anti-Microbial Activity. *A. Research J. Pharm. Chem.. Biol Sci.* **2**, 1116–1135 (2011).
- 62 Singh, N, Pandurangan, A, Rana, K, Anand, P, Ahmad, A. and Tiwari, A.K. Benzimidazole: A short review of their antimicrobial activities. *Int. Curr. Pharm. J.* **1**, 119–127 (2012).
- 63 Srestha, N., Banerjee, J. and Srivastava, S. A review on chemistry and biological significance of benzimidazole nucleus. *J. Pharm.* **4**, 28–41 (2014).
- 64 Siddiqui, N., Ahsan, W., Alam, M.S., Ali, R., Jain, S., Azad, B. and Akhtar, J. Triazoles: As potential bioactive agents. *Int. J. Pharm. Sci. Rev. Res.* **8**, 161–169 (2011).
- 65 Zhang, Q., Pan, J., Zheng, R.L. and Wang, Q. Redifferentiation of human hepatoma cell induced by 6-(p-chlorophenyl)-3-[1-(p-chlorophenyl)-5-methyl-1 H-1,2,3-triazol-4-yl]-s-triazolo[3,4-b]-1,3,4-thiadiazole (TDZ). *Pharmazie.* **60**, 378–382 (2005).
- 66 Asif, M. Antiviral and antiparasitic activities of various substituted triazole derivatives: A mini review. *Chem Int.* **1**, 71–80 (2015).

- 67 Wang, Y. and Zhou, C.H. Recent advances in the researches of triazole compounds as medicinal drugs. *Scientia Sinica Chemica*. **41**, 1429-1456 (2011)
- 68 Singhal, N., Sharma, P.K., Dudhe, R. and Kumar, N. Recent advancement of triazole derivatives and their biological significance. *J. Chem. Pharm. Res.* **3**, 126–133 (2011).
- 69 Kharb, R., Sharma, P.C. and Yar, M.S. Pharmacological significance of triazole scaffold. *J. Enzyme Inhib. Med. Chem.* **26**, 1–21 (2011).
- 70 Mi, J.L., Wu, J. and Zhou, C.H. Progress in anti-tumor agents:triazoles. *J. Chin. Pharm. Sci.* **23**, 84-86 (2008).
- 71 Mi, J.L., Zhou, C.H. and Bai, X., 2007. Advances in triazole antimicrobial agents. *J. Chin. Antibiot.* **32**, 587-593 (2003).
- 72 Rodriguez-Fernandez, E., Manzano, J.L., Benito, J.J., Hermosa, R., Monte, E. and Criado, J.J. Thiourea, triazole and thiadiazine compounds and their metal complexes as antifungal agents. *J. Inorg. Biochem.* **99**, 1558-1572 (2005).
- 73 Liu, Z.Q., Zhu, Q.Z., Li, F.Y., Zhang, L.N., Leng, Y. and Zhang, A.N-(5 substituted thiazol-2-yl)-2-aryl-3-(tetrahydro-2H-pyran- 4-yl)propanamides as glucokinase activators. *Med. Chem. Comm.* **2**, 531-535 (2011).
- 74 Ouellette, W., Jones, S. and Zubieta, J. Solid state coordination chemistry of metal-1,2,4-triazolates and the related metal-5-(pyrid-4-yl)tetrazolates. *Crystallography Eng. Comm.* **13**, 4457-4485 (2011).
- 75 Zhou, C.H., Gan, L.L., Zhang, Y.Y., Zhang, F.F., Wang, G.Z., Jin, L., Geng, R.X. Review on supermolecules as chemical drugs. *Sci. China, Ser. B, Chem.* **52**, 415-458 (2009).
- 76 Zhou, C.H., Zhang, F.F., Gan, L.L., Zhang, Y.Y. and Geng, R.X. Research in supermolecular chemical drugs. *Sci. China, Ser. B, Chem.* **39**, 208-252 (2009).
- 77 Zhou, C.H., Zhang, Y.Y., Yan, C.Y., Wan, K., Gan, L.L. and Shi, Y. Recent researches in metal supramolecular complexes as anticancer agents. *Anti-Cancer Agents. Med. Chem.* **10**, 371-395 (2010).
- 78 Lin, R., Connolly, P.J. and Huang, S. 1-Acyl-1H-[1,2,4]triazole-3,5-diamine analogues as novel and potent anticancer cyclin dependent kinase inhibitors: synthesis and evaluation of biological activities. *J. Med. Chem.* **48**, 4208–4211 (2005).
- 79 Pachuta-Stec, A., Rzymowska, J., Mazur, L., Mendyk, E., Pitucha, M. and Rzaczyńska, Z. Synthesis, structure elucidation and antitumour activity of N-substituted amides of 3-(3-ethylthio-1,2,4-triazol-5-yl)propenoic acid. *Eur J. Med. Chem.* **44**, 3788–3793 (2009).
- 80 Suma, B.V., Natesh, N.N., and Madhavan, V. Benzotriazole in medicinal chemistry: an overview. *J. Chem. Pharm. Res.* **3**, 375-381(2011).

- 81 Katritzky, A.R., Kim, S. and Widyan, K. The Baylis-Hillman reaction of substituted aminomethylbenzotriazoles. *Arkivoc.* **(iii)**, 91–101 (2008).
- 82 Furmiss, B.S., Hannaford, A.J., Smith, P.W.G. and Tatchell, A.R. *Vogel's textbook of practical organic chemistry.* Pearson . **5**, 1163 (2008).
- 83 Piccionello, A.P., and Guarcello, A. Bioactive compounds containing benzoxadiazole, benzothiadiazole, benzotriazole. *Curr. Bioact. Compd.* **6**, 266-283 (2010).
- 84 Singh, G., Kumar, R., Swett, J. and Zajc, B. Modular synthesis of N-vinyl benzotriazoles. *Org. Lett.* **15**, 4086-4089 (2013).
- 85 Milosevic, N.P., Dimova, V.B. and Perisic-Janjic, N.U. RP TLC data in correlation studies with in silico pharmacokinetic properties of benzimidazole and benztriazole derivatives. *Eur. J. Pharm. Sci.* **49**, 10-17 (2013).
- 86 Duncan, J.S., Gyenis, L., Lenehan, J., Bretner, M., Graves, L.M. Hayward, T.A. and Lichfield, D.W. An unbiased evaluation of CK2 inhibitors by chemoproteomics: characterization of inhibitor effects on CK2 and identification of novel inhibitor targets. *Mol. Cell. Proteomics* **7**, 1077-1088 (2008).
- 87 Entezar, M., Safari, M., Hekmati, M., Hekmat, S. and Azin, A. Modification of carboxylated multiwall nanotubes with benzotriazole derivatives and study of their anticancer activities. *Med. Chem. Res.* **23**, 487-495 (2014).
- 88 Szyszka, R.1., Grankowski, N., Felczak, K. and Shugar, D. Halogenated benzimidazoles and benzotriazoles as selective inhibitors of protein kinases CK I and CK II from *Saccharomyces cerevisiae* and other sources. *Biochem. Biophys. Res. Commun.* **208 (1)**, 418-24 (1995).
- 89 Pagano, M.A., Bain, J., Kazimierczuk, Z., Sarno, S., Ruzzane, M., Di Maira, G., Elliott, M., Orzeskjj, A., Cozza, G., Meggio, F., and Pinna. L.A. The selectivity of inhibitors of protein kinase CK2: an update. *Biochem. J.* **415**, 353-365 (2008).
- 90 Suma, B.V, Natesh, N.N. and Madhavan, V. Benzotriazole in medicinal chemistry : An overview. *J. Chem. Pharm. Res.* **3**, 375–381 (2011).
- 91 Patil, G.K., Patil, H.C., Patil, I.M., Borse, S.L., and Pawar, S.P. Benzotriazole—the molecule of diverse biological activities. *World. J. Pharm. Pharm Scis.* **4**, 532–548 (2015).
- 92 Ren, Y. Recent Development of Benzotriazole-based Medicinal Drugs. *Med. Chem. (Los Angeles).* **4**, 640–662 (2014).
- 93 Bajetta, E., Zilembo, N. and Bichisao, E. Aromatase inhibitors in the treatment of postmenopausal breast cancer. *Drugs Aging.***15**, 271–283 (1999).

- 94 Allen, G.J., Burdon, J. and Tatlow, J.C. Aromatic polyfluoro-compounds. Part XXVII. Reactions of pentafluoro-aniline, -N-methylaniline, and -N,N-dimethylaniline with nucleophiles. *J. Chem. Soc.* 6329-6336 (1965).
- 95 Cargill, M.R. Polyfluorinated Aromatic Systems for Liquid Crystal Display Applications, Durham theses, Durham University (2011).
- 96 Langille, K.R. and Peach, M.E. The thiolate anion as a nucleophile part I. Reactions with hexafluorobenzene, decafluorobiphenyl and hexachlorobenzene. *J. Fluorine Chem.* **1**, 407–414 (1972).
- 97 Brooke, G.M. The preparation and properties of polyfluoro aromatic and heteroaromatic compounds. *J. Fluorine Chem.* **86**, 1–76 (1997).
- 98 Aroskar, E.V., Brown, P.J.N., Plevey, R.G. and Stephens, R. Aromatic polyfluoro compounds. Part XLI. Some reactions of pentafluorobenzaldehyde. *J. Chem. Soc. C.* 1569-1575 (1968)
- 99 Ranjbar-Karimi, R., Danesteh, R. and Beiki-Shoraki, K. Synthesis of some fluorinated thiazolopyridine from pentafluoropyridine and 4-phenylsulfonyl tetrafluoropyridine. *Arab. J. Chem.* (2015).
- 100 Chambers, R.D., Hutchinson, J. and Musgrave, W.K.R. Polyfluoro-heterocyclic compounds. Part I. The preparation of fluoro-, chlorofluoro-, and chlorofluorohydro-pyridines. *J. Chem. Soc.* 3573-3576 (1964).
- 101 Banks, R.E. Haszeldine, R.N. Latham, J.V. and Young, I.M. Heterocyclic polyfluoro-compounds. Part VI. Preparation of pentafluoropyridine and chlorofluoropyridines from pentachloropyridine. *J. Chem. Soc.* 594-597 (1965)
- 102 Graham, J. Acid induced reactions of poly uoroaromatic compounds, Durham theses, Durham University (1969).
- 103 Cartwright, M.W., Sandford, G., Bousbaa, J., Yufit, D.S., Howard, J.A.K., Christopher, J A. and Miller, D.D. Imidazopyridine and pyrimidinopyridine systems from perfluorinated pyridine derivatives. *Tetrahedron.* **63**, 7027–7035 (2007).
- 104 Sandford, G., Slater, R., Yufit, D., Howard, J. and Vong, A. Tetrahydropyrido[3,4-b]pyrazine Scaffolds from Pentafluoropyridine. *J. Org. Chem.* **70**, 7208-7216 (2005).
- 105 Zhou, C.H., Zhang, F.F., Gan, L.L., Zhang, Y.Y. and Geng, R.X. Research in super molecular chemical drugs. *Sci Chin Ser. B: Chem.* **39**, 208-252 (2009).
- 106 Tang, Y.D., Zhang, J.Q., Zhang, S.L., Geng, R.X. and Zhou, C.H. Synthesis and characterization of thiophene-derived amido bis-nitrogen mustard and its antimicrobial and anticancer activities. *Chin. J. Chem.* **30**, 1831-1840 (2012).

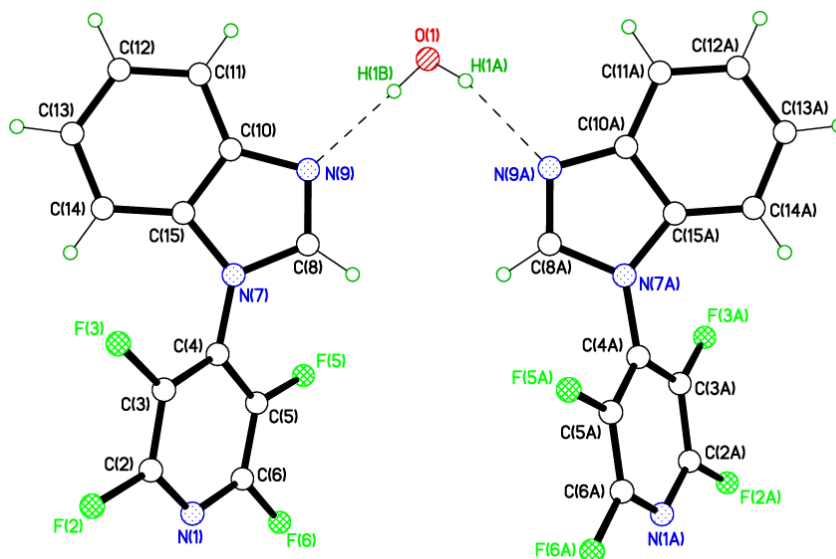
- 107 Duncan, J.S., Gyenis, L., Lenehan, J., Bretner, M., Graves, L.M. Haystead, T.A. and Litchfield, D.W. An unbiased evaluation of CK2 inhibitors by chemoproteomics: characterization of inhibitor effects on CK2 and identification of novel inhibitor targets. *Mol Cell. Proteomics* **7**, 1077-1088 (2008).
- 108 Yuan, J., Zhong, Y., Li SL., Zhao, X., Luan, GQ, Zhao, Z., Huang, J., Li, H. and XU, Y. Triazole and benzotriazole derivatives as novel inhibitors for p90 ribosomal S6 protein kinase 2: synthesis, molecular docking and SAR analysis. *Chin. J. Chem* **31**, 1192-1198 (2013).
- 109 Levitzki, A. and Gilon, C. Tyrphostins as molecular tools and potential antiproliferative drugs. *Trends. Pharmacol. Sci.* **12**, 171-4 (1991).
- 110 Levitzki, A. Signal-transduction therapy. A novel approach to disease management. *Eur. J. Biochem.* **226**, 1-13 (1994).
- 111 Levitzki, A. Tyrphostins: tyrosine kinase blockers as novel antiproliferative agents and dissectors of signal transduction. *Faseb. J.* **6**, 3275-82 (1992).
- 112 Roberts, P.J. and Der, C.J. Targeting the Raf-MEK-ERK mitogen-activated protein kinase cascade for the treatment of cancer. *Oncogene* **26**, 3291–3310 (2007).
- 113 McCubrey, J.A., Steelman, L.S., Chappell, W.H., Abrams, S.L., Wong, E.W., Chang, F., Lehmann, B., Terrian, D.M., Milella, M., Tafuri, A., Stivala, F., Libra, M., Basecke, J., Evangelisti, C., Martelli, A.M. and Franklin, R.A.. Roles of the Raf/MEK/ERK pathway in cell growth, malignant transformation and drug resistance. *Biochim. Biophys. Acta-Molecular Cell Res.* **1773**, 1263–1284 (2007).
- 114 Meier, F., Schittek, B., Busch, S., Garbe, C., Smalley, K., Satyamoorthy, K., Li, G. and Herlyn, M. The RAS RAF MEK ERK and PI3K AKT signalling pathways present molecular targets for the effective treatment of advanced melanoma. *Front. Biosci.* **10**, 2986-3001 (2005).
- 115 Huang, T., Karsy, M., Zhuge, J., Zhong, M. and Liu, D. B-Raf and the inhibitors: from bench to bedside. *J. Hematol. Oncol.* **6**, 30 (2013).
- 116 Davies, B.R., Logie, A., McKay, J.S., Martin, P., Steele, S, Jenkins, R., Cockerill, M., Cartlidge, S., and Smith P.D. AZD6244 (ARRY-142886), a potent inhibitor of mitogen-activated protein kinase/extracellular signal-regulated kinase 1/2 kinases: mechanism of action in vivo, pharmacokinetic/pharmacodynamic relationship, and potential for combination in preclinical models. *Mol. Cancer. Ther.* **6**, 2209–2219 (2007).
- 117 Herbst, R.S. Review of epidermal growth factor receptor biology. *Int. J. Radiat. Oncol. Biol. Phys.* **59**, 21–26 (2004).
- 118 Wang, Y., Schmid-Bindert, G. and Zhou, C. Erlotinib in the treatment of advanced non-small cell lung cancer: an update for clinicians. *Ther. Adv. Med. Oncol.* **4**, 19–29 (2012).

- 119 Ciardiello, F, Caputo, R, Bianco, R, Damiano, V, Pomatico, G, De Placido, S, Bianco A.R. and Tortora, G. Antitumor Effect and Potentiation of Cytotoxic Drugs Activity in Human Cancer Cells by ZD-1839 (Iressa), an Epidermal Growth Factor Receptor-selective Tyrosine Kinase Inhibitor. *Clin. Cancer. Res.* **6**, 2053–2063 (2000).
- 120 Levitzki, A. and Gazit, A. Tyrosine kinase inhibition: an approach to drug development. *Sci.* **267**, 1782-8 (1995).
- 121 Levitzki, A. Protein kinase inhibitors as a therapeutic modality. *Acc. Chem. Res.* **36(6)**, 462–469 (2003).
- 122 Payne, S. and Miles, D. Scott-Brown's Otorhinolaryngology: Head and Neck Surgery. *Scott-Brown's Otorhinolaryngol. Head Neck. Surg.* **3**, 34–46 (2008).
- 123 Wakeling, A.E., Guy, S.P., Woodburn, J.R., Ashton, S.E., Curry, B.J., Barker, A.J. and Gibson, K. H. ZD1839 (Iressa): an orally active inhibitor of epidermal growth factor signaling with potential for cancer therapy. *Cancer Res.* **62**, 5749-54 (2002).
- 124 Liu, P., Sharon, A. and Chu, C.K. Fluorinated nucleosides: Synthesis and biological implication. *J. Fluorine Chem.* **129**, 743–766 (2008).
- 125 Dolbier, W.R. Fluorine chemistry at the millennium. *J. Fluorine Chem.* **126**, 157–163 (2005).
- 126 Paul, A. and Bhattacharya, S. Chemistry and biology of DNA-binding small molecules. *Curr. Sci.* **102**, 212–231 (2012).
- 127 Bhambra, A.S., Edgar, M., Elsegood, M.R., Horsburgh, L., Kryštof, V., Lucas, P.D. Mojally, M., Teat, S.J., Warwick, T.G., Weaver, G.W. and Zeinali, F. Novel fluorinated benzimidazole-based scaffolds and their anticancer activity in vitro. *J. Fluorine Chem.* **188**, 99-109 (2016).
- 128 Sirajuddin, M., Ali, S., Haider, A., Shah, N.A., Shah, A. and Khan, M.R. Synthesis, characterization, biological screenings and interaction with calf thymus DNA as well as electrochemical studies of adducts formed by chlorides. *Polyhedron* **40**, 19–31 (2012).
- 129 Liu, Z., Qin, L. and Zard, S.Z. Radical ipso-Substitution of a Carbon-Fluorine Bond Leading to-7-Azindolines and Fluoro-7-Azaindoles. *Org. Lett.*, **16**, 2704–2707 (2014).
- 130 Althagbi, H.I., Lane, J.R., Saunders, G.C., and Webb, S.J. Engineering polar crystal structures by n-n stacking of N-perfluoroarylbenzimidazoles. *J. Fluorine Chem.* **166**, 88–95 (2014).
- 131 Beletskaya, I.P., Davydov, D.V., Gorovoi, M.S. and Kardashov, S.V. Selective N(1)-arylation of benzotriazole with activated aryl halides under conditions of phase transfer catalysis. *Russian Chemical Bulletin* **48**, 1533–1536 (1999).

6. Appendix

6.1. X-ray crystallography data

6.1.1. Compound 109 X-ray crystal structure data

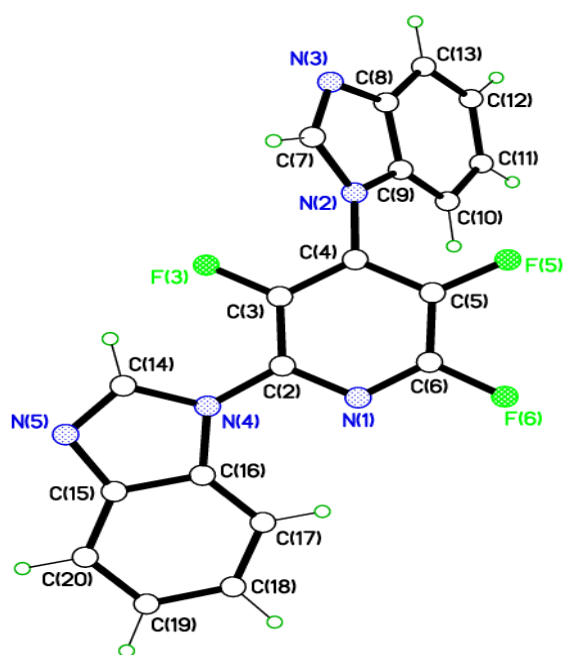


Crystal data and structure refinement

Identification code	gw85	
Chemical formula	$C_{12}H_6F_4N_3O_{0.50}$	
Formula weight	276.20	
Temperature	150(2) K	
Radiation, wavelength	MoK α , 0.71073 Å	
Crystal system, space group	monoclinic, Cc	
Unit cell parameters	$a = 27.76(4)$ Å	$\alpha = 90^\circ$
	$b = 7.483(10)$ Å	$\beta = 99.29(2)^\circ$
	$c = 11.133(15)$ Å	$\gamma = 90^\circ$
Cell volume	$2282(5)$ Å ³	
Z	8	
Calculated density	1.608 g/cm ³	
Absorption coefficient μ	0.148 mm ⁻¹	
F(000)	1112	
Crystal colour and size	colourless, $0.76 \times 0.46 \times 0.05$ mm ³	
Reflections for cell refinement	933 (θ range 3.31 to 21.56°)	
Data collection method	Bruker APEX 2 CCD diffractometer	

	rotation with narrow frames
θ range for data collection	2.82 to 28.49°
Index ranges	h -37 to 36, k 0 to 9, l 0 to 14
Completeness to θ = 26.00°	98.6 %
Intensity decay	0%
Reflections collected	2746
Independent reflections	2746 (R _{int} = 0.1161)
Reflections with F ² > 2σ	1450
Absorption correction	semi-empirical from equivalents
Min. and max. transmission	0.896 and 0.993
Structure solution	direct methods
Refinement method	Full-matrix least-squares on F ²
Weighting parameters a, b	0.1352, 0.0000
Data / restraints / parameters	2746 / 2 / 359
Final R indices [F ² > 2σ]	R1 = 0.0780, wR2 = 0.1981
R indices (all data)	R1 = 0.1376, wR2 = 0.2206
Goodness-of-fit on F ²	0.937
Extinction coefficient	0.0060(14)
Largest and mean shift/su	0.000 and 0.000
Largest diff. peak and hole	0.456 and -0.386 e Å ⁻³

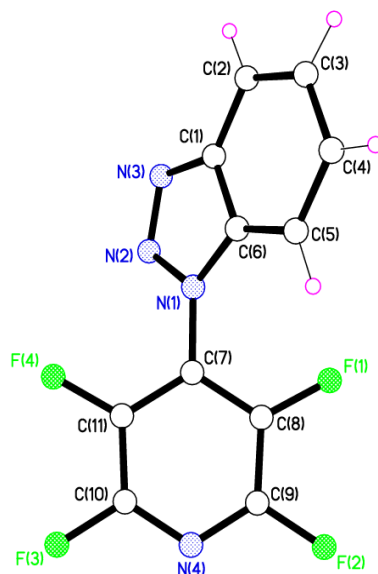
6.1.2. Compound 110 X-ray crystal structure data



Crystal data and structure refinement

Identification code	gw86
Chemical formula	C ₁₉ H ₁₀ F ₃ N ₅
Formula weight	365.32
Temperature	150(2) K
Radiation, wavelength	MoK α , 0.71073 Å
Crystal system, space group	Monoclinic, P2 ₁ /c
Unit cell parameters	a = 12.0121(6) Å α = 90° b = 8.7895(5) Å β = 100.5037(8)° c = 14.8138(8) Å γ = 90°
Cell volume	1537.84(14) Å ³
Z	4
Calculated density	1.578 g/cm ³
Absorption coefficient μ	0.124 mm ⁻¹
F(000)	744
Crystal colour and size	colourless, 0.67 × 0.50 × 0.20 mm ³
Reflections for cell refinement	7716 (θ range 2.71 to 30.56°)
Data collection method	Bruker APEX 2 CCD diffractometer
	ω rotation with narrow frames
θ range for data collection	2.71 to 30.59°
Index ranges	h -17 to 17, k -12 to 12, l -21 to 20
Completeness to θ = 30.59°	99.3 %
Intensity decay	0%
Reflections collected	17691
Independent reflections	4707 (R_{int} = 0.0258)
Reflections with $F^2 > 2\sigma$	3987
Absorption correction	semi-empirical from equivalents
Min. and max.transmission	0.921 and 0.976
Structure solution	direct methods
Refinement method	Full-matrix least-squares on F^2
Weighting parameters a, b	0.0741, 0.3637
Data / restraints / parameters	4707 / 0 / 284
Final R indices [$F^2 > 2\sigma$]	R1 = 0.0415, wR2 = 0.1189
R indices (all data)	R1 = 0.0483, wR2 = 0.1243
Goodness-of-fit on F^2	1.054
Largest and mean shift/su	0.001 and 0.000
Largest diff. peak and hole	0.546 and -0.256 e Å ⁻³

6.1.3. Compound 111 (X isomer) X-ray crystal structure data



Crystal data

$C_{11}H_4F_4N_4$	$F(000) = 536$
$M_r = 268.18$	$D_x = 1.729 \text{ Mg m}^{-3}$
Monoclinic, $P2_1/n$	Mo $K\alpha$ radiation, $\lambda = 0.71073 \text{ \AA}$
$a = 7.4413 (7) \text{ \AA}$	Cell parameters from 6886 reflections
$b = 13.0851 (12) \text{ \AA}$	$\theta = 2.5\text{--}30.6^\circ$
$c = 10.9628 (10) \text{ \AA}$	$\mu = 0.16 \text{ mm}^{-1}$
$\beta = 105.1556 (13)^\circ$	$T = 150 \text{ K}$
$V = 1030.32 (16) \text{ \AA}^3$	Block, colourless
$Z = 4$	$0.89 \times 0.43 \times 0.15 \text{ mm}$

Data collection

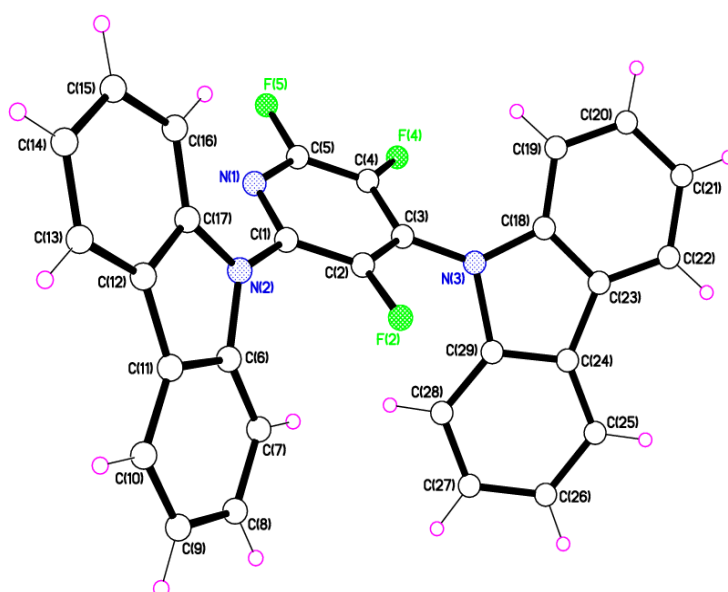
Bruker APEX 2 CCD area detector diffractometer	2817 reflections with $I > 2\sigma(I)$
Radiation source: fine-focus sealed tube	$R_{\text{int}} = 0.027$
ω rotation with narrow frames scans	$\theta_{\text{max}} = 30.6^\circ$, $\theta_{\text{min}} = 2.5^\circ$
Absorption correction: multi-scan SADABS v2012/1, Sheldrick, G.M., (2012)	$h = -10 \rightarrow 10$

$T_{\min} = 0.870, T_{\max} = 0.976$	$k = -18 \rightarrow 18$
12124 measured reflections	$l = -15 \rightarrow 15$
3156 independent reflections	

Refinement

Refinement on F^2	Primary atom site location: structure-invariant direct methods
Least-squares matrix: full	Hydrogen site location: difference Fourier map
$R[F^2 > 2\sigma(F^2)] = 0.038$	All H-atom parameters refined
$wR(F^2) = 0.115$	$w = 1/[\sigma^2(F_o^2) + (0.0686P)^2 + 0.2212P]$ where $P = (F_o^2 + 2F_c^2)/3$
$S = 1.04$	$(\Delta/\sigma)_{\max} < 0.001$
3156 reflections	$\Delta_{\max} = 0.41 \text{ e } \text{\AA}^{-3}$
188 parameters	$\Delta_{\min} = -0.24 \text{ e } \text{\AA}^{-3}$
0 restraints	

6.1.4. Compound 114 X-ray crystal structure data



Crystal data

$C_{29.02}H_{16.02}F_3N_3O_0$	$D_x = 1.392 \text{ Mg m}^{-3}$
$M_r = 463.77$	Mo $K\alpha$ radiation, $\lambda = 0.71073 \text{ \AA}$
Orthorhombic, $P2_12_12_1$	Cell parameters from 4470 reflections
$a = 8.1301 (5) \text{ \AA}$	$\theta = 2.2\text{--}22.0^\circ$
$b = 18.1470 (12) \text{ \AA}$	$\mu = 0.10 \text{ mm}^{-1}$
$c = 29.9929 (19) \text{ \AA}$	$T = 150 \text{ K}$
$V = 4425.1 (5) \text{ \AA}^3$	Plate, colourless
$Z = 8$	$0.40 \times 0.21 \times 0.05 \text{ mm}^3$
$F(000) = 1905$	

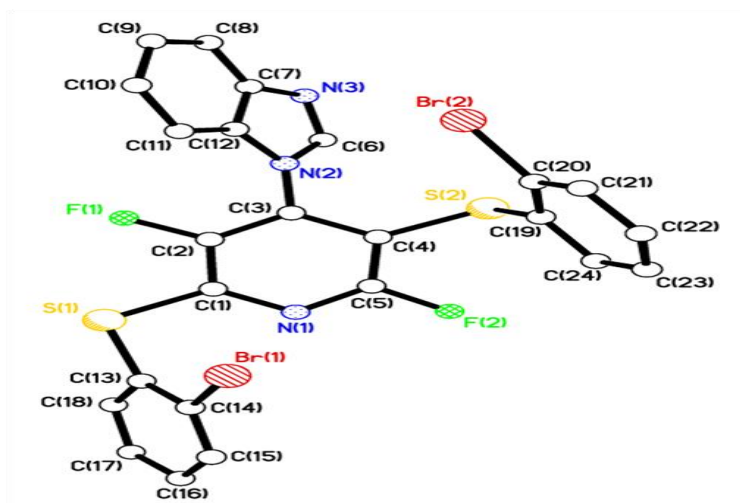
Data collection

Bruker APEX 2 CCD diffractometer	9768 independent reflections
Radiation source: fine-focus sealed tube	6291 reflections with $I > 2\sigma(I)$
Graphite monochromator	$R_{\text{int}} = 0.057$
ω rotation with narrow frames scans	$\theta_{\text{max}} = 27.1^\circ$, $\theta_{\text{min}} = 1.8^\circ$
Absorption correction: multi-scan <i>SADABS</i> v2012/1, Sheldrick, G.M., (2012)	$h = -10 \rightarrow 9$
$T_{\text{min}} = 0.961$, $T_{\text{max}} = 0.995$	$k = -23 \rightarrow 23$
30333 measured reflections	$l = -38 \rightarrow 36$

Refinement

Refinement on F^2	Secondary atom site location: difference Fourier map
Least-squares matrix: full	Hydrogen site location: inferred from neighbouring sites
$R[F^2 > 2\sigma(F^2)] = 0.045$	H-atom parameters constrained
$wR(F^2) = 0.089$	$w = 1/[\sigma^2(F_o^2) + (0.0303P)^2]$ where $P = (F_o^2 + 2F_c^2)/3$
$S = 1.00$	$(\Delta/\sigma)_{\max} = 0.001$
9768 reflections	$\Delta_{\max} = 0.15 \text{ e } \text{\AA}^{-3}$
760 parameters	$\Delta_{\min} = -0.15 \text{ e } \text{\AA}^{-3}$
546 restraints	Absolute structure: Flack x determined using 2058 quotients [[I+)-(I-)]/[(I+)+(I-)] (Parsons, Flack and Wagner, Acta Cryst. B69 (2013) 249-259).
Primary atom site location: dual	Absolute structure parameter: 0.5 (4)

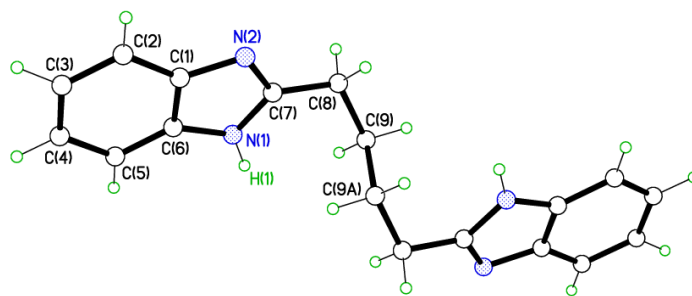
6.1.5. Compound 126 Xray crystal structure data



Crystal data and structure refinement

Identification code	gw83	
Chemical formula	$C_{24}H_{13}Br_2F_2N_3S_2$	
Formula weight	605.31	
Temperature	150(2) K	
Radiation, wavelength	MoK α , 0.71073 Å	
Crystal system, space group	triclinic, P $\bar{1}$	
Unit cell parameters	a = 8.2633(9) Å	$\alpha = 73.7151(15)^\circ$
	b = 10.5751(11) Å	$\beta = 78.7097(16)^\circ$
	c = 13.8671(14) Å	$\gamma = 70.2669(15)^\circ$
Cell volume	1088.0(2) Å ³	
Z	2	
Calculated density	1.848 g/cm ³	
Absorption coefficient μ	3.954 mm ⁻¹	
F(000)	596	
Crystal colour and size	colourless, 0.37 × 0.29 × 0.06 mm ³	
Reflections for cell refinement	4741 (θ range 2.30 to 28.42°)	
Data collection method	Bruker APEX 2 CCD diffractometer	
	ω rotation with narrow frames	
θ range for data collection	1.54 to 30.55°	
Index ranges	h -11 to 11, k -15 to 14, l -19 to 19	
Completeness to $\theta = 29.00^\circ$	99.5 %	
Intensity decay	0%	
Reflections collected	17054	
Independent reflections	6544 ($R_{int} = 0.0366$)	
Reflections with $F^2 > 2\sigma$	4835	
Absorption correction	semi-empirical from equivalents	
Min. and max.transmission	0.3224 and 0.797	
Structure solution	direct methods	
Refinement method	Full-matrix least-squares on F^2	
Weighting parameters a, b	0.0520, 1.3591	
Data / restraints / parameters	6544 / 0 / 298	
Final R indices [$F^2 > 2\sigma$]	R1 = 0.0421, wR2 = 0.1024	
R indices (all data)	R1 = 0.0660, wR2 = 0.1129	
Goodness-of-fit on F^2	1.032	
Largest and mean shift/su	0.001 and 0.000	
Largest diff. peak and hole	1.985 and -0.886 e Å ⁻³	

6.1.6. Compound 134 X-ray crystal structure data



Crystal data

$C_{18}H_{18}N_4$	$D_x = 1.324 \text{ Mg m}^{-3}$
$M_r = 290.36$	Mo $K\alpha$ radiation, $\lambda = 0.71073 \text{ \AA}$
Orthorhombic, $Pbca$	Cell parameters from 3582 reflections
$a = 8.788 (3) \text{ \AA}$	$\theta = 2.3\text{--}30.5^\circ$
$b = 9.340 (3) \text{ \AA}$	$\mu = 0.08 \text{ mm}^{-1}$
$c = 17.743 (5) \text{ \AA}$	$T = 150 \text{ K}$
$V = 1456.3 (8) \text{ \AA}^3$	Lath, colourless
$Z = 4$	$1.13 \times 0.23 \times 0.15 \text{ mm}$
$F(000) = 616$	

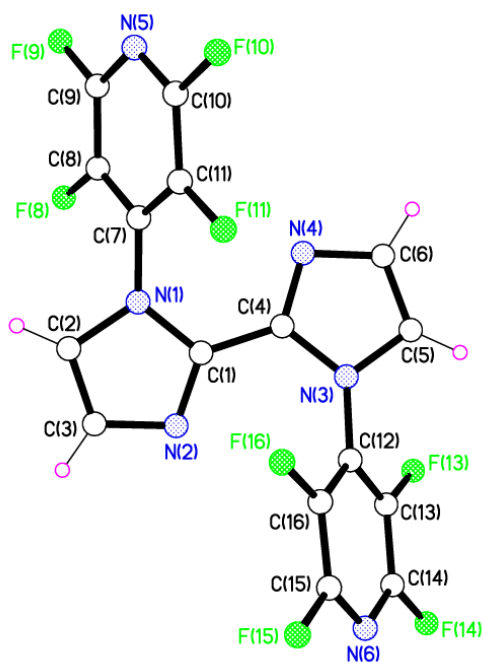
Data collection

Bruker APEX 2 CCD diffractometer	1773 reflections $\omega\tau\eta$ $I > 2\sigma(I)$
Radiation source: fine-focus sealed tube	$R_{\text{int}} = 0.047$
ω rotation with narrow frames scans	$\theta_{\text{max}} = 30.6^\circ$, $\theta_{\text{min}} = 2.3^\circ$
Absorption correction: multi-scan SADABS v2012/1, Sheldrick, G.M., (2012)	$h = -12 \rightarrow 12$
$T_{\text{min}} = 0.914$, $T_{\text{max}} = 0.988$	$\kappa = -13 \rightarrow 13$
15966 measured reflections	$\lambda = -25 \rightarrow 25$
2226 independent reflections	

Refinement data

Refinement on F^2	Primary atom site location: structure-invariant direct methods
Least-squares matrix: full	Hydrogen site location: difference Fourier map
$R[F^2 > 2\sigma(F^2)] = 0.042$	All H-atom parameters refined
$wR(F^2) = 0.115$	$w = 1/[\sigma^2(F_o^2) + (0.0566P)^2 + 0.3564P]$ where $P = (F_o^2 + 2F_c^2)/3$
$S = 1.05$	$(\Delta/\sigma)_{\max} < 0.001$
2226 reflections	$\Delta_{\mu\alpha\xi} = 0.34 \text{ \AA} \oplus^{-3}$
136 parameters	$\Delta_{\mu\nu\nu} = -0.21 \text{ \AA} \oplus^{-3}$
0 restraints	

6.1.7. Compound 137 X-ray crystal structure data



Crystal data

$C_{16}H_4F_8N_6$	$F(000) = 856$
$M_r = 432.25$	$D_x = 1.809 \text{ Mg m}^{-3}$
Monoclinic, $P2_1/c$	Mo $K\alpha$ radiation, $\lambda = 0.71073 \text{ \AA}$
$a = 7.4893 (7) \text{ \AA}$	Cell parameters from 7665 reflections
$b = 20.898 (2) \text{ \AA}$	$\theta = 2.2\text{--}30.5^\circ$
$c = 10.2489 (10) \text{ \AA}$	$\mu = 0.18 \text{ mm}^{-1}$
$\beta = 98.348 (2)^\circ$	$T = 150 \text{ K}$
$V = 1587.1 (3) \text{ \AA}^3$	Rod, colourless
$Z = 4$	$0.80 \times 0.23 \times 0.21 \text{ mm}$

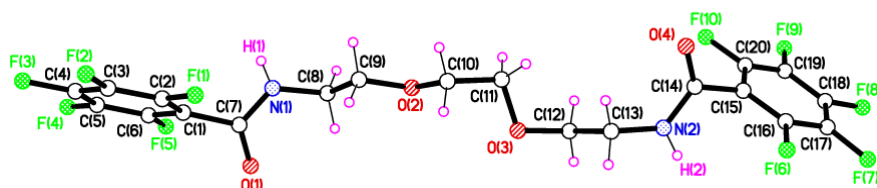
Data collection

Bruker APEX 2 CCD diffractometer	4039 reflections with $I > 2\sigma(I)$
Radiation source: fine-focus sealed tube	$R_{\text{int}} = 0.025$
ω rotation with narrow frames scans	$\theta_{\text{max}} = 30.6^\circ$, $\theta_{\text{min}} = 2.0^\circ$
Absorption correction: multi-scan SADABS v2009/1, Sheldrick, G.M., (2009)	$h = -10 \rightarrow 10$
$T_{\text{min}} = 0.869$, $T_{\text{max}} = 0.963$	$k = -29 \rightarrow 29$
18321 measured reflections	$l = -14 \rightarrow 14$
4813 independent reflections	

Refinement

Refinement on F^2	Primary atom site location: structure-invariant direct methods
Least-squares matrix: full	Secondary atom site location: all non-H atoms found by direct methods
$R[F^2 > 2\sigma(F^2)] = 0.037$	Hydrogen site location: difference Fourier map
$wR(F^2) = 0.104$	All H-atom parameters refined
$S = 1.04$	$w = 1/[\sigma^2(F_o^2) + (0.051P)^2 + 0.488P]$ where $P = (F_o^2 + 2F_c^2)/3$
4813 reflections	$(\Delta/\sigma)_{\max} = 0.001$
287 parameters	$\Delta_{\max} = 0.37 \text{ e } \text{\AA}^{-3}$
0 restraints	$\Delta_{\min} = -0.22 \text{ e } \text{\AA}^{-3}$

6.1.8. Compound 151 Xray crystal structure data



Crystal data

$C_{20}H_{14}F_{10}N_2O_4$	$F(000) = 3240$
$M_r = 536.33$	$D_x = 1.696 \text{ Mg m}^{-3}$
Monoclinic, $P2_1/c$	Synchrotron radiation, $\lambda = 0.7749 \text{ \AA}$
$a = 17.4161 (6) \text{ \AA}$	Cell parameters from 9918 reflections
$b = 14.3221 (5) \text{ \AA}$	$\theta = 2.3\text{--}25.1^\circ$
$c = 25.7502 (9) \text{ \AA}$	$\mu = 0.17 \text{ mm}^{-1}$
$\beta = 101.207 (2)^\circ$	$T = 150 \text{ K}$
$V = 6300.5 (4) \text{ \AA}^3$	Plate, colourless
$Z = 12$	$0.05 \times 0.03 \times 0.01 \text{ mm}^3$

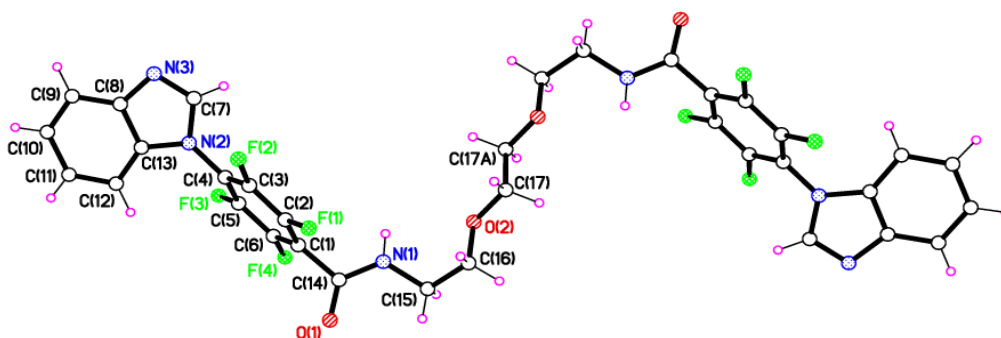
Data collection

Bruker D8 with PHOTON 100 detector diffractometer	9083 independent reflections
Radiation source: Advanced Light Station 11.3.1	6863 reflections with $I > 2\sigma(I)$
Silicon 111 monochromator	$R_{\text{int}} = 0.056$
Detector resolution: $10.42 \text{ pixels mm}^{-1}$	$\theta_{\text{max}} = 25.6^\circ$, $\theta_{\text{min}} = 2.1^\circ$
ω rotation with shutterless scans	$h = -19 \rightarrow 19$
Absorption correction: multi-scan SADABS v2012/1, Sheldrick, G.M., (2012)	$k = -15 \rightarrow 15$
$T_{\text{min}} = 0.992$, $T_{\text{max}} = 0.998$	$l = -28 \rightarrow 28$
44141 measured reflections	

Refinement

Refinement on F^2	Primary atom site location: iterative
Least-squares matrix: full	Secondary atom site location: difference Fourier map
$R[F^2 > 2\sigma(F^2)] = 0.055$	Hydrogen site location: mixed
$wR(F^2) = 0.142$	H atoms treated by a mixture of independent and constrained refinement
$S = 1.09$	$w = 1/[\sigma^2(F_o^2) + (0.0421P)^2 + 15.2253P]$ where $P = (F_o^2 + 2F_c^2)/3$
9083 reflections	$(\Delta/\sigma)_{\text{max}} < 0.001$
991 parameters	$\Delta_{\text{max}} = 0.83 \text{ e } \text{\AA}^{-3}$
0 restraints	$\Delta_{\text{min}} = -0.32 \text{ e } \text{\AA}^{-3}$

6.1.9. Compound 152 X-ray crystal structure data



Crystal data

$C_{34}H_{24}F_8N_6O_4$	$F(000) = 748$
$M_r = 732.59$	$D_x = 1.517 \text{ Mg m}^{-3}$
Monoclinic, $P2_1/n$	Synchrotron radiation, $\lambda = 0.7749 \text{ \AA}$
$a = 12.7854 (5) \text{ \AA}$	Cell parameters from 9938 reflections
$b = 8.9381 (4) \text{ \AA}$	$\theta = 2.5\text{--}33.6^\circ$
$c = 14.1393 (5) \text{ \AA}$	$\mu = 0.12 \text{ mm}^{-1}$
$\beta = 96.872 (2)^\circ$	$T = 150 \text{ K}$
$V = 1604.19 (11) \text{ \AA}^3$	Plate, colourless
$Z = 2$	$0.35 \times 0.18 \times 0.02 \text{ mm}^3$

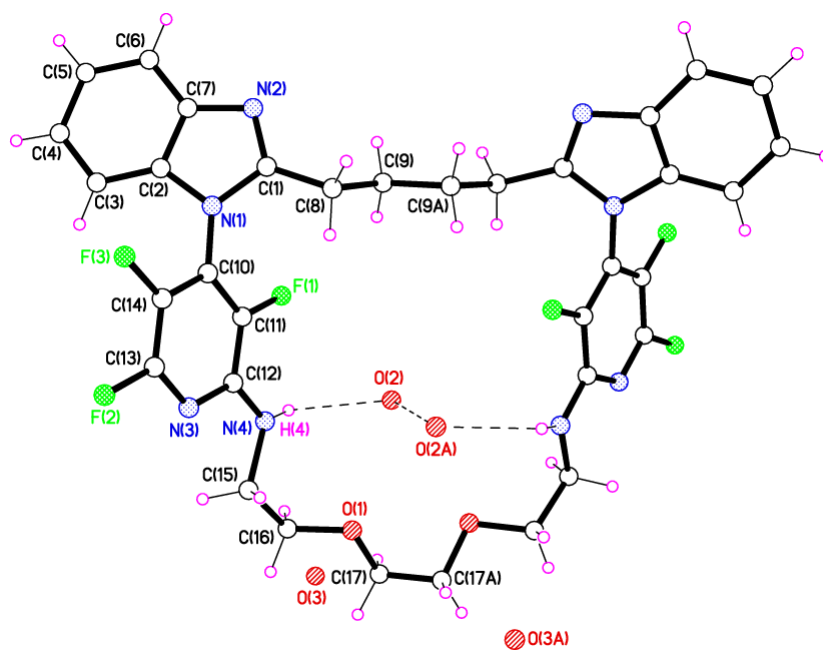
Data collection

Bruker D8 with PHOTON 100 detector diffractometer	4910 independent reflections
Radiation source: Advanced Light Station 11.3.1	3877 reflections with $I > 2\sigma(I)$
Silicon 111 monochromator	$R_{\text{int}} = 0.030$
ω rotation with shutterless scans	$\theta_{\text{max}} = 33.7^\circ$, $\theta_{\text{min}} = 2.2^\circ$
Absorption correction: multi-scan <i>SADABS</i> v2012/1, Sheldrick, G.M., (2012)	$h = -18 \rightarrow 18$
$T_{\text{min}} = 0.959$, $T_{\text{max}} = 0.998$	$k = -12 \rightarrow 12$
20949 measured reflections	$l = -20 \rightarrow 20$

Refinement

Refinement on F^2	Primary atom site location: interative
Least-squares matrix: full	Secondary atom site location: difference Fourier map
$R[F^2 > 2\sigma(F^2)] = 0.043$	Hydrogen site location: mixed
$wR(F^2) = 0.121$	H atoms treated by a mixture of independent and constrained refinement
$S = 1.07$	$w = 1/[\sigma^2(F_o^2) + (0.058P)^2 + 0.4702P]$ where $P = (F_o^2 + 2F_c^2)/3$
4910 reflections	$(\Delta/\sigma)_{\max} < 0.001$
239 parameters	$\Delta_{\max} = 0.41 \text{ e } \text{\AA}^{-3}$
0 restraints	$\Delta_{\min} = -0.20 \text{ e } \text{\AA}^{-3}$

6.1.10. Compound 181 X-ray crystal structure data



Crystal data

$C_{34}H_{30}F_6N_8O_2 \cdot 2.5(H_2O)$	$D_x = 1.478 \text{ Mg m}^{-3}$
$M_r = 741.70$	Synchrotron radiation, $\lambda = 0.7749 \text{ \AA}$
Orthorhombic, $P2_12_12$	Cell parameters from 5058 reflections
$a = 22.3299 (9) \text{ \AA}$	$\theta = 2.7\text{--}29.5^\circ$
$b = 6.0739 (3) \text{ \AA}$	$\mu = 0.15 \text{ mm}^{-1}$
$c = 12.2892 (5) \text{ \AA}$	$T = 100 \text{ K}$
$V = 1666.78 (13) \text{ \AA}^3$	Lath, colourless
$Z = 2$	$0.10 \times 0.03 \times 0.02 \text{ mm}^3$
$F(000) = 770$	

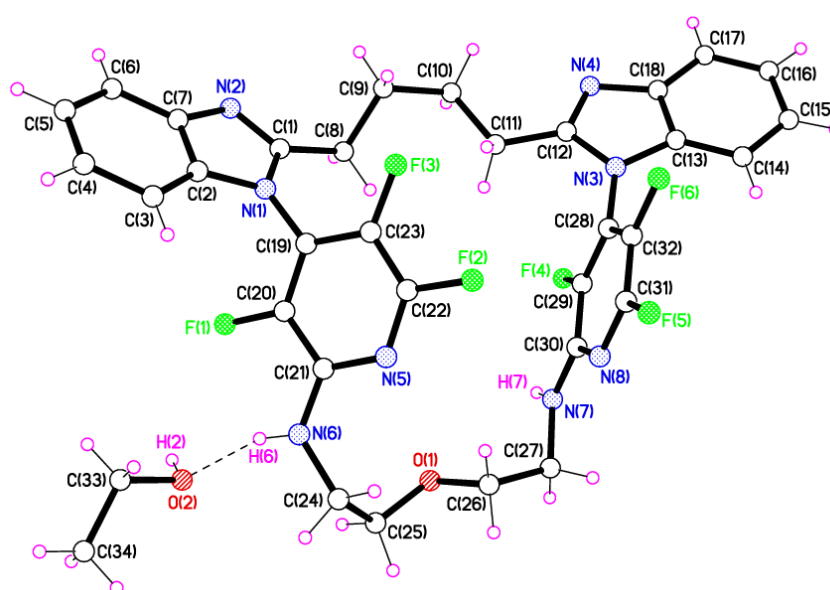
Data collection

Bruker APEX 2 CCD area detector diffractometer	3344 reflections with $I > 2\sigma(I)$
Radiation source: ALS Station 11.3.1	$R_{\text{int}} = 0.068$
ω & ϕ rotation with narrow frames scans	$\theta_{\text{max}} = 30.8^\circ$, $\theta_{\text{min}} = 2.7^\circ$
Absorption correction: multi-scan <i>SADABS</i> v2012/1, Sheldrick, G.M., (2012)	$h = -29 \rightarrow 29$
$T_{\text{min}} = 0.985$, $T_{\text{max}} = 0.997$	$k = -8 \rightarrow 8$
16401 measured reflections	$l = -16 \rightarrow 16$
4015 independent reflections	

Refinement

Refinement on F^2	Hydrogen site location: inferred from neighbouring sites
Least-squares matrix: full	H-atom parameters constrained
$R[F^2 > 2\sigma(F^2)] = 0.053$	$w = 1/[\sigma^2(F_o^2) + (0.0652P)^2 + 0.4696P]$ where $P = (F_o^2 + 2F_c^2)/3$
$wR(F^2) = 0.140$	$(\Delta/\sigma)_{\max} < 0.001$
$S = 1.05$	$\Delta_{\max} = 0.29 \text{ e } \text{\AA}^{-3}$
4015 reflections	$\Delta_{\min} = -0.38 \text{ e } \text{\AA}^{-3}$
278 parameters	Extinction correction: <i>SHELXL</i> , $F_c^* = kFc[1+0.001xFc^2\lambda^3/\sin(2\theta)]^{-1/4}$
49 restraints	Extinction coefficient: 0.015 (3)
Primary atom site location: intrinsic phasing	Absolute structure: Flack x determined using 1238 quotients $[(I+)-(I-)]/[(I+)+(I-)]$ (Parsons, Flack and Wagner, <i>Acta Cryst. B</i> 69 (2013) 249-259).
Secondary atom site location: difference Fourier map	Absolute structure parameter: 0.4 (5)

6.1.11. Compound 183 X-ray crystal structure data



Crystal data

$C_{32}H_{26}F_6N_8O \cdot C_2H_6O$	$F(000) = 2896$
$M_r = 698.67$	$D_x = 1.436 \text{ Mg m}^{-3}$
Monoclinic, $C2/c$	Mo $K\alpha$ radiation, $\lambda = 0.71073 \text{ \AA}$
$a = 14.1373 (7) \text{ \AA}$	Cell parameters from 7141 reflections
$b = 17.2114 (8) \text{ \AA}$	$\theta = 2.2\text{--}27.7^\circ$
$c = 27.3518 (13) \text{ \AA}$	$\mu = 0.12 \text{ mm}^{-1}$
$\beta = 103.7199 (8)^\circ$	$T = 150 \text{ K}$
$V = 6465.4 (5) \text{ \AA}^3$	Tablet, colourless
$Z = 8$	$0.25 \times 0.18 \times 0.07 \text{ mm}^3$

Data collection

Bruker APEX 2 CCD area detector diffractometer	5498 reflections with $I > 2\sigma(I)$
Radiation source: fine-focus sealed tube	$R_{\text{int}} = 0.047$
ω rotation with narrow frames scans	$\theta_{\text{max}} = 28.3^\circ$, $\theta_{\text{min}} = 1.9^\circ$
Absorption correction: multi-scan <i>SADABS</i> v2012/1, Sheldrick, G.M., (2012)	$h = -18 \rightarrow 18$
$T_{\text{min}} = 0.971$, $T_{\text{max}} = 0.992$	$k = -22 \rightarrow 22$
33520 measured reflections	$l = -36 \rightarrow 36$
8064 independent reflections	

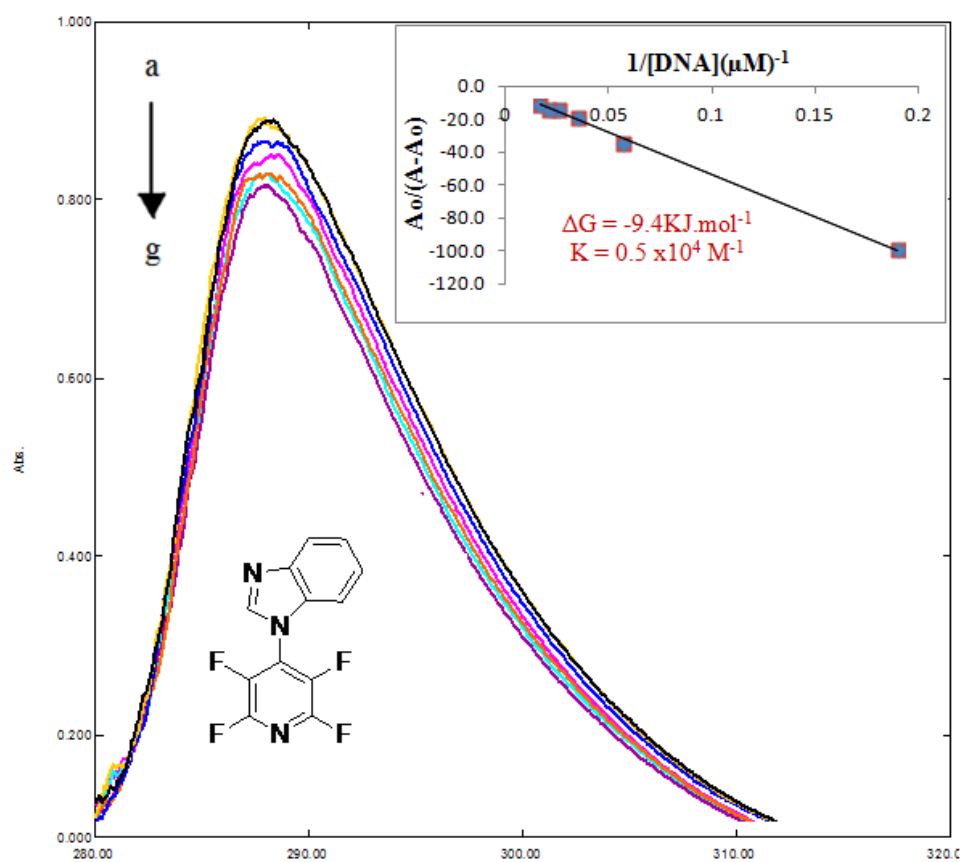
Refinement

Refinement on F^2	Primary atom site location: structure-invariant direct methods
Least-squares matrix: full	Hydrogen site location: mixed
$R[F^2 > 2\sigma(F^2)] = 0.042$	H atoms treated by a mixture of independent and constrained refinement
$wR(F^2) = 0.101$	$w = 1/[\sigma^2(F_o^2) + (0.0375P)^2 + 2.548P]$ where $P = (F_o^2 + 2F_c^2)/3$
$S = 1.03$	$(\Delta/\sigma)_{\max} = 0.001$
8064 reflections	$\Delta_{\max} = 0.24 \text{ e } \text{\AA}^{-3}$
477 parameters	$\Delta_{\min} = -0.21 \text{ e } \text{\AA}^{-3}$
15 restraints	

6.2. UV-Visible spectroscopy data

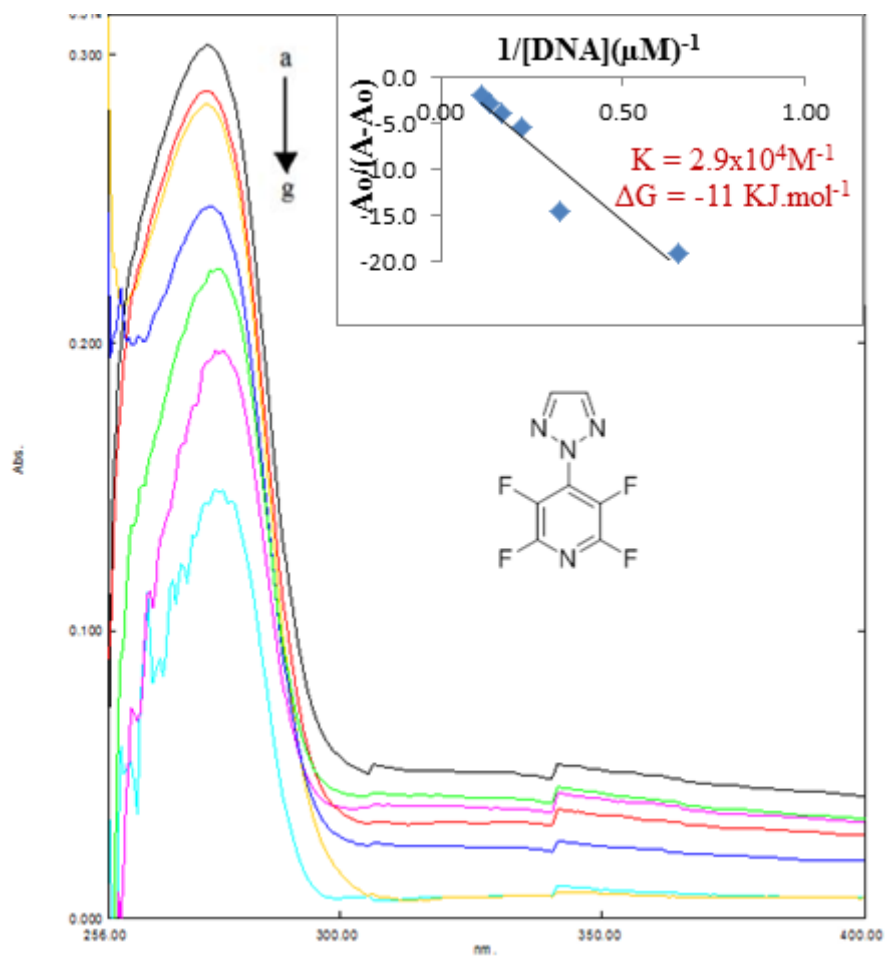
The spectra showed the absorbance of the of synthesis compounds in absence (a) and presence of 5.2 μM (b), 18 μM (c), 28 μM (d), 39 μM (e), 48 μM (f) and 57 μM (g) of DNA. The arrow shows increasing of DNA concentration. Inside graph is plot of $A_0/(A-A_0)$ vs. $1/[\text{DNA}]$ for determination K and ΔG values.

6.2.1. UV-visible spectroscopy of compound 108



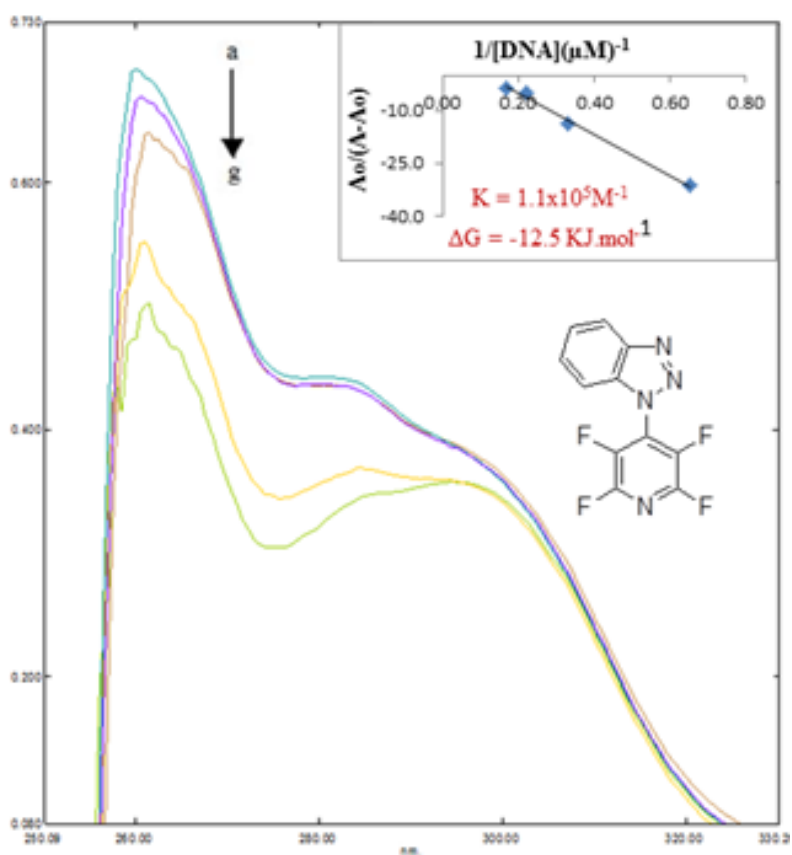
Absorption spectra of $1 \times 10^{-5} \text{ M}$ of compound 108 ($R^2 = 0.9976$ for six points)

6.2.2. UV-visible spectroscopy of compound 111



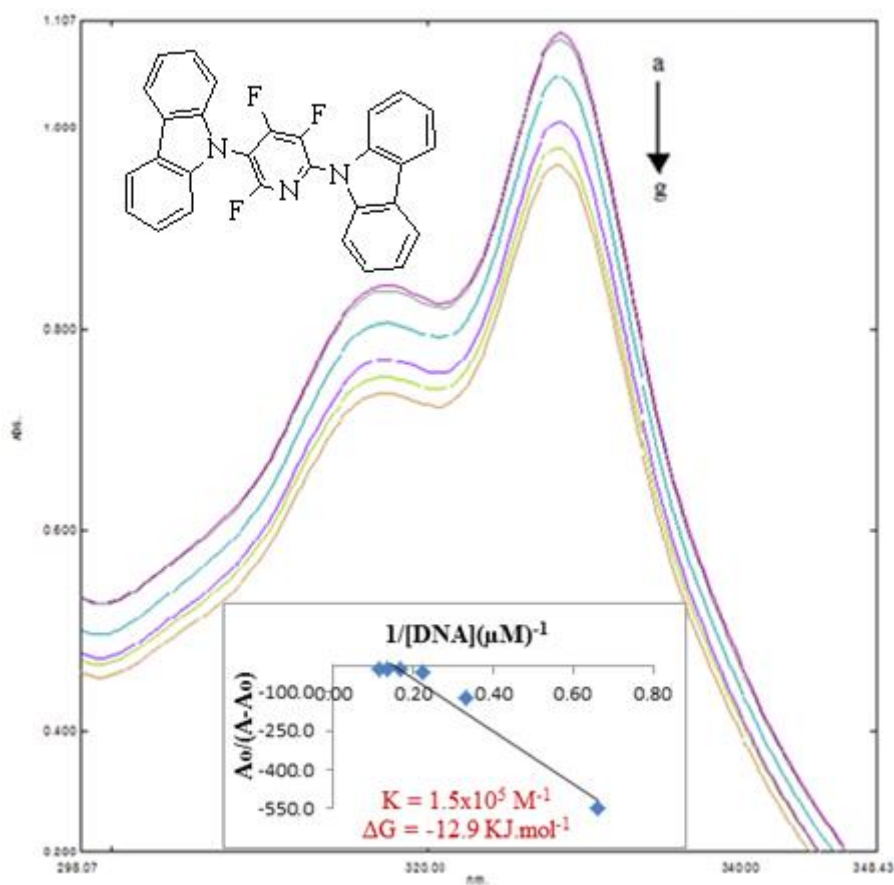
Absorption spectra of $9 \times 10^{-5} \text{ M}$ of compound 112. ($R^2 = 0.9529$ for six points)

6.2.3. UV-visible spectroscopy of compound 113



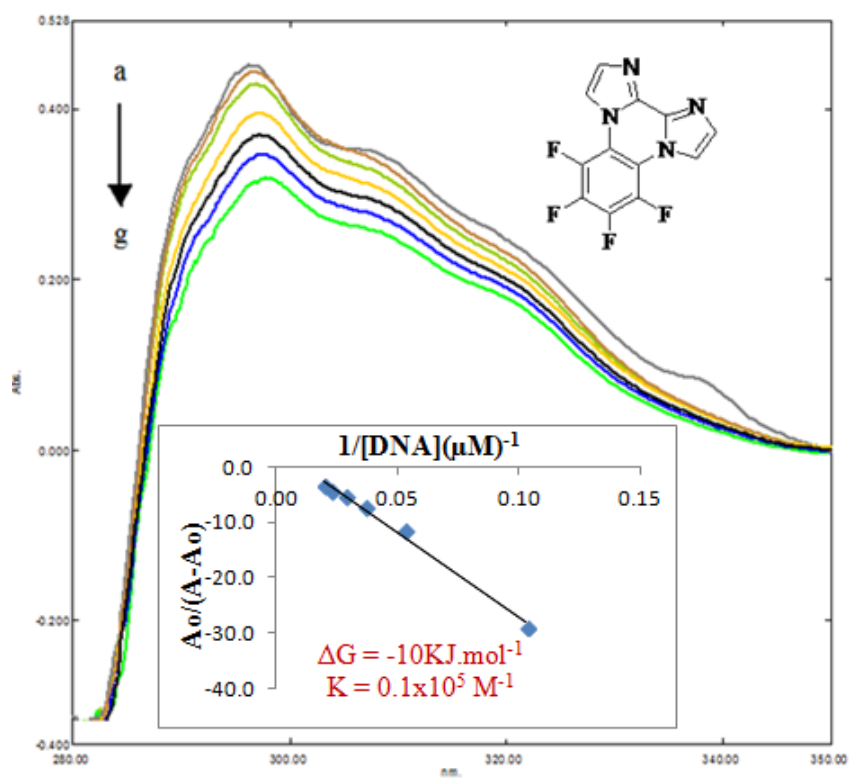
Absorption spectra of 2×10^{-5} M of compound 113. ($R^2 = 0.9940$ for six points)

6.2.4. UV-visible spectroscopy of compound 114



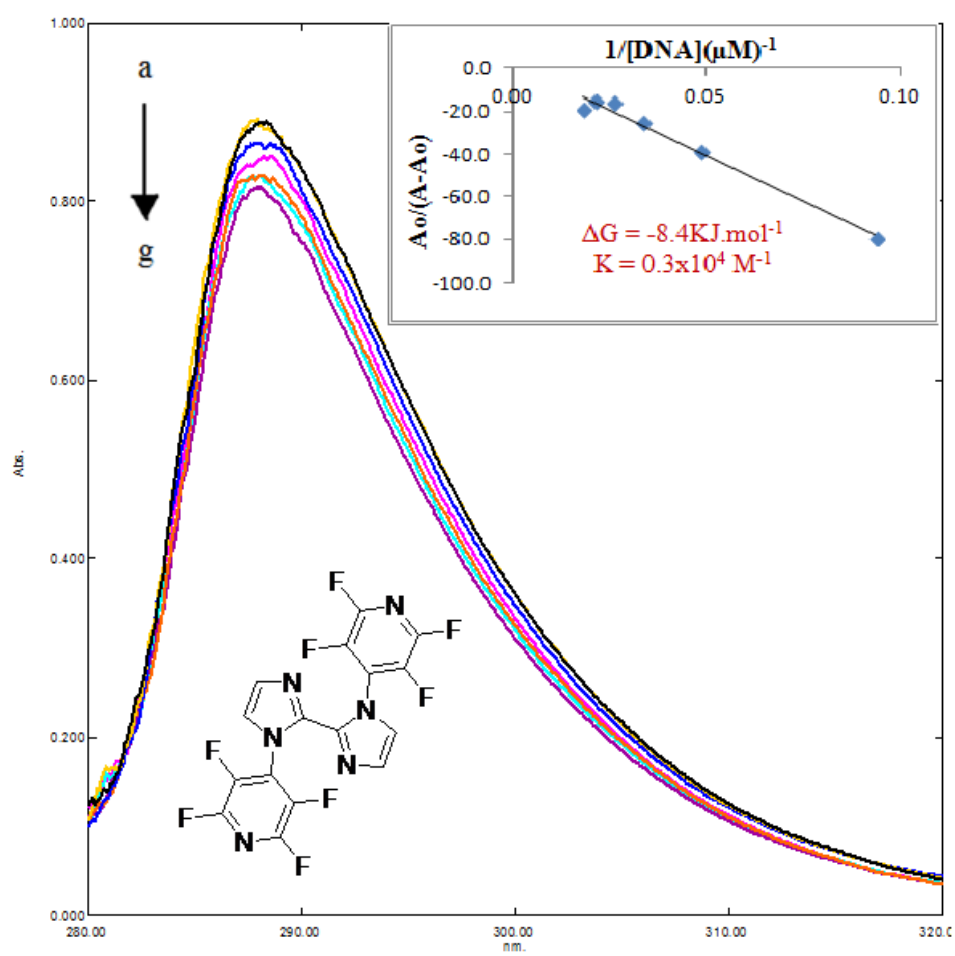
Absorption spectra of $3.8 \times 10^{-5} \text{ M}$ of compound 114. ($R^2 = 0.9563$ for six points)

6.2.5. UV-visible spectroscopy of compound 137



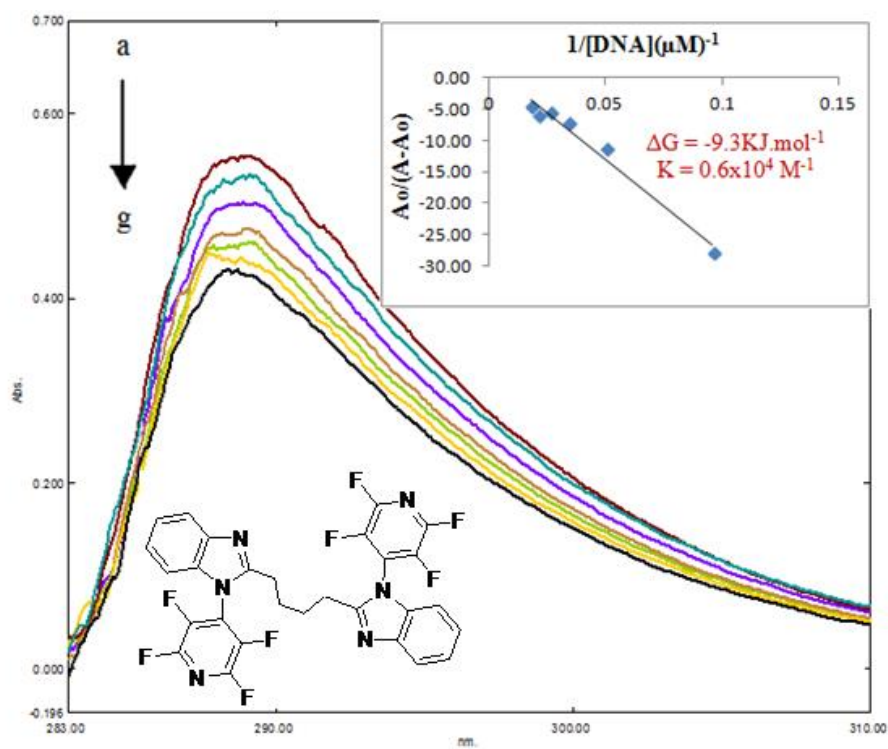
Absorption spectra of $1 \times 10^{-5} \text{ M}$ of compound 137 ($R^2 = 0.9912$ for six points)

6.2.6. UV-visible spectroscopy of compound 138



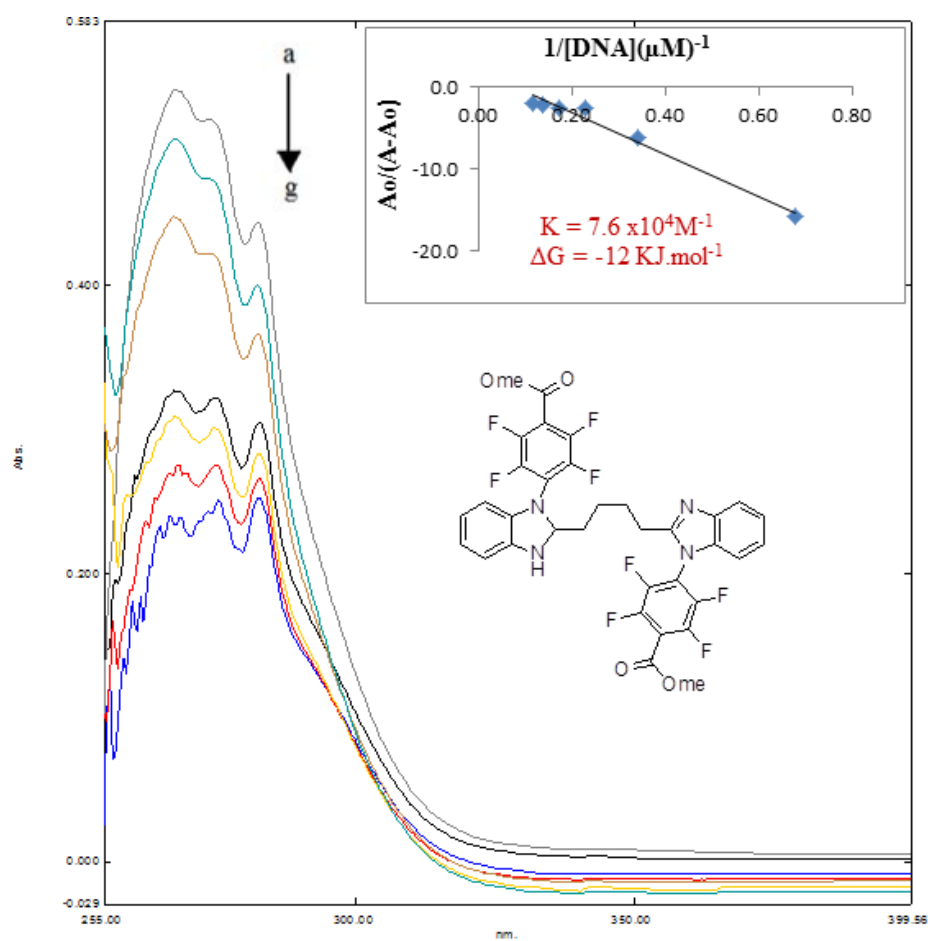
Absorption spectra of $1 \times 10^{-5} \text{ M}$ of compound 138 ($R^2 = 0.9826$ for six points)

6.2.7. UV-visible spectroscopy of compound 143



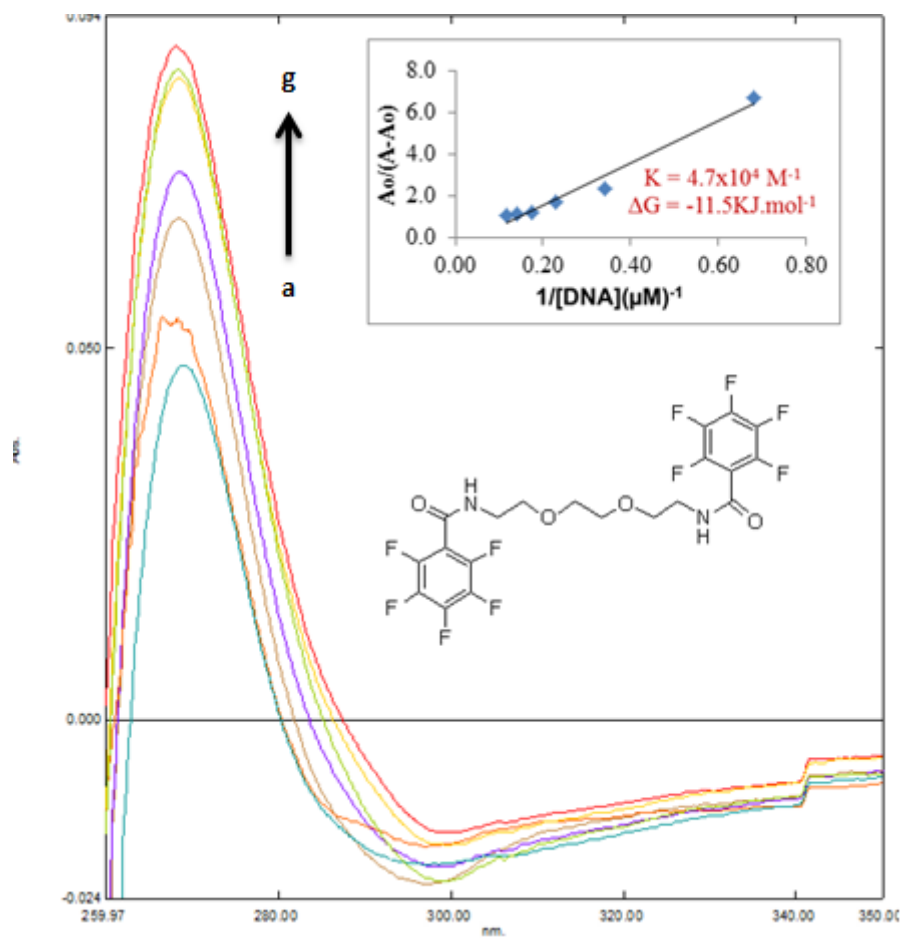
Absorption spectra of $1 \times 10^{-5} \text{ M}$ of compound 143. ($R^2 = 0.9744$ for six points)

6.2.8. UV-visible spectroscopy of compound 148



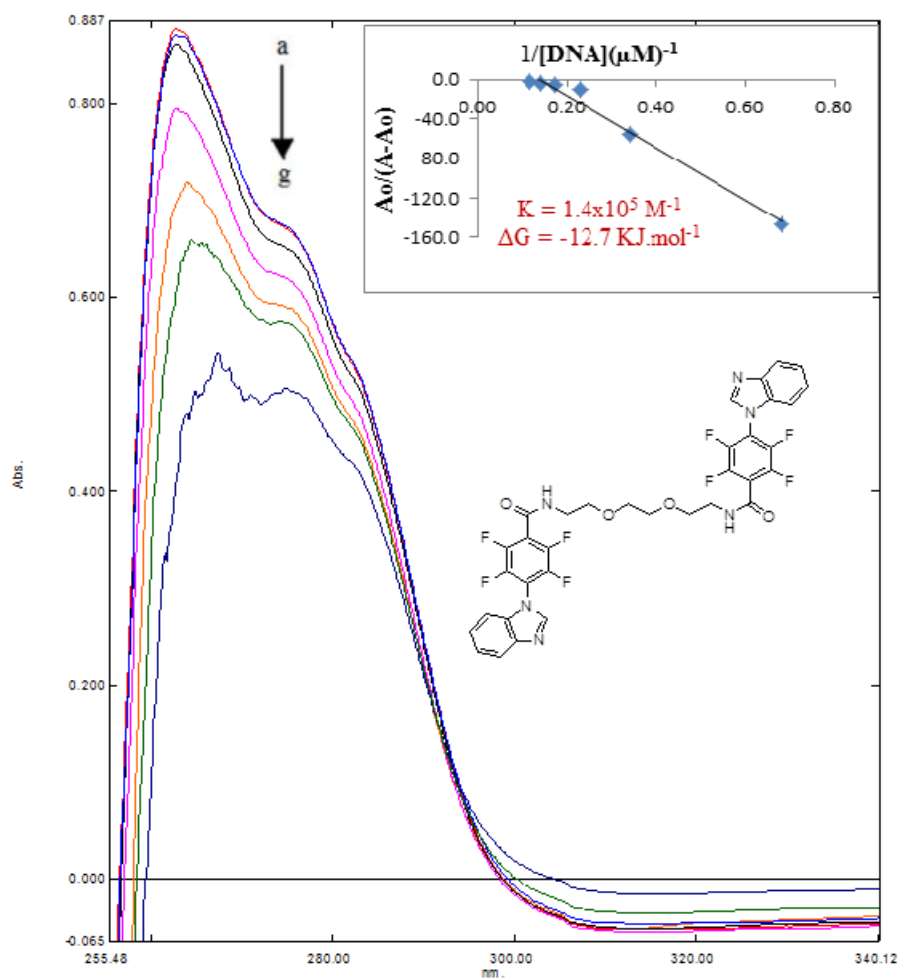
Absorption spectra of $3.8 \times 10^{-5} \text{ M}$ of compound 148. ($R^2=0.9785$ for six points)

6.2.9. UV-visible spectroscopy of compound 151



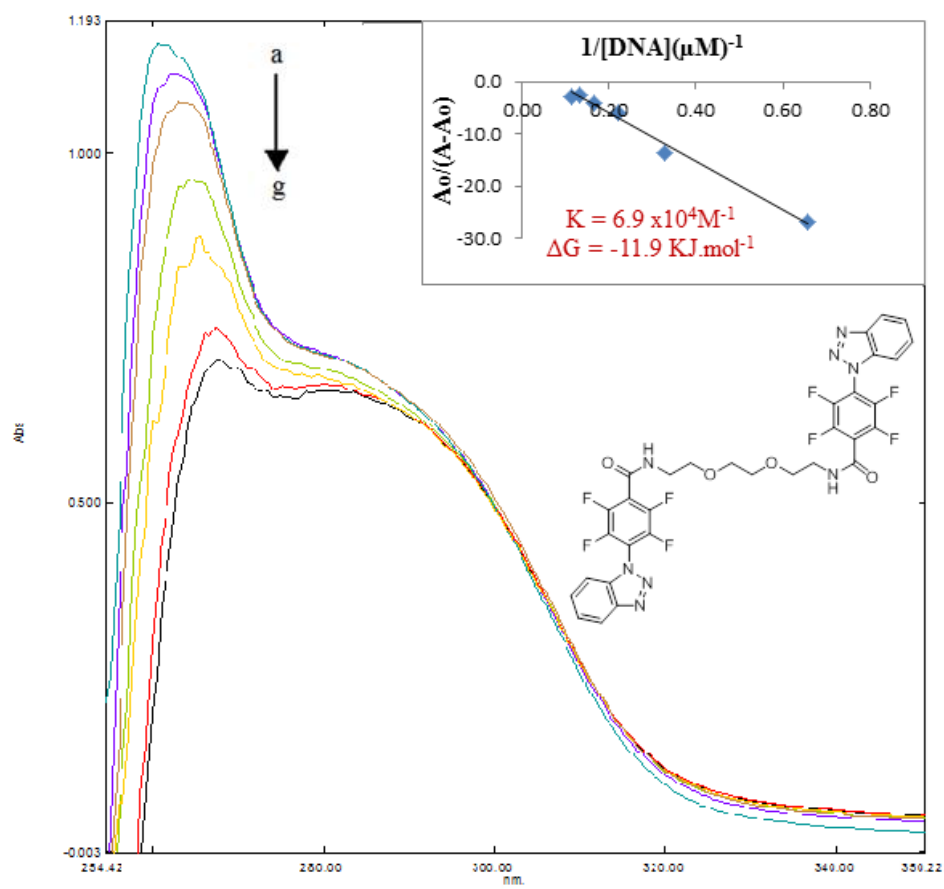
Absorption spectra of $6.5 \times 10^{-5} M$ of compound 151. ($R^2 = 0.971$ for six points)

6.2.10. UV-visible spectroscopy of compound 152



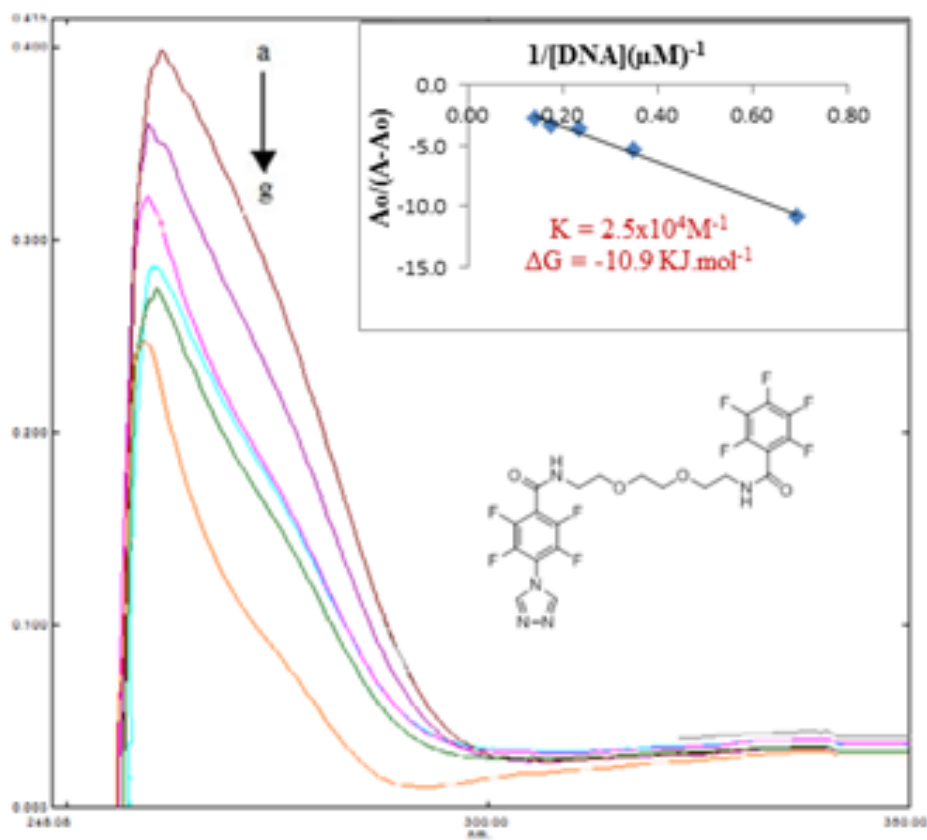
Absorption spectra of $3.8 \times 10^{-5} M$ of compound 152 ($R^2 = 0.9824$ for six points)

6.2.11. UV-visible spectroscopy of compound 161



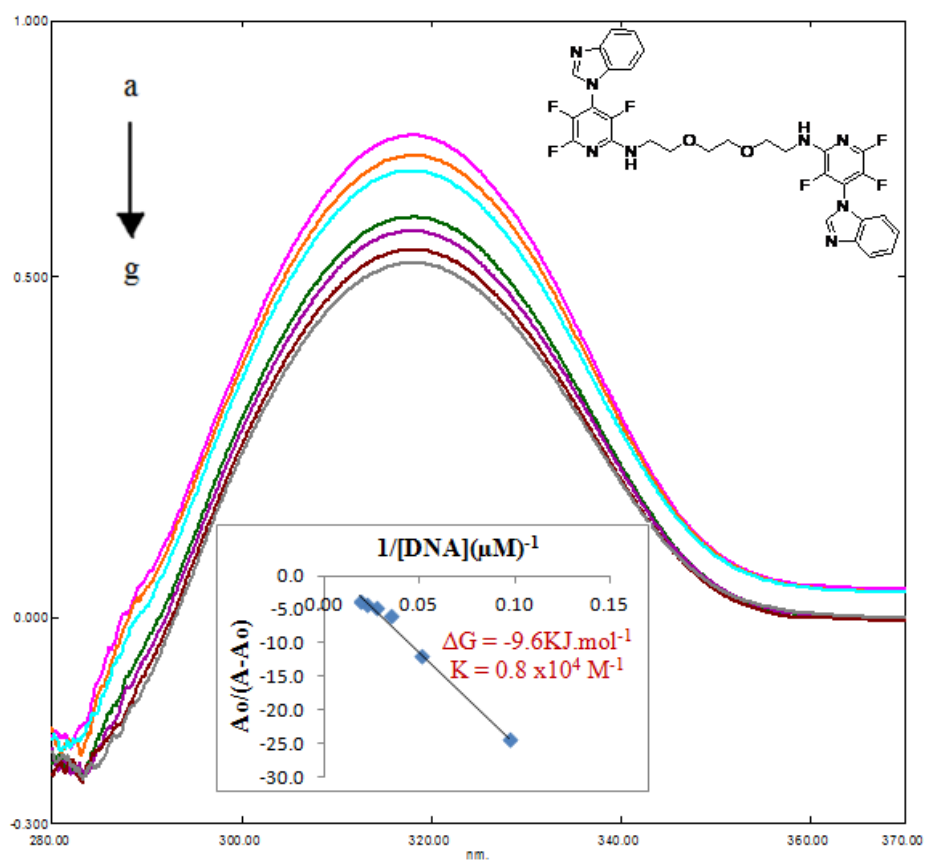
Absorption spectra of $3.8 \times 10^{-5} \text{M}$ of compound 161. ($R^2 = 0.9886$ for six points)

6.2.12. UV-visible spectroscopy of compound 162



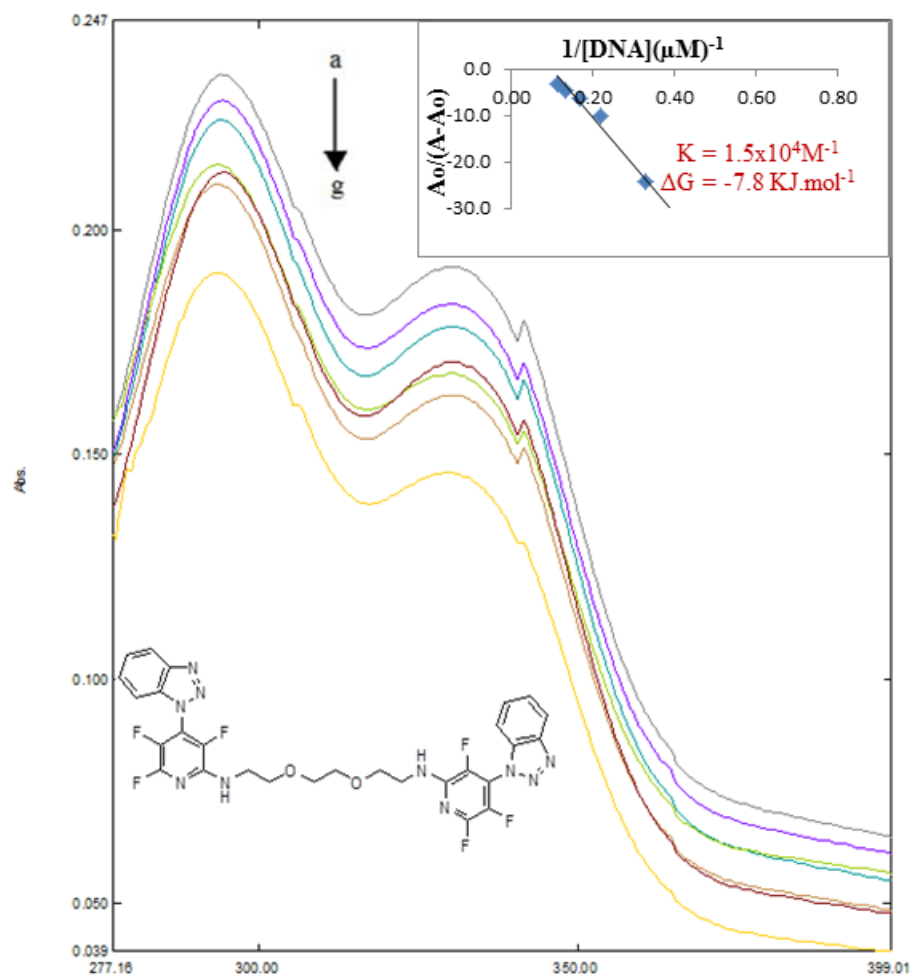
Absorption spectra of $9 \times 10^{-5} \text{ M}$ of compound 162 ($R^2 = 0.9951$ for six points)

6.2.13. UV-visible spectroscopy of compound 163



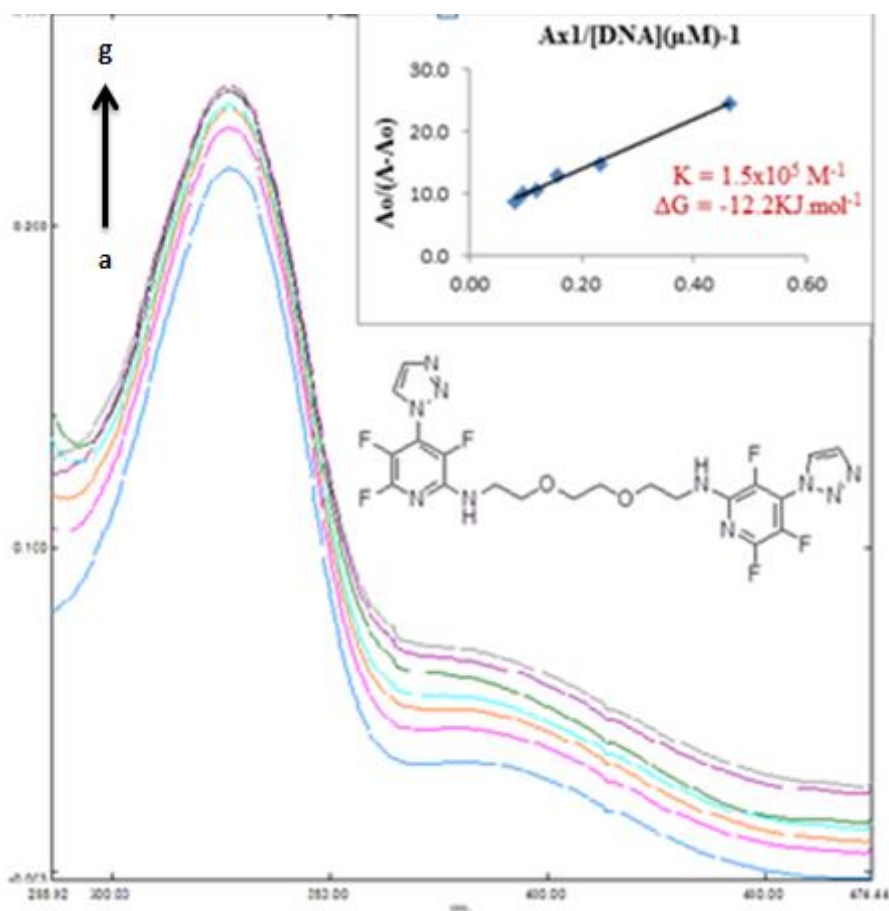
Absorption spectra of $1 \times 10^{-5} \text{ M}$ of compound 163. ($R^2 = 0.9909$ for six points)

6.2.14. UV-visible spectroscopy of compound 164



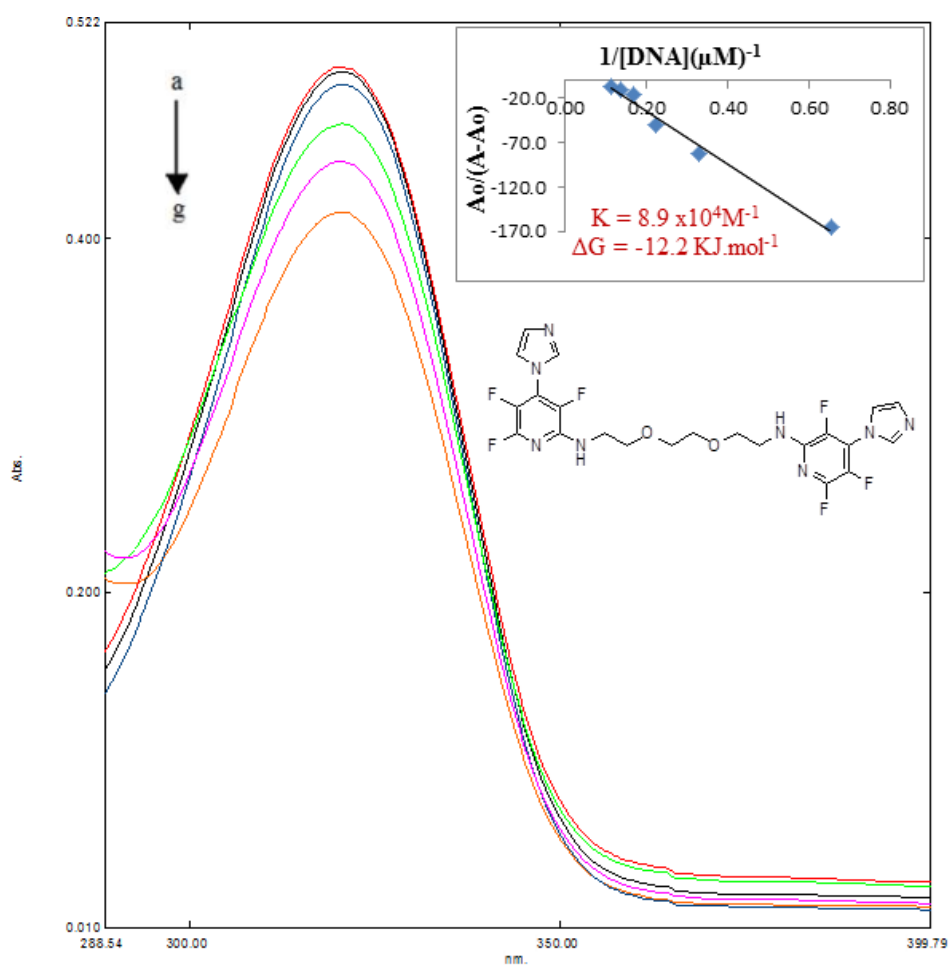
Absorption spectra of $9 \times 10^{-5} \text{ M}$ of compound 164. ($R^2 = 0.9949$ for six points)

6.2.15. UV-visible spectroscopy of compound 165



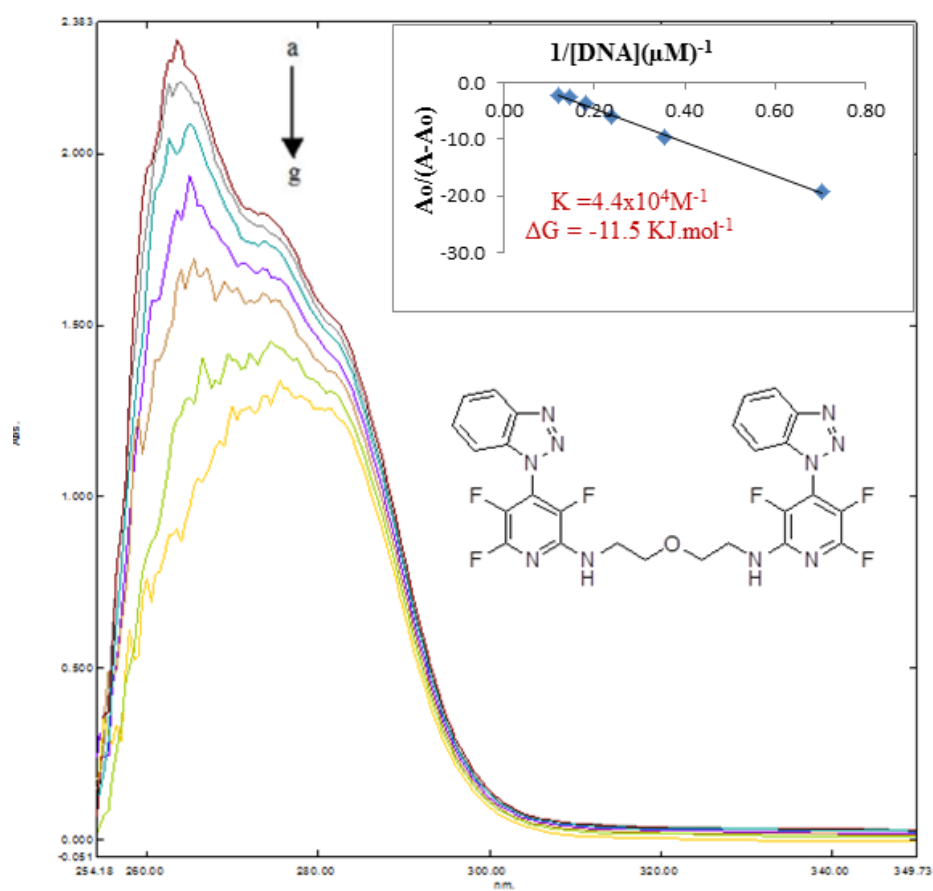
Absorption spectra of $7 \times 10^{-5} \text{ M}$ of compound 165. ($R^2 = 0.9933$ for six points)

6.2.16. UV-visible spectroscopy of compound 166



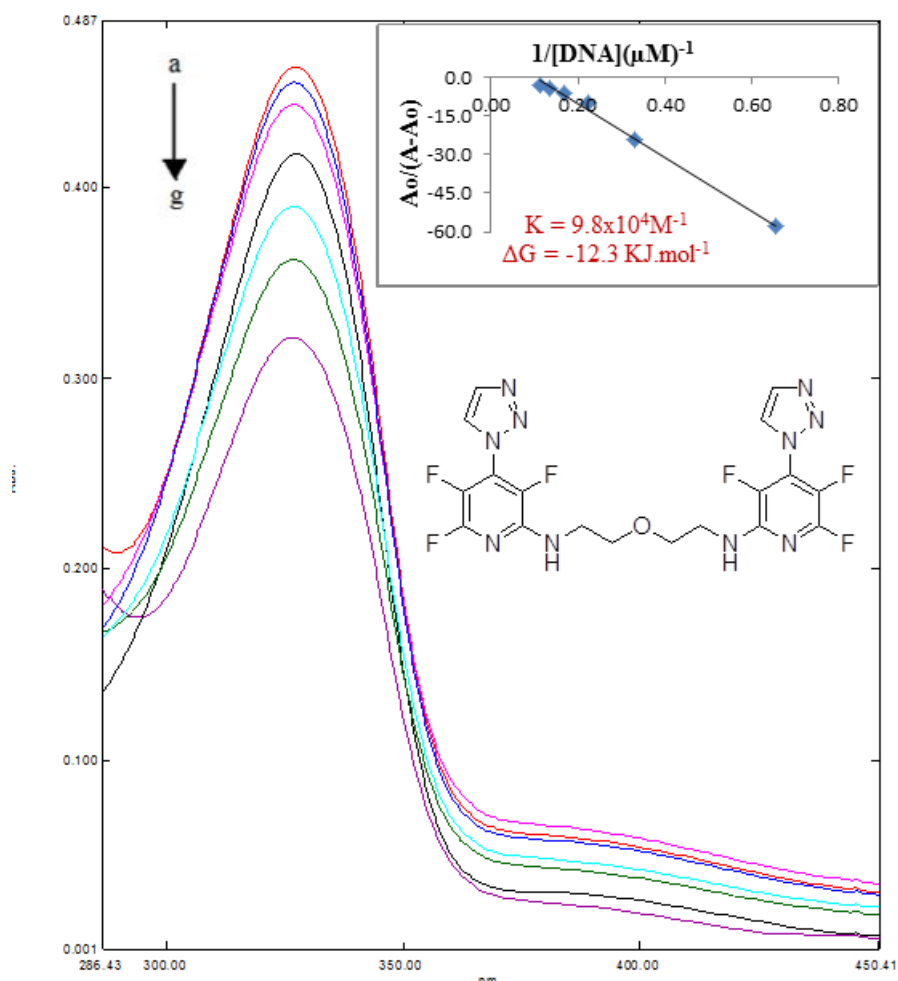
Absorption spectra of $3.8 \times 10^{-5} M$ of compound 166. ($R^2 = 0.9837$ for six points)

6.2.17. UV-visible spectroscopy of compound 169



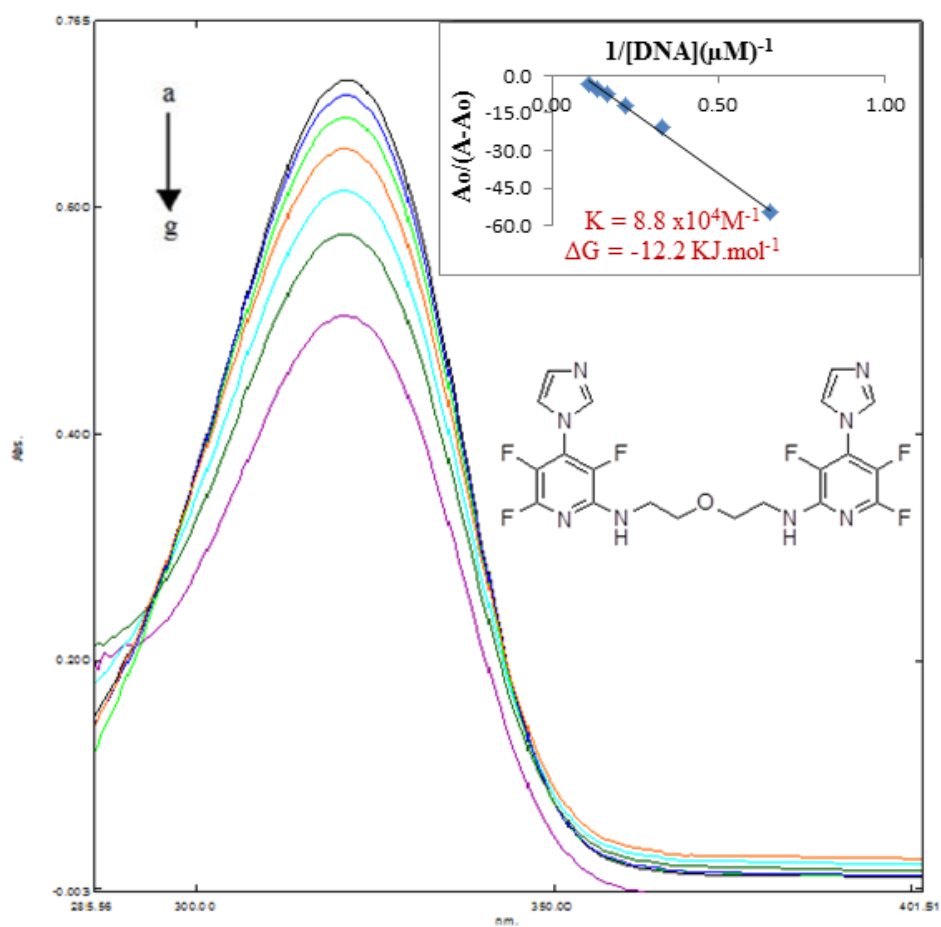
Absorption spectra of $9 \times 10^{-5} \text{ M}$ of compound 169 ($R^2 = 0.9973$ for six points)

6.2.18. UV-visible spectroscopy of compound 170



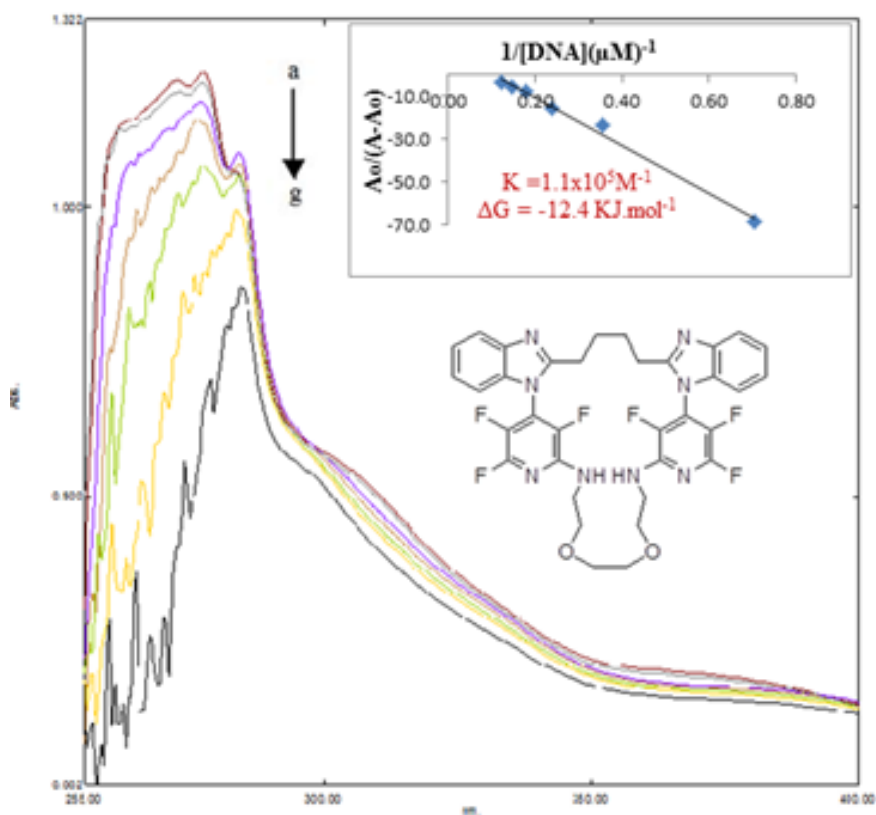
Absorption spectra of $3.8 \times 10^{-5} M$ of compound 170 ($R^2 = 0.9949$ for six points)

6.2.19. UV-visible spectroscopy of compound 171



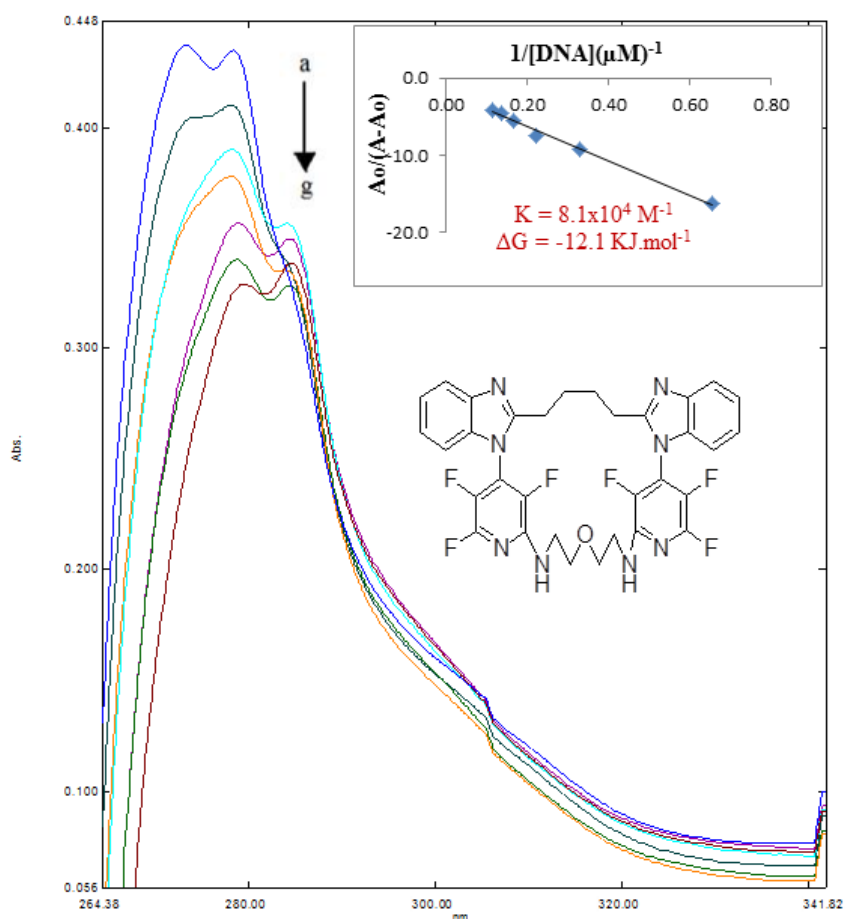
Absorption spectra of 3.8×10^{-5} M of compound 171. ($R^2 = 0.9961$ for six points)

6.2.20. UV-visible spectroscopy of compound 181



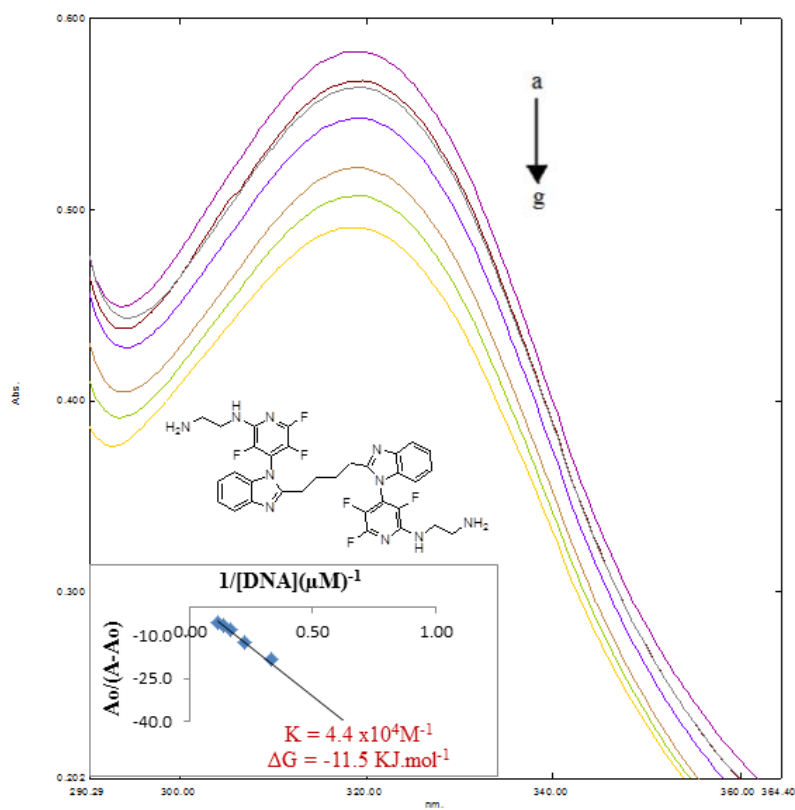
Absorption spectra of $9 \times 10^{-5} \text{ M}$ of compound 181 ($R^2 = 0.9923$ for six points)

6.2.21. UV-visible spectroscopy of compound 183



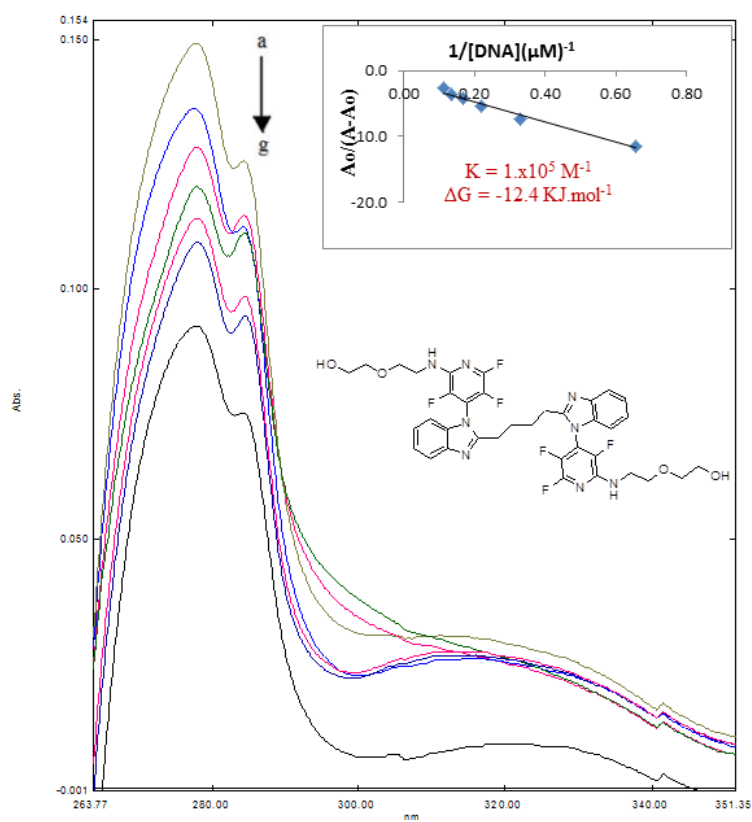
Absorption spectra of $3.8 \times 10^{-5} \text{ M}$ of compound 183. ($R^2 = 0.9934$ for six points)

6.2.22. UV-visible spectroscopy of compound 187



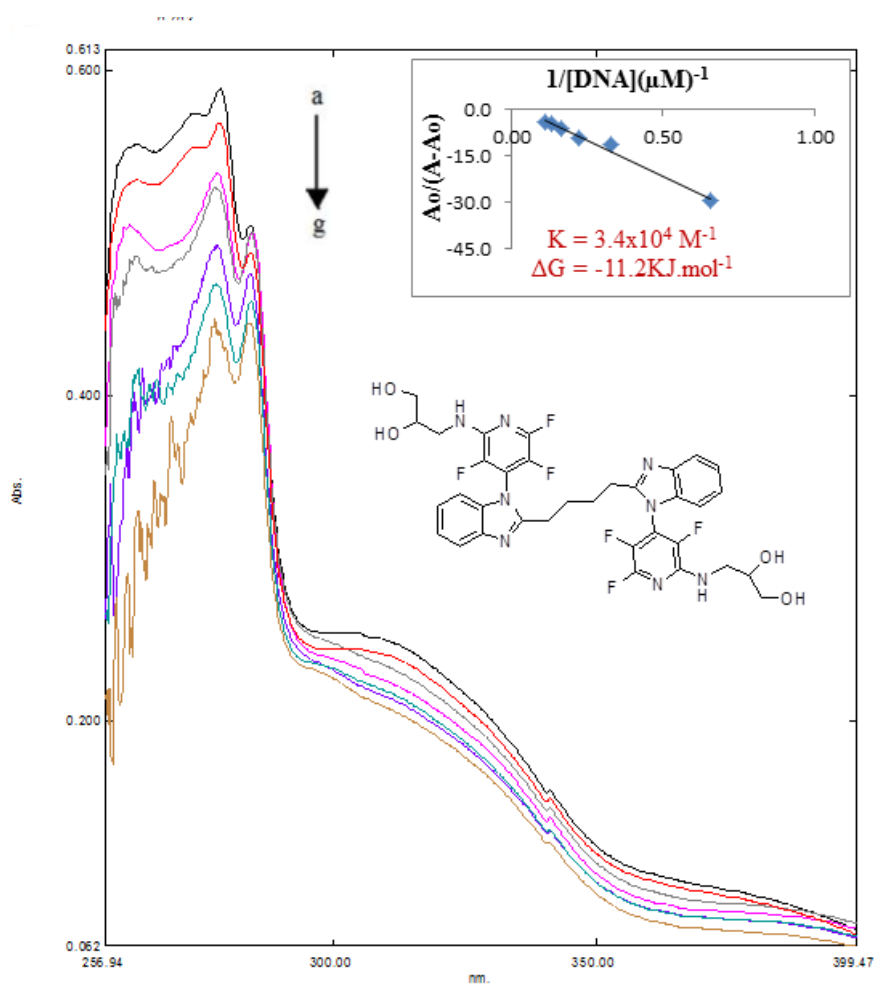
Absorption spectra of $3.8 \times 10^{-5} M$ of compound 187 in ($R^2 = 0.9837$ for six points)

6.2.23. UV-visible spectroscopy of compound 189



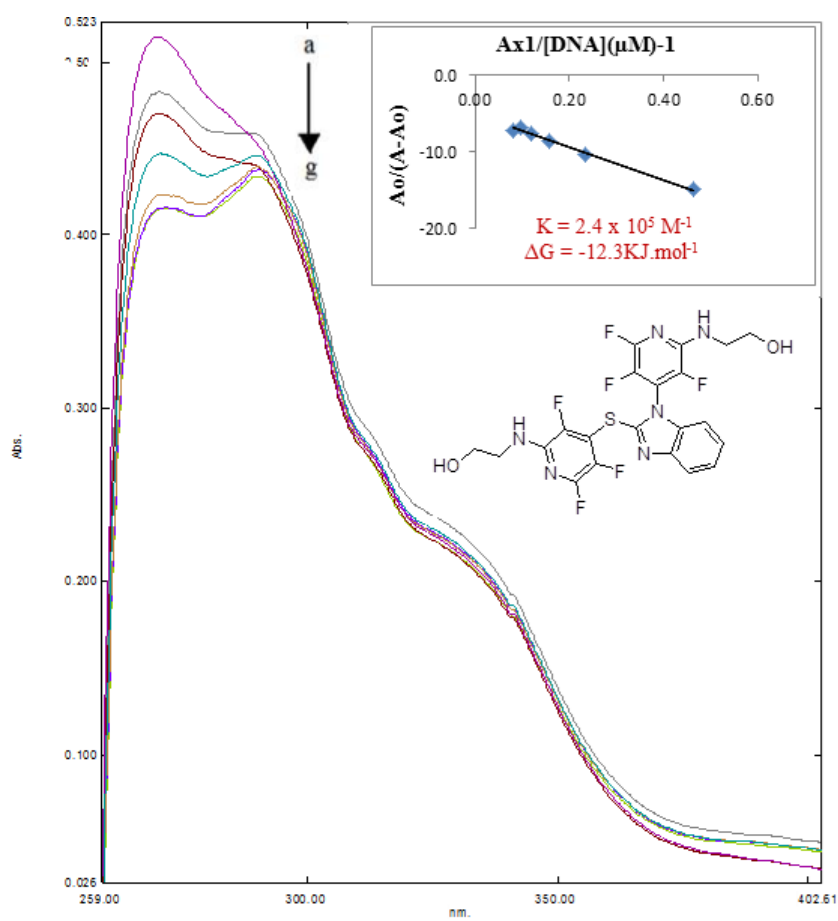
Absorption spectra of $3.8 \times 10^{-5} M$ of compound 189. ($R^2 = 0.9769$ for six points)

6.2.24. UV-visible spectroscopy of compound 191



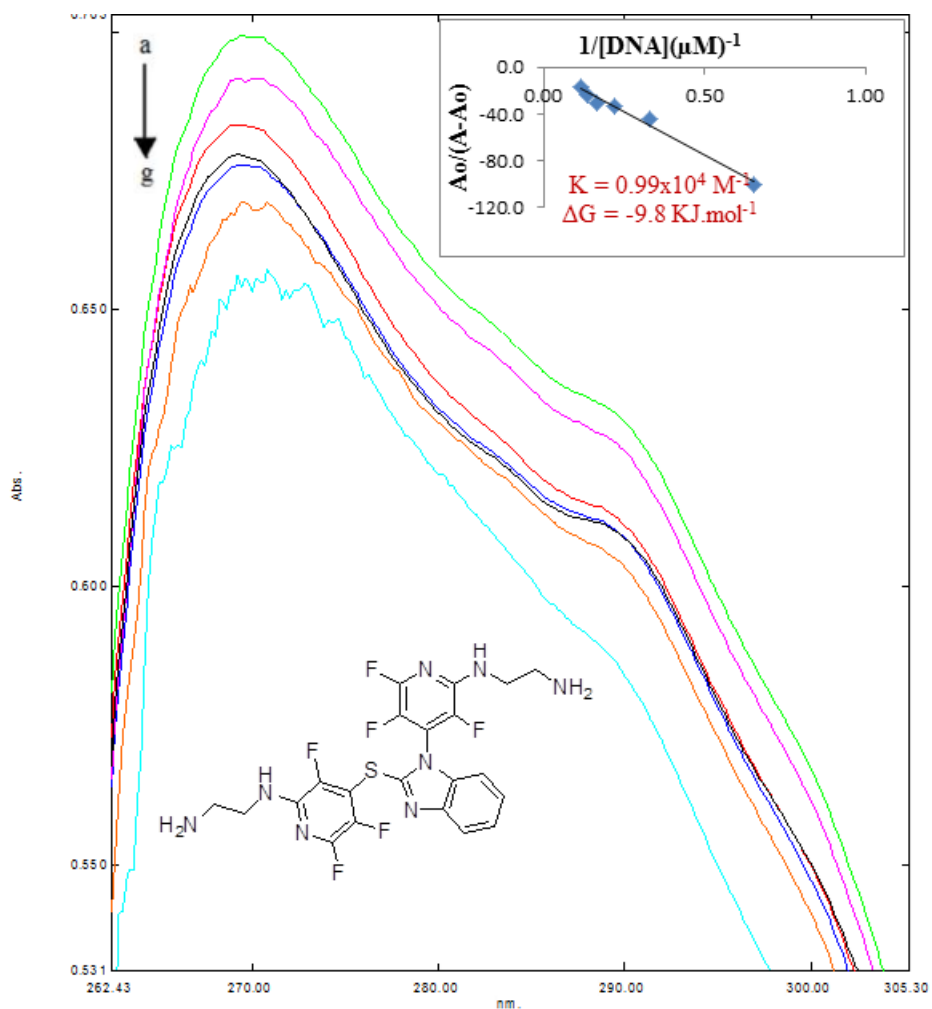
Absorption spectra of $3.8 \times 10^{-5} \text{ M}$ of compound 191. ($R^2=0.9866$ for six points)

6.2.25. UV-visible spectroscopy of compound 195



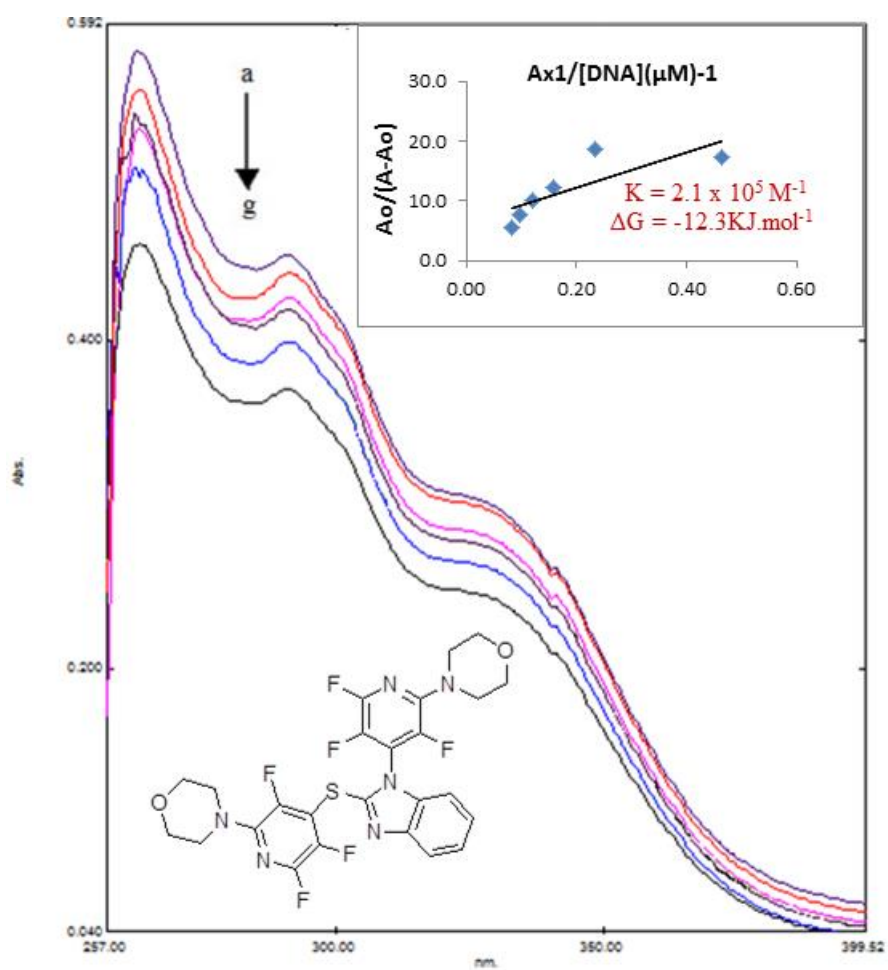
Absorption spectra of $3.8 \times 10^{-5} M$ of compound 195. ($R^2 = 0.9689$ for six points)

6.2.26. UV-visible spectroscopy of compound 196



Absorption spectra of $3.8 \times 10^{-5} M$ of compound 196. ($R^2 = 0.9848$ for six points)

6.2.27. UV-visible spectroscopy of compound 198

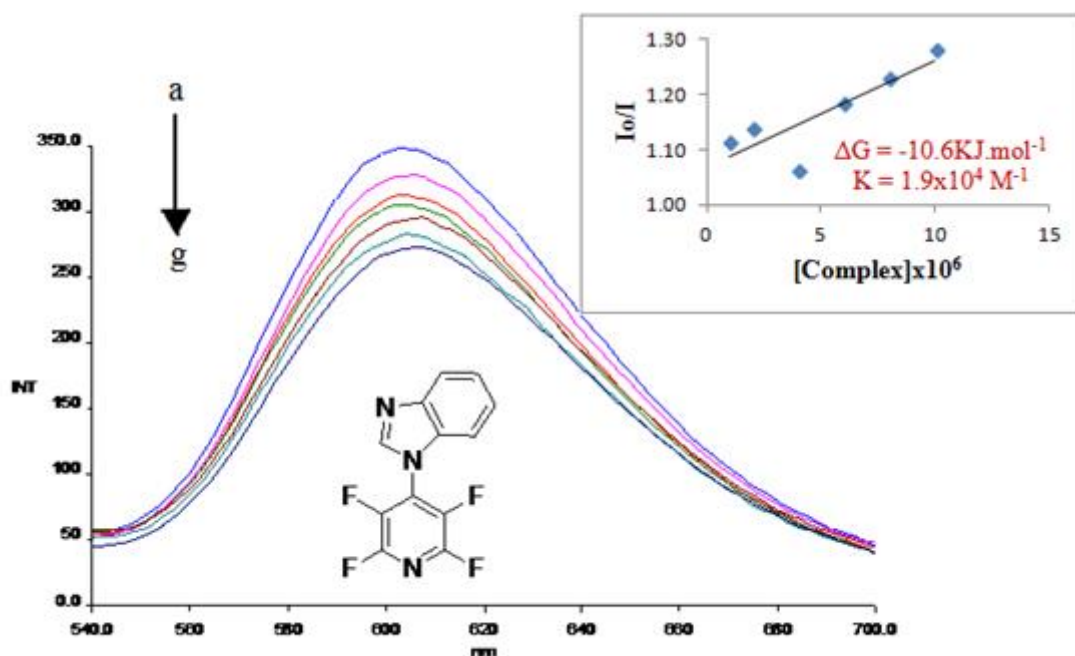


Absorption spectra of $9 \times 10^{-5} M$ of compound 198. ($R^2=0.8887$ for six points)

6.3. Fluorescence spectroscopy data for the ethidium boromide displacement assay

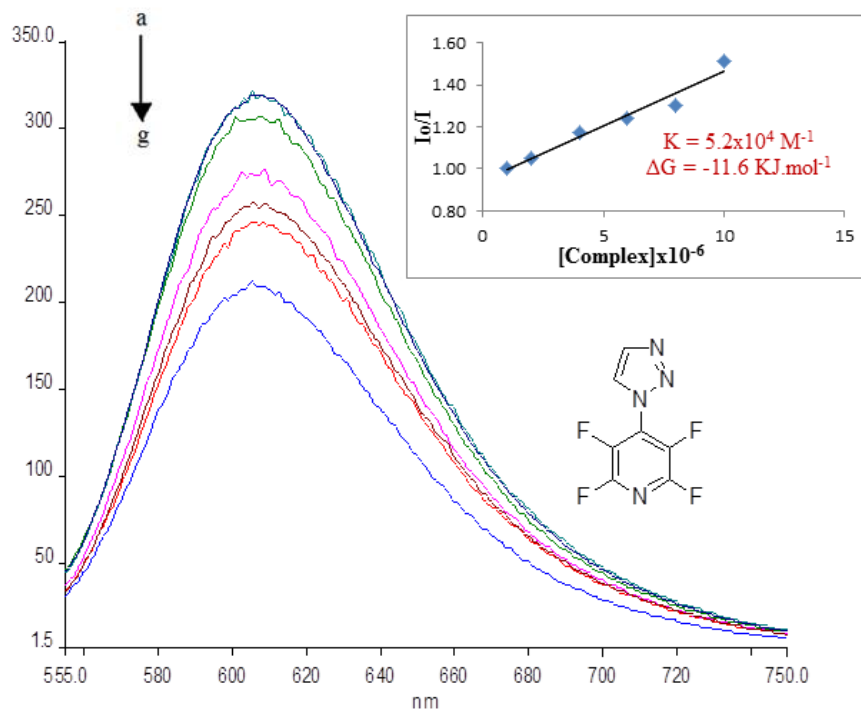
Emission spectra of SS-DNA in trisma base buffer on titration of the successfully synthesised compounds. $K_{ex} = 480 \text{ nm}$; $[EB] = 1 \times 10^{-6} \text{ M}$; $[DNA] = 1.5 \times 10^{-4} \text{ M}$. The arrow shows the increase of the complex concentration (a) 0.0 , (b) 1×10^{-6} , (c) 2×10^{-6} , (d) 4×10^{-6} , (e) 6×10^{-6} , (f) 8×10^{-6} , (g) $1 \times 10^{-6} \text{ M}$. Inside graph in plot of I_0 / I vs. complex concentration for determination of k and ΔG values.

6.3.1. Fluorescence spectra of compound 108



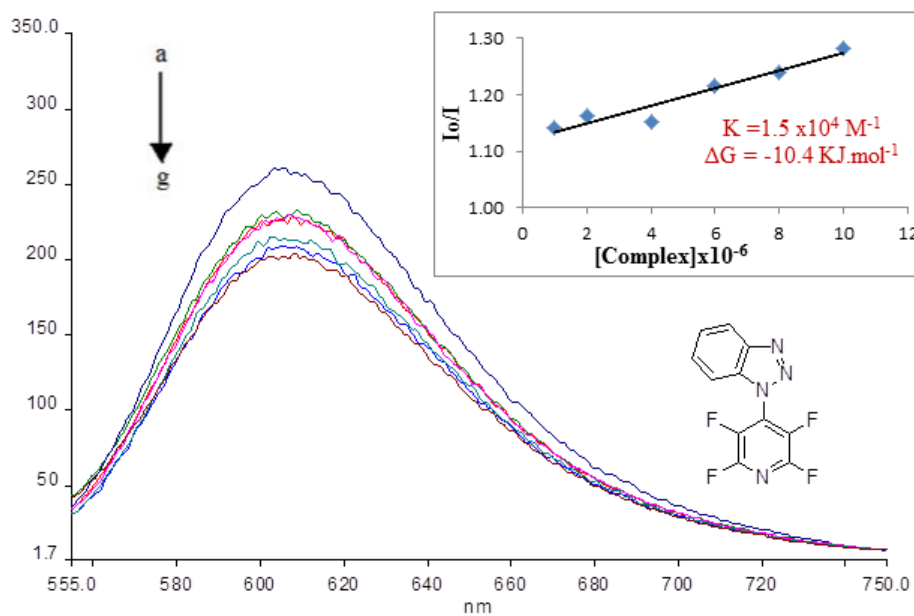
$R^2 = 0.7217$ for six points

6.3.2. Fluorescence spectra of compound 111



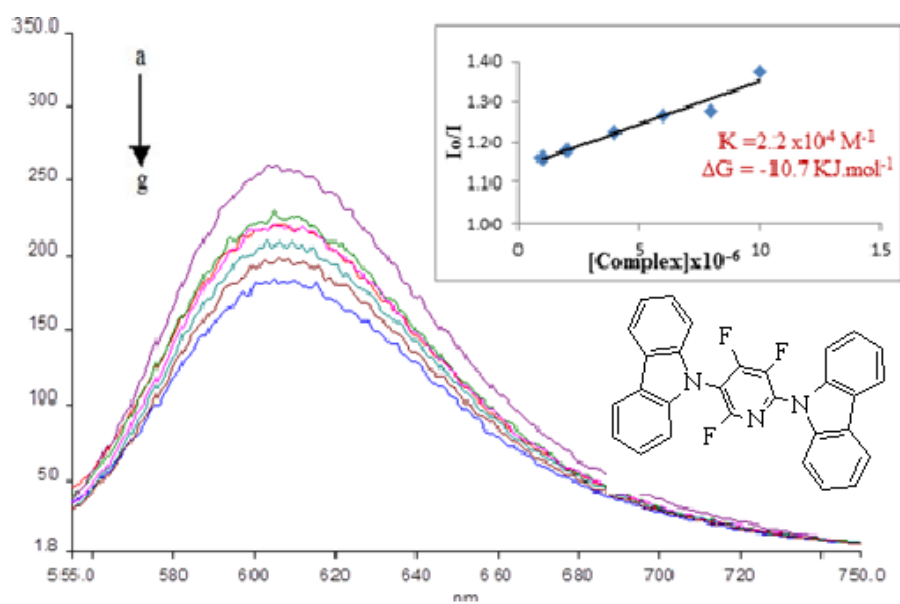
$R^2 = 0.965$ for six points.

6.3.3. Fluorescence spectra of compound 113



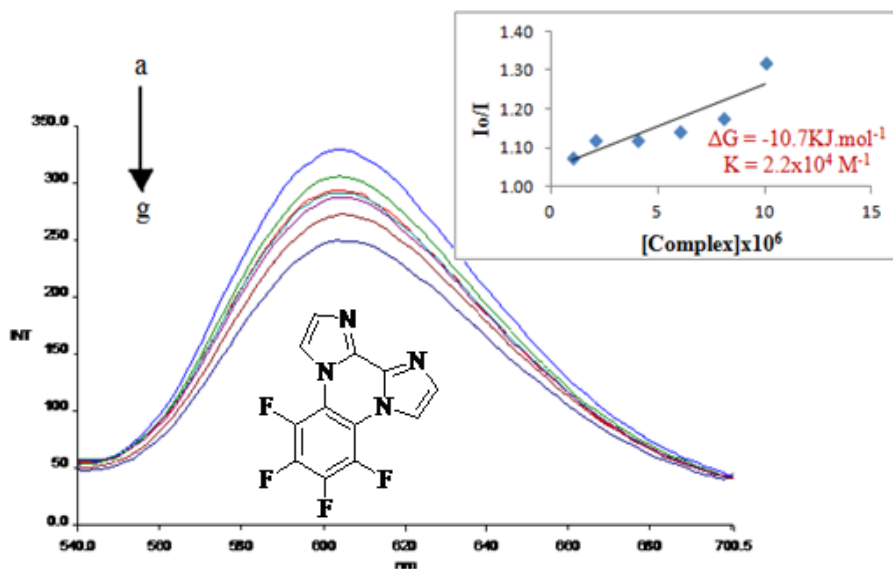
$R^2 = 0.9296$ for six points.

6.3.4. Fluorescence spectra of compound 114



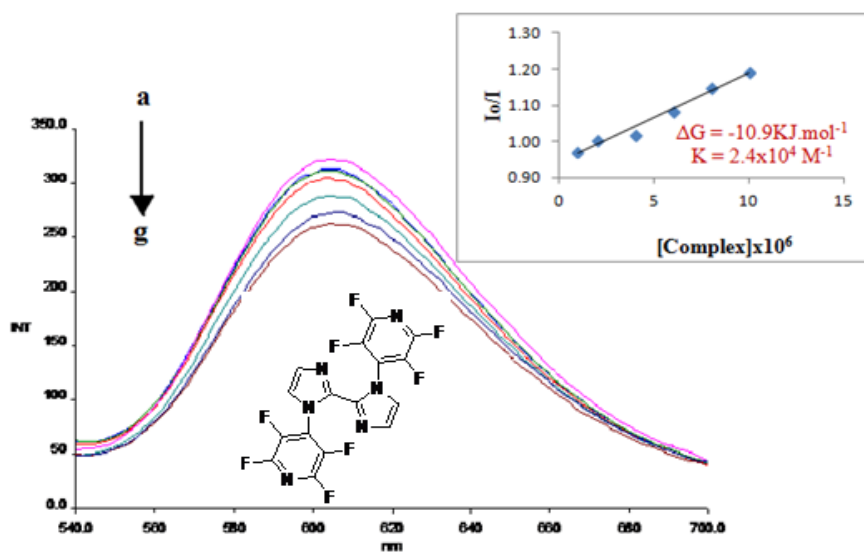
$R^2 = 0.9472$ for six point

6.3.5. Fluorescence spectra of compound 137



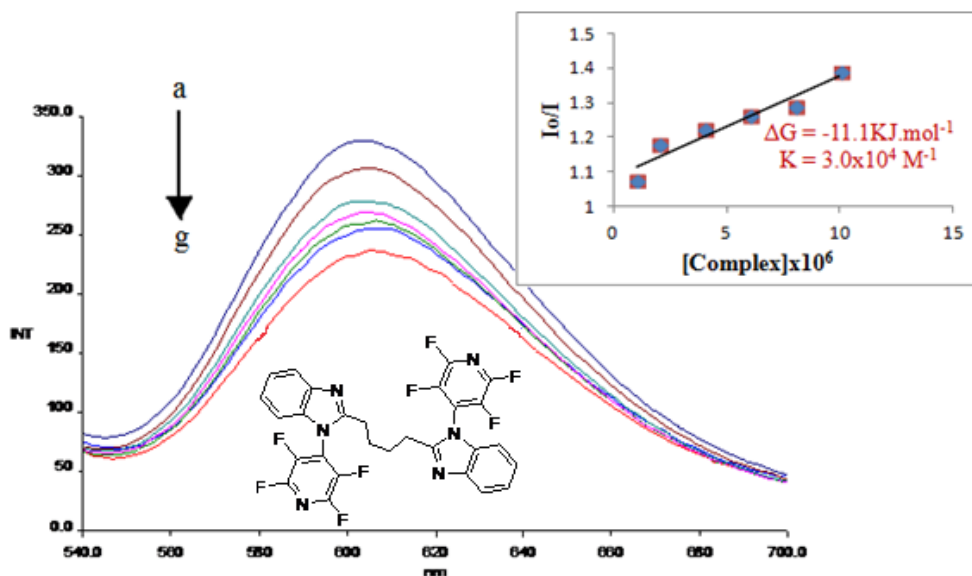
$R^2 = 0.7375$ for six points

6.3.6. Fluorescence spectra of compound 138



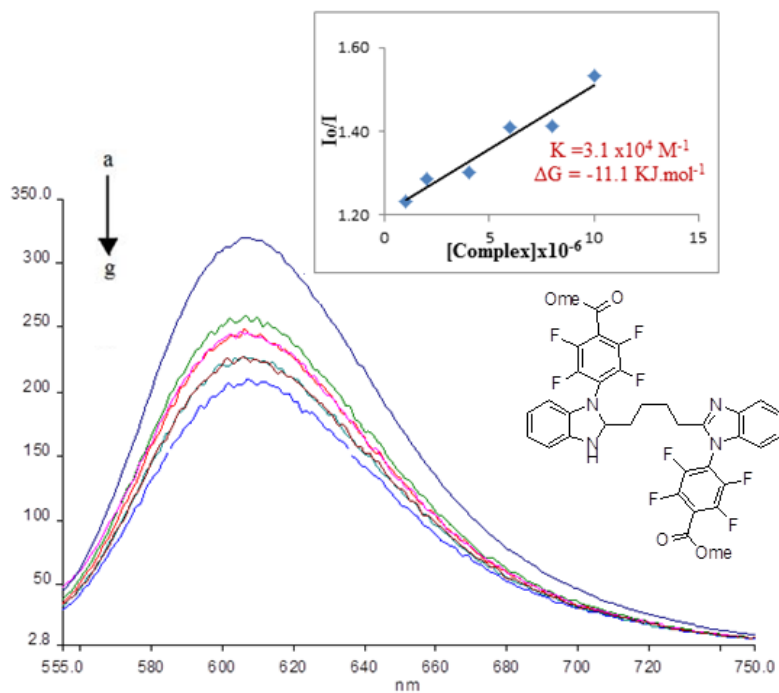
$R^2 = 0.9786$ for six points

6.3.7. Fluorescence spectra of compound 143



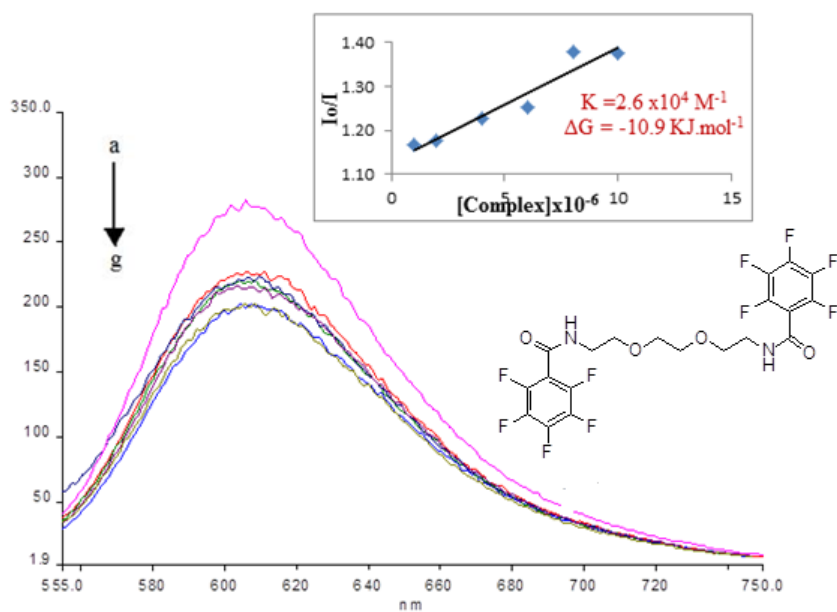
$R^2 = 0.9921$ for six points

6.3.8. Fluorescence spectra of compound 148



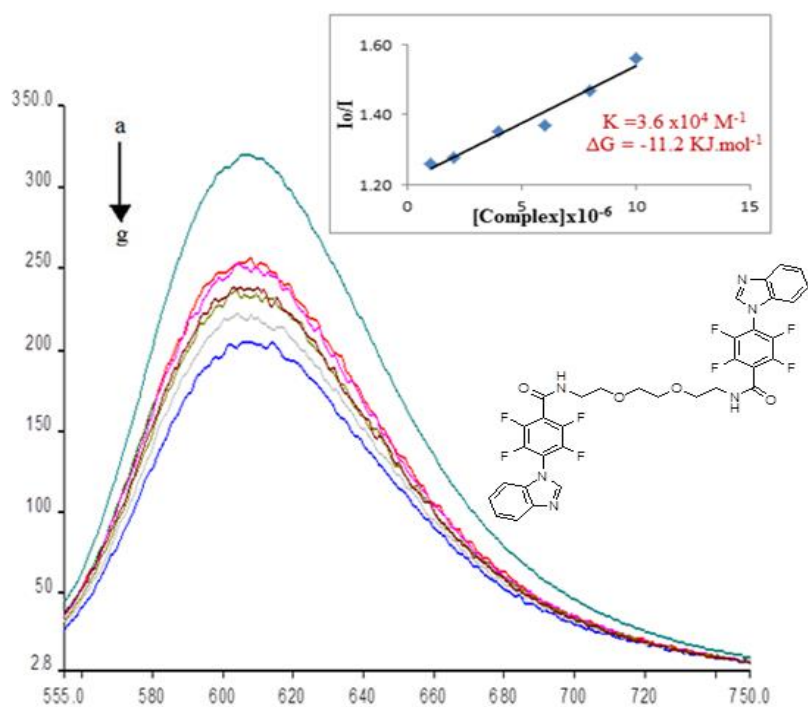
R² = 0.9414 for six points

6.3.9. Fluorescence spectra of compound 151



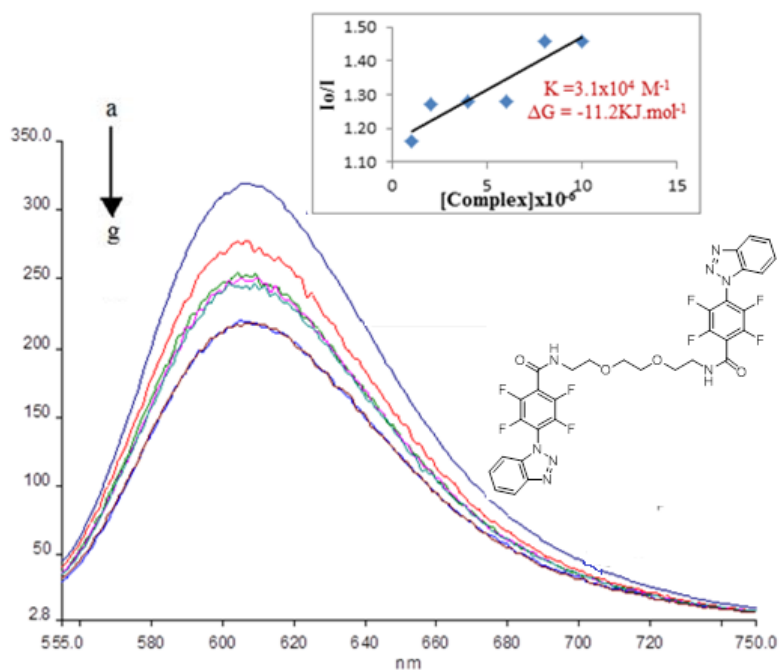
R² = 0.9318 for six point

6.3.10. Fluorescence spectra of compound 152



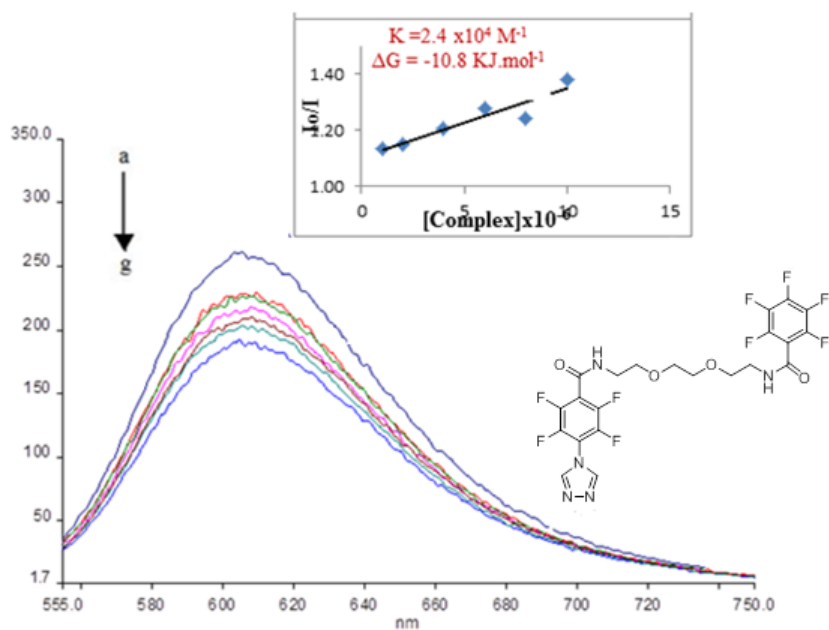
$R^2 = 0.9622$ for six points

6.3.11. Fluorescence spectra of compound 161



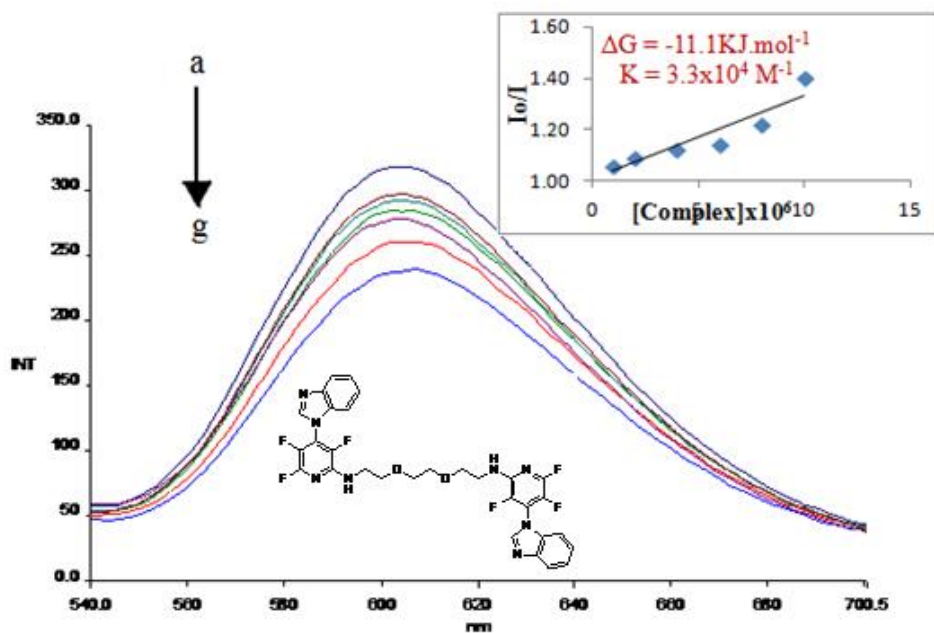
$R^2 = 0.8476$ for six points.

6.3.12. Fluorescence spectra of compound 162



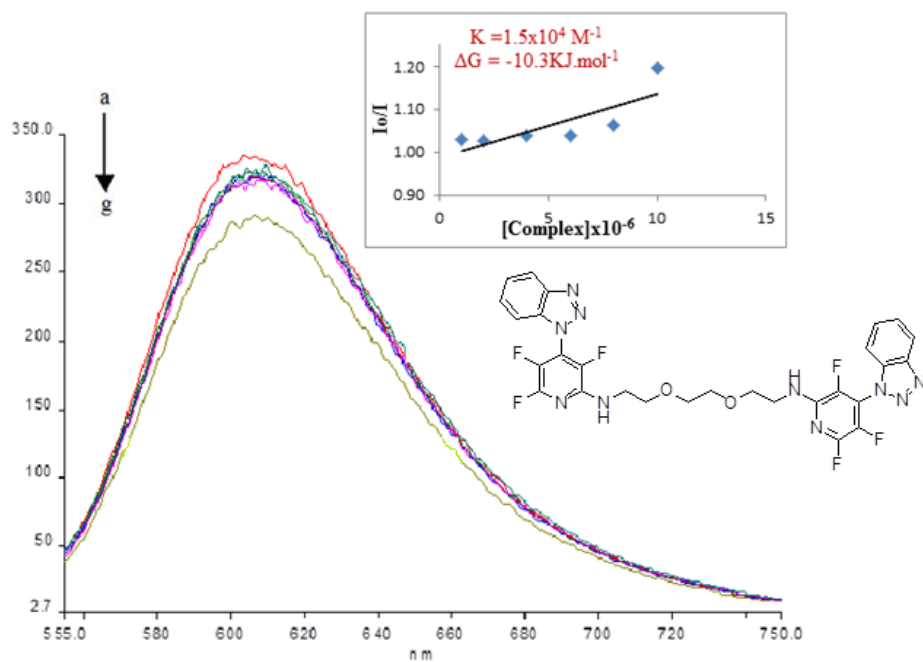
$R^2 = 0.8765$ for six points.

6.3.13. Fluorescence spectra of compound 163



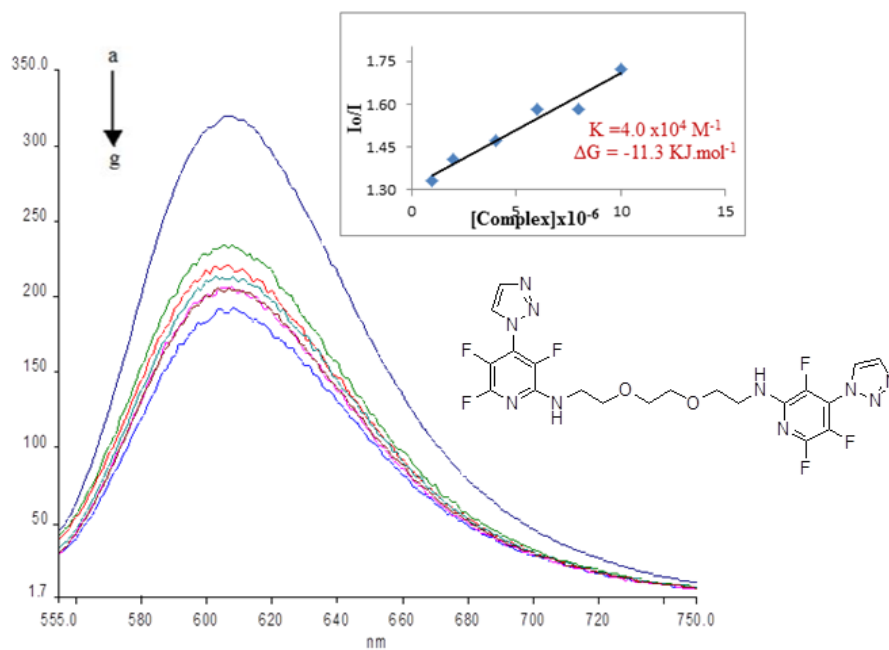
$R^2 = 0.8559$ for six points

6.3.14. Fluorescence spectra of compound 164



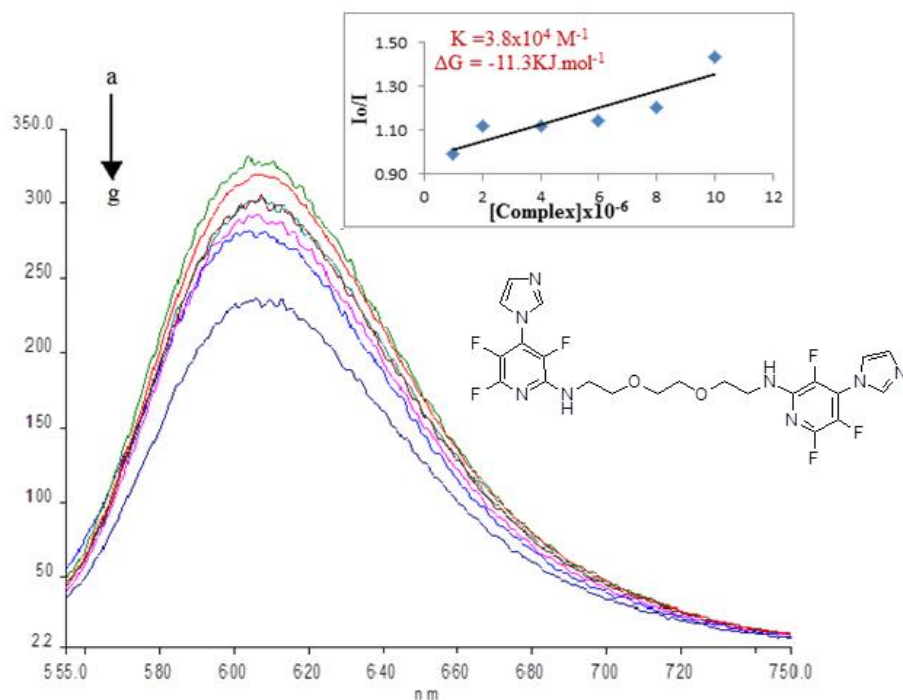
$R^2 = 0.6235$ for six point

6.3.15. Fluorescence spectra of compound 165



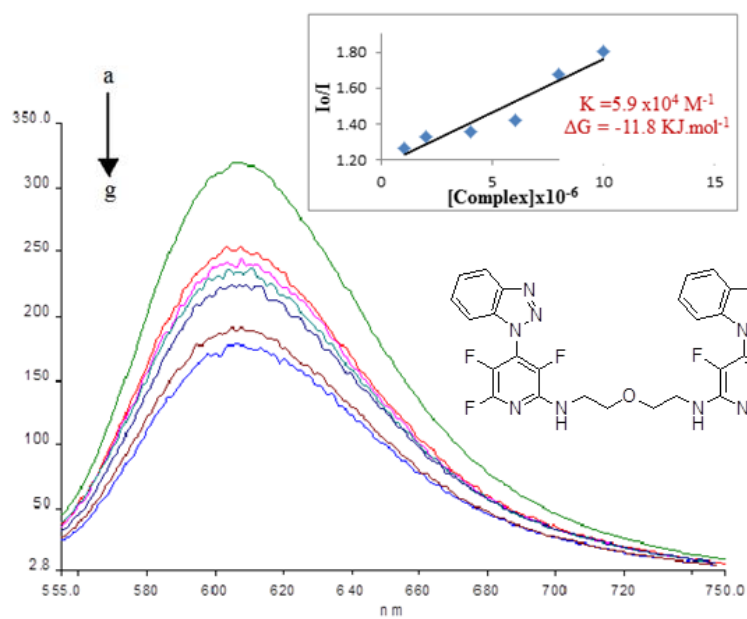
$R^2 = 0.9601$ for six points.

6.3.16. Fluorescence spectra of compound 166



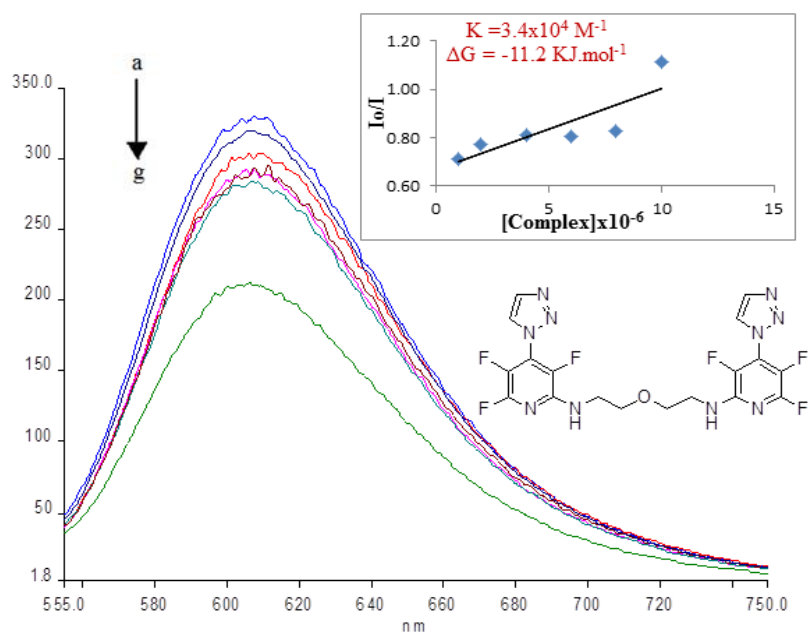
$R^2 = 0.819$ for six points.

6.3.17. Fluorescence spectra of compound 169



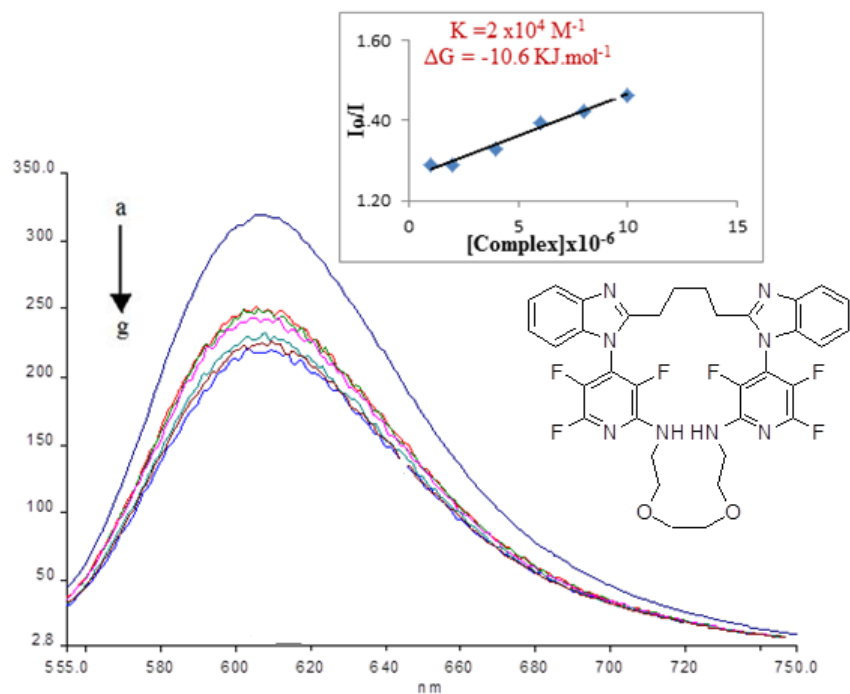
$R^2 = 0.9221$ for six points

6.3.18. Fluorescence spectra of compound 170



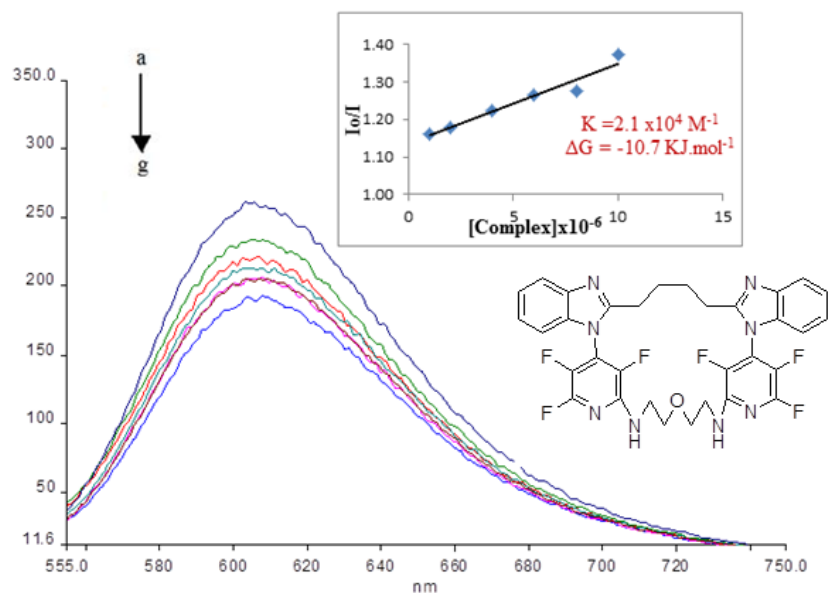
R² = 0.7004 for six points.

6.3.19. Fluorescence spectra of compound 181



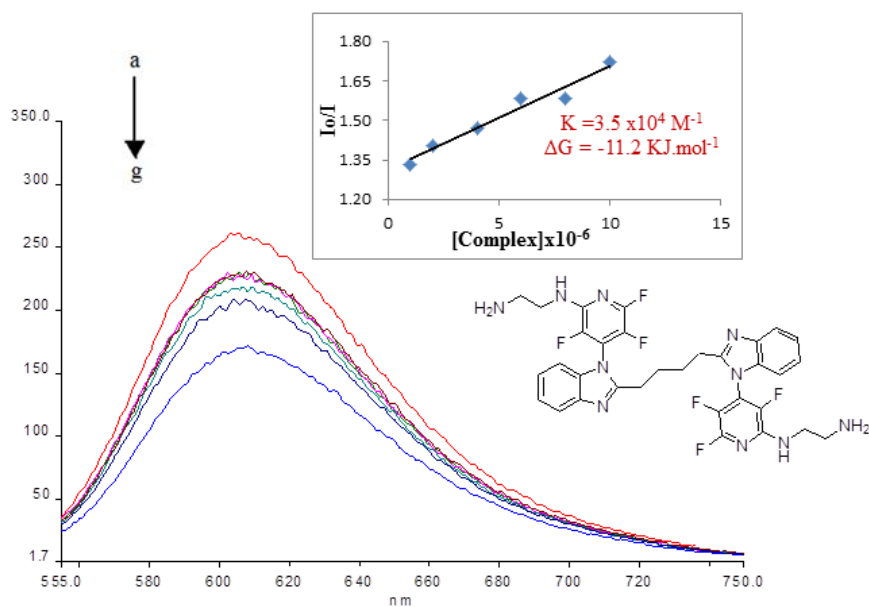
R² = 0.9827 for six point

6.3.20. Fluorescence spectra of compound 183



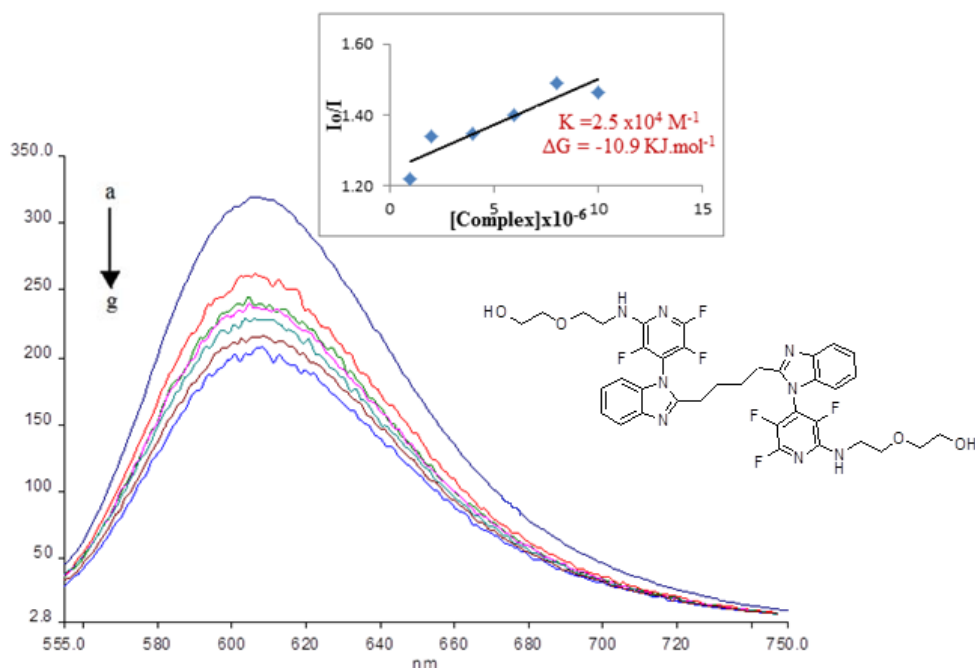
R² = 0.9456 for six point

6.3.21. Fluorescence spectra of compound 187



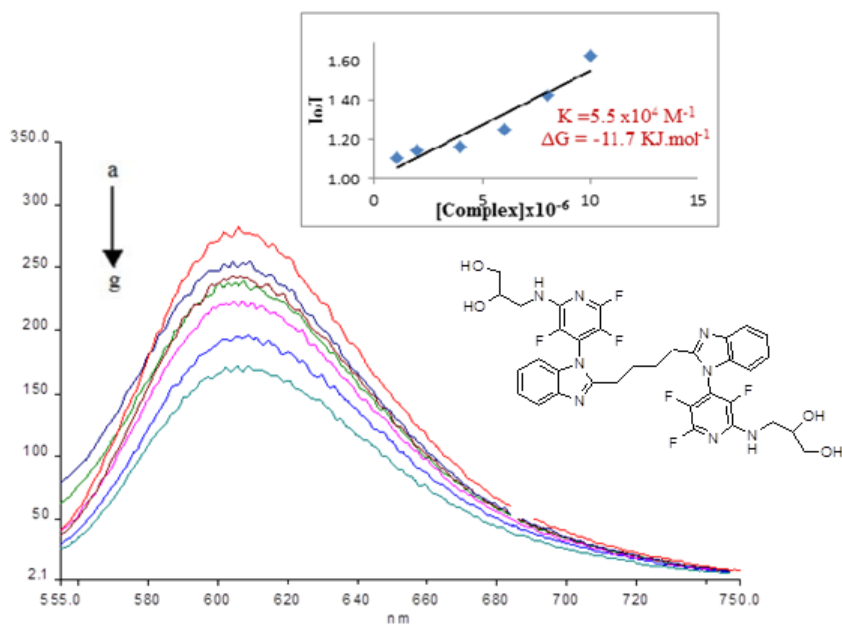
R² = 0.9601 for six points

6.3.22. Fluorescence spectra of compound 189



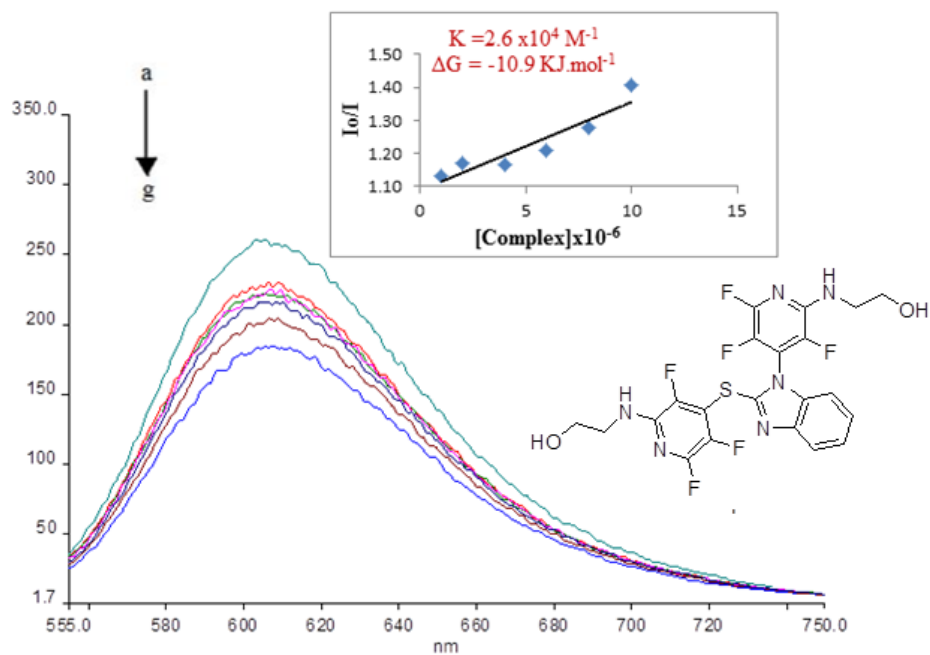
$R^2 = 0.8443$ for six point

6.3.23. Fluorescence spectra of compound 191



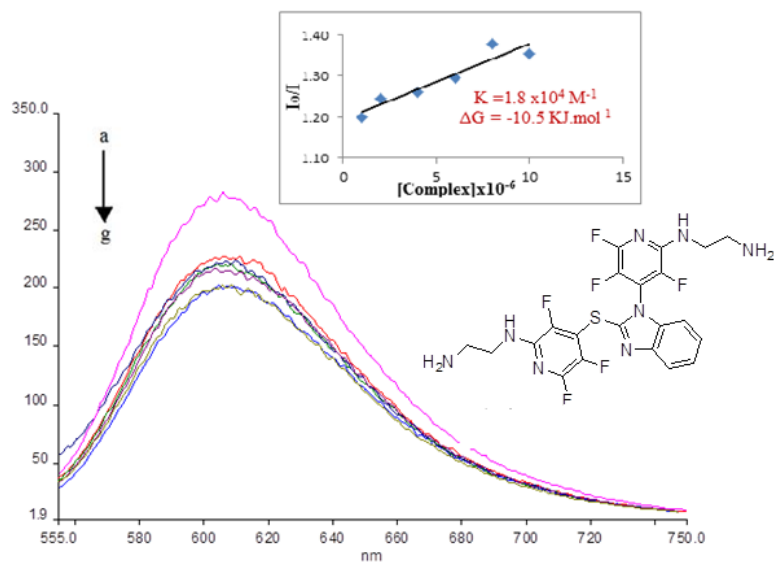
$R^2 = 0.9071$ for six point

6.3.24. Fluorescence spectra of compound 195



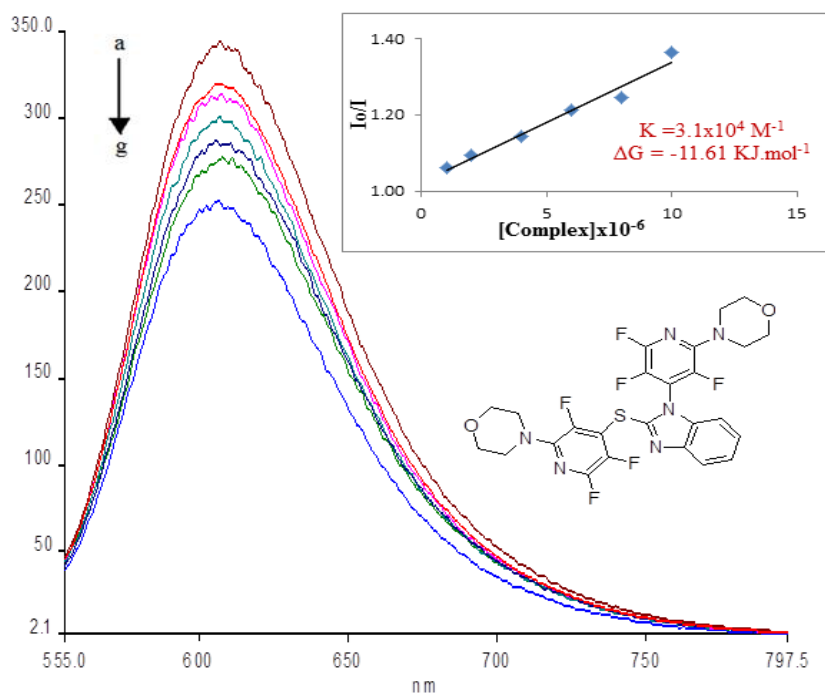
$R^2 = 0.8712$ for six point

6.3.25. Fluorescence spectra of compound 196



$R^2 = 0.8935$ for six point

6.3.26. Fluorescence spectra of compound 198



$R^2 = 0.9744$ for six points.